Characterization of the relationship between two RBM5 family members

by

Julie Jennifer Loiselle

A thesis submitted in partial fulfillment
of the requirements for the degree of
Doctor of Philosophy (PhD) in Biomolecular Sciences

The Faculty of Graduate Studies
Laurentian University
Sudbury, Ontario, Canada

THESIS DEFENCE COMMITTEE/COMITÉ DE SOUTENANCE DE THÈSE
Laurentian Université/Université Laurentienne
Faculty of Graduate Studies/Faculté des études supérieures

Title of Thesis Titre de la thèse	Characterization of the relationship between two RBM5 family members
Name of Candidate Nom du candidat	Loiselle, Julie
Degree Diplôme	Doctor of Philosophy
Department/Program Département/Programme	Biomolecular Sciences
Date of Defence Date de la soutenance	July 31,2017

APPROVED/APPROUVÉ

Thesis Examiners/Examinateurs de thèse:

Dr. Leslie Sutherland
(Supervisor/Directeur(trice) de thèse)

Dr. Eric Gauthier
(Committee member/Membre du comité)

Dr. Amadeo Parissenti
(Committee member/Membre du comité)

Dr. Doug Gray
(External Examiner/Examinateur externe)

Dr. T.C. Tai
(Internal Examiner/Examinateur interne)

Approved for the Faculty of Graduate Studies
Approuvé pour la Faculté des études supérieures
Dr. David Lesbarrères
Monsieur David Lesbarrères
Dean, Faculty of Graduate Studies
Doyen, Faculté des études supérieures

ACCESSIBILITY CLAUSE AND PERMISSION TO USE

Abstract

RNA binding proteins (RBPs) control all aspects of RNA metabolism, and a single RBP can have numerous downstream effects. Alterations to their expression and/or function can, therefore, have remarkable consequences. For instance, decreased levels of the RNA binding motif domain (RBM) protein *RBM5* are associated with increased risk of a number of cancer types, and *RBM10* mutations can be lethal. Although these consequences are quite severe, little is known regarding the range of processes and events influenced by these two homologous RBPs. In fact, previous RBM5 and RBM10 functional studies were largely focused only on their abilities to promote two processes; apoptosis and cell cycle arrest. Potentially by control of these processes, RBM5 and RBM10 were shown to influence one event: differentiation. The objectives of this study were to identify all cellular processes and events enriched by changes in *RBM5* and/or *RBM10* expression in a particular cultured cell line, and to determine the extent of functional overlap for RBM5 and RBM10 in these cells. Towards these goals, a list of *RBM5* and *RBM10* mRNA targets and differentially expressed genes was determined using next generation sequencing techniques. Our data suggest that RBM5 and RBM10 do influence a wide range of cellular processes and events. Although there is overlap in *RBM5* and *RBM10* mRNA targets and differentially expressed genes, these RBPs can have antagonistic functions; for example our data suggest that RBM5 prevents the transformed state, whereas RBM10 actually promotes it in an *RBM5*-null environment. Furthermore, we present a working model by which RBM5 may regulate RBM10's protransformatory function. Finally, we demonstrate a relationship between RBM5 and RBM10 in non-transformed cells. The results presented herein provide insight not only into the roles and regulation of RBM5 and RBM10, but of RBPs in general. Taken together,

the results presented in the four papers included in this thesis expand the knowledge base of RBM5 and RBM10, which provides insight into the disease states associated with their disrupted expression or function. Our findings are thus relevant to a wide range of scientific fields including molecular, developmental and cancer biology.

Keywords

RNA binding proteins, RBM5, RBM10, RIP-Seq, RNA-Seq, Transcriptional studies, Small cell lung cancer, Myoblasts, Regulation of RNA binding proteins

Co-Authorship Statement

Chapter 2. Insight into the role of alternative splicing within the RBM10v1 exon 10 tandem donor site

I determined *RBM10* splice variant expression levels in GLC20 cells by RNA-Seq (Figure 2.3A). In addition, ST and I performed protein modeling. ST carried out all initial molecular biology experiments and is responsible for Figure 2.1D,E,F and Figure 2.2. CP performed the final RT-PCR experiment presented in Figure 2.1B. BK performed the final Western Blot presented in Figure 2.1Ci. JR performed the final NUMB RNA expression experiment, and produced the graph. AM performed the FISH analysis. LCS conceived the project and developed the model. ST prepared the first draft of the manuscript, and LCS wrote the final draft.

Chapter 3. RBM5 reduces small cell lung cancer growth, increases cisplatin sensitivity and regulates key transformation-associated pathways

I wrote the manuscript, and my results are presented in all 8 tables and Figures 3.3, 3.4, 3.5 (Sp1 section only), 3.6, 3.7, 3.8, 3.11, 3.12, 3.13, and 3.14. JR grew the GLC20 cells (parental and sublines) (Figure 3.1F) and performed cell growth and apoptosis assays (Figures 3.9 and 3.10). LCS established the stable RBM5-expressing GLC20 sublines and revised the manuscript. JL, JR and LCS conceived and designed the experiments. Additional acknowledged contributions are as follow; NRM characterized the GLC20 cell line (Figures 3.1 and 3.2), BK analyzed RBM5 antibodies (Figure 3.5), ST help prepare RNA-Seq samples and SH extracted RNA from the primary tissue specimens.

Chapter 4. RBM10 promotes transformation-associated processes in small cell lung cancer and is directly regulated by RBM5

I wrote the manuscript, prepared all figures and was corresponding author. My results are included in both tables and Figures 4.1, 4.2, 4.3A,B, 4.4, 4.5, 4.6A,B,D, 4.7, 4.8. I also developed the model (Figures 4.9 and 4.10). JR established the stable RBM10KD clones, and performed Western blot and MTT assays (Figure 4.3C,D,E and 4.6C). LCS revised the manuscript.

Chapter 5. Post-transcriptional regulation of Rbm5 expression in undifferentiated H9c2 myoblasts

I wrote the manuscript, prepared all figures and was corresponding author. Some work was performed by me at the end of my masters, but specifically during my PhD studies I performed transient RBM5 knockdown experiments (two biological replicates) (Figure 5.2) and analyzed RBM5 overexpression experiments (Figure 5.3). I also contributed to the analysis of the stable RBM5KD clones (Figure 5.1) and designed the model (Figure 5.4). LCS established the stable RBM5KD clones and revised the manuscript. ST screened all stable RBM5KD H9c2 clones generated by LCS (Figure 5.1).

Acknowledgments

I would first and foremost like to thank my supervisor, Dr. Leslie Sutherland. You have been an amazing mentor, and words cannot express my gratitude. Your dedication to the success of your students is unmatched, and has shaped me into the researcher I have become. Thank you for your friendship, patience, support and encouragement, which have helped me through the more difficult times and taught me how to approach and overcome all new challenges.

Thank you to my committee members, Dr. Éric Gauthier and Dr. Amadeo Parissenti, for their insights, guidance and support throughout my doctoral studies. Thank you also to the past and present members of the Sutherland lab group, particularly, Sarah Hunt, Jose Knee and Justin Roy, for supporting me through the ups and downs of research, and making the lab such a friendly and happy environment. To all members of the Health Sciences North Research Institute, it's been a pleasure working alongside such exceptional researchers.

I am very appreciative of the funding I received from the Natural Sciences and Engineering Research Council of Canada (NSERC) and the Northern Cancer Foundation, which have allowed me to focus on research throughout my studies.

A special thank you to my wonderful husband, Mathieu, who believes in me even when I don't believe in myself. I will be forever grateful for your strong, unwavering love and support. Thank you also to Henri and Hugo, my two beautiful boys, who inspire me every day to be the best I can be. Finally, to my all of my family and friends, particularly my parents, I cannot thank you enough for your encouragement throughout all of my studies. Having such a strong support system has allowed me to dream big and accomplish this significant goal.

Table of Contents

List of Abbreviations

7-AAD – 7-aminoactinomycin D

DMSO – dimethyl sulfoxide

EC50 – half-maximal effective concentration

EGFR – epidermal growth factor receptor

EMT – epithelial to mesenchymal transition

FIDEA – functional interpretation of differential expression analysis

FISH – fluorescent in situ hybridization

FPKM - fragments per kilobase of transcript per million mapped reads

GSAASeq – gene set association analysis with sequence permutation

KD – knockdown

KEGG – Kyoto encyclopedia of genes and genomes

MSigDB – molecular signatures hallmark database

MTT - 3-(4,5-dimethylthiazol-2-yl)-2,5-diphenyltetrazolium bromide

n.s – not significant

NCI – National Cancer Institute

NSCLC – non small cell lung cancer

OTB – Ontario Tumour Bank

PCR – polymerase chain reaction

PDGF – platelet derived growth factor

RBM – RNA binding motif

RBP – RNA binding protein

RIP – RNA Immunoprecipitation

RNP – ribonucleoprotein

RRM – RNA recognition motif

SCLC – small cell lung cancer

shRNA – short hairpin RNA

siRNA – small interfering RNA

TARP syndrome – Talipes equinovarus, Atrial septal defect, Robin sequence, and Persistence of the left superior vena cava

UTR – untranslated region

VEGF – vascular endothelial growth factor

List of Tables

List of Figures

1 Introduction

1.1 RNA binding proteins

Proteins are the end result of the central dogma of molecular biology, by which DNA encodes RNA, and RNA in turn can encode proteins. Proteins play a key role in almost every cellular process, from DNA replication to cell structure, and even form the extracellular environment (O'Connor and Adams, 2010). RNA binding proteins (RBPs) are a large and broad class of proteins that regulate all aspects of RNA metabolism (Glisovic et al., 2008). Their interaction with RNA can be accomplished *via* one or more consensus RNA binding sequences that form domains within the RBP (Lunde et al., 2007).

1.1.1 RNA binding domains

RBPs' are classified, in large part, by the RNA binding domains present within their primary sequence. While certain RBPs have unconventional RNA binding domains, most contain one or more conventional domains, defined by consensus sequences. Such sequences include RNA-recognition motifs (RRM), zinc-finger domains, K-homology domains, S1 domains, arginine-rich motifs, cold-shock domains and double-stranded RNA-binding motifs (Castello et al., 2016; Lunde et al., 2007). Many RBPs have more than one type of RNA binding domain, which combined with other structural features of the protein, determine the specificity of the RBP with regards to RNA targets, as well as the functional consequences of the protein-RNA interaction (Allain et al., 2000; Lunde et al., 2007). By far the most abundant RNA binding domain is the

RRM, also known as RNA binding motif or ribonucleoprotein motif, with about 0.5 to 1% of human genes coding this sequence (Lunde et al., 2007; Venter et al., 2001).

The RRM domain is approximately 90 amino acids in length, and is characterized by two consensus ribonucleoprotein (RNP) sequences. RNP1 and RNP2 are eight and six amino acids long, respectively, with the RNP1 sequence being more conserved than that of RNP2 (Bandziulis et al., 1989). Structurally, the RRM domain folds to form a four stranded β-sheet with two α-helixes in a βαββαβ arrangement (Hoffman et al., 1991; Nagai et al., 1990; Oubridge et al., 1994). The RNP domains are found on the internal two β-sheets of the RRM structure, and form its main RNA binding surface (Lunde et al., 2007; Oubridge et al., 1994). Each RRM domain can only recognize up to eight nucleotides in the target RNA (Maris et al., 2005; Price et al., 1998). Having one RRM domain thus does not provide a high level of specificity for an RBP regarding RNA targets. In fact, many RBPs have multiple RRM domains and/or other types of RNA binding sequences, significantly increasing their ability to interact with only specific RNA molecules (Auweter et al., 2006). It is important to note that the three dimensional structure of a whole RBP, as well as the individual RNA binding domains within it, plays a role in defining the protein's RNA targets. Large-scale studies predicting RNA-binding sites must thus account for both primary sequence and structural influences in their design (Li et al., 2014).

1.1.2 Function of RBPs

The list of proteins classified as RBPs is still growing, and consequently so are the functions they're associated with (Castello et al., 2016). It is understood that RBPs influence all aspects of RNA metabolism, from transcription to transport, including alternative splicing, translation,

stability and degradation, usually as part of ribonucleoprotein particles (RNPs) (Glisovic et al., 2008). RBPs are, therefore, involved in regulating the nature, quantity and functionality of gene expression products.

RBPs can interact with various types of RNA, including messenger RNA (mRNA) (or pre-mRNA), ribosomal RNA (rRNA), transfer RNA (tRNA), small nuclear RNA (snRNA), short interfering RNA (siRNA), microRNA (miRNA), and long non-coding RNA (lncRNA) (Ferre et al., 2016; Han et al., 2004). These interactions result in varied downstream effects. For instance, DNA-damage response RBPs not only regulate gene expression but also mediate DNA repair (Dutertre and Vagner, 2016). RBPs can also influence cellular processes, such as cell migration and metastasis, *via* interaction with other proteins, like focal adhesion proteins (de Hoog et al., 2004). Some RBPs, such as MRPP2, even have enzymatic activities (Castello et al., 2015). In large part due to next generation sequencing techniques and large screens, new roles for RBPs are still being elucidated and the extent of the influence of RBPs on the regulation of cellular processes is still being unraveled.

It is important to note that one single RBP can itself affect multiple aspects of RNA metabolism. For instance, the RNA binding protein Hu antigen R (HuR) interacts with target mRNAs to (1) stabilize and protect the mRNAs from decay, (2) translationally upregulate their expression, or (3) translationally downregulate their expression (Srikantan and Gorospe, 2012). The effect of HuR on a particular target depends in part on HuR's phosphorylation status at the time of protein-RNA interaction (Popovitchenko et al., 2016; Srikantan and Gorospe, 2012). A HuR related protein, AU-binding factor 1 (AUF1), also affects multiple aspects of RNA metabolism.

For instance, AUF1 can promote mRNA translation and even gene transcription (Aigner et al., 2001; Panda et al., 2014). In this manner, AUF1 regulates myogenesis, muscle regeneration and telomerase activity (Panda et al., 2014; Pont et al., 2012). AUF1 can also promote mRNA stability; AUF1 increases the parathyroid hormone transcript stability, which is in turn responsible for regulating serum calcium levels (Sela-Brown et al., 2000). On the other hand, AUF1 can de-stabilize mRNAs and promote their degradation, such as those for inflammatory cytokines or mRNAs of proteins involved in cell-cycle checkpoints (Pont et al., 2012). AUF1 and HuR thus influence many processes *via* a number of RNA regulatory mechanisms. Understanding that RBPs often have multifaceted roles is, therefore, very important when characterizing the functions of such proteins.

1.1.3 Regulation of RBP expression

As one single RBP can influence many processes, one would anticipate their expression and activity to be tightly regulated. In fact, the expression and activity of RBPs themselves can be modulated at any point from transcription to post-translational modifications. This regulation can result from auto-regulation, or interactions with other RBPs (Buratti and Baralle, 2011; Pullmann et al., 2007).

For instance, members of the Fox family, which include *RBM9* (*Fox-2*), can auto-regulate the alternative splicing of *Fox* mRNA (Damianov and Black, 2010). In fact, Fox proteins inhibit exon inclusion during *Fox* alternative splicing, resulting in a translated variant with reduced RNA binding capabilities (Nakahata and Kawamoto, 2005). This exclusion variant represses

Fox's influence on the alternative splicing of other genes, thus Fox proteins not only autoregulate their alternative splicing, but also their own function (Damianov and Black, 2010).

HuR is another RBP that has multiple levels of regulation. First, *HuR* is transcriptionally regulated by NF-κB. Second, *HuR* mRNA's cytoplasmic export, stabilization and translation are promoted by HuR protein (Pullmann et al., 2007; Yi et al., 2010). Third, additional factors decrease *HuR* translation, such as miR-519 (Abdelmohsen et al., 2010). Finally, HuR's function, stabilization and cytoplasmic localization are controlled post-transcriptionally by a number of factors *via* HuR post-translational modifications such as phosphorylation, methylation and ubiquitination (Srikantan and Gorospe, 2012).

Interestingly, RBPs are key targets for posttranscriptional modifications, including phosphorylation, methylation and acetylation. These changes can impact RBP interaction with RNA targets or other proteins, ultimately influencing function (Blackwell and Ceman, 2012; Thapar, 2015). For instance, phosphorylation of the RNA-binding protein DAZL, an important regulator of spermatogenesis, inhibits its interaction with poly(A)-binding protein, resulting in decreased translation of DAZL RNA targets (Williams et al., 2016). On the other hand, acetylation of KHDRBS1 enhanced its RNA binding activity (Babic et al., 2004). These numerous levels of control highlight the importance of regulated RBP expression and function to normal cellular processes.

1.1.4 Dysregulation of RBPs and disease

Due to their influence on all aspects of RNA metabolism and their strict regulation, it is not surprising that dysregulation of RBPs can have severe downstream consequences. Interestingly, disease-linked mutations can be found within various regions of RBPs, not only specific RNA-binding regions (Castello et al., 2013). RBP mutations can thus impair not only protein-RNA interactions, but also protein-protein interactions, complex formation and enzymatic function – all resulting in impaired RNA metabolism with important downstream consequences (Castello et al., 2013; Lunde et al., 2007).

Altered RBP expression and/or function is associated with a wide spectrum of diseases, but most are of neurological, muscular, sensory or neoplastic origin (Castello et al., 2013; Lukong et al., 2008). As regulation of alternative splicing is controlled by RBPs, and this process occurs at a high rate in the brain and throughout development, these findings are not surprising. The consequences of aberrant RBPs can be as varied as the associated disease. For instance, a point mutation in *Qk1* was embryonically lethal in mice (Justice and Bode, 1988; Shedlovsky et al., 1988). Interestingly, the lethal mutation prevented *Qk1* homodimerization, and did not interfere with RNA binding (Chen and Richard, 1998), suggesting that critical *Qk1* functions are dependent on more than only its ability to bind RNA. In other cases, RBP alterations can have an impact on the capacities of the affected individual. This is the case for Fragile X syndrome, which is the most frequent form of heritable mental retardation (Crawford et al., 2001). Genetically, this syndrome is usually caused by a CGG expansion in the 5’ untranslated region (UTR) of the gene encoding the FMR1 RBP (Garber et al., 2008). The associated phenotypic characteristics depend on the level of methylation of the CG islands in these expansion segments within *FMR1*’s 5’ UTR, with the most severe cognitive impairments presenting in patients with

complete methylation of this region (Garber et al., 2008). Other diseases associated with irregularly expressed RBPs include spinal muscular atrophy, the main monogenic cause of death in infants (Crawford and Pardo, 1996), and TARP syndrome, an abnormal developmental condition usually resulting in death prior to or soon after birth (Johnston et al., 2010). The impact of these RNA binding protein-associated diseases can thus be very serious, once again highlighting the importance of RBPs to numerous aspects of biology at both the cell and organism level.

RBPs also play a very important role in cancer development (Wurth, 2012). As RBPs can influence protein expression levels of oncogenes or tumor suppressors, deregulated RBP expression, as observed in certain cancers, could be key to the establishment of the transformed state (Wurth, 2012). For instance, the expression of the RNA binding protein KHDRBS1 is increased in a number of cancers and promotes the alternative splicing of many cancer-associated genes, including *CD44* and *CCND1*, towards their transformation-promoting variant (Matter et al., 2002; Paronetto et al., 2010; Rajan et al., 2008; Wurth, 2012). In addition, a tumor suppressor, *RBM5*, is downregulated in a variety of cancers (Kim et al., 2010; Miller et al., 2009; Peng et al., 2013; Welling et al., 2002; Zhao et al., 2012). As described below, although some studies have begun to elucidate *RBM5*'s role in the cell and contribution to diseased states, much remains to be determined.

1.2 RBM5

RNA binding motif domain protein, RBM5, is coded for on chromosome 3 at position 3p21.3 and was first cloned by Wei et al in 1996 (Wei et al., 1996) under the name LUCA-15. The *RBM5* transcript is approximately 3 kb, divided into 25 exons, and codes for a protein of 815 amino acids.

1.2.1 *RBM5* alternative splice variants

Alternative splicing dramatically increases the variety of proteins translated from a single primary transcript (pre-mRNA molecule). Although the RNA sequence of these isoforms may be very similar, the resulting proteins can have very distinct properties, such as variations in stability, localization, activity, and protein and RNA partners (Kelemen et al., 2013). *RBM5* is alternatively spliced, and its variants have been quite well characterized. Three *RBM5* alternative splice variants retain introns and are targets for non-sense mediated decay (Sutherland et al., 2005). The truncated proteins for which they code are thus rarely, if ever, translated (Sutherland et al., 2005). These variants are *RBM5Δ6* in which exon 6 is deleted, *RBM5+6* in which intron 6 is retained, and *RBM5+5+6* in which introns 5 and 6 are retained (Maquat and Carmichael, 2001; Sutherland et al., 2000; Sutherland et al., 2005). Interestingly, a truncated form of *RBM5+5+6*, termed *RBM5+5+6t* or Clone 26, is not degraded by non-sense mediated decay and encodes a protein product of approximately 21 kDa (Masilamani et al., 2012). This is likely due to splicing of intron 5 from the *RBM5+5+6t* transcript (Rintala-Maki and Sutherland, 2009). Finally, an antisense transcript of *RBM5* is also transcribed. Originally, this transcript was

thought to be only 326 bp and span from introns 6 to 5 (*Je2*) (Sutherland et al., 2000); however, it was later discovered that the transcript codes all the way into intron 4 (including intron 5) of *RBM5*. This transcript was termed *LUST*, for LUCA-15-specific transcript (Rintala-Maki and Sutherland, 2009). Interestingly, one study showed opposing roles for Clone 26 and *Je2* in regards to apoptosis sensitization; therefore, the alternative splicing of RBM5 may have important functional consequences (Sutherland et al., 2000).

1.2.2 Primary structure

Proteins translated from alternative splice variants will have different primary structures. Primary structure is important as it controls higher order structures, and is used to identify consensus functional motifs. Many of these consensus functional motifs encode RNA binding domains. *RBM5* codes for two RRM domains, through which RNA binding and regulation of alternative splicing can occur (Figure 1) (Song et al., 2012). RBM5 also has two zinc finger motifs, one C2H2-type and one RanBP2-type. The former can bind both DNA and RNA, and may be particularly important for protein-protein interactions (Brayer et al., 2008), while the latter has been shown to directly interact with pre-mRNA and regulate alternative splicing (Loughlin et al., 2009). Other RBM5 consensus functional motifs include: (1) an OCRE domain that may influence splicing regulation (Bonnal et al., 2008; Callebaut and Mornon, 2005), (2) two bipartite nuclear localization signals, (3) an arginine-rich N-terminal domain that can directly bind RNA and regulate/influence RNA binding capabilities, and direct proteins to specific nuclear locations involved in splicing (Bayer et al., 2005; Li and Bingham, 1991), and (4) a G-patch domain that may be involved in RNA processing, as it is commonly found in RNA binding proteins (Aravind

and Koonin, 1999; Banerjee et al., 2015). These motifs predict the RNA binding and alternative splicing modulatory capabilities of RBM5. As many of these motifs are lost upon alternative splicing of RBM5, this may be one means of regulating RBM5's RNA binding capabilities.

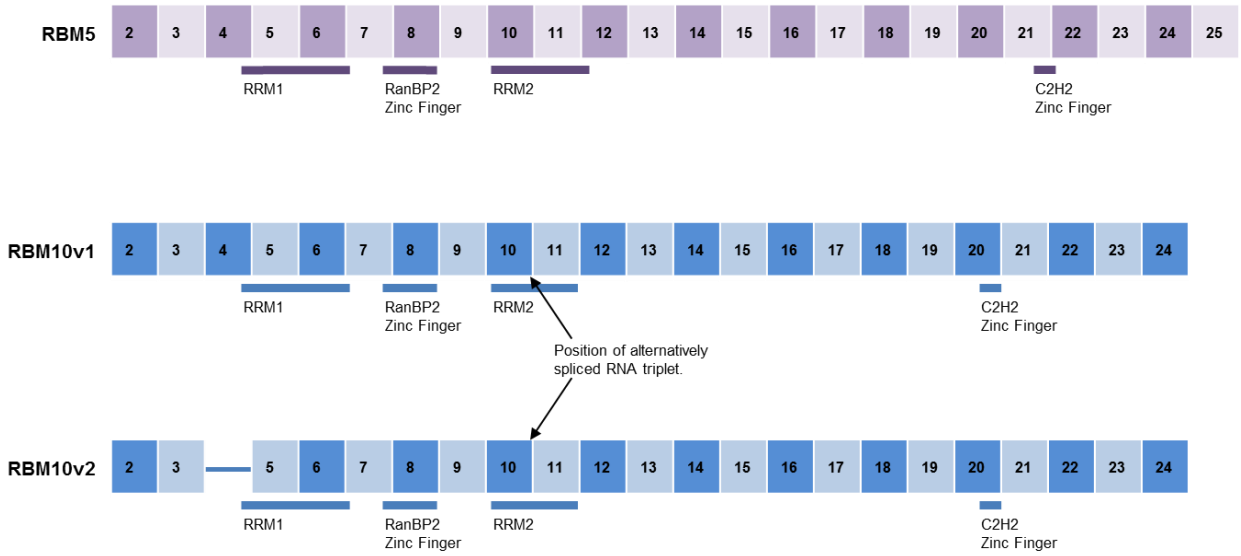

Figure 1.1: RBM5 and RBM10 RNA binding domains. Translated RBM5 and RBM10 exons are represented by boxes. Numbers indicated within a box designates the exon it represents within the corresponding transcript. Box size does not represent exon length. Location of RBM5 and RBM10 RNA binding domains are indicated by the thick line under the corresponding exon(s) boxes, and the type of RNA binding domain is indicated underneath. Arrows point to the location of the alternatively spliced RNA triplet in RBM10v1 and RBM10v2, which results in the +/- valine variants of RBM10v1 and RBM10v2.

1.2.3 Function

As mentioned, the function of RBPs can often be multifaceted. Functional studies regarding RBM5, however, have focused on the full-length variant, and its effect on apoptosis and cell cycle arrest. For instance, *RBM5* overexpression in a human leukemic cell line altered the expression of 35 apoptosis and proliferation-associated genes (Mourtada-Maarabouni et al., 2006) and arrested cells in the G1 cell cycle phase (Mourtada-Maarabouni et al., 2003). Cell

cycle arrest was also associated with *RBM5* overexpression in a prostate cancer and a fibrosarcoma cell line (Edamatsu et al., 2000; Zhao et al., 2012). *RBM5*'s role in apoptosis promotion has been demonstrated in a number of cell lines, including breast, lymphoblastoid and prostate cancer cell lines. This increase in apoptosis was also shown to occur when apoptosis was triggered by either Fas, TNFα or TRAIL; the ligands of all three main death receptors (Rintala-Maki and Sutherland, 2004; Sutherland et al., 2000; Zhao et al., 2012). Furthermore, fibroblast xenografts showed a significant reduction in growth when *RBM5* was expressed (Oh et al., 2002). RBM5 can thus modulate the cell cycle and apoptosis in a number of different human cell lines, both cancerous and non-transformed, however, the potential impact of RBM5 on other cellular processes remains to be determined.

RBM5 may play a particularly important role in cells which line the lower respiratory tract. This is suggested by its 70-95% downregulation in lung cancer, of which there are two main types; non-small cell lung cancer (NSCLC) and small cell lung cancer (SCLC) (Travis W.D., 2004). In fact, *RBM5* is encoded within a region called the human lung tumor suppressor locus (Wei et al., 1996), as deletions within this region of the short arm of chromosome 3 (3p21.3) are the earliest and most frequent genetic alterations observed in lung cancers (Hung et al., 1995; Lerman and Minna, 2000; Wistuba et al., 2000). In line with this, *RBM5* is deleted in various lung cancer cell lines (Lerman and Minna, 2000). In patient lung tumors, however, *RBM5* is still expressed (Wistuba et al., 2000), although significantly downregulated (Liang et al., 2012; Oh et al., 2002; Shao et al., 2012). Taken together, these findings suggest that downregulation of *RBM5* may be a key step in lung cancer development and/or progression. Only three studies have investigated *RBM5*'s role in lung cancer cells. In the first study, undertaken by Oh *et al.* in 2006, investigators

overexpressed *RBM5* in an NSCLC cell line (A549) and found that increased RBM5 expression was associated with promotion of apoptosis and G1 cell cycle arrest (Oh et al., 2006). They also showed that *RBM5* expression slowed xenograft tumor growth (Oh et al., 2006). In 2011, Kobayashi *et al.* showed that *RBM5* expression in the H1299 NSCLC cell line inhibited cell growth by both p53-dependent and independent mechanisms (Kobayashi et al., 2011). Finally, Shao *et al.* showed that *RBM5* overexpression in A549 cells promoted apoptosis, and that injections of bacteria carrying the RBM5 plasmid decreased xenograft tumor size (Shao et al., 2012). These studies support a tumor suppressive role for RBM5 in NSCLC. The role of RBM5 in SCLC, however, has yet to be determined. The majority of the work presented herein was thus performed in a SCLC-derived cell line. Results thus not only expand our knowledge of RBM5 function, but also shed light on the molecular basis of SCLC.

1.2.4 Mechanism of action

The primary structure of RBM5 suggests RNA binding capabilities. Identification of all RNAs bound by RBM5 could thus give important insight into the scope of RBM5's influence in the cell. Prior to commencing my doctoral studies, an RNA binding consensus sequence targeted by RBM5 had yet to be determined. A few studies, however, characterized the binding capabilities of individual RBM5 RNA binding domains. For instance, the RRM2 of RBM5 preferentially bound CU and GA rich sequences (Song et al., 2012). Furthermore, RBM5's RanBP2-type zinc finger had an affinity for the GGU motif (Nguyen et al., 2011). Three direct RBM5 RNA targets had also been confirmed in human cell lines, and RBM5 regulated alternative splicing in all three instances; caspase-2 (*CASP2*) mRNA (Fushimi et al., 2008), activation induced cytidine

deaminase (*AID*) mRNA (Jin et al., 2012) and Fas antisense transcript 1 (*FAS-AS1*), a lncRNA (Sehgal et al., 2014). In regards to the *CASP2* transcript, RBM5 promoted exon 9 exclusion, and thus higher levels of the proapoptotic form of caspase-2, by binding to the UC-rich region in intron 9 (Fushimi et al., 2008). In *AID*, RBM5 promoted exon 4 exclusion and consequently a truncated protein product, by binding to the pyrimidine tract in intron 3 (Jin et al., 2012). RBM5's binding to the lncRNA *FAS-AS1*, however, did not influence the alternative splicing of *FAS-AS1* itself, but rather inhibited RBM5's ability to alternatively splice another transcript (Bonnal et al., 2008; Sehgal et al., 2014). Interestingly, 11 direct RBM5 mRNA targets have been identified in mouse spermatid differentiation (O'Bryan et al., 2013). In addition, RBM5 was shown to influence the alternative splicing of two other transcripts, although direct protein-RNA interactions have yet to be established in this regard: (1) *c-FLIP*, for which RBM5 promoted exon 7 exclusion, and thus higher levels of the apoptosis regulating form (Bonnal et al., 2008; Chang et al., 2002), and (2) *DMD*, for which RBM5 influenced exons 40 and 72 skipping (O'Leary et al., 2009). Taken together, these findings suggest that RBM5's regulation of alternative splicing is important in both cancer and development, and that the downstream effects can vary depending on the system.

Supporting its role as a regulator of alternative splicing, RBM5 was first shown to be a component of prespliceosomal complexes by Hartmuth *et al.* (Hartmuth et al., 2002). More specifically, immunoprecipitation of spliceosomal complexes A and B identified RBM5 as a component of only spliceosomal complex A, and not B (Behzadnia et al., 2007; Deckert et al., 2006). These results suggest a role for RBM5 in the early steps of alternative splicing. Isolation of other factors involved in splicing showed that RBM5 also interacted with (a) the splicing

factor U2AF^{65} (Bonnal et al., 2008) and (b) the spliceosomal complex component DHX15, resulting in stimulation of its helicase activity (Niu et al., 2012). RBM5 thus directly participates in the regulation of alternative splicing, and interacts with many spliceosomal components.

1.2.5 Expression and regulation

RBM5 is ubiquitously expressed in human non-tumor tissues and cell lines (Sutherland et al., 2000; Timmer et al., 1999b). *RBM5* expression, however, is decreased in many cancers, including vestibular schwannomas (Welling et al., 2002), biliary tract cancers (Miller et al., 2009), stage III serous ovarian carcinoma (Kim et al., 2010), prostate cancer (Zhao et al., 2012), and pancreatic cancer (Peng et al., 2013). In fact, *RBM5* was one of nine genes downregulated within a 17 gene signature associated with metastasis in human (Ramaswamy et al., 2003) and murine (Qiu et al., 2004) solid tumors. These expression studies strongly suggest a tumor suppressor activity for *RBM5* across various tumor types.

Little is known about the regulation of *RBM5*, and thus how its expression is modulated in these various cancerous states. In regard to transcriptional regulation, the promoter region of *RBM5* has been shown to be mutated in melanomas (Smith et al., 2015), but not hypermethylated, at least in lung cancers (Oh et al., 2008). In addition, a Ras mutant, Ras(G12V), influenced *RBM5* expression, although the exact mechanism involved remains to be determined (Edamatsu et al., 2000). Ras is a guanine exchange factor involved in signal transduction, ultimately controlling processes such as the cell cycle and cell death (Khosravi-Far and Der, 1994). Ras(G12V), a constitutively active Ras mutant, downregulated *RBM5* expression, and thus Ras' promotion of

cell growth and survival may, in part, be accomplished *via* modulation of *RBM5* expression (Edamatsu et al., 2000). In regard to posttranscriptional modifications, RBM5 has only been shown to be phosphorylated (Rintala-Maki et al., 2007). This phosphorylation was dependent on the presence of growth factors, and was reversible, suggesting phosphorylation of RBM5 may regulate its apoptotic functions (Shu et al., 2007). Additional studies are required to gain a complete understanding of the factors that regulate *RBM5* expression.

RBM5 shares a high degree of homology with another RNA binding motif domain protein, RBM10. In fact, at the protein level this similarity is approximately 50% (Sutherland et al., 2005). It has been suggested that the duplication of similar functioning genes to different genomic locations, such as 3p21.3 (*RBM5*) and Xp11.23 (*RBM10*), could be an evolutionary means of both expanding gene expression and providing an additional level of regulation (Timmer et al., 1999a). The study described herein also included an examination of *RBM10*, to determine if *RBM5* and *RBM10* do in fact have similar functions, and if they interact or influence each other's function.

1.3 RBM10

RBM10 is coded for on the X-chromosome at position p11.23 (Coleman et al., 1996; Thiselton et al., 2002) and was first cloned from bone marrow in 1995 (Nagase et al., 1995). The full length *RBM10* transcript is approximately 3.5 kb long, divided into 24 exons, and translated into a protein of 930 amino acids (Johnston et al., 2010).

1.3.1 Alternative splice variants

Like 95% of multi-exon containing transcripts (Pan et al., 2008), *RBM10* can be alternatively spliced. The main *RBM10* alternative splice variant, *RBM10v2,* is produced by alternatively splicing the fourth exon from *RBM10,* resulting in a protein of 853 amino acids (Johnston et al., 2010; Sutherland et al., 2005). As depicted in Figure 1, the alternative splicing of exon 4 of *RBM10* does not alter the number of RNA binding domains. It would be likely, however, to impact *RBM10*'s overall protein structure and could thus alter function, as discussed above.

The level of homology between RBM5 and RBM10 is approximately 50%, with RBM10v1 sharing 49% identity with RBM5, and RBM10v2 sharing 53% (Sutherland et al., 2005). Exons 4, 9 and 15 are particularly different between *RBM5* and *RBM10* and are the main cause of the variation between both proteins (Sutherland et al., 2005). Of note, these non-homologous exons are located right before consensus functional motifs, suggesting similar functionality for *RBM5* and *RBM10,* but potentially different specificity.

1.3.2 Primary structure

Like RBM5, RBM10 contains a number of consensus functional motifs. These include two RRM domains, an OCRE domain and a G-patch domain, all involved in RNA binding and/or regulation of alternative splicing (Inoue et al., 1996; Sutherland et al., 2005). The OCRE domain has also been suggested to have nuclear localization abilities, along with the two other nuclear localization signals present within the RBM10 sequence (Inoue et al., 2008; Xiao et al., 2013). In addition, RBM10 has two zing finger motifs, one C2H2-type and one RanBP2-type, similar to

RBM5. The presence of these motifs suggests that RBM10 may, like RBM5, bind RNA and affect which alternative variants are expressed.

1.3.3 Function

Functionally, RBM10 has been much less studied than RBM5, but again, most studies have centered on a role involving apoptosis promotion and cell cycle arrest. In fact, the first functional study published regarding RBM10 correlated *RBM10* expression with decreased cell proliferation and increased apoptosis in hypertrophic primary chondrocytes (James et al., 2007). In 2012, our group confirmed that RBM10 promoted apoptosis in two human cancer cell lines, and associated increased RBM10 expression with increased TNFα transcription (Wang et al., 2012). Notably, as knockdown of only RBM5 or RBM10 has significant effects, both proteins do not functionally compensate for each other. Correlational studies from human tissues support an apoptosis-promoting role for RBM10, as *RBM10* mRNA expression in breast cancer samples correlated with increased mRNA expression of BAX, a proapoptotic protein, and p53, a tumor suppressor with transcriptional activity (Martinez-Arribas et al., 2006). Unexpectedly, however, this study also correlated *RBM10* expression with increased mRNA expression of *VEGF*, a potent promoter of angiogenesis (Martinez-Arribas et al., 2006). These findings suggest a tumor suppressor role for *RBM10*, but that additional studies are required to more clearly understand how this role is achieved.

1.3.4 Mechanism of action

The primary sequence of RBM10 suggests RNA binding and alternative splicing capabilities. No direct RBM10 RNA targets, however, had been identified prior to the start of this research project. In addition, RBM10 had not yet been shown to modulate the alternative splicing of any transcript. Interestingly, the rat equivalent of RBM10, S1-1, bound poly(G) and poly(U) RNA homopolymers (Inoue et al., 1996). S1-1 also bound the 3'UTR of the angiotensin receptor type 1 (*AT-1*) transcript and increased the transcript's stability, ultimately leading to downregulation of its transcription (Mueller et al., 2009). At the amino acid level, RBM10v1 and v2 share an 85 and 96% identity with S1-1, respectively, suggesting similar functionality (Sutherland et al., 2005). RBM10 may thus have an affinity for poly(G) and (U) motifs, and its binding may post-transcriptionally influence RNA expression.

Protein-protein interaction studies support a regulatory role for *RBM10* in alternative splicing. For instance, immunoprecipitation of spliceosomal complexes identified RBM10 as a component of spliceosomal complexes A and B (Behzadnia et al., 2007; Deckert et al., 2006; Rappsilber et al., 2002). Interestingly, RBM10 also interacted with the 2A-DUB deubiquitinase protein complex, which influences histone modifications (Zhu et al., 2007). RBM10 may, therefore, also epigenetically regulate gene transcription through changes in the posttranslational modification of histones. Taken together, these results suggest that RBM10 may, like many RBPs, influence various aspects of RNA metabolism and highlights that a lot remains to be determined regarding how RBM10 exerts its potential tumor suppressor properties.

1.3.5 Expression and regulation

RBM10 is expressed at levels marginally lower than RBM5 in most, if not all, human cells (GeneCards data), even though one *RBM10* allele is silenced due to X chromosome inactivation (Coleman et al., 1996; Thiselton et al., 2002). *RBM10* expression is especially important during development, as *RBM10* mutations are the cause of TARP syndrome (Gorlin et al., 1970; Johnston et al., 2010). This condition is characterized by many developmental abnormalities, particularly craniofacial deformities such as cleft palate, glossoptosis (tongue displacement) and micrognathia (undersized jaw), which can cause difficulties eating and breathing (Gorlin et al., 1970). Sadly, usually due to various heart conditions associated with the disease, the affected children die before, or soon after, birth (Gorlin et al., 1970; Gripp et al., 2011; Johnston et al., 2010). If significant medical attention is provided, however, there have been reports of children with TARP syndrome living up to three years (Gripp et al., 2011). These cases have permitted doctors to observe other phenotypic consequences of embryonic *RBM10* mutations, including chronic lung disease, visual impairment, significant intellectual disability and an inability to eat or sit independently (Gripp et al., 2011). The severe impact of *RBM10* mutations in these children strongly suggests a critical role for *RBM10* in fetal development. This is supported by my recent findings showing RBM10 expression to be regulated during rat skeletal and cardiac muscle cell differentiation (Loiselle and Sutherland, 2014). Interestingly, the only post-transcriptional modification identified regarding RBM10 was its phosphorylation by c-Src tyrosine kinase (Amanchy et al., 2008). Furthermore, this phosphorylation event was shown to be part of the platelet derived growth factor (PDGF) signaling pathway, an important regulator of cell differentiation and disease, further suggesting the importance of RBM10 to normal development (Amanchy et al., 2008; Heldin et al., 1998).

Unlike *RBM5, RBM10* expression is not significantly altered in cancer. Likely for this reason, the regulation of *RBM10* expression has yet to be studied. *RBM10*, however, is mutated in select cancer types. For instance, *RBM10* was found to be truncated in 7% of lung adenocarcinomas (Imielinski et al., 2012), and had a frameshift mutation in pancreatic intraductal papillary mucinous neoplasms (Furukawa et al., 2011). Despite this, in a mutational screen of 441 tumors of various cancer types including breast, pancreatic and lung, only one breast and one prostate cancer sample, respectively, had an *RBM10* mutation (Kan et al., 2010). The importance of functional *RBM10* in regards to the transformed state, therefore, remains to be determined.

1.4 Study objectives

1.4.1 Overview

RNA binding proteins regulate all aspects of RNA metabolism, and their dysregulation can have fatal consequences. Elucidating the broad and often multifaceted roles of specific RNA binding proteins will help us to better understand their influence on cellular processes, and thus how the associated pathways are regulated. Together with a better comprehension of the regulation of RBPs, studies in this area may contribute to the development of therapeutic options aimed at restoring or modifying RBP expression in diseases associated with their aberrant expression.

1.4.2 Hypothesis

RBPs often have multifaceted functions. Functional data relating to *RBM5* and *RBM10*, however, have been largely limited to their abilities to promote cell cycle arrest and apoptosis. Through the regulation of these processes, RBM5 and RBM10 can modulate cancer cell division and death. *RBM5* and *RBM10* expression is key for proper development, since (1) mutations in *RBM10* are the causative agent of TARP syndrome (Johnston et al., 2010), (2) *RBM5* is an important splicing factor in spermatid differentiation (O'Bryan et al., 2013), and (3) my master's thesis work determined that *RBM5* and *RBM10* expression is regulated during rat myoblast differentiation (Loiselle and Sutherland, 2014). Of note, cell cycle arrest and apoptosis are essential processes involved in differentiation (Andres and Walsh, 1996; Sandri and Carraro, 1999; Walsh and Perlman, 1997; Wang and Walsh, 1996; Yahi et al., 2006), therefore, it may be *via* the control of these processes that *RBM5* and *RBM10* influence differentiation. In fact, cell cycle arrest and apoptosis are crucial processes involved in a number of complex events, such as epithelial to mesenchymal transition (EMT) and angiogenesis. Consistent with this view, apoptotic resistance is important to EMT initiation (Franco et al., 2010; Savagner, 2010; Valdes et al., 2002), and endothelial cell proliferation and apoptosis are essential for proper angiogenesis (Savagner, 2010). To summarise, RBM5 and RBM10 have been shown to influence the processes of apoptosis and cell cycle, and the event of differentiation. Entering into this study, I **hypothesized** that processes influenced by changes in RBM5 and RBM10 expression are not limited to apoptosis and cell cycle regulation. I also **hypothesized** that RBM5 and RBM10 influence many events in addition to differentiation. Finally, based on their structural similarities, I **hypothesized** some overlap in functional roles for RBM5 and RBM10.

1.4.3 Objectives

Based on these hypotheses, my **objectives** were to **(1)** identify all cellular processes and events enriched by changes in RBM5 and/or RBM10 expression in a particular cultured cell line, and **(2)** to determine the extent of functional overlap for RBM5 and RBM10 in these cells.

To accomplish the first objective, I had three specific aims: (1) to identify RBM5 and RBM10 direct mRNA targets using RNA immunoprecipitation followed by next generation sequencing (RIP-Seq), (2) to identify genes whose expression and/or alternative splicing was altered by changes in RBM5 or RBM10 expression using RNA-Seq, and (3) to determine processes and events influenced by RBM5 and RBM10, by carrying out functional analyses on the above RIP-Seq and RNA-Seq data from Aims 1 and 2.

To accomplish the second objective, I aimed to compare RBM5 and RBM10 targets and downstream effects. To do this, I compared RBM5 and RBM10 RIP-Seq and RNA-Seq results, at both the gene expression and process/event level.

1.4.4 Rationalization for models and techniques

Many factors come into play when choosing an *in vitro* model. One of the most important features is the suitability of the system for the project at hand. As we aimed to perform target identification studies, a system with null levels of *RBM5* or *RBM10* would be optimal since it would provide a wild-type (endogenously unaltered) negative control. Another factor to consider is clinical relevance. As mentioned, *RBM5* is downregulated in 95% of SCLCs, and *RBM10* is

mutated in approximately 7% of lung cancers (Imielinski et al., 2012; Network, 2014). The impact of this downregulation and mutation, respectively, however, remains to be determined. With a survival rate of only about 5%, it is clear that a better understanding of the molecular mechanisms underlying SCLC is required (Lee et al., 2006; Lekic et al., 2012; Micke et al., 2002). Examining RBM5 and RBM10 function in a SCLC system would thus provide meaningful insight into how altered expression of RBM5 or RBM10 might impact SCLC development and progression. The GLC20 cell line filled both of these criteria; it is a SCLC cell line with a homozygous deletion of RBM5. This system presented, therefore, an appropriate model for aggressive SCLC and provided optimal experimental conditions for RBM5 target identification studies. The parental GLC20 cell line was established from the tumor of a male SCLC patient that showed no clinical response to a treatment regimen of cyclophosphamide, doxorubicin and vincristine (Smit et al., 1992). Five stable GLC20 sublines were established by various members of the Sutherland lab, each with particular levels of *RBM5* and *RBM10* expression, respectively. Table 1.1 summarizes the GLC20 sublines used in this study.

Table 1.1: GLC20 sublines used throughout this body of work.

GLC20 subline	Stably transfected plasmid or shRNA	*RBM5* expression (FPKM)	*RBM10* expression (FPKM)	Origin
pcDNA3	pcDNA3	0 (endogenous)	47 (endogenous)	Pooled population
T2	pcDNA3.RBM5	58 (overexpressed)	49 (endogenous)	Pooled population
C4	pcDNA3.RBM5	388 (overexpressed)	52 (endogenous)	Clonal population
G300.3	Hush 300 (control shRNA)	0 (endogenous)	55 (endogenous)	Clonal population
G29/30.4	Hush 29 and Hush 30 (target RBM10 exon 6)	0 (endogenous)	43 (knockdown)	Clonal population

Fragments Per Kilobase of transcript per Million mapped reads (FPKM) values represent RNA expression levels, as determined by RNA-Seq.

Using this SCLC model, we set out to assemble a comprehensive list of RBM5 and RBM10 mRNA targets. To this end, I used RIP-Seq. This technique provides the nucleotide sequence of all mRNA molecules within a cell that are associated with the protein of interest. This level of resolution allows researchers to identify the exact splice variant of a gene with which their protein of interest interacts. The first step of RIP-Seq involves identification of an antibody specific for the protein of interest. With this antibody, the protein of interest is immunoprecipitated, then all associated mRNAs are sequenced using next generation sequencing techniques. It is important to note that existing protein-protein interactions within the cell, of the protein of interest and any potentially complexed proteins, are not broken during this procedure. All mRNAs associated directly with the protein of interest, or associated with it *via* another protein, would therefore be detected. As RBM5 and RBM10 are both components of spliceosomal complexes (Behzadnia et al., 2007; Deckert et al., 2006; Rappsilber et al., 2002), this technique was anticipated to minimally identify all transcripts whose alternative splicing

may be influenced by RNP complexes containing RBM5 and RBM10. For these reasons, RIP-Seq was anticipated to provide the most comprehensive list of RBM5 and RBM10 mRNA targets, and thus the best ability to distinguish direct mRNA targets for RBM5 and RBM10, from indirect effects of their modulated expression.

Following mRNA target identification, we set out to determine all processes/events affected by changes in *RBM5* and *RBM10* expression levels. Many techniques available are biased in that they are directed towards particular cellular processes, such as apoptosis, proliferation, mitochondrial activity or cell cycle arrest. In order to capture all processes influenced by *RBM5* and *RBM10*, I performed RNA-Seq on our GLC20 sublines. RNA-Seq provides a single nucleotide resolution snapshot of all transcripts present within a cell. I was, therefore, able to identify the differences in gene expression and alternative splicing amongst the isogenic sublines, and consequently gained a comprehensive view of influenced processes and events, through an analysis of altered signaling pathways.

Extending findings from a transformed system to a non-transformed system broadens the importance of an observed phenomenon. We, therefore, decided to extend our research past our SCLC-model, to determine if any potential RBM5/RBM10 relationship was restricted to transformed state. The non-transformed model chosen involved H9c2 rat myoblasts. This particular model was selected since both RBM5 and RBM10 had been previously suggested to be important to H9c2 differentiation (Loiselle and Sutherland, 2014). In addition, apoptosis, cell cycle arrest and alternative splicing, all processes previously associated with RBM5 and/or RBM10, are key to muscle cell differentiation (Andres and Walsh, 1996; Revil et al., 2010;

Sandri and Carraro, 1999; Walsh and Perlman, 1997; Wang and Walsh, 1996; Yahi et al., 2006). Finally, *RBM5* and *RBM10* are expressed in a number of tissues types, including muscle, further suggesting they may be important to muscle cells as well as non-transformed cells in general (Coleman et al., 1996; Loiselle and Sutherland, 2014; Timmer et al., 1999b).

1.4.5 Chapter 2

Although alternative splice variants are transcribed from the same gene, their effects in cells can be completely opposite. It is, therefore, important to know which splice variants of a gene are expressed within a system prior to undertaking functional studies. To this end, our first step was to clearly define which *RBM5* and *RBM10* alternative splice variants were present in our SCLC GLC20 model. As GLC20 cells are endogenously *RBM5*-null, all *RBM5* transcripts expressed would necessarily derive from the exogenous, intron-less *RBM5* wildtype cDNA sequence introduced. In regards to *RBM10*, both main *RBM10* splice variants, *RBM10v1* and *RBM10v2*, had been previously well characterised (Sutherland et al., 2005). It remained unclear, however, if both *RBM10v1* and *RBM10v2* had an additional variant differing by only one amino acid. Furthermore, if these variants did exist, it remained to be determined whether or not it was the result of an *RBM10* allele mutation or alternative splicing. To this end, in Chapter 2, we performed a comprehensive analysis regarding the alternative splicing of *RBM10*. Using GLC20 cells, we demonstrated that there were two full-length *RBM10v1* and *RBM10v2* splice variants, respectively, differing by the presence or absence of only one valine residue ((+/-) valine) (Figure 1). In addition, we showed that these variants were the result of alternative splicing, not mutations in *RBM10* alleles. In this chapter, we also explored the functional implications of these

(+/-) valine RBM10 isoforms, using protein modeling and gene expression data. Taken together, this work was the first to demonstrate that both *RBM10v1* and *RBM10v2* have (+/-) valine variants, and that these variants are the result of alternative splicing. Our data suggest that the presence of the valine residue can impact the helical structure of RBM10's RRM2 domain, possibly affection its RNA binding ability.

1.4.6 Chapters 3 & 4

Having characterized *RBM10* splice variants in the GLC20 cell line, I went on to the main objectives of my doctoral studies: **(1)** identify all cellular processes and events enriched by changes in RBM5 and/or RBM10 expression in a particular cultured cell line, and **(2)** to determine the extent of functional overlap for RBM5 and RBM10 in these cells. To capture potential new roles for RBM5 and RBM10, next generation sequencing techniques were used; mRNA targets were identified using RIP-Seq, and potential processes and events altered by these proteins were discovered using RNA-Seq (some of which were confirmed using selected targeted functional assays). Results for RBM5 and RBM10, respectively, were then compared to evaluate the degree, and potential significance, of any overlapping roles. An important relationship between RBM5 and RBM10 was also evaluated, as described in Chapter 4. In addition, in Chapter 3, the clinical significance of *RBM5* downregulation to SCLC was evaluated in terms of chemotherapy, sensitivity and the similarity between RBM5-altered pathways and those modified in tumors from SCLC patients. As GLC20 cells show some drug resistance, but are still able to undergo death upon exposure to cisplatin (Figure 3.2), they were deemed to be an appropriate model for specific drug-sensitization studies. In all, this work is the first

comprehensive analysis of processes altered by RBM5 and RBM10 expression, and provides a comprehensive list of their mRNA targets in a SCLC cell line. These manuscripts also show RBM5 directly regulates RBM10 function, and a working model is presented that describes this relationship and its functional consequences.

1.4.7 Chapter 5

Having discovered a significant relationship between RBM5 and RBM10 in the GLC20 SCLC cells, we extended our research past cancer cell lines to determine if any potential RBM5/RBM10 relationship was restricted to the transformed state, or if it was a more general phenomenon across cell types, species, and transformation-status. Non-transformed H9c2 rat myoblasts were used for the reasons described above. We determined that *RBM5* expression was post-transcriptionally regulated in rat myoblasts and that *RBM10* expression was influenced by the expression levels of *RBM5*. A model describing this regulation was proposed. This work is the first to describe the post-transcriptional regulation of *RBM5* in a non-transformed system, as well as show a relationship between RBM5 and RBM10 outside of tumor cells.

1.4.8 Impact statement

A single RBP can influence RNA metabolism in a variety of ways, and consequently have multiple downstream effects. It is, therefore, critical to elucidate the wide range of processes each RBP can potentially influence when determining an RBP's role(s) and function(s). Together, this knowledge would help to better understand pathway regulation and potential pathway-linkages. The body of work presented in this dissertation is the first comprehensive

analysis of the roles and relationship of two related RBPs, RBM5 and RBM10. I show not only potential pathways they influence, both directly and as a downstream consequence of their expression, but also the complex functional associations between these two proteins in transformed and non-transformed cells. The particularly significant regulation of RBM10 by RBM5, discovered and described in this work, truly highlights the complexity of RNA metabolism, and pathway regulation. Understanding the scope of function of RBM5 and RBM10 not only helps to continue to evolve our knowledge of RNA binding proteins in general, but also to gain comprehensive insight into the impact of their downregulation and mutation in various disease states such as SCLC.

Chapter 2

2 Insights into the role of alternative splicing within the RBM10v1 exon 10 tandem donor site

Tessier SJ, Loiselle JJ, McBain A, Pullen C, Koenderink BW, Roy JG and Sutherland LC. (2015) *Insight into the role of alternative splicing within the RBM10v1 exon 10 tandem donor site.* **BMC Research Notes**. **8**(46).

Full text, open access document can be accessed through the journal's website:
https://bmcresnotes.biomedcentral.com/articles/10.1186/s13104-015-0983-5

Tessier et al. BMC Research Notes (2015) 8:46
DOI 10.1186/s13104-015-0983-5

BMC Research Notes

SHORTREPORT Open Access

Insight into the role of alternative splicing within the RBM10v1 exon 10 tandem donor site

Sarah J Tessier[1], Julie J Loiselle[2], Anne McBain[3], Celine Pullen[1], Benjamin W Koenderink[4], Justin G Roy[5] and Leslie C Sutherland[1,2,4,5,6,7*]

Abstract

Background: RBM10 is an RNA binding protein involved in the regulation of transcription, alternative splicing and message stabilization. Mutations in RBM10, which maps to the X chromosome, are associated with TARP syndrome, lung and pancreatic cancers. Two predominant isoforms of RBM10 exist, RBM10v1 and RBM10v2. Both variants have alternate isoforms that differ by one valine residue, at amino acid 354 (RBM10v1) or 277 (RBM10v2). It was recently observed that a novel point mutation at amino acid 354 of RBM10v1, replacing valine with glutamic acid, correlated with preferential expression of an exon 11 inclusion variant of the proliferation regulatory protein NUMB, which is upregulated in lung cancer.

Findings: We demonstrate, using the GLC20 male-derived small cell lung cancer cell line - confirmed to have only one X chromosome - that the two (+/−) valine isoforms of RBM10v1 and RBM10v2 result from alternative splicing. Protein modeling of the RNA Recognition Motif (RRM) within which the alteration occurs, shows that the presence of valine inhibits the formation of one of the two α-helices associated with RRM tertiary structure, whereas the absence of valine supports the α-helical configuration. We then show 2-fold elevated expression of the transcripts encoding the minus valine RBM10v1 isoform in GLC20 cells, compared to those encoding the plus valine isoform. This expression correlates with preferential expression of the lung cancer-associated NUMB exon 11 inclusion variant.

Conclusions: Our observations suggest that the ability of RBM10v1 to regulate alternative splicing depends, at least in part, on a structural alteration within the second RRM domain, which influences whether RBM10v1 functions to support or repress splicing. A model is presented.

Keywords: RBM10, RNA binding protein, RRM, Alternative splicing, Regulation, NUMB

* Correspondence: lsutherland@amric.ca
[1]Department of Biology, Laurentian University, 935 Ramsey Lake Road, Sudbury, ON P3E 2C6, Canada
[2]Biomolecular Sciences Program, Laurentian University, 935 Ramsey Lake Road, Sudbury, ON P3E 2C6, Canada
Full list of author information is available at the end of the article

Acknowledgements: The authors would like to dedicate this manuscript to Charles Buys, Professor Emeritus, University of Groningen, who passed away earlier this year. Professor Buys provided the GLC20 cell line for this study. Work was funded by NSERC Grant # 9043429 to L.C.S., the Northern Cancer Foundation and the Northeastern Ontario Cancer Therapeutics Research Initiative (CTRI).

2.1 Introduction

The RNA binding protein RBM10 is capable of regulating the expression of a number of genes including some involved in apoptosis (e.g., FASR) [1] and cell proliferation (e.g., NUMB) [2]. In all of the reported cases but one, this expression regulation takes the form of alternative splicing regulation [1-4]. The one gene whose expression is not regulated by RBM10-mediated alternative splicing is the angiotensin receptor 1 (AT1), where RBM10 influences AT1 expression by binding within the transcript's 3′-untranslated region (UTR), stabilising the message and subsequently contributing to a decreased rate of transcription [4]. How RBM10 accomplishes these disparate functions remains to be determined.

The region(s) within the RBM10 protein that is involved in any of the RNA-protein interactions identified to date has not been defined although it likely involves at least one of two RNA Recognition Motifs (RRM) and two zinc fingers (ZnF) [5]. On the other hand, two consensus motifs within the target RNA with which the RBM10 protein binds have been defined as CUCUGAA CUC and CGAUCCCU [2]. Using HeLa cells, Bechara et al. [2] reported that RBM10 interactions occurred predominantly within the upstream intron of an excluded alternate exon but predominantly downstream of an included alternate exon. On the other hand, using HEK293 cells, Wang et al. [3] reported that RBM10 interactions occurred in the vicinity of the 5′- and 3′-splice sites within both the upstream and downstream introns of alternate exons, though predominant binding in the vicinity of the upstream 3′-splice site was associated with less exon skipping. Obviously, much remains to be elucidated concerning the regulation of these interactions.

Mutations in *RBM10* have been noted in cells associated with lung and pancreatic cancers and the neuromuscular disorder TARP syndrome [3,6-10] (summarized in Table 2.1). In one lung study, 12/183 (7%) adenocarcinoma specimens had *RBM10* mutations, each patient having a different mutation (5/12 being missense, 5/12 truncating and 2/12 splice-site) [10]. In another lung study, a mutation - caused by a T to A substitution and consequent valine (V) to glutamic acid (E) substitution within the second RRM (RRM2) of RBM10 - was reported in A549 lung adenocarcinoma cells, with consequences for NUMB alternative splicing [2]. In the blood cells of patients with TARP syndrome, six different mutations were identified [6-8], and a six exon-spanning deletion (aa 651–889) that codes for a truncated RBM10 isoform with an inability to regulate alternative splicing [3].

Table 2.1: *RBM10* mutations.

Phenotype	Mutation effect	Mutation	Exon	Protein	Reference
NSCLC	Missense		2	E4K	Imielinski et al. [10]
NSCLC	Missense		2	R6H	Imielinski et al. [10]
TARP syndrome	Frameshift	c.159delC	3	p.Lys54SerfsX80	Gripp et al. [7]
NSCLC	Nonsense		3	E67	Imielinski et al. [10]
TARP syndrome		c.448C>T	4	p.Gln150X	Johnston et al. [8]
NSCLC	Nonsense		5	R157fs	Imielinski et al. [10]
NSCLC	Nonsense		7	Y206	Imielinski et al. [10]
NSCLC	Nonsense		8	R230	Imielinski et al. [10]
TARP syndrome		c.724+2T>C	8		Johnston et al. [8]
NSCLC	Missense		10	1316F	Imielinski et al. [10]
TARP syndrome	Nonsense	c.1235G>A	12	p.Trp412X	Johnston et al. [6]
NSCLC	Missense		16	Y580F	Imielinski et al. [10]
NSCLC	Splice site		17	Y596	Imielinski et al. [10]
Pancreatic neoplasm	Frameshift	c.1817-1818insA	17	p.E606EfsX37	Furukawa et al. [9]
TARP syndrome	Frameshift	c.1893-1894insA	17	p.Pro632ThrfsX41	Johnston et al. [6]
TARP syndrome	Deletion	aa651-889	18-23		Wang et al. [3]
NSCLC	Missense		18	R685L	Imielnski et al. [10]
TARP syndrome		c.2176C>T	20	p.Arg726X	Johnston et al. [8]
NSCLC	Nonsense		21	E810	Imielinski et al. [10]
NSCLC	Splice site		22	V846	Imielinski et al. [10]

The pre-mRNA for RBM10 is alternatively spliced to yield two predominant protein isoforms: a 930 amino acid (aa) (~103.5 kDa) isoform that includes exon 4, referred to as RBM10 variant 1 (RBM10v1), and an 853 aa (~94.5 kDa) isoform that lacks exon 4, referred to as RBM10v2. In addition to the two major RBM10 variants, the Ensembl Database lists a variant of RBM10v2 that is one amino acid shorter (852 aa). The 7 April 2003 Gen-Bank deposition version 1 for this RBM10v2(V277del) isoform (NM_152856.1) describes it as having an "alternate donor splice site" compared to RBM10v1. Indeed, a tandem donor splice site of the configuration GYNGYN was identified in RBM10 exon 10 (as GTGGTG) from a screen of expressed sequence tags (ESTs) for variants generated from upstream and downstream tandem repeat triplets [11]. Utilization of the downstream triplet (the "e" site referred to in [11]) would result in the inclusion of a valine at amino acid 277 for RBM10v2 and 354 for RBM10v1. For clarity throughout this manuscript, we will refer to the longer RBM10v2 isoform as RBM10v2 (V277), the shorter RBM10v2 isoform as RBM10v2 (V277del), the longer RBM10v1 isoform as RBM10v1 (V354) and the shorter RBM10v1 isoform as RBM10v1 (V354del).

Our comprehensive review of the literature and various protein databases suggested that the presence of RBM10v1(V354del) is by no means generally recognized and that there appears to be some confusion as to its legitimacy and the mechanism by which it is generated. For instance, RBM10v1(V354del) has been identified as RBM10 "missing" valine 354 (UniProt – P98175-2), and as a mismatch of I353 with valine (on the Protein Data Bank website). For an overview of RBM10v1 isoforms described in various databases and references, see Table 2.2. In the study presented herein using a small cell lung cancer cell line, we confirm the existence of two full-length RBM10v2 transcripts, RBM10v2(V277) and RBM10v2(V277del), and prove the

existence of two full-length RBM10v1 transcripts, RBM10v1(V354) and RBM10v1(V354del). We then demonstrate that the presence or absence of valine alters the tertiary structure of the second RNA Recognition Motif (RRM2) within the RBM10 protein. Finally, we show that 2-fold higher levels of the transcripts encoding the minus- compared to the plus- valine isoforms of both RBM10v1 and RBM10v2 correlates with higher levels of the lung cancer associated NUMB exon 11 inclusion variant, compared to the exon 11 exclusion variant.

Table 2.2: RBM10v1 isoforms reported in various database and references.

Origin	Sequence	Reference
Databases		
Ensembl	STIVEAA	ENST00000377604
NIH GenBank	STIVEAA	NM_005676
	STIEAA	NM_001204467
NIH GenBank	STIVEAA	NP_005667
	STIEAA	NP_001191396
EMBL-EBI InterPro	STIVEAA	P98175
UniProtKB	STIVEAA	P98175-1
	STI-EAA	P98175-2
neXtprot beta	STIVEAA	iso1
	STI-EAA	iso2
USCSC	STIVEAA	uc004dhf.3
	STI-EAA	uc004dhh.3
HUGE	STI-EAA	KIAA0122/GenBank D50912
References		
Bechara et al. [2]	Minus valine isoform; STI(E)EAA	
Inoue et al. [1]	STI-EAA	KIAA0122

2.2 Materials and methods

2.2.1 Cell culture and differentiation

GLC20 cells were kindly provided by Charles Buys (University of Groningen, The Netherlands). Cells were cultured in RPMI supplemented with 10% fetal bovine serum (FBS). JKM1 [24],

Jurkat Clone E6 [25], MCF-7 [26], MDA-MB-231 [27] and TF-1 cells [25] were grown as previously described. A549 (from ATCC) and HeLa cells (provided by Hoyun Lee, AMRIC) were grown in DMEM/ F-12 medium supplemented with 10% FBS. TK6 cells (provided by Elliot Drobetsky, University of Montreal) were grown in DMEM/F-12 medium supplemented with 10% fetal horse serum. BEAS-2B cells (purchased from ATCC) were grown in LHC-9 medium, on plates pre-coated with 0.01 mg/ml fibronectin, 0.03 mg/ml collagen and 0.01 mg/ ml bovine serum albumin. Media and sera were purchased from Life Technologies (Burlington, Canada).

2.2.2 Fluorescent in situ hybridization (FISH)

Slides were prepared from a cell suspension using standard cytogenetic techniques. Slides were denatured at 75°C for 2 mins and hybridized overnight at 37°C with Spectrum Green (X chromosome) and Spectrum Red (Y chromosome) (Vysis, Abbott Molecular, Mississauga, Canada). Following hybridization the slides were washed in 0.4×SSC/0.3% NP40 at 73°C for 2 mins, then 2.0×SSC/ 0.1% NP40 at 23°C for 1 min. Slides were dried in the dark then stained with Vysis DAPI II and the coverslips applied. Images were captured using an Olympus BX60 microscope equipped with a mercury bulb and camera. Images were processed with Cytovision software from Genetix.

2.2.3 RNA extraction, reverse-transcription and PCR

RNA was isolated from cell pellets using Tri-Reagent (Molecular Research Center, Inc., Cedarlane, Burlington, Canada). Reverse transcription was carried out using 1 μg of RNA, and MMLV (for expression level reactions) or SuperScript II (for sequencing) reverse transcriptase (Life Technologies). Amplification of cDNA by polymerase chain reaction (PCR) was performed using gene-specific primers RBM10F and RBM10RS (exon 4 spanning) [27] (Figure 2.1Bi) or RBM10v1/v2R (also exon 4 spanning) [20] (Figure 2.1Bii), NUMBF(exon10): 5′-TAGAAGGGGAGG CAGAGAGC-3′ and NUMBR(exon12): 5′-CTCAGAGG GAGTACGTCTAT-3′ and GAPDH [28] (all primers purchased from AlphaDNA, Montreal, Canada). End-point PCR reaction conditions: (1) 95°C for 5 minutes, (2) gene-specific cycle number (40 cycles for RBM10, 28 and 40 cycles for NUMB, and 19 (Figure 2.3Bi) or 25 (Figures 2.1Bii and 2.3Bii) cycles for GAPDH) of 95°C for 30 seconds, 62°C (RBM10F + RS), 55°C (RBM10F + v1/v2R), 61°C (NUMB), 59°C (GAPDH) for 30 seconds, 72°C for 45 seconds, and (3) 72°C for 10 minutes. The samples were visualized following electrophoresis through a 2% (40 mM Tris-acetate, 10 mM EDTA, pH 8.0) (TAE) agarose gel containing SYBR®safe DNA gel stain (Life Technologies).

For sequencing of full-length RBM10, nested PCR was carried out, using RBM10FNhe1: 5′-CTA GCT AGC TAG TGG CTG GGA AGT GAA ACG GAG CCA GCG-3′ and RBM10RL: 5′-TGG CTG GGG AGT GGG CTG G-3′ primers for Reaction 1 and RBM10FNhe1 and RBM10RHindIII: 5′-CCC AAG CTT GGC TGG GCC TCG TTG AAG CG-3′ primers for Reaction 2, Platinum Pfx Polymerase (Life Technologies) and 5 μl of Reaction 1 as template for Reaction 2. PCR reaction conditions: Reaction 1: (1) 95°C for 2 minutes, (2) 18 cycles of 94°C

for 10 seconds, 66°C for 1 minute, 68°C for 3 minutes; Reaction 2: (3) 22 cycles of 94°C for 10 seconds, 62°C for 1 minute, 68°C for 3 minutes, (4) 72°C for 5 minutes.

2.2.4 Immunoblotting

Western blotting was carried out as previously described [20]. RBM10 antibody was used at a dilution of 1:500. The in vitro transcription/translation reactions were carried out using a TNT® T7 Quick Coupled Transcription/ Translation Kit (Promega, through Fisher Scientific, Nepean, Canada), and plasmid constructs pcDNA3.RBM10v1 or pcDNA3.RBM10v2 [20].

2.2.5 Sequencing

Full-length RBM10v1 and RBM10v2 amplicons were separated by agarose gel electrophoresis (note, no full-length RBM10v2 amplicon was detectable in the GLC20 cells) and cDNA was excised using a QIAquick gel extraction kit (Qiagen, Toronto, Canada). DNA quantity (absorbance at 260 nanometers (nm)) and purity (ratio of the absorbance at 260 and 280 nm) were determined using a Nano-Drop 2000C spectrophotometer (Fisher Scientific, Ottawa, Canada), and the samples were sent for sequencing.

Samples were sequenced, using the Sanger technique, by the MOBIX Lab - DNA Sequencing and Oligo Synthesis Facility (McMaster University, Hamilton, Canada). Internal primers (sequences available upon re-quest) were generated by MOBIX. Bi-directional, over-lapping sequence reads of ~600 bp were generated, as detailed in Figure 2.1D.

2.3 Results

2.3.1 Evidence that alternative splicing occurs within exon 10

The GLC20 cell line was established from a small cell lung cancer (SCLC) of male origin [12]. It is RBM5-null and was determined, by FISH, to contain only one X chromosome (Figure 2.1A). Alternative splicing of the X-linked RBM10 gene [13], to generate both RBM10v1 and RBM10v2, was confirmed in the GLC20 cells, using RT-PCR (Figure 2.1B). Most of the cancer, or transformed, cell lines that we have tested express more RBM10v1 than RBM10v2, at both the mRNA (Figure 2.1B) and protein (Figure 2.1C and data not shown) levels. This observation is particularly true for GLC20 cells, which express such a small amount of RBM10v2 protein that it is technically challenging to detect.

To estimate functionality of RBM10 in the GLC20 cells, sequencing of cDNA was carried out. Only full-length RBM10v1 cDNA was sequenced because full-length RBM10v2 cDNA could not be amplified from the GLC20 cells. Mixed sequence was observed beginning at the 3′-end of exon 10, with either the forward or reverse primer. At that point in time (June 2014), the Ensembl Database listed two different RBM10v2 isoforms, we are herein designating RBM10v2(V277) and RBM10v2(V277del) (corresponding to GenBank Accession Numbers NM_ 001204466.1 and NM_152856.2). To determine if the mixed sequencing read in the GLC20 RBM10v1 sample was the result of a mixture of transcripts with different exon 10 3′-end sequences, we designed primers immediately 3′- to the anticipated modified triplet site in the cDNA (refer to Figure 2.1D for primer locations), thereafter expecting an unambiguous sequence read. Indeed, clear sequence was obtained, thereby delineating the altered region as the last three nucleotides of exon 10 (Figure 2.1E).

The presence of a mixture of two different isoforms of RBM10v1 suggested either an alternative splicing event or two RBM10 alleles, the later possibility being unlikely since we had confirmed only one X chromosome by FISH analysis (Figure 2.1A). Since there remained the possibility of an RBM10 gene duplication with allelic variation, we decided to sequence RBM10v1 cDNA from additional cell lines, theorizing that if the same mixed read was observed in other cells it would suggest alternative splicing. We sequenced transcripts from both male and female-derived cell lines, since one RBM10 allele is silenced as the result of X chromosome inactivation in female somatic cells [14,15], therefore whether male or female-derived, cell lines would theoretically have only one RBM10 gene that is transcribed. RBM10v1 and RBM10v2 cDNA was sequenced in A549 (a male-derived lung adenocarcinoma cell line), HeLa (a female-derived cervical adenocarcinoma cell line) and BEAS-2B (a male-derived non-cancerous SV40/adenovirus-transformed lung cell line). Sequencing data revealed the same nucleotide variation in exon 10 of RBM10v1 and exon 9 of RBM10v2 in all three cell lines, therefore suggesting that the two isoforms of RBM10v1 are, as originally surmised within GenBank deposition NM_152856.1 and by Hiller et al. [11], the result of an alternative splicing event. An example of how this might occur is presented diagrammatically in Figure 2.1F.

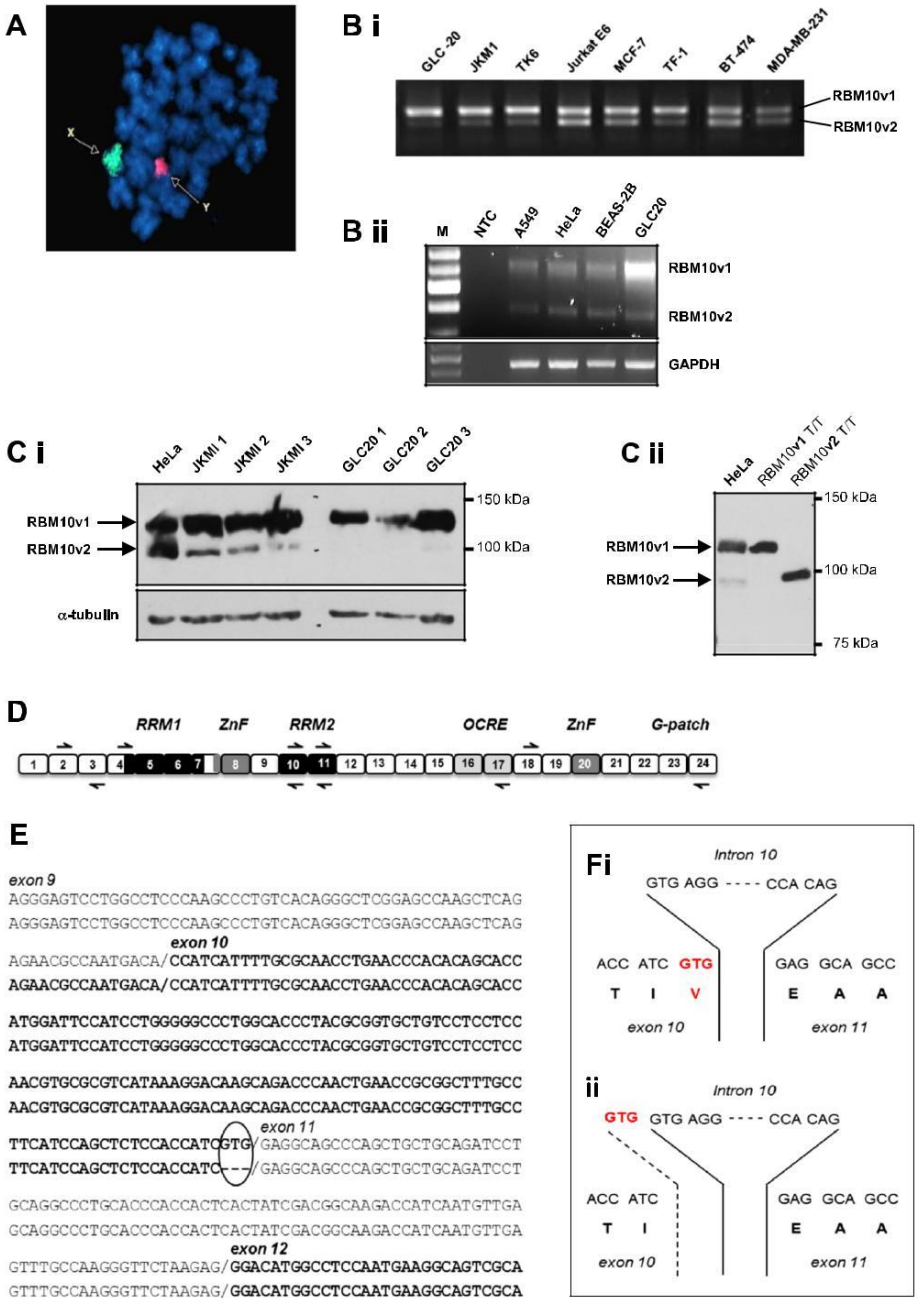

Figure 2.1 Alternativge splicing of RBM10. (A) FISH analysis of GLC20 cells, with painted X and Y chromosomes, demonstrating the presence of only one X chromosome. (B) RBM10v1 and RBM10v2 RNA expression in various cell lines, including GLC20. Representative raw RT-PCR data using RBM10 exon 4 spanning primers. Bi: RBM10F with RBM10RS primers. Bii: RBM10F with RBM10v1/v2R primers. M: 100 bp DNA ladder (FroggaBio Inc., Toronto, Canada). NTC: no template control. (C) Protein expression by Western blot. Ci shows RBM10 expression in whole cell lysates from three cell lines, including GLC20. The numbers 1, 2 and 3 after JKM1 and GLC20 delineate cells from three biological replicates. Cii includes control HeLa protein and in vitro translated RBM10v1 and RBM10v2 protein, to confirm the location of RBM10v2 is the cell line extracts. (D) Cartoon of full-length RBM10v1 mRNA, not drawn to scale. Boxes represent exons. Left and right black arrows represent primer placement for sequencing. Approximate positioning of consensus functional motifs is indicated by text and differential shading. (E) Alignment of the two GLC20 RBM10v1 isoform sequences. Circled area indicates the region that differs between the two RBM10v1 isoforms. (F) Nucleotide and amino acid sequences of the RBM10v1 exon10/intron 10/exon 11 donor and acceptor sites for (i) RBM10v1(V354), and (ii) RBM10v1(V354del).

Sequence variation that occurs as a result of alternative splicing at the 3′-ends of exons with tandem repeats such as GYNGYN, is regulated partly by U1snRNA binding and partly by the presence of CGGG and GGGT sequons in the downstream intron, particularly if the downstream intron is shorter than 200 nucleotides (nts) [11]. Intron 10 of RBM10 is 171 nts and contains three CGGG sequons, two GGGT sequons and one CGGGGT sequon, suggesting that co-expression of the two RBM10v1 isoforms is indeed a regulated alternative splicing event. The stimuli that control this regulation remain to be determined, but are unlikely limited to male, lung or cancer cells, since both RBM10v1(V354) and RBM10v1(V354del) were present in A549, HeLa, BEAS-2B and GLC20 cells.

2.3.2 Structural consequences of alternative splicing of RBM10v1

RBM10v1 and RBM10v2 both contain two RRMs (refer to Figure 2.1D) defined as ~75-85 amino acids that three dimensionally form four β-sheets flanked by two α-helices. The most conserved sequences within any RRM comprise the RNP2 and RNP1 domains (reviewed in [5]), RNP1 having the most highly conserved sequence of the two. Notably, amino acid 354 in RBM10v1 is located in approximately the middle of RRM2, at the beginning of the second α-helix and near to the end of β-sheet three, which is encoded by the highly conserved RNP1 domain [16].

Valines have a high free energy that is associated with α-helix disruption and since α-helices are known to contribute to the stabilization of RNA/protein interactions, disruption of the α-helix by

a valine insertion would be predicted to destabilize any RNA/protein interaction. In RBM10, the placement of the altered amino acid adjacent to the highly conserved β-sheet three structure suggested that any potential alteration to the second α-helical structure within RRM2 might have a significant effect on overall protein conformation, and consequently, the ability to interact with RNA. Indeed, Bechara et al. [2] recently described a G to T mutation in the terminal exon 10 codon of RBM10, which changed the amino acid coded from valine (V) to a glutamic acid (E). This single mutation had dramatic functional consequences, manifesting as an altered ability to splice specific downstream targets, such as pre-mRNA encoding the proliferation regulatory protein NUMB [2].

To better understand how a change to this residue might contribute to RBM10 functional alterations we compared the structures of a valine-retaining, a glutamic acid-substituting and a valine-lacking amino acid within RRM2. We uploaded these altered RBM10v1 RRM2 sequences into SwissProtKB/Swiss-Prot (www.expasy.org), a program that predicts a two-dimensional configuration and ranks it against similar configurations of previously crystalized structures. A crystal structure for a minus-valine RBM10 RRM2 (designated 2m2d) [17,18] was the reference structure for the V354, V354E and V354del RBM10v1 RRM2 predictions. We also uploaded the RRM2 sequences into Phyre^2 (the Protein Homology/analogY Recognition Engine v2.0, www.sbg.bio.ic.ac.uk). To visualize a rotatable three-dimensional structure, the structure predictions for V354, V354E and V354del from both Swiss ProtKB and Phyre^2 were uploaded into the Yasara modeling program (Yet Another Scientific Artificial Reality Application, www.yasara.org). A comparison of all the predictions (Figure 2.2) revealed that the addition of

valine did, as anticipated, disrupt the α-helical structure and thus the classic configuration of an RRM domain (shown as a colour change from dark blue to cyan by the Yasara software). Exclusion of the valine was associated with an α-helix. Substitution of the V for an E resulted in two slightly different configurations, depending on the prediction program used: both programs, however, predicted a change to, but a retention of, an α-helical structure compared to either the V354del or the V354. These modelling results suggest that conformational changes to the RBM10v1 protein could be responsible for altering the protein's ability to interact with RNA.

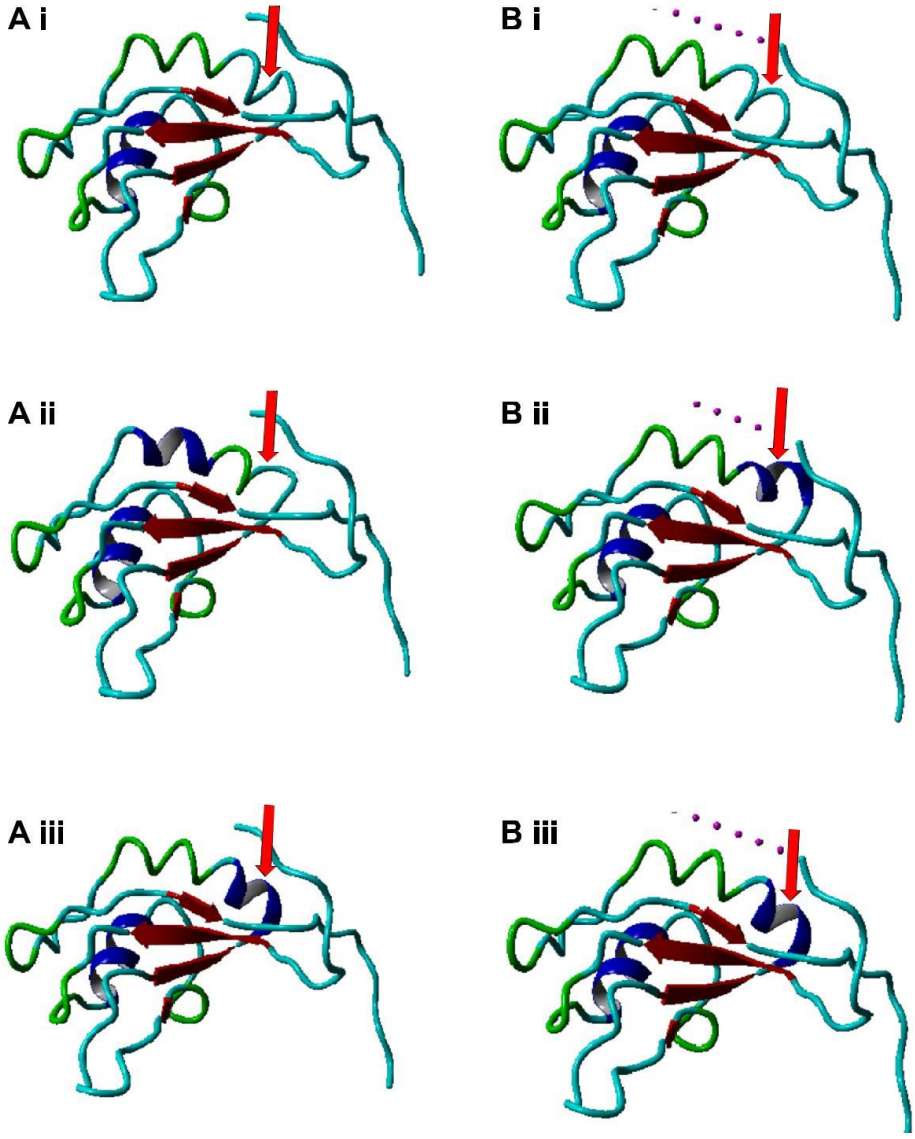

Figure 2.2 Conformation of RBM10v1 RRM2. The RBM10 RRM2 conformation was modeled using SwissProtKB (A) or Phyre[2] (B). (i) Isoforms V354. (ii) Isoforms V354E. (iii) Isoforms V354del. Arrow indicates the position of the +/− valine. Yasara structure colors indicate beta-sheets (red), alpha-helixes (dark blue), turns (green) and random coils (cyan).

2.3.3 Functional consequences of alternative splicing of RBM10v1

Using PAR-CLIP technology Bechara et al. [2] identified an RBM10 cluster in the 3′-splice site region preceding NUMB exon 11 (the current Ensembl exonic designation for the previously referred to NUMB exon 9) [2]. They then went on to demonstrate, using an A549 non-small cell

lung cancer (NSCLC) cell line with an RBM10v1 (V354E) mutation (herein referred to as A549-JV), that expression of recombinant RBM10v1 protein, with either a valine or a glutamic acid at amino acid 354, altered NUMB splicing. With valine present (RBM10v1(V354)), there was preferential NUMB exon 11 exclusion - associated with NOTCH repression and decreased proliferation. On the other hand, the glutamic acid-containing isoform (RBM10v1(V354E)) demonstrated preferential NUMB exon 11 inclusion – associated with NOTCH activation and increased proliferation. Recognizing that a V354E substitution would not necessarily have a similar effect as a V354del, but taking into consideration our structural predictions, the fact that the valine to glutamic acid mutation occurred at exactly the same site as the RBM10v1 alternative splicing of RBM10v1(V354) to RBM10v1(V354del) suggested to us that regulated alternative splicing of RBM10v1 has functional significance and is important to lung cancer.

Considering that RBM10v1(V354) expression correlated with preferential NUMB exon 11 exclusion and RBM10v1(V354E) expression correlated with preferential NUMB exon 11 inclusion [2] and that expression of the exon 11 retaining NUMB transcript is frequently increased in lung adenocarcinomas [19], one might predict that (a) downregulation of RBM10v1(V354) is one means by which lung cancer cells circumvent proliferation controls, and (b) more RBM10v1(V354del) than RBM10v1 (V354) is expressed in lung cancers. Interestingly, we have whole transcriptome-sequencing data (manuscript in preparation) demonstrating that in the GLC20 small cell lung cancer cells and three stable GLC20 sublines, transcripts encoding RBM10v1(V354del) and RBM10v2(V277del) have ~2-fold higher expression than transcripts encoding RBM10v1(V354) and RBM10v2(V277) (Figure 2.3A). When NUMB exon 11

alternative splicing was examined in the GLC20 cells, as predicted, preferential expression of the NUMB exon 11 inclusion variant was observed (Figure 2.3B).

NUMB splicing was also examined in HeLa and BEAS-2B cells as well as our A549 cells (herein referred to as A549-LS) that, unlike those used by Valcárcel and colleagues [2], express transcripts encoding both RBM10v1 (V354) and RBM10v1(V354del), as opposed to only RBM10v1(V354E). If RBM10v1(V354del) functions in a similar manner to RBM10v1(V354E) - to generate the NUMB exon 11 inclusion transcript - then we anticipated A549-LS cells would express both the NUMB exon 11 inclusion and exclusion transcripts. We also anticipated more of the NUMB exon 11 exclusion transcript in the A549-LS cells (resulting from RBM10v1(V354) expression), compared to the A549-JV subline (which lacks RBM10v1(V354)). As shown in Figure 2.3B, and confirming the observations of Valcárcel and colleagues [2], the A549-LS subline expressed both NUMB variants, but significantly more of the NUMB exclusion variant than the inclusion variant (as opposed to the A549-JV subline that expressed predominantly the NUMB exon 11-inclusion transcript: see [2], Figure Six C, upper panel, lane 14). In the transformed but non-tumourigenic BEAS-2B bronchial epithelial cells, we predicted a lower NUMB exon 11 inclusion to exclusion ratio, based on the previously reported observations that the ratio of NUMB exon 11 inclusion to exon 11 exclusion is higher in lung cancer than in normal cells [19] and our hypothesis that the RBM10v1(V354del) isoform is more prevalent in cancer cells. As shown in Figure 2.3B, the BEAS-2B cells did indeed have the lowest NUMB exon 11 inclusion to exclusion ratio of the four cell lines examined. Finally, as expected, and previously shown by Bechara et al. [2], HeLa cells had a clearly higher inclusion

to exclusion expression ratio. The only unexpected observation from this cell line RNA analysis was the high level of the NUMB exon 11 exclusion variant in the A549-LS cells, considering they are a lung cancer cell line. Determination of the relative expression levels of the transcripts encoding RBM10v1(V354) and RBM10v1(V354del) isoforms in this subline would help to resolve this conundrum.

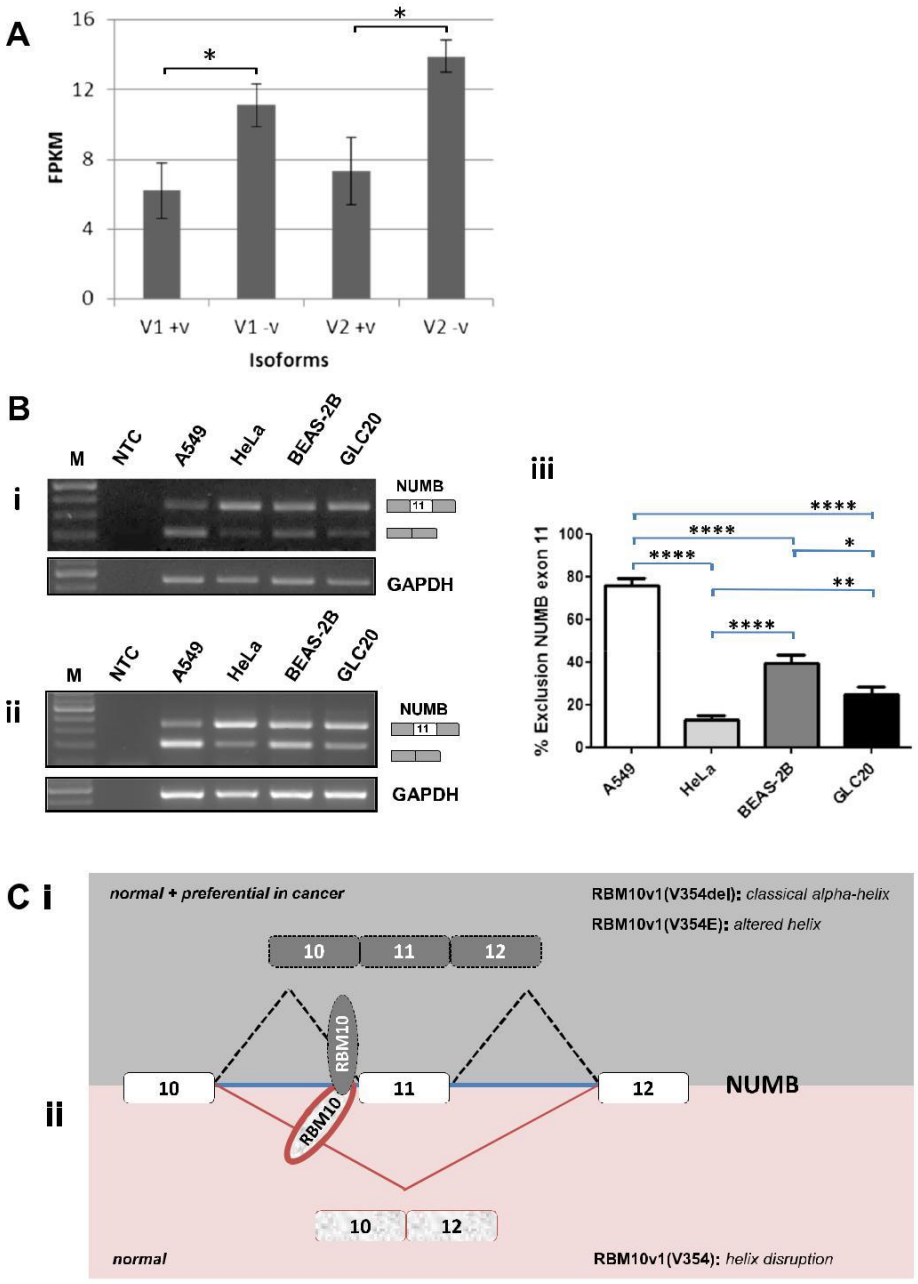

Figure 2.3 Functional effects associated with RBM10 variant expression. (A) In GLC20 cells, comparative expression levels of RBM10v1 and RBM10v2 transcripts encoding the valine-retaining and valine-lacking isoforms, as determined by RNA-seq. *$p < 0.05$. (B) NUMB alternative splicing in A549, HeLa, BEAS-2B and GLC20 cells. (i) and (ii) are 2% agarose gels with SYBR®safe, showing representative amplicon expression levels following end-point PCR with (i) 28 cycles, or (ii) 40 cycles, using NUMB exon 11-spanning primers and (i) 19 cycles or (ii) 25 cycles for GAPDH. (iii) Following densitometry of amplicons from six end-point PCR reactions (three at 28 cycles and three at 40 cycles) of the two different cDNA preparations from one RNA extraction for each cell line, the percentage of the NUMB exon 11 exclusion variant was calculated and plotted. Error bars represent the standard error of the mean. Significances were calculated using an unpaired Student's t-test, with *$p < 0.05$, **$p < 0.01$ and ****$p < 0.0001$. (C) Model depicting how the +/− valine isoforms of RBM10v1 might influence NUMB exon 11 alternative splicing. The plus and minus valine isoforms are present, at low levels, in normal cells, and contribute to the production of both the exon 11 inclusion and exclusion variants of NUMB. Both RBM10 isoforms are able to bind NUMB pre-mRNA, but the minus valine isoform of RBM10v1 does so with higher affinity, having the classical α-helix structure. The plus valine isoform does not bind as efficiently, thereby interfering with recognition of the intron 10 3′splice site, resulting in NUMB exon 11 exclusion.

2.4 Discussion

RBM10 is an apoptosis regulatory protein [20] and its paralogue, RBM5 functions in the same capacity, but has the added ability to regulate the cell cycle [21,22]. Based on the findings of Bechara et al. [2], it appears that RBM10 is also able to regulate the cell cycle, via the NOTCH signaling pathway [2]. Is the regulation of RBM10v1(V354) versus RBM10v1(V354del) alternative splicing a means by which normal cells temporarily modulate proliferation prior to a repair versus apoptosis event? Have cancer cells hijacked this alternative splicing mechanism as one means of circumventing proliferation controls? Of the mutations identified so far in pancreatic cancer and NSCLCs, none occurs at this site to permanently generate the minus valine isoform, except the mutation described by Bechara et al. [2] in a lung adenocarcinoma cell line (see Table 2.1). It is therefore difficult to predict how important the regulation of this alternative splicing event is to cancer initiation and/or progression. We have initiated studies to more thoroughly characterise the expression of transcripts encoding the two RBM10v1 and RBM10v2 isoforms in primary lung cancer specimens. Additional studies relating to protein expression are also warranted, as are studies concerning the regulation of this expression.

In an attempt to align our observations with those of Bechara et al. [2] and Wang et al. [3] we propose a model to explain how changes in RBM10v1 splicing might be predicted to regulate NUMB splicing. The model takes into consideration the following observations. Firstly, overexpression of RBM10 correlates with NUMB exon 11 exclusion [2,3]. Secondly, in lung cancer there is preferential expression of the NUMB exon 11 inclusion variant. Thirdly, in lung cancer RBM10 is highly expressed [10], but while in our A549, HeLa, BEAS-2B and GLC20

cells transcripts encoding both RBM10v1 isoforms were observed, there was two-fold more RBM10v1(V354del) than RBM10v1(V354) in the GLC20 SCLC cells. Our model does not attempt to reconcile the somewhat conflicting binding data previously reported [2,3].

Our model, depicted in Figure 2.3C, posits that RBM10v1 (V354) and RBM10v1(V354del) are both expressed in normal cells, but that in cancers RBM10v1(V354del) is preferentially expressed. RBM10v1(V354) and RBM10v1 (V354del) are both capable of interacting with pre-mRNA, and do so in the vicinity of the upstream intronic 3′-splice site of the alternate exon. RBM10v1(V354del), however, has a higher affinity interaction with pre-mRNA than RBM10v1(V354) (resulting from its ability to form the second α-helix within RRM2). In its capacity as a higher affinity binder, RBM10v1(V354del) is able to function as an auxiliary splicing factor. As for RBM10v1 (V354), disruption of the second α-helical structure within RRM2 generates an RBM10v1 isoform that interacts with the same pre-mRNA as RBM10v1(V354del) but in a manner that impedes splicing. As a result of either less efficient or lower affinity binding or an inability to optimally interact with other auxiliary/splicing factors, expression of RBM10v1(V354) functions to increase the splicing of the alternative transcript. In our model, the increase in the NUMB exon 11 inclusion transcript that is associated with downregulation of RBM10 results from the presence of reduced levels of the competing, less efficient binding, RBM10v1(V354) isoform and consequently more binding of the higher affinity RBM10v1(V354del) isoform, resulting in more of the NUMB exon 11 inclusion product. According to our model, therefore, alternative splicing regulation by RBM10 depends not only

on the ratio of RBM10v1(V354) to RBM10v1(V354del), but on the total levels of RBM10v1 protein as well.

Exactly how the structural change associated with a valine insertion at amino acid 354 of RBM10v1 results in splicing changes is unknown. Multiple binding motifs have been identified for RBM10 [2] as have multiple potential binding regions within pre-mRNA [2,3], suggesting that interaction of RBM10 with pre-mRNA targets may be a dynamic and flexible phenomenon. And while expression of RBM10 is more frequently associated with alternate exon exclusion [1-3,23], it is also associated with alternate exon inclusion [2,3]. Perhaps binding and function of RBM10 is more influenced by tertiary structure than primary sequence of the protein, and the multiple sequence motifs and binding regions identified within pre-mRNAs reflect interactions with different RBM10 isoforms that each assume a slightly different conformation.

To note just prior to submission of this manuscript, Ensembl (which had not, at least during the course of this investigation, listed RBM10v1(V354del) in its database) removed the RBM10v2(V277del) isoform, thereby eliminating all reference to the minus-valine isoforms. The minus valine isoforms are those which form the classic α-helical structure associated with the RRM domains (as shown herein), RNA transcripts encoding the minus valine isoform of RBM10v1 exist in multiple cell types (as shown herein), and functional studies demonstrate the apoptotic regulatory ability [20] and alternative splicing ability [2] of RBM10v1(V354del). We therefore suggest that the alternative splicing of RBM10v1, and likely RBM10v2, is a regulated event worthy of consideration in functional studies.

2.5 References

1. Inoue A, Yamamoto N, Kimura M, Nishio K, Yamane H, Nakajima K. RBM10 regulates alternative splicing. FEBS Lett. 2014;588:942–7.

2. Bechara EG, Sebestyen E, Bernardis I, Eyras E, Valcarcel J. RBM5, 6, and 10 Differentially Regulate NUMB Alternative Splicing to Control Cancer Cell Proliferation. Mol Cell. 2013;52:720–33.

3. Wang Y, Gogol-Doring A, Hu H, Frohler S, Ma Y, Jens M, et al. Integrative analysis revealed the molecular mechanism underlying RBM10-mediated splicing regulation. EMBO Mol Med. 2013;5:1431–42.

4. Mueller CF, Berger A, Zimmer S, Tiyerili V, Nickenig G. The heterogenous nuclear riboprotein S1-1 regulates AT1 receptor gene expression via transcriptional and posttranscriptional mechanisms. Arch Biochem Biophys. 2009;488:76–82.

5. Sutherland LC, Rintala-Maki ND, White RD, Morin CD. RNA binding motif (RBM) proteins: a novel family of apoptosis modulators? J Cell Biochem. 2005;94:5–24.

6. Johnston JJ, Teer JK, Cherukuri PF, Hansen NF, Loftus SK, Chong K, et al. Massively parallel sequencing of exons on the X chromosome identifies RBM10 as the gene that causes a syndromic form of cleft palate. Am J Hum Genet. 2010;86:743–8.

7. Gripp KW, Hopkins E, Johnston JJ, Krause C, Dobyns WB, Biesecker LG. Long-term survival in TARP syndrome and confirmation of RBM10 as the disease-causing gene. Am J Med Genet A. 2011;155A:2516–20.

8. Johnston JJ, Sapp JC, Curry C, Horton M, Leon E, Cusmano-Ozog K, et al. Expansion of the TARP syndrome phenotype associated with de novo mutations and mosaicism. Am J Med Genet A. 2014;164A:120–8.

9. Furukawa T, Kuboki Y, Tanji E, Yoshida S, Hatori T, Yamamoto M, et al. Whole-exome sequencing uncovers frequent GNAS mutations in intraductal papillary mucinous neoplasms of the pancreas. Sci Rep. 2011;1:161.

10. Imielinski M, Berger AH, Hammerman PS, Hernandez B, Pugh TJ, Hodis E, et al. Mapping the hallmarks of lung adenocarcinoma with massively parallel sequencing. Cell. 2012;150:1107–20.

11. Hiller M, Huse K, Szafranski K, Rosenstiel P, Schreiber S, Backofen R, et al. Phylogenetically widespread alternative splicing at unusual GYNGYN donors. Genome Biol. 2006;7:R65.

12. Smit EF, de Vries EG, Timmer-Bosscha H, de Leij LF, Oosterhuis JW, Scheper RJ, et al. In vitro response of human small-cell lung-cancer cell lines to chemotherapeutic drugs; no correlation with clinical data. Int J Cancer. 1992;51:72–8.

13. Nagase T, Seki N, Tanaka A, Ishikawa K, Nomura N. Prediction of the coding sequences of unidentified human genes. IV. The coding sequences of 40 new genes (KIAA0121-KIAA0160) deduced by analysis of cDNA clones from human cell line KG-1. DNA Res. 1995;2:167–210.

14. Coleman MP, Ambrose HJ, Carrel L, Nemeth AH, Willard HF, Davies KE. A novel gene, DXS8237E, lies within 20 kb upstream of UBE1 in Xp11.23 and has a different X inactivation status. Genomics. 1996;31:135–8.

15. Thiselton DL, McDowall J, Brandau O, Ramser J, d'Esposito F, Bhattacharya SS, et al. An integrated, functionally annotated gene map of the DXS8026-ELK1 interval on human Xp11.3-Xp11.23: potential hotspot for neurogenetic disorders. Genomics. 2002;79:560–72.

16. Song Z, Wu P, Ji P, Zhang J, Gong Q, Wu J, et al. Solution structure of the second RRM domain of RBM5 and its unusual binding characters for different RNA targets. Biochemistry. 2012;51:6667–78.

17. Kopp J, Schwede T. The SWISS-MODEL Repository of annotated three-dimensional protein structure homology models. Nucleic Acids Res. 2004;32:D230–4.

18. Kiefer F, Arnold K, Kunzli M, Bordoli L, Schwede T. The SWISS-MODEL Repository and associated resources. Nucleic Acids Res. 2009;37:D387–92.

19. Misquitta-Ali CM, Cheng E, O'Hanlon D, Liu N, McGlade CJ, Tsao MS, et al. Global profiling and molecular characterization of alternative splicing events misregulated in lung cancer. Mol Cell Biol. 2011;31:138–50.

20. Wang K, Bacon ML, Tessier JJ, Rintala-Maki ND, Tang V, Sutherland LC. RBM10 Modulates Apoptosis and Influences TNA-a Gene Expression. Journal of Cell Death. 2012;5:1–19.

21. Mourtada-Maarabouni M, Keen J, Clark J, Cooper CS, Williams GT. Candidate tumor suppressor LUCA-15/RBM5/H37 modulates expression of apoptosis and cell cycle genes. Exp Cell Res. 2006;312:1745–52.

22. Oh JJ, Razfar A, Delgado I, Reed RA, Malkina A, Boctor B, et al. 3p21.3 tumor suppressor gene H37/Luca15/RBM5 inhibits growth of human lung cancer cells through cell cycle arrest and apoptosis. Cancer Res. 2006;66:3419–27.

23. Zheng S, Damoiseaux R, Chen L, Black DL. A broadly applicable high-throughput screening strategy identifies new regulators of Dlg4 (Psd-95) alternative splicing. Genome Res. 2013;23:998–1007.

24. Sutherland LC, Edwards SE, Cable HC, Poirier GG, Miller BA, Cooper CS, et al. LUCA-15-encoded sequence variants regulate CD95-mediated apoptosis. Oncogene. 2000;19:3774–81.

25. Shu Y, Rintala-Maki ND, Wall VE, Wang K, Goard CA, Langdon CE, et al. The apoptosis modulator and tumour suppressor protein RBM5 is a phosphoprotein. Cell Biochem Funct. 2007;25:643–53.

26. Rintala-Maki ND, Abrasonis V, Burd M, Sutherland LC. Genetic instability of RBM5/LUCA-15/H37 in MCF-7 breast carcinoma sublines may affect susceptibility to apoptosis. Cell Biochem Funct. 2004;22:307–13.

27. Rintala-Maki ND, Goard CA, Langdon CE, Wall VE, Traulsen KE, Morin CD, et al. Expression of RBM5-related factors in primary breast tissue. J Cell Biochem. 2007;100:1440–58.

28. Rintala-Maki ND, Sutherland LC. LUCA-15/RBM5, a putative tumour suppressor, enhances multiple receptor-initiated death signals. Apoptosis. 2004;9:475–84.

Chapter 3

3 RBM5 reduces small cell lung cancer growth, increases cisplatin sensitivity and regulates key transformation-associated pathways

Loiselle JJ, Roy JG and Sutherland LC. (2016) *RBM5 reduces small cell lung cancer growth, increases cisplatin sensitivity and regulates key transformation-associated pathways.* **Heliyon**. **2**(11) e00204.

Full text, open access document can be accessed through the journal's website:
http://www.heliyon.com/article/e00204/

Heliyon

ELSEVIER

Received:
27 September 2016
Revised:
7 November 2016
Accepted:
22 November 2016

Heliyon 2 (2016) e00204

RBM5 reduces small cell lung cancer growth, increases cisplatin sensitivity and regulates key transformation-associated pathways

Julie J. Loiselle [a], Justin G. Roy [b], Leslie C. Sutherland [a,b,c,*]

[a] Biomolecular Sciences Program, Laurentian University, Sudbury, ON P3E 2C6, Canada

[b] Department of Chemistry and Biochemistry, Laurentian University, Sudbury, ON P3E 2C6, Canada

[c] Health Sciences North Research Institute (HSNRI), 41 Ramsey Lake Road, Sudbury, ON P3E 5J1, Canada

* Corresponding author at: 41 Ramsey Lake Road, Sudbury, ON, P3E 5J1, Canada.

E-mail address: lsutherland@hsnri.ca (L.C. Sutherland).

http://dx.doi.org/10.1016/j.heliyon.2016.e00204

3.1 Abstract

Small cell lung cancer (SCLC) is the most aggressive type of lung cancer, with almost 95% of patients succumbing to the disease. Although *RBM5*, a tumor suppressor gene, is downregulated in the majority of lung cancers, its role in SCLC is unknown. Using the GLC20 SCLC cell line, which has a homozygous deletion encompassing the *RBM5* gene locus, we established stable *RBM5* expressing sublines and investigated the effects of *RBM5* re-expression. Transcriptome and target identification studies determined that RBM5 directly regulates the cell cycle and apoptosis in SCLC cells, as well as significantly downregulates other important transformation-associated pathways such as angiogenesis and cell adhesion. RNA sequencing of paired non-tumor and tumor SCLC patient specimens showed decreased RBM5 expression in the tumors, and expression alterations in the majority of the same pathways that were altered in the GLC20 cells and sublines. Functional studies confirmed *RBM5* expression slows SCLC cell line growth, and increases sensitivity to the chemotherapy drug cisplatin.

Overall, our work demonstrates the importance of *RBM5* expression to the non-transformed state of lung cells and the consequences of its deletion to SCLC development and progression.

3.2 Introduction

According to the American Cancer Society, more people die from primary cancers of the lung than from any other type of cancer. The most aggressive type of lung cancer occurs in the “small cells”, found in the main bronchi (Travis et al., 2004). Small cell lung cancer (SCLC) almost

exclusively occurs in people with a history of tobacco smoking (Jackman and Johnson, 2005; Travis et al., 2004).

Lung cancer initiation and progression are attributed at the molecular level to many factors, but arguably the most interesting is the loss of heterozygosity in a few regions throughout the short arm of chromosome three. Notably, allelic loss within the 3p21.3 region is evidenced even in pre-neoplastic tissue from smokers (Wistuba et al., 2000). An overlapping homozygous deletion within 3p21.3, noted in lung and breast tumors, harbors a number of tumor suppressor genes (Lerman and Minna, 2000). RNA Binding Motif 5 (*RBM5*), a putative lung cancer tumor suppressor gene (Sutherland et al., 2010), resides near the end of the telomeric deletion breakpoint that was noted in three SCLC cell lines (Lerman and Minna, 2000). In the majority of lung cancers (including SCLC and non-small cell lung cancer (NSCLC)), expression of *RBM5* is downregulated but present (Oh et al., 2002). The cause of this downregulation is unknown, but does not appear to result from gene mutation or promoter hypermethylation (Oh et al., 2008; Oh et al., 2007), suggesting allelic loss may be responsible. The almost universal downregulation of *RBM5* in all types of lung cancer does suggest it plays an important role in lung cancer initiation and/or progression. *RBM5* was, in fact, identified as one of nine downregulated genes within a 17 gene signature associated with metastasis in various human solid tumors, including lung (Ramaswamy et al., 2003).

Previous functional work relating to RBM5 in a variety of cancer cell lines identified it as a modulator of the cell cycle and apoptosis, partially via its influence on alternative splicing (Bechara et al., 2013; Oh et al., 2002). In regards to lung cancer specifically, some functional

work regarding RBM5 has been performed using a lung adenocarcinoma cell line (A549), which showed that increased *RBM5* expression correlated with (a) G_1 cell cycle arrest (Network, 2014; Shao et al., 2012), and (b) increased apoptosis (Oh et al., 2006; Shao et al., 2012). No functional work, however, has been undertaken for RBM5 in SCLC. This project set out to determine the importance of RBM5 in SCLC, in order to better understand the consequences of its downregulation to the development and progression of this disease. Furthermore, since SCLC is the most aggressive type of lung cancer, with 95% of patients eventually succumbing to the disease (Govindan et al., 2006), it is clear that a better understanding of this disease, as well as more effective treatment options, are required.

GLC20 is a SCLC cell line derived from small cells within a lung tumor biopsy (Smit et al., 1992). The cells have two 3p21 homozygous deletions, one of which includes *RBM5*, making the cells an attractive model in which to study the functional consequences of RBM5 re-expression (Angeloni, 2007; Kok et al., 1994). We established two *RBM5* expressing populations, with different levels of *RBM5*, and conducted transcriptome analyses to identify the pathways affected by altering the levels of *RBM5*. Target identification experiments were carried out to determine which of these pathways were directly affected by RBM5. To validate our findings, we (a) compared our in vitro transcriptomic results to transcriptomic data from two paired non-tumor/tumor patient specimens with a 50% downregulation of *RBM5* expression, and (b) experimentally examined the effects of no versus low versus high *RBM5* expression on cell proliferation and apoptosis. Our results suggest that RBM5 is a key SCLC suppressor and guardian of the non-transformed phenotype.

3.3 Materials & methods

3.3.1 Cell culture

SCLC GLC20 cells were a kind gift from the late Dr. Charles Buys from the University of Groningen (Groningen, Netherlands). GLC20 cells and sublines pcDNA3, T2 and C4 were maintained in RPMI 1640 (Gibco, Life Technologies) supplemented with 10% fetal bovine serum (FBS, Gibco) (termed complete media), with the addition of 0.1 mg/mL G418/Geneticin (Gibco) for pcDNA3, T2 and C4 sublines. Cells were maintained at 37 °C with 5% CO_2 in a humidified chamber.

3.3.2 Southern blotting

Genomic DNA was isolated by spooling, following overnight incubation in Tail Buffer (1% SDS, 0.1 M NaCl, 0.1 M EDTA, 0.05 M Tris, pH8), treated with 50 µg/ ml of RNase A (Amersham Biosciences) and cleaned using Qiagen Genomic-tip 100/G columns, following the manufacturer's instructions. The Southern blot was prepared and probed as previously described (Rintala-Maki and Sutherland, 2009). The *RBM5* probe was prepared using the PROSTAR HF single tube RT-PCR System (Stratagene), labelling with radioactive phosphate, and cleaning with a G25 sepharose column, following manufacturer's instructions.

3.3.3 GLC20 apoptosis profiles

GLC20 cells were diluted 1:2 in a 24 well plate 24 h before treatment. The following day, cells were treated with cisplatin (Sigma-Aldrich) dissolved in dimethyl sulfoxide (DMSO) and/or

etoposide (Sigma-Aldrich) dissolved in DMSO. Cells were then incubated for varying amounts of time, as shown in Fig. 3.2, at 37 °C in a 5% CO_2 humidified incubator.

3.3.4 Western blotting

Primary antibodies used were rabbit anti-RBM5 LUCA-15-UK (non-commercially available) (1:2,500 or 1:5,000) (Sutherland et al., 2000), rabbit anti-human PARP (1:1,500–1:2,000, C2-10: BD Pharmingen) and mouse anti-α-tubulin primary antibody (1:10,000, sc-8035, Santa Cruz Biotechnology, Inc.). Secondary antibodies used were goat anti-mouse HRP-conjugated secondary antibody (1:10,000, sc-2005; Santa Cruz Biotechnologies Inc.) or goat anti-rabbit HRP-conjugated secondary antibody (1:10,000, sc-2004; Santa Cruz Biotechnologies Inc.). Protein was exposed using Amersham ECL Western blotting detection reagents (GE-Healthcare) to Amersham Hyperfilm (GE-Healthcare). Film was then developed using a SRX-101A medical film processor (Konica Minolta Medical and Graphic Inc.).

3.3.5 Establishment of stable RBM5-expressing GLC20 sublines

GLC20 sublines were established following DMRIE-C transfection with pcDNA3 or pcDNA3.RBM5, and stable selection with G418 at 1.0 mg/ml in soft agar for 120 days. Detailed protocol is as follows; Cells were passaged 1:2, 24–48 h prior to transfection. 10 ml of cell culture (~ 2×10^6 cells) were used in each transfection, with 24 μl DMRIE-C (Life Technologies) and 8 μg total DNA (pcDNA3 or pcDNA3.RBM5). DMREI-C and DNA were incubated for ~30 min prior to cell addition. The cell/DMREI-C/DNA mix was then incubated at 37 °C and 5% CO_2 for 4 h, and the transfection terminated by adding serum. Transfected cells were selected using G418, at a concentration of 1.0 mg/ml, a concentration previously

determined to kill all untransfected cells by seven days. Following transfection, a clonal population of cells was established following plating in soft agar, as previously described (Longthorne and Williams, 1997). Four empty vector transfected clones and five RBM5 transfected clones were picked following 36 days of G418 selection in soft agar. After 120 days of continuous growth in G418 (following the first dilution of 10 ml of stably transfected cells, the selection reagent concentration was reduced from 1.0 to 0.1 mg/ml), only two of the five RBM5-transfected clones survived. One of these, designated C4, as well as one empty vector control clone, were used in subsequent studies. A second transfection was carried out in order to generate a pooled population of RBM5-transfected cells (eventually designated T2).

3.3.6 RNA extraction

GLC20 RNA samples were isolated using Tri-Reagent (BioCan Scientific). For RNA templates used in PCR, reverse transcription was performed as previously described (Loiselle and Sutherland, 2014). In regards to the Ontario Tumour Bank (OTB) tissue samples, 20 mg of tissue was cut with a sterile blade from fresh frozen tissue specimens that had been stored at −80 °C. The 20 mg tissue piece was transferred to a Bessman Tissue Pulverizer (VWR) that had been placed in liquid nitrogen for 10 min. Once the pulverizer was secured, a hammer was used to smash the tissue until it obtained a powder-like consistency. Powdered tissue was transferred to a solution containing Buffer RLT (Qiagen) and 0.14 mM β-mercaptoethanol, and homogenized using a Polytron PT 1300 D Homogenizer (Kinematica). The lysate was centrifuged for 3 min at 17000 x g to pellet tissue matter that did not homogenize. Supernatant was transferred to an Allprep DNA/RNA/Protein Mini Kit spin column (Qiagen) and RNA was extracted according to

manufacturer's instructions. It is important to note that RNA was extracted from two 20 mg pieces of tissue, and combined.

3.3.7 PCR

RBM5 genomic DNA PCR was performed using Gen1E2Fc (exon 2: 5′-CTTCAGTGGGACAATGGGTTCAGA-3′) and Gen2E3I2R (exon 3/intron 2: 5′-CCACTACGCTCTGTTCTACTCACTCTGCCA-3′) primers, with the follow-ing PCR amplification program 95 °C 5 min, [95 °C 30 s/65 °C 30 s/68 °C 2 min] (40 cycles), 68 °C 10 min. *RBM5* RT-PCR was performed using LU15(2) (exon 4) and LU15(3) (exon 8) primers, as previously described (Sutherland et al., 2000).*GAPDH* was amplified using GAPDH-F (exon 6: 5′ AACACAGTCCATGC-CATCAC 3′) and GAPDH-R (exon 7: 5′ TCCACCACCCTGTTGCTGTA), with an annealing temperature of 58−59 °C and 25–35 amplification cycles. PCR and product visualization were carried out as previously described (Loiselle and Sutherland, 2014). Approximate primer locations shown in Fig. 3.1G.

3.3.8 RNA-Sequencing and analyses

Extracted RNA was sent to the Donnelly Sequencing Centre (Toronto, Canada) for Illumina TruSeq stranded mRNA library preparation with Ribozero depletion, followed by paired-end high throughput sequencing using the Illumina HiSeq 2500 platform.

All four untreated GLC20 subline samples were multiplexed together during sequencing, as were the four cisplatin-treated samples. It is important to note that there were some differences between sample preparation and sequencing for cisplatin treated and untreated RNA-Seq

samples; (1) untreated samples were DNase treated prior to sequencing, (2) reads were 100 bp for untreated samples and 125 bp for cisplatin treated samples, and (3) untreated samples were sequenced in duplicate (multiplexed on each of two paired-end lanes), while treated samples were not sequenced in duplicate. Due to the longer read length for the cisplatin treated samples and overall higher output, however, similar depth was achieved for treated and untreated samples. Nonetheless, we only ran analysis within the treated and untreated groups, and compared the outputs, so as to not potentially introduce sequencing biases into our analyses. All four OTB specimens (two paired tumor and non-tumor specimens) were also multiplexed and sequenced in duplicate.

Transcriptome sequencing data quality was verified by FastQC (Babraham Bioinformatics, http://www.bioinformatics.bbsrc.ac.uk/projects/fastqc/). All specimens had quality score distributions over all sequences above 37 (on a phred 33 quality scale). Primers and adapters used for sequencing were then removed using cutadapt version 1.4.2 (Martin, 2011) using a quality cut-off of 26, as recommended (Del Fabbro et al., 2013). Following trimming, data quality was verified using FastQC. Trimmed reads were analyzed using the Tuxedo suite tools as follows: (1) TopHat 2.0.11 (Kim et al., 2013) was used to align reads to the human reference genome USCS hg19, (2) Cufflinks 2.1.1 (Trapnell et al., 2010) was used to assemble the mapped reads and obtain FPKM values for each investigated gene and isoform, (3) Cuffdiff 2.1.1 (Trapnell et al., 2013) was used to investigate differential expression, and (4) CummeRbund (Trapnell et al., 2010) was used for visualization. Samtools (Li et al., 2009) and Picard (http://broadinstitute.github.io/picard/) were used to assess mapping quality. For untreated and treated GLC20 subline RNA-Seq samples, all samples had a very good percentage of overall mapped

reads and concordantly mapped paired reads, with small standard deviations, permitting comparison between samples; in untreated samples 94.06% ± 0.44% (SD) reads mapped, with 89.18% ± 0.28% being concordant for both forward and reverse reads, and in the cisplatin treated samples 94.51% ± 0.87% reads were mapped, with 91.73 ± 1.07 of paired reads mapping concordantly. Values were slightly lower for OTB patient specimens, as expected, with 89.84 ± 3.08% reads mapped and 86.06 ± 2.87% concordant.

Prior to differential expression analysis, gene expression levels in both control samples (parental GLC20 and GLC20.pcDNA3) were compared to see if they were sufficiently similar to be combined into one experimental group; more replicates provides greater power and accuracy in RNA-Seq experiments (Liu et al., 2014). In fact, gene expression levels in both samples were very highly correlated ($r = 0.9699$ in untreated samples and $r = 0.9813$ in cisplatin treated samples), and thus both controls were combined into one experimental group.

Pathway enrichment was investigated using the FIDEA (Functional Interpretation of Differential Expression Analysis) program (D'Andrea et al., 2013) with the KEGG database (Kanehisa and Goto, 2000; Kanehisa et al., 2016). Pathway analysis was also performed using GSAASeqSP (Gene Set Association Analysis for RNA-Seq with Sample Permutation) (Xiong et al., 2014) with the Molecular Signatures Database (MSigDB) Hallmark gene set collection (Liberzon et al., 2015). Since each program uses a different algorithm in their calculations, and each gene set/functional interaction pathway set is curated separately, with different foci, a broad view of affected cellular processes affected is gained, and results can be compared between programs to identify the most robust changes.

For analysis of alternative splicing events in our RNA-Seq data, stringent parameters were used in order to identify alternative splicing events: (1) the expression of at least one alternative splice variant had to be significantly upregulated, and (2) the expression of at least one other alternative splice variant had to be significantly downregulated.

3.3.9 RNA immunoprecipitation followed by next generation sequencing (RIP-Seq)

The basic RIP technique was carried out as previously described (Jain et al., 2011). RNA associated with the immunoprecipitated samples was sequenced by the Donnelly Sequencing Centre. Illumina TruSeq Stranded Total RNA library preparation, including Ribozero Gold depletion, was performed along with random priming. Samples were sequenced in duplicate on the Illumina HiSeq 2500 platform, with each run being paired-ended, 125 bp reads.

RIP-Seq results were analyzed using the Tuxedo Pipeline (Trapnell et al., 2012), with the same quality control steps used for RNA-Seq analysis. Using the FPKM and log2-fold change values generated by Cuffdiff, the following inclusion criteria were used to distinguish RBM5 targets from IP contaminants: the RBM5 RIP sample target had to have (1) an FPKM value greater than one, (2) a log2-fold change greater than one, and (3) a positive log2-fold change (meaning it was more highly expressed than in the control RIP).

3.3.10 Cell counting, cell growth and cell death assays

Cells were plated at 10,000 per well in 96-well flat-bottom plates at a density of 50 cells/μL, in triplicate wells per treatment. Cells were left for 24 h at 37 °C with 5% CO_2 in a humidified chamber. After 24 h, the cells were treated with the following conditions: left untreated, saline (0.9% NaCl in H_2O) control, 1.0 μM cisplatin in saline for 0, 2, 4, 6, 8 and 10 days, or 0.1, 0.5, 10.0 and 100.0 μM cisplatin for 4 and 8 days. Cisplatin (Sigma) was prepared, as previously described (Hall et al., 2014), in saline at a concentration of 1.0 mg/mL. The cells were then counted every other day by transferring cells to a 96-well Vee-bottom plate and subjecting them to centrifugation at 500 x g for 5 min at 21 °C. The supernatant was discarded and cells treated with 0.25% Trypsin-EDTA for 10 min at 37 °C with 5% CO_2 in a humidified chamber. Complete media was added to cells and they were subjected to centrifugation at 500 x g for 5 min 21 °C. Cells were resuspended in complete media and counted in a 1:1 ratio of cells in complete media and 0.2% nigrosin, using a hemocytometer.

Live cells were counted as cells with intact membranes, characterized by a lack of blue/purple nigrosin within the cells, and dead cells were counted as cells without intact membranes, characterized by the presence of blue/purple nigrosin within the cell. Live cell counts were used to monitor cell growth, relative to day 0 counts, and the average of biological triplicates was plotted. A two-way ANOVA was performed with Bonferroni post-hoc analysis, comparing all subline cell growth to the pcDNA3 subline, calculated using Graphpad Prism 5. Percent intact membrane by nigrosin was calculated using the following equation: percent intact membrane by nigrosin = number of live cells divided by (number of live cells + number of dead cells) x 100.

Percent intact membrane by nigrosin for the 1.0 μM cisplatin values was also made relative to saline controls, and the average of biological triplicates was plotted. A two-way ANOVA was performed with Bonferroni post-hoc analysis, comparing all subline results to the pcDNA3 subline, calculated using Graphpad Prism 5. Day eight cisplatin results were made relative to the saline control for the calculation of EC50 values. EC50 values were calculated using 'log (inhibitor) vs. response (three parameters)' on Graphpad Prism 5, and the average of biological triplicates was plotted with the saline control represented at 10^{-10} M on the graphs. A one-way ANOVA was performed with Tukey post-hoc analysis, comparing all sublines to the pcDNA3 subline.

3.3.11 Apoptosis assays − Fluorescent microscopy

GLC20 cells and sublines were counted and 2.0×10^6 cells were plated in T75 flasks at a cell density of 50 cells/μL. After 24 h incubation at 37 °C with 5% CO_2 in a humidified chamber, cells were either exposed to 5.0 μM cisplatin or left untreated for 4 days. A fraction of cells was collected by centrifugation at 149 x g for 7 min at 21 °C and supernatant was discarded, followed by centrifugation at 5,900 x g for 2 min at 21 °C, with supernatant discarded, and the pellet stored at −80 °C for PARP cleavage analysis by Western Blot.

Another fraction of cells was used for apoptosis analysis by fluorescent microscopy. These cells were subjected to centrifugation at 149 x g for 7 min at 21 °C, supernatant was discarded, and the cells were treated with 0.25% Trypsin-EDTA for 10 min at 37 °C with 5% CO_2 in a humidified chamber, to obtain a single cell suspension. Cells were then washed two times in complete media and centrifuged at 500 x g for 5 min at 21 °C, with changes in media between each

centrifugation, then counted in a 1:1 ratio of cells in complete media and 0.2% nigrosin, using a hemocytometer. 0.5×10^6 cells were resuspended at a 1000 cell/μL density in cold PBS for fluorescence analysis. If fewer than 0.5×10^6 cells were counted, cells were adjusted to a smaller volume at a 1000 cell/μL density in cold PBS.

Before staining, cells were washed three times in cold PBS at 5,900 x g for 2 min at 21 °C, with changes in cold PBS between centrifugations, then resuspended in Annexin V binding buffer (10 mM HEPES, 140 mM NaCl, and 2.5 mM $CaCl_2$) at a density of 1000 cells/μL. Cells were triple stained with 7-aminoactinomycin D (7AAD) in DMSO, Annexin V-AlexaFlour® 488 conjugated, and Hoescht 33342 Nucblue® Live Cell Stain ReadyProbe Reagent (all Life Technologies) at 0.02 mg/ mL, 5 μL/100 μL, and 1 drop/500 μL concentrations, respectively, at 21 °C for 15 min in the dark. Cells were then washed three times in cold Annexin V binding buffer at 5,900 x g for 10 min at 21 °C, then resuspended in 100 μL of cold PBS.

Samples were loaded into Cytospin™ columns (Symport, VWR International) that were pre-loaded with a microscope slide (VistaVision, VWR International). Cells were centrifuged onto the microscope slides at 500 rpm for 2 min 21 °C in a Shandon Cytospin™ 4 cytocentrifuge (Thermo Scientific), rotor # 4127 0806 59930093. Samples on slides were air-dried, then fixed with 4% paraformaldehyde (Sigma-Aldrich) in PBS at 21 °C in the dark for 10 min. Slides were washed sequentially in three changes of PBS, then air-dried. 90% glycerol (Sigma-Aldrich) in PBS was added to the samples and a No. 1 coverslip (VWR) was placed on top of the sample. The cover slip was sealed with nail polish and the slides stored at 4 °C in the dark until visualized (~24 h later).

Cells were visualized using an Olympus 1 × 73 Microscope (Olympus Life Sciences). Fluorphores were excited using Lumen Dynamics Xcite 120 LED (Lumen Dynamics), Olympus LED PS and LBM laser systems (Olympus Life Sciences). Fluorescence emission spectra were captured for Hoescht 33342 (Ex: 250 nm/Em: 461 nm), AlexaFlour® 488 (Ex: 495 nm/Em: 519 nm), and 7-AAD (Ex: 546 nm/Em: 647 nm). In addition to fluorphores, cell morphology was observed using phase contrast (images not included). Images of the stained cells were captured using the Olympus DP80 camera (Olympus Life Sciences) and CellSens Dimensions imaging software (Olympus Life Sciences). Images obtained that were later counted underwent no post-production adjustments. Images presented underwent post-production adjustments using the 'Adjust Display' function in the CellSens Dimensions imaging software. In brief, background colour intensities were excluded from the images using the histogram tool. Colour threshold intensity was then increased. These changes were applied to all the images and at the same intensities.

Exposure times and gain were made constant during the imaging of each biological replicate. Although exposure times varied, the Hoechst 33342 stain was exposed for roughly 250 milliseconds (ms), the Annexin V- Alex-Fluor 488 stain was exposed for roughly 2 seconds (s) with a gain of 2X, and the 7-AAD stain was exposed for roughly 800 ms. All images were taken using a 40X objective lens. 'Live' events were defined as cells with visually uncondensed nuclei, stained with Hoechst 33342, and lacking green Annexin V stain or red 7-AAD stain. 'Early Apoptosis' events were defined as cells that had either or both green Annexin V stain (indicative of phosphatidylserine flipping) and condensed nuclei (condensed blue Hoechst 33342 staining).

Lastly, ‘Late Apoptosis/Necrosis’ was defined as the loss of membrane integrity, which was indicated by the presence of the red stain of 7-AAD (made purple/pink in images). Three biological replicates were performed. For each biological replicate, the events were totalled between ten fields of view counted. A minimum of 300 events was counted per biological replicate. Values were then transformed to a percentage of the total number of events that were counted, for each biological replicate. The average of the three biological replicates was presented and one-way ANOVA was performed between the sublines for each defined event. Tukey post-hoc analysis was done, comparing all the sublines to the pcDNA3 subline.

3.4 Results & discussion

3.4.1 Establishment of a GLC20 model for SCLC studies relating to RBM5

GLC20 cells are *RBM5*-null and were established from a tumor that was multidrug resistant (doxorubicin, cyclophosphamide and vincristine), a common characteristic of advanced SCLC. As depicted in Fig. 3.1A, the breakpoint for the GLC20 deletion is upstream of RBM5, and the entire RBM5 gene is deleted (Lerman and Minna, 2000). We verified the absence of *RBM5* DNA, RNA and protein (Fig. 3.1B–E).

To better understand the impact of RBM5 downregulation on SCLC, stable populations of *RBM5* expressing cells were established. Two *RBM5*-expressing sublines were established, one clonal (designated GLC20.C4 or “C4”) and one from a pooled population of *RBM5*-expressing transfectants (designated GLC20.T2 or “T2”) (Fig. 3.1F). We also established an empty vector control subline (GLC20. pcDNA3 or “pcDNA3”).

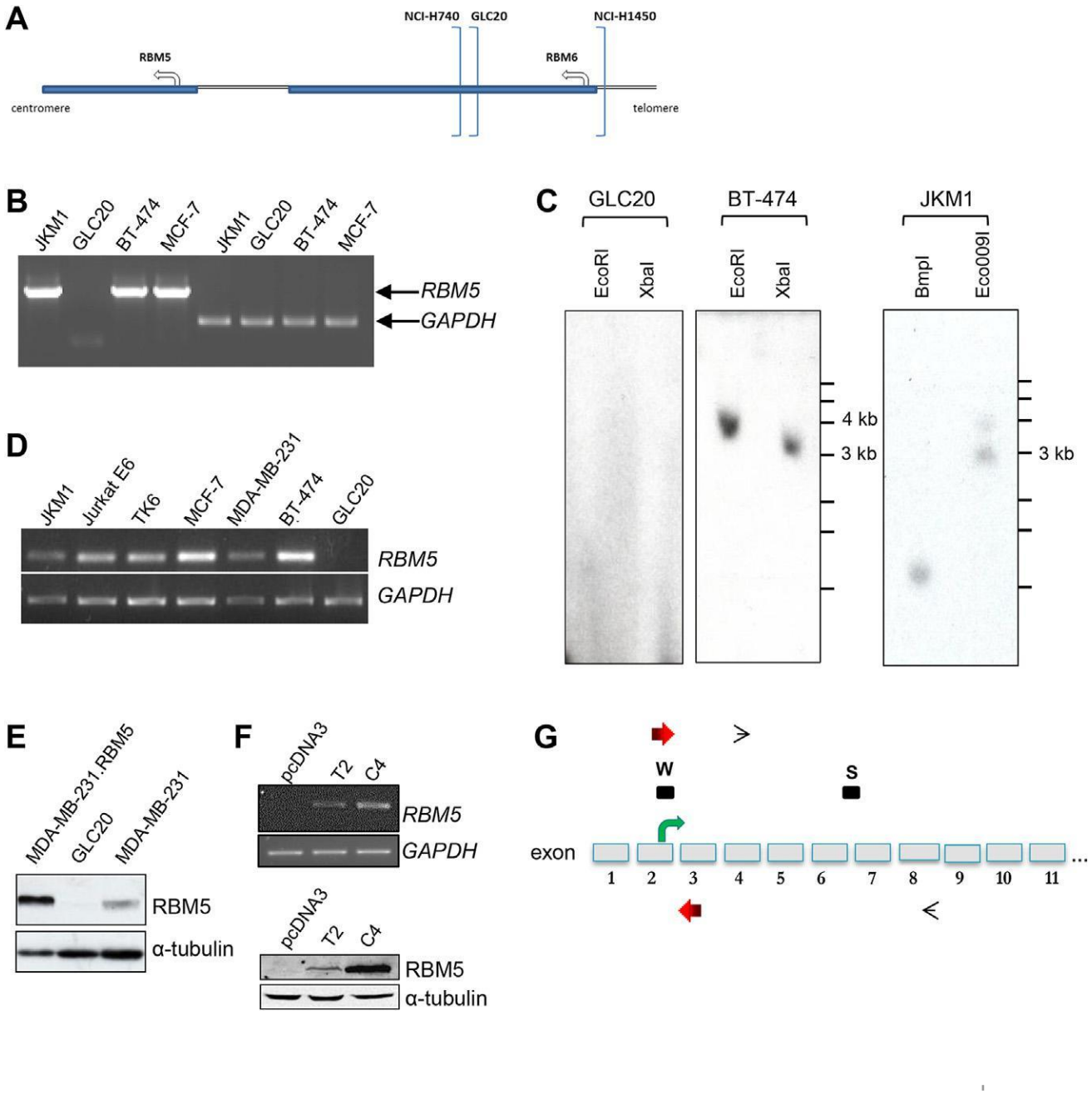

Figure 3.1 Characterization of wildtype GLC20 cells and RBM5 expressing sublines. (A) Cartoon of location of deletion breakpoints in various lung cell lines. (B) Genomic DNA PCR results from different cell lines. (C) RBM5 Southern Blot. (D) RT-PCR results from different cell lines. (E) Western Blot. (F) RBM5 expression in GLC20 stable transfectants by RT-PCR and Western Blot. (G) Cartoon of 5′ end of RBM5 gene, not drawn to scale, showing approximate locations of various probes. Box marked "W": Western antibody LUCA-15 UK; box marked "S": Southern probe; RT-PCR primers LU15(2) and LU15(3) (black thin open arrowheads); genomic PCR primers Gen1E2Fc and Gen2E3I2R (red thick arrows).

To ensure that a GLC20 model would be useful for functional studies relating to RBM5, chiefly known as a modulator of apoptosis, we examined their cell death profile when exposed to various apoptogenic agents. The highly resistant nature of GLC20 cells to chemotherapy was demonstrated (Fig. 3.2), since cisplatin exposure, without etoposide, required a concentration of 80 μg/ml (226 μM) to be somewhat effective at promoting apoptosis by 24 h post exposure (Fig. 3.2A, lanes 1–3). GLC20 cells are, however, capable of undergoing apoptosis, since PARP cleavage was observed 24 h following co-administration of 10 μg/ml (33 μM) cisplatin and 10 or 20 μg/ml (17 or 34 μM) etoposide (Fig. 3.2A, lanes 4–9), and almost complete following 40 to 48 h incubation with these agents (Fig. 3.2B lanes 4–9). Thus, although these cells are highly drug resistant, they are capable of experiencing cisplatin-mediated apoptosis.

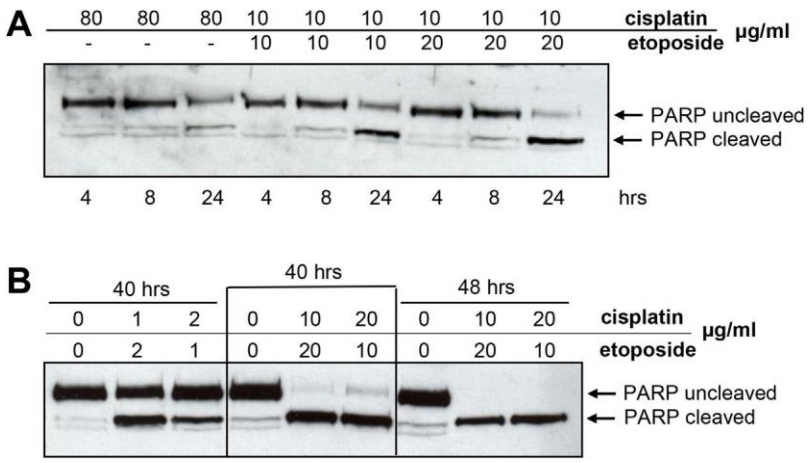

Figure 3.2 Apoptosis induction by various apoptogenic stimuli. GLC20 cells were treated with cisplatin with or without etoposide, for the various times indicated. Details in Materials & methods. See Figure S2 for full blots.

3.4.2 RNA-Seq shows that over 12% of the transcriptome is differentially expressed by RBM5 in GLC20 cells, SLC25A53 is the most altered gene, and pathways relating to cancer are the most likely impacted

To investigate if and how RBM5 expression influences GLC20 cells, deep sequencing of the transcriptome (RNA-Seq) of the parental GLC20 cells and three sublines was carried out. See Materials & methods for an explanation of the "control" used in sequencing analyses.

Firstly, we confirmed *RBM5* expression levels within the transcriptomic data for T2 and C4 (Fig. 3.3A). Differential expression testing (refer to Materials & methods) identified that 12.5% of the transcriptome examined was significantly differentially expressed between control and T2, and 18.4% between control and C4 (Fig. 3.3B). Furthermore, over 50% of the genes that were differentially expressed in T2 were also differentially expressed in C4, suggesting that any effect in C4 is not likely the result of a clonal effect related to subclone establishment. Solute Carrier Family 25 Member 53 (*SLC25A53*) was the most significantly differentially expressed gene in both T2 and C4 compared to control (based on log2 (fold-change); 1112.1 FPKM (Fragments Per Kilobase of transcript per Million mapped reads) to 0.068 FPKM in control vs. C4, and 1127.3 FPKM to 0.073 FPKM in control vs. T2). This gene is part of a large family of transporters that control various cellular functions, although a particular role for SLC25A53 has yet to be identified (Palmieri, 2013). Other highly downregulated genes common to both T2 and C4 include *CD9*, Discs Large Homolog Associated Protein 1 (*DLGAP1*), and Feline Sarcoma (*FES*). Interestingly, CD9 and FES have previously been associated with cell adhesion and tumor metastasis, with the effect of their expression seeming to be cell type-specific (Delfino et al., 2006; Huan et al., 2015; Kanda et al., 2009; Rappa et al., 2015). Of the two, only CD9 has been investigated in regards to SCLC specifically, and low expression levels were linked to increased motility and invasiveness (Funakoshi et al., 2003). The fact that *RBM5* expression decreased *CD9* expression was thus unexpected, as we hypothesized that RBM5 would promote a non-

transformed state in SCLC cells. However, *CD9* gene expression levels in our control were much lower than those in our clinical SCLC tumor samples (described below) (average of 6.6 FPKM in our cell line control and 109.1 FPKM in tumor samples), suggesting that although RBM5's influence on *CD9* may be statistically significant, it may not be physiologically relevant in our system.

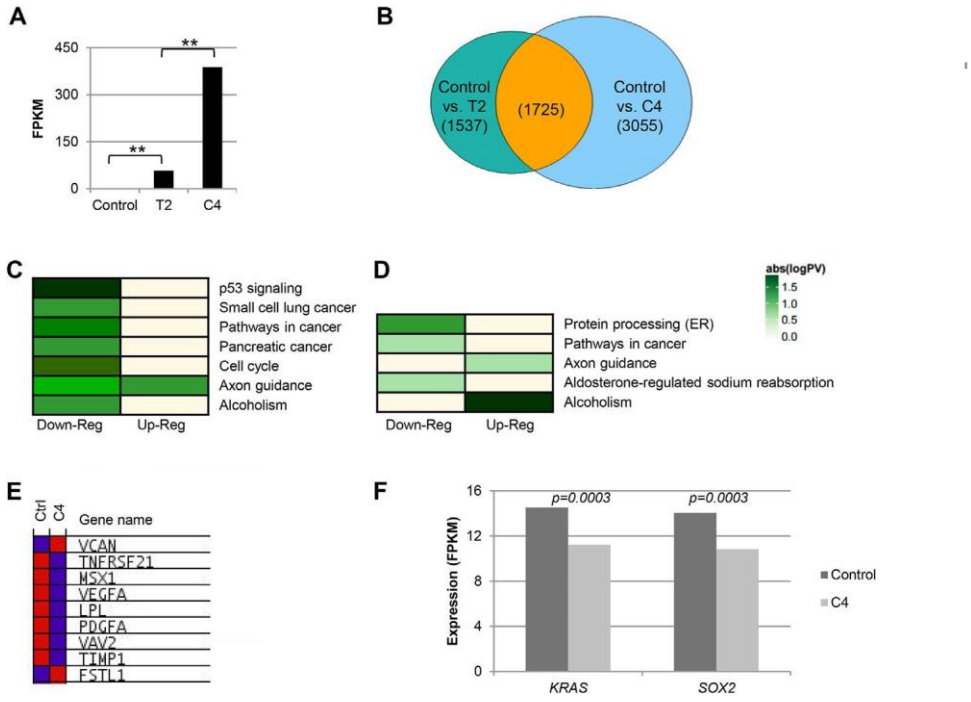

Figure 3.3 Transcriptome analysis of GLC20 sublines. (A) RBM5 expression in control, T2 and C4 samples as determined by RNA-Seq. **p < 0.01. (B) Venn diagram demonstrating significantly differentially expressed genes between T2 and C4 compared to control, respectively, as determined by RNA-Seq. Number of genes in each group indicated in parenthesis. (C and D) FIDEA pathway analysis results for altered KEGG pathways in control vs T2 (C) and C4 (D) samples, respectively, from RNA-Seq transcriptome data. (E) GSAASeqSP blue-pink o'gram representing the expression levels of core enriched genes within the MSigDB Angiogensis Hallmark gene set in control and C4 (RNA-Seq data). Blue indicates low expression, whereas red indicates high expression levels. Genes listed in order of Rank Metric Score. (F) KRAS and SOX2 expression in control and C4 samples as determined by RNA-Seq.

On the other hand, two genes other than *RBM5* were highly upregulated in both T2 and C4 compared to control; *MKRN3* and *ZNF85*. Of note, the former has been previously associated with development, particularly the onset of puberty, which is in line with the pathway results presented below (Abreu et al., 2013).

Using two different pathway analysis programs, we went on to determine the functional implications of genes differentially expressed upon expression of *RBM5*. First, the Functional Interpretation of Differential Expression Analysis (FIDEA) (D'Andrea et al., 2013) program with the Kyoto Encyclopedia of Genes and Genomes (KEGG) pathway database (Kanehisa and Goto, 2000; Kanehisa et al., 2014) was used, thus differentially expressed genes are placed in known signaling pathways to determine if these pathways are significantly up- or downregulated. Analysis results are presented in Fig. 3.3C and D. Pathways in cancer was significantly downregulated in both T2 and C4 compared to control. Other transformation-related pathways were also downregulated upon *RBM5* expression in T2 such as the cell cycle, small cell lung cancer and pancreatic cancer. The fact that these pathways were not also significantly changed in C4 may be due to the larger number of differentially expressed genes in this sample, which may mask the effect of RBM5 on these particular cancer-related pathways. In addition, both axon guidance and alcoholism were significantly altered in both T2 and C4. This is very interesting since axon guidance, as well as alcoholism, have been shown to play a substantial role in cancer development and progression (Chedotal et al., 2005; Forsyth et al., 2010).

To complement our KEGG pathway results, we used an additional pathway analysis program − the Gene Set Association Analysis for RNA-Seq with Sample Permutation (GSAASeqSP) program (Xiong et al., 2014) - as it takes into account inherent bias present in RNA-Seq data. In combination with the Broad Institute's Molecular Signatures Database (MSigDB) Hallmark gene set (Liberzon et al., 2015), genes are grouped based on established biological processes, and enriched gene sets determined. We identified 12 and 17 gene sets with false discovery rates

(FDR) at or below 10% in T2 and C4, respectively, compared to control. Over half of these T2 altered gene sets were common to C4, once again suggesting that any effect seen in C4 is not likely due to a clonal effect related to subclone establishment. Gene sets with FDR at or below 10% in control vs. C4 are presented in Table 3.1, along with their FDR in control vs. T2. Interestingly, many differentially expressed gene sets are important to development, which validates our experimental findings, as RBM5 was recently shown to be involved in myogenesis, spermatogenesis and neuronal development (Fushimi et al., 2008; Loiselle and Sutherland, 2014; O'Bryan et al., 2013). Furthermore, apoptosis and TNFα signaling, both pathways RBM5 has been previously associated with in Jurkat T lymphoblastoid cells (Rintala-Maki and Sutherland, 2004; Sutherland et al., 2000) and MCF-7 cells (Rintala-Maki et al., 2004) were altered in T2 and C4. Fig. 3.4 lists the core enriched genes in these gene sets and how their expression changed upon RBM5 expression in C4, highlighting the importance of RBM5 to these cellular functions.

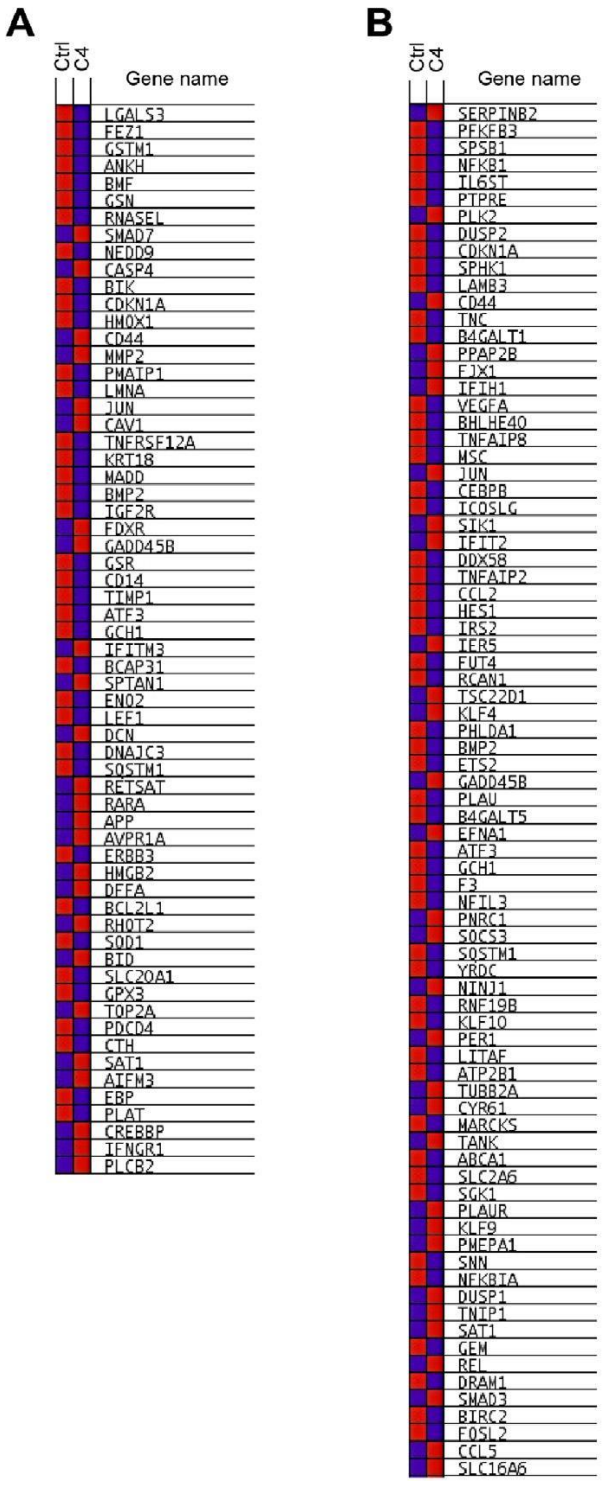

Figure 3.4 Expression changes of core enriched genes in RBM5-altered gene sets. GSAASeqSP blue-pink o'gram representing the expression changes of core enriched genes from the MSigDB Hallmark Apoptosis (A) and TNFα signaling via NFκB (B) gene sets in control vs. C4 samples (RNA-Seq data). Blue indicates low expression, whereas red indicates high expression. Genes listed in order of Rank Metric Score.

Other gene sets identified in this GSAASeqSP analysis are important to the transformed state, supporting our KEGG pathway results and providing additional insight into the role of RBM5 in SCLC cells. These gene sets (Table 3.1) include genes involved in (a) angiogenesis, where *RBM5* expression (in T2 and C4) correlated with significantly decreased expression of pro-angiogenic factors, such as Vascular Endothelial Growth Factor A (*VEGFA*) (Fig. 3.3E), (b) epithelial to mesenchymal transition (EMT), and (c) the immune response. RBM5 may, therefore, not only promote a non-transformed state, but be important for identification and elimination of cells that adopt cancerous characteristics.

Table 3.1: Altered gene sets Altered gene sets with FDR below 10% between control and C4 samples, as determined by GSAASeqSP analysis with the MSigDB Hallmark gene set using the samples' RNA-Seq results. Ranked based on FDR value in control vs. C4 analysis. FDR value in control vs. T2 samples is also indicated for the given pathways. Italics indicates FDR values above 10%.

	Control vs. C4	Control vs. T2
Gene Set	FDR	FDR
Hedgehog signaling	0.000	0.033
Angiogenesis	0.000	0.067
Apoptosis	0.054	0.28
Androgen response	0.058	0.067
Myogenesis	0.064	0.183
Estrogen response late	0.064	0.033
TNFα signaling via NF-κB	0.070	0.075
Coagulation	0.071	0.115
IL2 STAT5 signaling	0.075	0.125
UV response down	0.076	0.226
Apical surface	0.078	1.000
Cholesterol homeostasis	0.080	0.113
IL6 JAK STAT3 signaling	0.083	0.147
Estrogen response early	0.087	0.057
Inflammatory response	0.094	0.432
KRAS signaling up	0.100	0.114
Epithelial to mesenchymal transition	0.100	0.073

Taken together, these RNA-Seq pathway analysis results for the GLC20 sublines indicate that in SCLC cells, *RBM5* expression is very important to the maintenance of the non-transformed state, particularly via regulation of cell death, angiogenesis, cell-cell adhesion and immune response pathways.

3.4.3 RBM5 regulates expression of SCLC-associated genes

To investigate the influence of *RBM5* expression particularly on SCLC-associated pathways, we examined the expression of previously identified lung cancer-associated genes in our GLC20 sublines. In a report released by the National Cancer Institute (NCI) in June 2014, entitled Scientific Framework for Small Cell Lung Cancer, a list of 37 ‘Genes of Interest in SCLC’ was compiled. Interestingly, the expression of 43.2% of these ‘Genes of Interest in SCLC’ (16/37) significantly changed expression in C4, compared to control (Table 3.2), with 11 of these differentially expressed genes changing expression in a manner that would promote suppression of tumor growth upon *RBM5* expression; *BCL2*, *CCNE1*, *COBL*, *CREBBP*, *EPHA7*, *MED12L*, *MYCL1*, *RAB37*, *SLIT2*, *SMO* and *SOX2*. Furthermore, 11 of the 21 non-differentially expressed genes had very low expression in the control and C4 (FPKM below one), and thus may not play an important role in GLC20 cells. The observation that *RBM5* expression influences the expression levels of so many NCI-collated ‘Genes of Interest in SCLC’ highlights (1) the importance of RBM5 to SCLC, (2) the impact that *RBM5* gene deletion may have on the development of lung cancer, and (3) the effect that re-establishment of *RBM5* expression may have on SCLC tumors.

Table 3.2: Expression of NCI 'Genes of Interest in SCLC' in control and C4 samples, as determined by RNA-Seq. Expression values are expressed as FPKM. Italics identify genes with non-significant differential expression between control and C4 and expression below one FPKM in both samples.

Gene name	Control	C4	p-value	Significance
BCL2†	1.8307	0.2914	0.00005	Yes
CCNE1†	18.139	10.6106	0.00005	Yes
CDK14‡	17.0371	19.8042	0.0083	Yes
CDKN2A	78.3537	89.0263	0.0378	No
COBL†	0.885007	0.011419	0.004	Yes
CREBBP‡	5.47952	6.5709	0.0018	Yes
DMBX1	0.048243	0.102193	1	No
EP300	7.62326	7.82019	0.789641	No
EPHA7‡	20.1031	26.6501	0.0001	Yes
FGFR1	0.171331	0.212293	1	No
GPR113	0.475767	0.661619	0.6777	No
GPR133	0.003737	0	1	No
GPR55	0.001965	0	1	No
GRID1	0.553261	0.587185	0.6624	No
LRRK2	0.068785	0.016732	1	No
MED12L†	3.18195	0.191165	0.00005	Yes
MLL (KMT2A)	11.1758	11.5143	0.5842	No
MYCL†	11.114	8.99515	0.0044	Yes
NOTCH1‡	4.87757	6.22612	0.00005	Yes
NOTCH2‡	3.44146	4.85108	0.00005	Yes
NOTCH3	0.06277	0.11642	1	No
PIK3CA	9.39427	8.64243	0.1883	No
PPEF2	0.037315	0.063875	1	No
PRKD3	26.8136	28.0848	0.4054	No
PTEN†	17.1134	14.0056	0.0007	Yes
PTPRD	0	5.72938	1	No
RAB37†	0.660452	0.186656	0.00005	Yes
RASGRF1	0.00182	0.006163	1	No
RASGRF2	0.377979	0.006163	1	No
RB1	6.22425	6.86606	0.1533	No
RUNX1T1‡	5.11373	8.39718	0.00005	Yes
SLIT2‡	5.19232	9.74325	0.00005	Yes
SMO†	5.93771	3.35434	0.00005	Yes
SOX2†	14.0653	10.8382	0.0003	Yes

Table 3.2.
(Continued)

Gene name	Control	C4	p-value	Significance
STK38	20.2447	18.0817	0.0533	No
TP53	2.85615	3.40231	0.2023	No
TRRAP	13.9452	12.2657	0.0716	No

† Indicates genes significantly downregulated in C4.
‡ Indicates genes significantly upregulated in C4.

In addition to these NCI-collated 'Genes of Interest in SCLC', we examined the influence of RBM5 expression on Sex-determining region Y-box 2 (*SOX2*) and Kirsten Rat Sarcoma Viral Oncogene Homolog (*KRAS*), as overexpression of the former has been observed in many types of lung cancers and is linked with tumor initiation (Tam and Ng, 2014), and activation of the latter occurs in approximately 30% of smoking-associated lung adenocarcinomas (Unni et al., 2015). In our C4 samples, *SOX2* and *KRAS* were significantly downregulated (Fig. 3.3F), suggesting once again the importance of RBM5 expression in lung tissue.

3.4.4 Alternative splicing accounts for a minority of the differential gene expression

RBM5 influences processes such as apoptosis and cell cycle arrest in a variety of cancer cell lines at least in part via the modulation of alternative splicing of key factors, such as *NUMB* and CASPASE 2 (*CASP2*) (Bechara et al., 2013; Fushimi et al., 2008). To see if RBM5 influences processes in SCLC via modulation of alternative splicing, we mined our RNA-Seq data for significant alternative splicing changes.

In the control vs. T2 group, 2,546 variants were significantly differentially expressed (5.12% of the 49,772 variants examined), with 10 genes showing a significant change from one alternative splice variant to another (Table 3.3). In the control vs. C4 group, 4,180 variants were differentially expressed, with 47 genes showing a significant change from one alternative splice variant to another (Table 3.4). The greater number of alternative splicing events occurring in the C4 subline, compared to T2, suggests an additive effect of RBM5 on alternative splicing, which was expected. There was no overlap, however, of splicing events between T2 and C4, potentially due to the stringent search parameters used, and no significant enrichment of these splicing events in any KEGG pathway or MSigDB Hallmark gene set. Furthermore, the number of significant alterations in splicing between control and T2 and C4, respectively, was much lower than expected, given the high number of differentially expressed genes (even considering the stringent search parameters). This suggests that modulation of alternative splicing is not the only means by which RBM5 influences important transformation-associated pathways in SCLC. RBM5 may, for instance, regulate gene expression levels by influencing transcription or stabilizing transcripts, as has been shown for other RNA-binding proteins, including the RBM5-related protein RBM10 (Guallar and Wang, 2014; Mueller et al., 2009). We therefore proceeded to carry out binding studies in order to identify targets with which RBM5 interacts, either directly or indirectly, and thereby gain a better understanding of how RBM5 influences the identified pathways.

Table 3.3: Genes with at least one alternative splice variant significantly upregulated, and at least one alternative splice variant significantly downregulated between control and T2 (RNA-Seq results). Each row indicates expression levels of a different variant for the given gene. Arranged alphabetically, by gene.

	Control vs. T2		
Gene name	Log2 (fold-change)	p-value	q-value
BAG6	0.633915	0.0002	0.00279
	-2.0923	0.0027	0.03018
EML1	1.18146	0.004	0.04069
	-0.321613	0.0019	0.02236
FERMT2	-0.682011	0.0012	0.01589
	0.326233	0.0039	0.04029
INF2	-0.707866	5e-05	0.00106
	1.40674	5e-05	0.00106
IQCE	-1.59194	0.0004	0.00645
	0.571945	0.0045	0.04469
KCTD15	0.509451	0.0006	0.00906
	-0.932889	5e-05	0.00106
KIF2A	1.13138	5e-05	0.00106
	-1.01307	5e-05	0.00106
LIG3	1.44254	0.0003	0.00434
	-0.360436	0.0007	0.01032
LIPA	0.547552	0.0005	0.0078
	-0.676966	5e-05	0.00106
ZBTB14	-1.18342	0.0025	0.02843
	2.62976	0.001	0.01382

Table 3.4: Genes with at least one alternative splice variant significantly upregulated, and at least one alternative splice variant significantly downregulated between control and C4 (RNA-Seq results). Each row indicates expression levels of a different variant for the given gene. Arranged alphabetically, by gene.

	Control vs. C4		
Gene	log2 (fold-change)	p-value	q-value
ADAM22	0.983	8E-04	0.007
	-0.691	0.006	0.0374
ADAT2	-0.412	0.002	0.0155
	0.885	1E-04	0.0011
AR	0.444	5e-05	0.0006
	-0.979	0.002	0.0119
ASAP1	-0.454	0.003	0.0219
	0.722	5e-05	0.0006
ASPH	1.693	1E-04	0.0011
	-0.679	0.005	0.0327
ATG16L1	0.718	5e-05	0.0006
	-0.648	0.003	0.0204
BCKDHB	0.544	0.004	0.0242
	-0.531	2E-04	0.0016
BZW2	-1.239	0.001	0.0091
	0.281	0.002	0.0125
C14orf93	-1.649	8E-04	0.0066
	1.096	0.002	0.0149
C8orf59	-0.413	0.004	0.0267
	0.564	0.001	0.0098
CDK13	0.711	1E-04	0.0011
	-0.303	0.003	0.0201
CEP41	1.715	0.006	0.0395
	-0.482	5e-05	0.0006
CEP78	-1.025	5e-05	0.0006
	1.100	5e-05	0.0006
CTNNB1	0.498	0.004	0.0281
	-0.689	5e-05	0.0006
DMTF1	-0.427	0.002	0.0155
	1.026	0.001	0.0091
DST	-0.791	5e-05	0.0006
	0.740	4E-04	0.0034
GGA1	1.047	8E-04	0.007

Table 3.4. (Continued)

	Control vs. C4		
Gene	log2 (fold-change)	p-value	q-value
	-1.099	0.002	0.0161
	1.028	0.001	0.0091
HMGXB4	0.567	5e-05	0.0006
	-0.764	5e-05	0.0006
KIAA1958	1.630	1E-04	0.0011
	-1.107	4E-04	0.0034
LIMA1	1.434	0.003	0.0213
	-0.742	5e-05	0.0006
MAPKAP1	0.660	5e-05	0.0006
	-0.474	0.001	0.0105
MUM1	0.479	0.004	0.0248
	-0.875	5e-05	0.0006
MYO1B	0.763	5e-05	0.0006
	0.906	0.001	0.0098
	-1.790	0.004	0.0273
NAP1L1	-0.41	0.001	0.0109
	0.404	0.002	0.0167
NUMB	-1.472	0.008	0.0499
	0.951	0.005	0.0314
	-0.516	8E-04	0.0066
PAXBP1	-1.167	0.005	0.0319
	1.058	5e-05	0.0006
PCBP2	-1.724	0.002	0.0177
	0.652	0.006	0.0356
PDE1C	-0.722	8E-04	0.007
	0.911	5e-05	0.0006
PDHA1	-0.269	0.007	0.0435
	2.175	0.003	0.0195
PHF8	0.834	2E-04	0.0021
	-0.396	0.006	0.0374
PTK2	0.558	0.003	0.0231
	-0.666	5e-05	0.0006
RAC1	0.297	0.006	0.0389
	-1.588	5e-05	0.0006
RBBP5	-1.255	5e-05	0.0006
	0.472	0.002	0.017

Table 3.4. (Continued)

	Control vs. C4		
Gene	log2 (fold-change)	p-value	q-value
RBFOX2	0.971	5e-05	0.0006
	-0.499	3E-04	0.0026
RPAP3	-1.041	0.005	0.0309
	0.308	0.005	0.0303
RTN1	0.501	4E-04	0.0034
	-2.439	3E-04	0.003
SLC29A1	-0.849	5e-05	0.0006
	0.395	0.005	0.0325
SLC9A6	-1.393	5e-05	0.0006
	0.492	0.006	0.0364
SSBP3	0.785	5e-05	0.0006
	-0.597	3E-04	0.003
SYT1	1.903	5e-05	0.0006
	-5.079	1E-04	0.0011
TPM1	1.473	5e-05	0.0006
	-0.922	0.004	0.0258
UGGT1	0.626	5e-05	0.0006
	-0.95	5e-05	0.0006
UPF3B	0.927	5e-05	0.0006
	-1.231	5e-05	0.0006
ZBTB20	-1.234	0.004	0.0261
	0.746	6E-04	0.0055
ZNF260	0.424	2E-04	0.0021
	-0.933	0.001	0.0098
ZNF566	0.791	0.004	0.0273
	-0.804	5E-04	0.0043
ZNF655	-1.174	0.005	0.034
	0.690	0.007	0.0425

3.4.5 RIP-Seq identified RBM5 RNA targets regulate RNA metabolism and cell cycle pathways, ZNRF3 being the most enriched gene

Although some studies have investigated RBM5's binding motif (Bechara et al., 2013; Ray et al., 2013), the number of identified RNA targets that are directly bound by RBM5 is low. In cancer cell lines, only three directly bound RNA targets have been identified to date; Caspase-2 (CASP2) (Fushimi et al., 2008), the antisense transcript of FAS (FAS-AS1) (Sehgal et al., 2014), and Activation-induced cytidine deaminase (AID) (Jin et al., 2012). In mouse spermatid differentiation, 11 RNA targets have been identified (O'Bryan et al., 2013). In its capacity as a component of spliceosomal complexes (Hegele et al., 2012; Niu et al., 2012), RBM5 is also likely capable, however, of binding many important RNA targets indirectly (e.g., via another protein within the complex).

In order to identify direct and indirect RNA targets of the RBM5 protein in GLC20 cells, we used RNA Immunoprecipitation followed by next generation sequencing (RIP-Seq). RIP-Seq experiments were performed using our non-commercially available RBM5-specific LUCA-15UK antibody (Sutherland et al., 2000) because, as demonstrated in Fig. 3.5, the commercially available antibodies that were tested were not specific for RBM5. Two different negative controls were used in each of two RIP-Seq replicates, to ensure the validity of identified RBM5 targets. Firstly, a non-specific IgG IP in C4 cells (vs. LUCA-15UK IP in C4 cells), and secondly, LUCA-15UK IP in GLC20.pcDNA3 cells (vs. LUCA-15UK IP in C4 cells). Western blots showing successful IP of RBM5 for both replicates are presented in Fig. 3.6A.

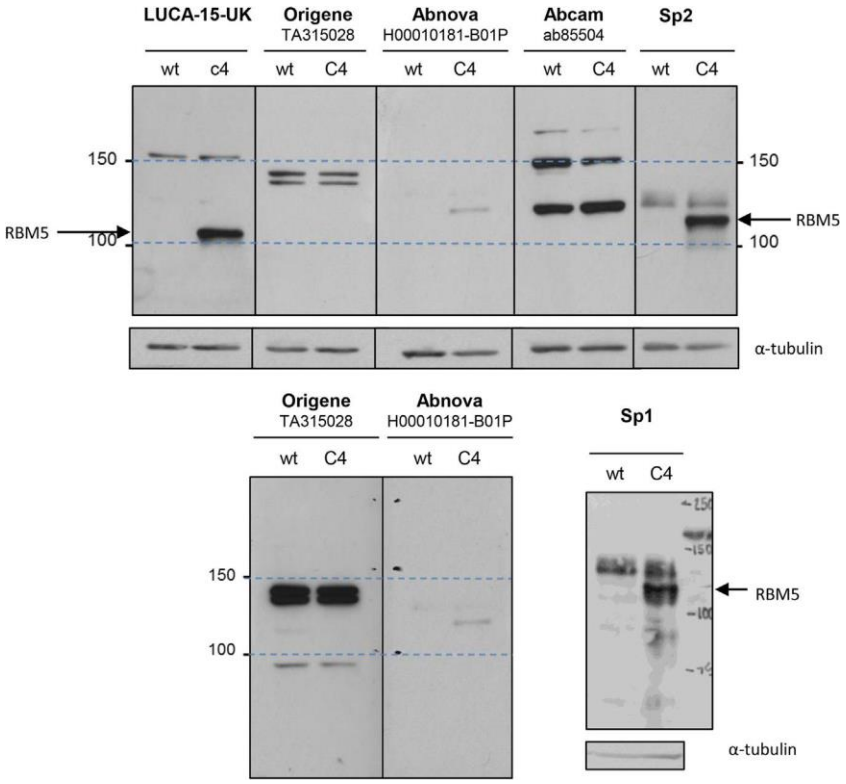

Figure 3.5 RBM5 antibody testing. The same whole cell lysate from either GLC20 cells (wt) or GLC20.C4 RBM5 containing cells (C4) was loaded in alternate lanes and probed with the antibodies indicated. The LUCA-15-UK blot was probed with a 1:1000 antibody dilution, overnight at 4 °C, and exposed for 2 min. The upper Origene blot was probed with a 1:3000 antibody dilution, for 3 h at RT, and exposed for 60 min. The lower Origene blot was reprobed with a 1:500 antibody dilution, overnight at 4 °C, and exposed for 60 min. The upper Abnova blot was probed with a 1:500 antibody dilution, for 3 h at RT, and exposed for 60 min. The lower Abnova blot was reprobed with a 1:350 antibody dilution, overnight at 4 °C, and exposed for 60 min. The Abcam blot was probed with a 1:2500 antibody dilution, overnight at 4 °C, and exposed for 5 min. The Sp1 and Sp2 blots were probed with a 1:5000 antibody dilution, for 3 h at RT, and exposed for 1 min. All commercially available antibodies (therefore excluding Sp1 and Sp2 – a gift from Juan Valcárcel − and LUCA-15-UK) interacted with product around the same molecular weight as RBM5 even in GLC20 cells, making them unsuitable for use in RIP-Seq experiments.

RNA from both RIP-Seq experiments was sequenced. The distribution of gene expression values in our control vs. RBM5 RIP samples is presented in Fig. 3.6B, for genes with FPKMs < 5000 (10 genes had FPKMs above 5000). This figure highlights the high level of gene expression in our RBM5 RIP samples, compared to the control, confirming the success of our technique. We identified 773 genes as RBM5 targets (see Materials & methods for exclusion details), a not unexpectedly large number since this technique identifies all RNA bound by a complex of which RBM5 is a part.

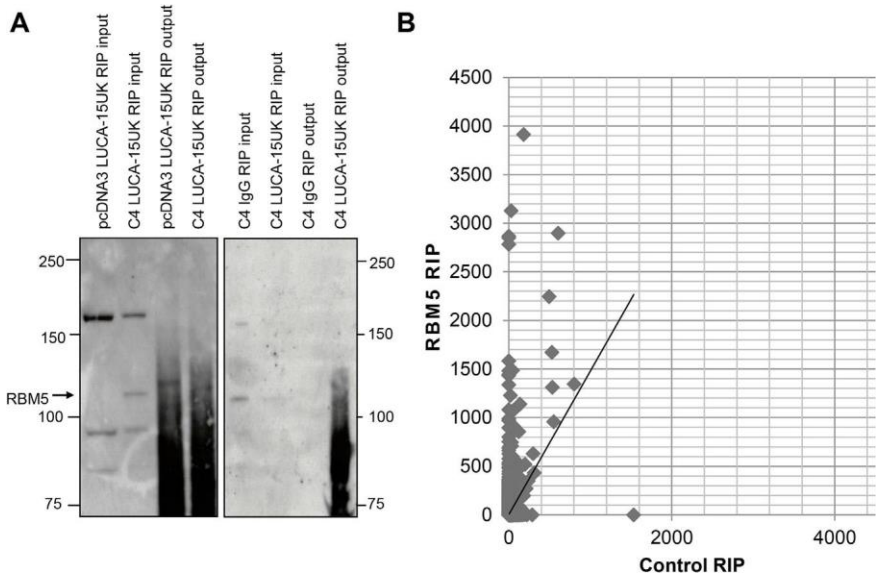

Figure 3.6 RBM5 RIP-Seq optimization and quality control. (A) Raw Western Blot data demonstrating successful immunoprecipitation of RBM5. (B) Scatterplot representing expression of genes with FPKM < 5000 in control and RBM5 RIP samples, respectively. All Western Blot ladder sizes are in kilodaltons (kDa).

The most significant RBM5 targets included Zinc & ring finger 3 (*ZNRF3*), Suppressor of cancer cell invasion (*SCAI*), Growth factor receptor-bound protein 2 (*GRB2*), Zw10 kinetochore protein (*ZW10*), DEP domain containing (*DEPDC1*) and Activating transcription factor 2 (*ATF2*). None of these genes were detected in the control IP and all had FPKM values above 350 in the RBM5 RIP (*ZNRF3* had the highest count with 1.23×10^7 FPKM, followed by *SCAI* with 2866.53 FPKM and *GRB2* with 1482.74 FPKM). Interestingly, these six genes have all been shown to play important roles in the control of the cell cycle and proliferation. It is important to note that the previously identified direct RBM5 targets - *CASP2*, *FAS* and *AID* - were not identified in our RIP-Seq experiments. Lack of detection of these potentially direct targets could be a cell type-specific phenomenon, since neither *FAS* nor *AID* were expressed above 0.1 FPKM in our samples.

To determine the importance of these targets to cellular functions, pathway analysis was carried out on RIP-Seq identified RBM5 RNA targets. FIDEA analysis, using the KEGG database, identified only three significantly changed pathways; 'Spliceosome' (hsa03040) (with a Benjamini value of 1.37×10^{-4}),'RNA transport' (hsa03013) (1.53×10^{-3}) and 'Ribosome' (hsa03010) (9.07×10^{-3}). These results support our findings that RBM5 influences important pathways in SCLC via regulation of alternative splicing and other pre- and/or post-transcriptional processes. These results also help to confirm the success of our technique, since RBM5 was previously shown to be a key component of spliceosomal complexes (Hegele et al., 2012; Niu et al., 2012).

As with our RNA-Seq data, we used an additional pathway analysis program to support our results. For this RIP-Seq data, our second program was Cytoscape with the Reactome FI Network plugin, as the GSAASeq program is designed specifically for RNA-Seq data. Using Reactome, we found 68 pathways with an FDR < 8% (Table 3.5), many involved in gene expression and mRNA splicing/ metabolism. Interestingly, there was an enrichment of RBM5 targets in the EGFR pathway (Fig. 3.7), as well as many cell cycle pathways and the 'Apoptosis induced DNA fragmentation' pathway (Fig. 3.8), supporting our RNA-Seq results and suggesting that RBM5 may play a direct role in regulating the cell cycle and apoptosis in SCLC cells.

Table 3.5: RBM5 RIP-Seq results, showing top enriched pathways (FDRs below 8%), identified by Cytoscape Reactome FI Plugin tool using the Reactome Pathway Database.

Reactome Pathway	FDR
Nonsense-Mediated Decay (NMD)	5.88E-05
NMD enhanced by the Exon Junction Complex	5.88E-05
Influenza Infection	6.67E-05
HATs acetylate histones	7.14E-05
Influenza Life Cycle	7.69E-05
Processing of Capped Intron-Containing Pre-mRNA	8.33E-05
GTP hydrolysis and joining of the 60S ribosomal subunit	9.09E-05
NMD independent of the Exon Junction Complex	1.00E-04
mRNA Splicing	1.00E-04
mRNA Splicing - Major Pathway	1.00E-04
Influenza Viral RNA Transcription and Replication	1.05E-04
Eukaryotic Translation Elongation	1.11E-04
L13a-mediated translational silencing of Ceruloplasmin expression	1.25E-04
3' -UTR-mediated translational regulation	1.25E-04
Eukaryotic Translation Initiation	1.67E-04
Cap-dependent Translation Initiation	1.67E-04
Cell Cycle, Mitotic	2.27E-04
Formation of a pool of free 40S subunits	2.38E-04
Translation	2.50E-04
Attenuation phase	2.61E-04
Metabolism of proteins	3.08E-04
Translation initiation complex formation	3.20E-04
Ribosomal scanning and start codon recognition	3.20E-04
Chromatin modifying enzymes	3.33E-04
Chromatin organization	3.33E-04
SRP-dependent cotranslational protein targeting to membrane	6.88E-04
Cellular responses to stress	6.97E-04
Cell Cycle	7.10E-04
Activation of the mRNA upon binding of the cap-binding complex and eIFs, and subsequent binding to 43S	7.33E-04
Mitochondrial biogenesis	7.35E-04
Viral mRNA Translation	7.59E-04
Peptide chain elongation	7.59E-04
Eukaryotic Translation Termination	7.59E-04
HSF1-dependent transactivation	9.14E-04
Organelle biogenesis and maintenance	1.00E-03
Gene Expression	1.00E-03
Calnexin/calreticulin cycle	1.84E-03

Table 3.5. (Continued)

Reactome Pathway	FDR
Deadenylation of mRNA	2.11E-03
G2/M Transition	2.21E-03
Transcriptional activation of mitochondrial biogenesis	2.53E-03
Mitotic G2-G2/M phases	2.81E-03
N-glycan trimming in the ER and Calnexin/Calreticulin cycle	4.26E-03
EGFR downregulation	4.67E-03
Cellular response to heat stress	6.91E-03
ISG15 antiviral mechanism	7.04E-03
Antiviral mechanism by IFN-stimulated genes	7.04E-03
M Phase	7.45E-03
Formation of the ternary complex, and subsequently, the 43S complex	1.07E-02
Activation of gene expression by SREBF (SREBP)	1.11E-02
Deadenylation-dependent mRNA decay	1.11E-02
Regulation of PLK1 Activity at G2/M Transition	1.12E-02
Regulation of cholesterol biosynthesis by SREBP (SREBF)	1.84E-02
Cellular Senescence	2.37E-02
Mitotic Anaphase	2.40E-02
Mitotic Prometaphase	2.51E-02
Mitotic Metaphase and Anaphase	2.55E-02
Resolution of Sister Chromatid Cohesion	3.48E-02
Centrosome maturation	4.44E-02
Recruitment of mitotic centrosome proteins and complexes	4.44E-02
Loss of Nlp from mitotic centrosomes	6.15E-02
Loss of proteins required for interphase microtubule organization from the centrosome	6.15E-02
mRNA Splicing – Minor Pathway	7.52E-02
MicroRNA (miRNA) biogenesis	7.79E-02
Initiation of Nuclear Envelope Reformation	7.79E-02
Nuclear Envelope Reassembly	7.79E-02
Recycling of eIF2:GDP	7.79E-02
Apoptosis induced DNA fragmentation	7.79E-02
Activator of DNA fragmentation factor	7.79E-02

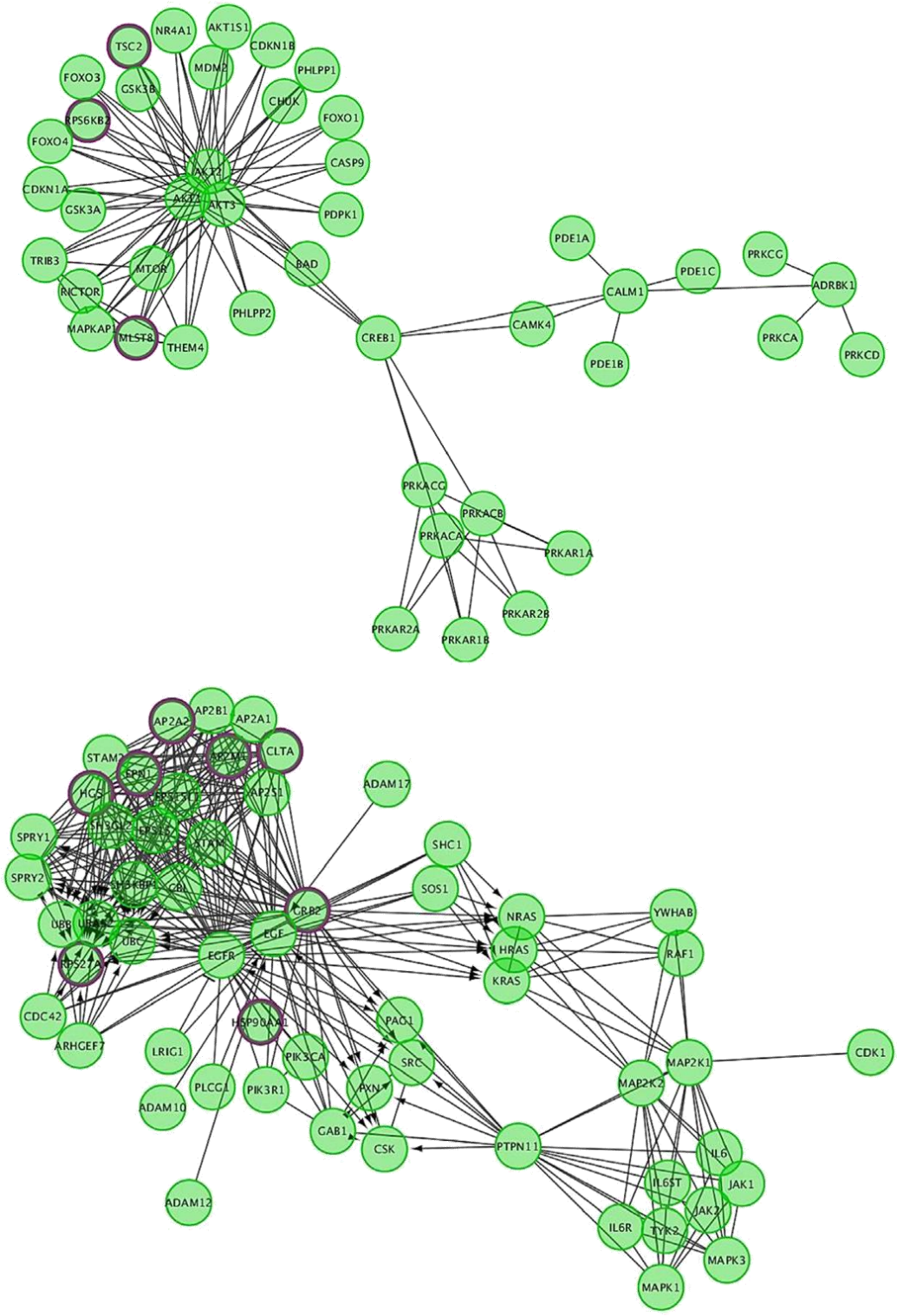

Figure 3.7 RBM5 targets in the EGFR signaling pathway. Network analysis results of RBM5 targets (identified by RIP-Seq) in a portion of the EGFR Signaling pathway. Purple indicates that the gene was identified as an RBM5 target.

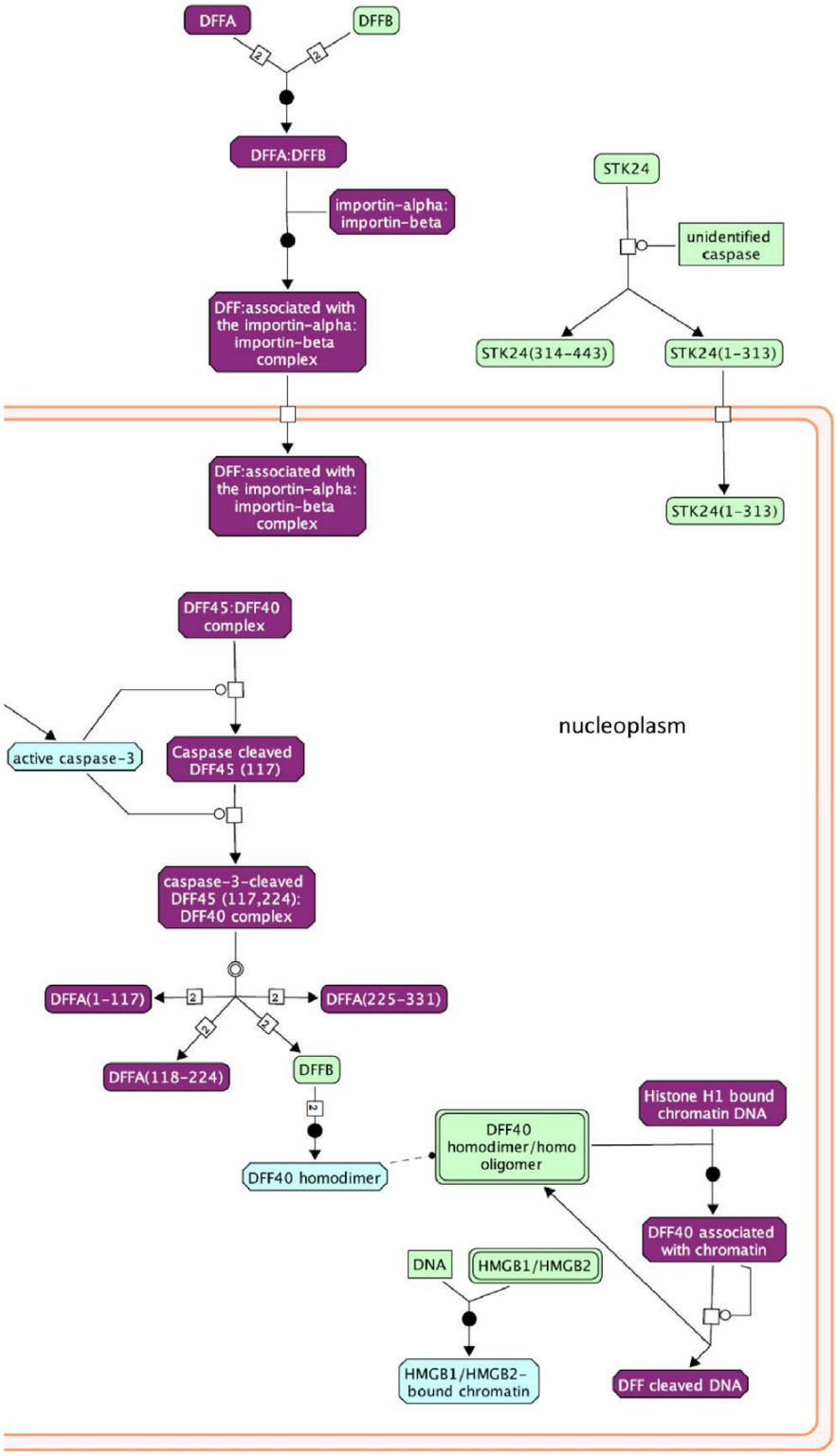

Figure 3.8 RBM5 targets in the Apoptotic Execution Phase pathway. Pathway analysis results of RBM5 targets (identified by RIP-Seq) in a portion of the Reactome Apoptotic Execution Phase pathway. Purple indicates that the gene was identified as an RBM5 target.

It is interesting to note that of all the genes shown in our RNA-Seq experiments to experience a significant change in alternative splicing upon RBM5 expression in T2 or C4 (Table 3.3 and Table 3.4), only one, ArfGAP with SH3 Domain, Ankyrin Repeat and PH Domain (ASAP1), was identified as an RBM5 target in our RIP-Seq experiments. This suggests that the effect of *RBM5* expression on alternative splicing largely results from downstream consequences of changes in *RBM5* expression, as opposed to a targeted RBM5 interaction with the alternatively spliced transcript.

Taken together, our RNA-Seq and RIP-Seq pathway analyses revealed that RBM5 directly influences many processes involved in the maintenance of a non-transformed state, and this by means distinct from regulation of alternative splicing.

3.4.6 Functionally, RBM5 inhibits cell growth and sensitizes cells to cisplatin–mediated apoptosis

In other cancer cell lines, RBM5 has been shown to regulate the cell cycle and modulate responses to apoptogenic stimuli (Kobayashi et al., 2011; Oh et al., 2006; Rintala-Maki and Sutherland, 2004). Since we identified ‘Cell Cycle’ (Fig. 3.3C and D) and ‘Apoptosis’ (Table 3.1) as pathways likely influenced by the differentially expressed genes in T2 and C4, respectively, we decided to validate our sequencing data by carrying out functional studies.

To see if and how RBM5 affects the cell cycle in SCLC, we performed a proliferation and membrane integrity assay using our GLC20 cells and sublines. As shown in Fig. 3.9A, C4 had significantly decreased cell numbers, relative to the vector control, by day six, while membrane integrity was unaffected (Fig. 3.9B). This suggests that when RBM5 levels are high, such as in

C4, RBM5 slows cell cycle progression in untreated SCLC cells, thereby promoting a non-transformed state, a result that supports our RNA-Seq findings.

In North America, due to the usual late stage diagnosis and consequent metastasis, SCLC tumors are not commonly resected, but rather treated with a combination of platinum-based agents such as cisplatin or carboplatin, and the topoisomerase inhibitor etoposide (Gaspar et al., 2012; Jackman and Johnson, 2005; Johnson et al., 2014; Travis et al., 2004). Initially, the patient may show a complete response to the treatment, but most will relapse as the cancer develops resistance (Jackman and Johnson, 2005). Understanding how SCLC cells develop resistance to these drugs is thus of great importance. We therefore included a platinum-based treatment in our functional analysis, and determined the effects of *RBM5* expression on SCLC cells' response to the drug. Cisplatin was our drug of choice since, as demonstrated in Fig. 3.2, GLC20 cells are already quite resistant to cisplatin, making them a good model for a drug sensitization study. Interestingly, *RBM5* overexpression in the cisplatin-resistant NSCLC cell line A549 reduced resistance to cisplatin, manifesting as increased cisplatin-induced apoptosis (Li et al., 2012), thus we expected that RBM5 expression in our SCLC cell line would have a similar effect.

The GLC20 parental cell line and sublines were treated with 1 μM cisplatin, and cell proliferation and membrane integrity assessed. Both T2 and C4 cells showed significantly decreased cell numbers, relative to the vector control, following 10 days of cisplatin exposure (Fig. 3.9A), and a significant decrease in membrane integrity by day four (Fig. 3.9B). In addition, the IC_{50} for cisplatin in both of the *RBM5* expressing sublines was significantly lower than the vector control (Fig. 3.9C).

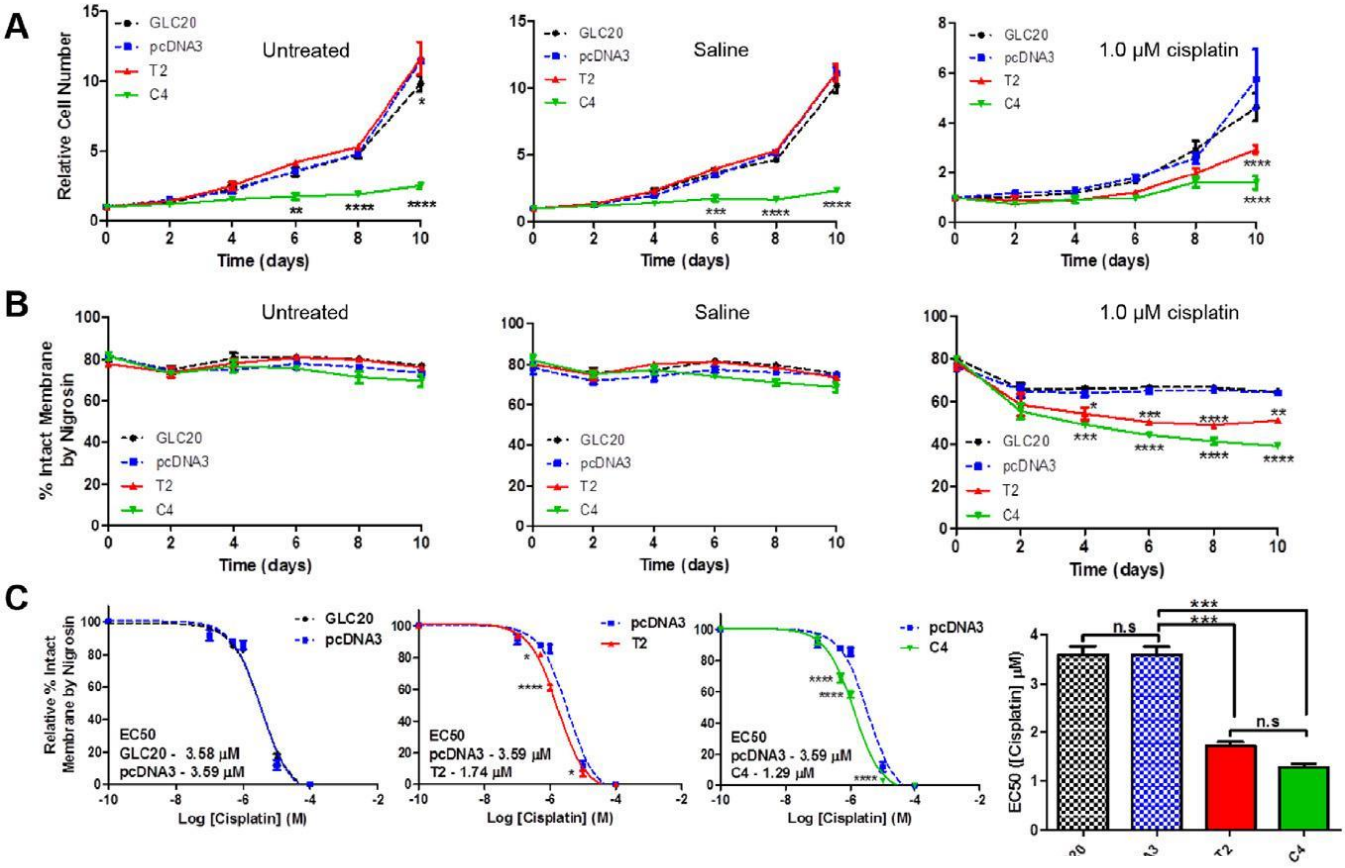

Figure 3.9 Effect of RBM5 expression +/- cisplatin on cell proliferation and membrane integrity. (A and B) GLC20 sublines were left untreated, or exposed to either a saline control or 1.0 µM cisplatin and cell numbers (A) or membrane integrity (B) monitored every other day by cell counting using a hemocytometer. Average of three biological replicates carried out in technical triplicate with standard error is displayed. A two-way ANOVA was performed between pcDNA3 and the other sublines, with Bonferroni post-hoc analysis. (C) GLC20 subline membrane integrity was monitored after eight days of exposure to various concentrations of cisplatin. Results represent the average of three biological replicates performed in technical triplicate with standard error using the calculated average EC_{50} (calculated from Graphpad Prism 5, 'non-linear fit − log(inhibitor) vs response (3 parameters)'). Graph represents the average EC_{50} of three biological replicates. One-way ANOVA was performed with Tukey post-hoc analysis, between sublines, with *p < 0.05, **p < 0.01, ***p < 0.001 and ****p <0.0001.

To determine if the decreased membrane integrity observed in T2 and C4 upon cisplatin treatment was due to increased apoptosis, we examined apoptotic marker expression using fluorescence microscopy. When cells were untreated, no significant change in the level of cell death was observed between sublines (Fig. 3.10A and B), consistent with our membrane integrity results (Fig. 3.9B). Following four days of exposure to 5 μM cisplatin, however, significantly more cells were observed in both early and late stage apoptosis in the C4 cells, compared to the vector control (Fig. 3.10C and D). Furthermore, Poly(ADP-Ribose) Polymerase (PARP) cleavage was significantly increased in the C4 cells, following cisplatin treatment (Fig. 3.10E and F). (An insignificant increase in cisplatin-mediated apoptosis was observed in the T2 subline, by Western blot (Fig. 3.10E and F) and fluorescence microscopy (Fig. 3.10C and D)).

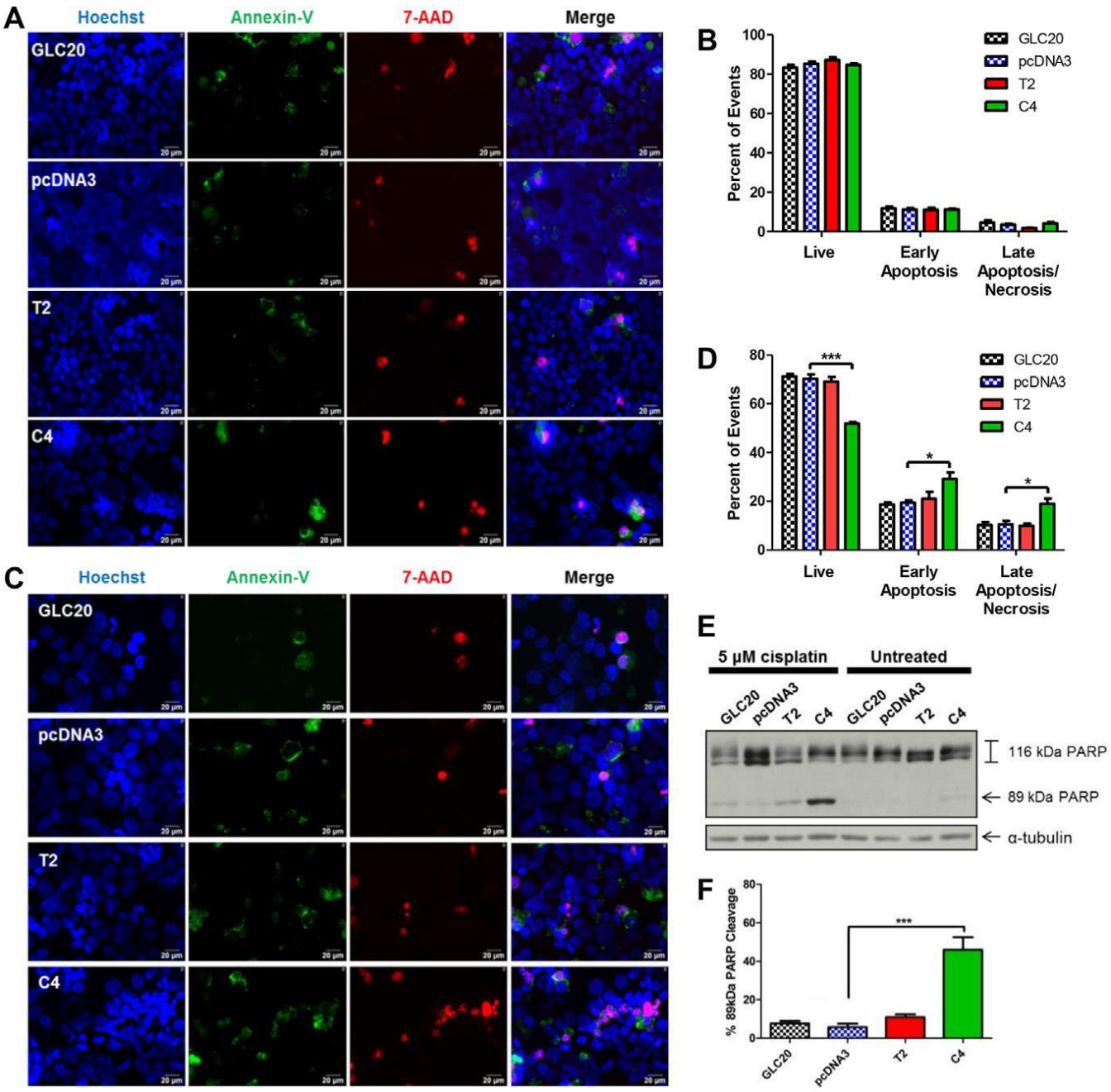

Figure 3.10 Effect of RBM5 expression +/- cisplatin on apoptosis. GLC20 sublines were left untreated (A, B) or treated with 5 μM cisplatin (C, D, E, F) and collected after four days for fluorescence microscopy (A, C) or PARP cleavage analysis (E, F). Average number of Live (only Hoechst/blue), Early Apoptosis (condensed Hoechst/blue and/or Annexin-V/green) and Late Apoptosis/Necrosis (7-AAD/Red) fluorescence microscopy events from three biological replicates, each with 10 different fields of view, with standard error, for the untreated cells (B) and 5 μM cisplatin (D). (E) A representative Western blot for PARP cleavage, in the cisplatin-treated samples, with (F) densitometric analysis of 'percent 89kDa PARP cleavage product' [(89kDa cleaved PARP/total PARP)x100], with standard error, from three biological replicates, using the AlphaEase FC, '1D-Multi' analysis tool. One-way ANOVA was performed with Tukey post-hoc analysis, between sublines, with *$p < 0.05$ and ***$p < 0.001$.

These results suggest that *RBM5* expression does in fact sensitize cells to cisplatin's pro-apoptotic effects, being in line with our RNA-Seq and RIP-Seq data, which suggest that RBM5 influences the regulation of apoptotic pathways.

3.4.7 In cisplatin-treated GLC20 cells, RNA-Seq shows that 7% of the transcriptome is differentially expressed by RBM5, and that DSG2 and ATP11C are the most altered genes, potentially driving the observed downstream effects of RBM5 expression

Having demonstrated that *RBM5* expression can significantly influence a SCLC cell line's response to cisplatin, at least in terms of cell proliferation, membrane integrity and apoptosis, we decided to examine this influence on a more global level, by performing RNA-Seq on the cells treated with 5 μM cisplatin for four days.

We identified 1,797 differentially expressed genes in the control vs. T2 group (7% of genes examined), 1,225 in the control vs. C4 group (4.7%), with 457 genes being common to both groups. Fewer differentially expressed genes in C4 compared to T2 was an unexpected finding, based on our RNA-Seq data from the untreated samples, and was possibly due to the increased rate of apoptosis in the high *RBM5* expressing cells, limiting the measurable effect on gene expression by RNA-Seq.

The most highly upregulated genes common to treated T2 and C4 cells were Protein Phosphatase 1 Regulatory Inhibitor Subunit 1A (*PPP1R1A*) and Makorin Ring Finger Protein 3 (*MKRN3*). MKRN3 has been shown to be important to development, particularly the onset of puberty

(Abreu et al., 2013), which is in line with previously identified RBM5 functions, as described above.

The most highly downregulated genes common to treated T2 and C4 include (a) Translocase of Outer Mitochondrial Membrane 40 Like (*TOMM40L*), which is a component of the outer mitochondrial membrane translocase, and thus influences many mitochondrial processes (Humphries et al., 2005), (b) ATPase Phospholipid Transporting 11C (*ATP11C*), whose cleavage (or downregulation) is required for phosphatidylserine exposure and consequent phagocytosis during apoptosis (Segawa et al., 2014; Yabas et al., 2016), and (c) Desmoglein 2 (*DSG2*), a ubiquitously expressed cell adhesion protein upregulated in many epithelial-derived cancers (Brennan and Mahoney, 2009; Harada et al., 1996; Kurzen et al., 2003) and shown to promote cell cycle progression and apoptosis-resistance (Brennan et al., 2007; Gupta et al., 2015). These three genes thus play an important role in cell survival, and it may be via their downregulation that RBM5 slows SCLC growth and sensitizes them to cisplatin-mediated apoptosis. Interestingly, *ATP11C* and *DSG2* are also significantly downregulated in untreated T2 and C4 cells, suggesting that cisplatin treatment may complement/enhance the effect of RBM5's expression on SCLC.

FIDEA analysis using the KEGG database showed that no pathways were downregulated and two pathways were significantly enriched in our control vs. T2 group; 'Axon guidance' (Benjamini value of 2.02×10^{-6}) and 'Retrograde endocannabinoid signaling' (Benjamini value of 4.22×10^{-4}). In our control vs. C4 group, only 'Axon guidance' was significantly enriched (Benjamini value of 9.44×10^{-3}). These results are very interesting since axon guidance is

involved in the establishment of a transformed state (Chedotal et al., 2005), and was also significantly altered in our untreated T2 and C4 samples, suggesting cisplatin treatment may complement this particular RBM5 function. Absence of 'Retrograde endocannabinoid signaling' in the control vs. C4 group might explain the presence of fewer differentially expressed genes in the C4 vs. T2 group.

Using the GSAASeqSP program with the MSigDB Hallmark gene set, we identified 24 enriched gene sets with FDRs < 10% between cisplatin-treated control and T2, and 18 between control and C4, of which 16 were common between both (Table 3.6). It is important to note that only 12 MSigDB Hallmark gene sets were identified as significantly enriched in our untreated control vs. T2 samples, and 17 in untreated control vs. C4. The greater number of significantly changed pathways in the treated samples, but with fewer genes differentially expressed overall, suggests once again that cisplatin directs the effect of RBM5's expression to particular genes. Noticeably, 10 of the 16 enriched pathways that were common to the T2 and C4 cisplatin treated sample sets were also enriched in the untreated C4 samples at a FDR of 10% or lower, demonstrating that cisplatin exposure did not totally alter the influence of RBM5 expression on the SCLC cell's transcriptomes.

Table 3.6: Altered gene sets with FDRs below 10% between both cisplatin-treated control and T2, and control and C4 samples, respectively, as determined by GSAASeq analysis with the MSiDB Hallmark gene set using the samples' RNA-Seq results. Ranked based on FDR value in control vs. C4 analysis.

	Control vs. T2		Control vs. C4	
Gene set	p-value	FDR	p-value	FDR
TGFβ signaling	0.0	0.05	0.0	03
Notch signaling	0.2	0.07	0.0	0.04
EMT	0.0	0.00	0.0	0.04
Myogenesis	0.0	0.05	0.0	0.04
Estrogen response early	0.0	0.04	0.0	0.05
Coagulation	0.0	0.04	0.0	0.05
Angiogenesis	0.0	0.00	0.1	0.07
Androgen response	0.0	0.05	0.0	0.07
UV response down	0.0	0.05	0.0	0.08
Apoptosis	0.0	0.04	0.0	0.08
Inflammatory response	0.0	0.03	0.0	0.08
Estrogen response late	0.0	0.03	0.0	0.08
KRAS signaling up	0.0	0.04	0.0	0.08
TNFα signaling via NFκB	0.0	0.03	0.0	0.08
IL2 STAT5 signaling	0.0	0.04	0.0	0.08
Apical junctions	0.0	0.04	0.0	0.09

The 'Apoptosis' gene set was one of the significantly enriched pathways identified by GSAASeqSP in cisplatin-treated T2 and C4 samples, compared to control, which is in line with the functional work presented herein (Fig. 3.9 and Fig. 3.10). In cisplatin-treated T2 samples, 72 genes from this 'Apoptosis' gene set were significantly enriched compared to control, and 58 in C4. Of these genes, 35 were common between both groups (Fig. 3.11), suggesting that many of the same apoptotic pathways were significantly affected in both samples. T2 had 37 uniquely differentially expressed genes while C4 had 23, suggesting that a wider range of apoptotic processes were significantly affected by cisplatin in T2.

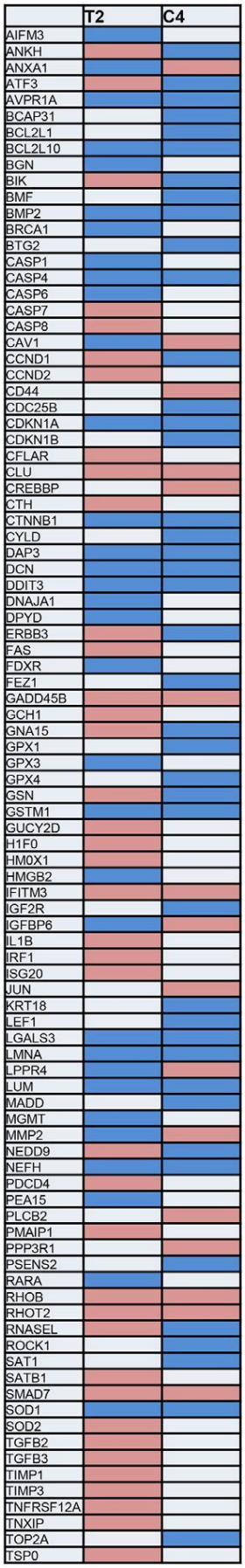

Figure 3.11 Expression of apoptosis-related genes in cisplatin treated samples. Adapted GSAASeqSP blue-pink o'gram representing the expression changes of core enriched genes from the MSigDB Hallmark Apoptosis gene set in cisplatin treated control vs. T2 and control vs. C4. Blue indicates decreased expression compared to control, whereas red indicates increased expression compared to control. Genes listed in alphabetical order.

Interestingly, *SMAD7* was the top enriched gene common to both T2 and C4 cisplatin-treated samples (third most enriched gene in both samples). Since SMAD7 has been shown to sensitize lung cells to cisplatin-mediated apoptosis (Jeon et al., 2012), it may be an important mediator of RBM5's sensitizing effect regarding cisplatin-induced promotion of apoptosis.

To further investigate which specific apoptotic processes were enriched in our cisplatin-treated samples, we analyzed the enriched genes from the 'Hallmark Apoptosis' gene set, as identified by GSAASeqSP, using the Reactome plug-in for Cytoscape (as described for RIP-Seq samples) (Fig. 3.12). These results confirmed that a wider range of apoptotic processes were influenced in the T2, compared to the C4, population; the 'Intrinsic pathway for apoptosis' and the 'Apoptotic execution' phase were significantly enriched in both cisplatin-treated T2 and C4 samples, however 'Caspase-8 activation' and the 'Extrinsic pathway' were only significantly enriched in T2 (Fig. 3.13 and Fig. 3.14). These T2-specific pathways are part of the early steps of apoptosis, suggesting that many cells in the cisplatin-treated T2 population were beginning the apoptotic process, but had not yet fully committed to programmed cell death. The cisplatin-treated C4 population, however, had a significant enrichment of the 'Intrinsic pathway for apoptosis' subgroups 'Activation of BH3-only proteins' and 'BH3-only proteins associate with and inactivate anti-apoptotic BCL-2 members'. These BH3-only proteins are essential for apoptosis (Shamas-Din et al., 2011).

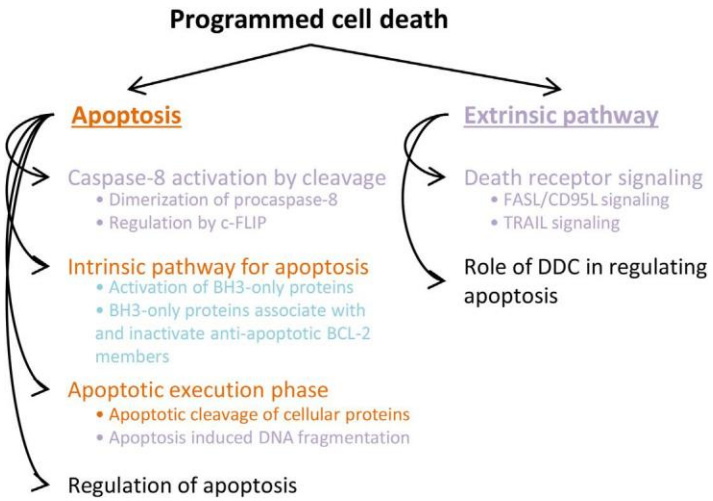

Figure 3.12 Enriched 'Programmed cell death' pathways in cisplatin treated samples. Diagram illustrating the Reactome 'Programmed cell death' pathways enriched with an FDR below 10% in cisplatin-treated control vs. T2 (purple), control vs. C4 (blue) or control vs. T2 and C4 (orange).

A

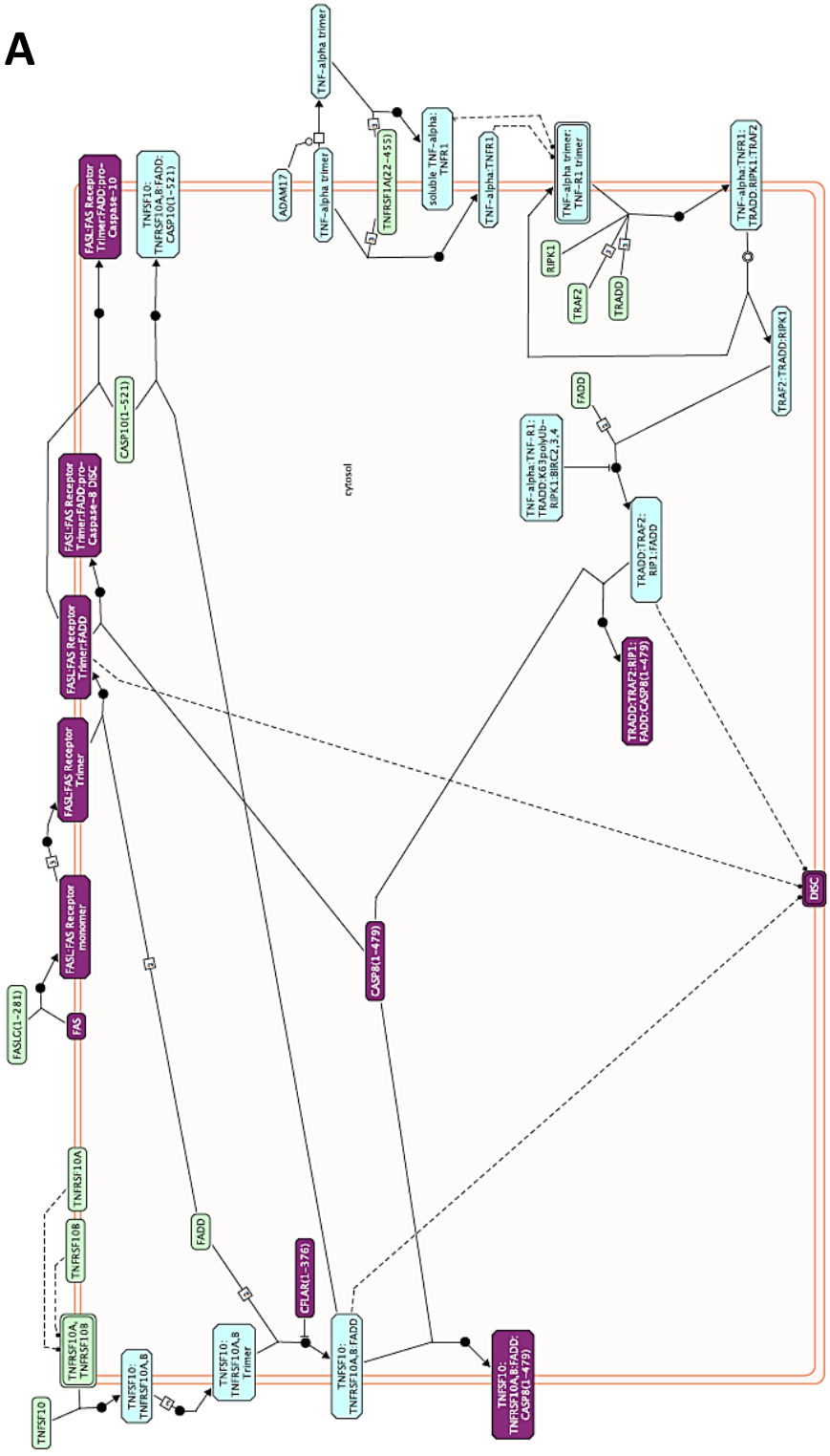
TNF-alpha trimer
ADAM17
TNF-alpha trimer
TNFRSF1A(22-455)
soluble TNF-alpha: TNFR1
TNF-alpha:TNFR1
TNF-alpha trimer: TNF-R1 trimer
TNF-alpha:TNFR1: TRADD:RIPK1:TRAF2
FASL:FAS Receptor Trimer:FADD:pro-Caspase-10
TNFSF10: TNFRSF10A,B:FADD: CASP10(1-521)
RIPK1
TRAF2
TRADD
TRAF2:TRADD:RIPK1
CASP10(1-521)
FADD
cytosol
FASL:FAS Receptor Trimer:FADD:pro-Caspase-8 DISC
TNF-alpha:TNF-R1: TRADD:K63polyUb-RIPK1:BIRC2,3,4
FASL:FAS Receptor Trimer:FADD
TRADD:TRAF2: RIP1:FADD
FASL:FAS Receptor Trimer
TRADD:TRAF2:RIP1: FADD:CASP8(1-479)
FASL:FAS Receptor monomer
DISC
CASP8(1-479)
FASLG(1-281)
FAS
TNFRSF10A
TNFRSF10B
FADD
CFLAR(1-376)
TNFSF10
TNFRSF10A, TNFRSF10B
TNFSF10: TNFRSF10A,B
TNFSF10: TNFRSF10A,B Trimer
TNFSF10: TNFRSF10A,B:FADD
TNFSF10: TNFRSF10A,B:FADD: CASP8(1-479)

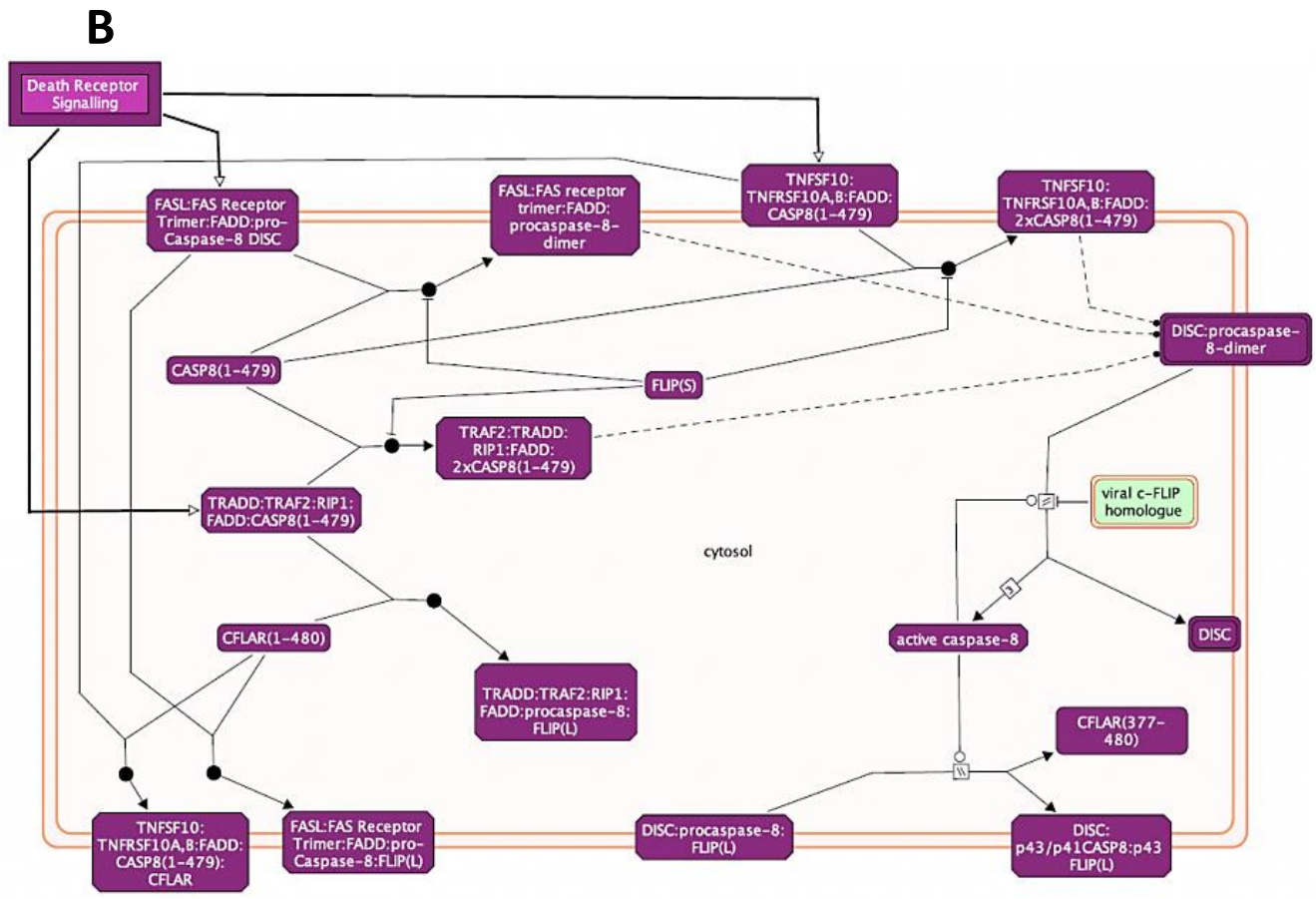

Figure 3.13 Gene enrichment for apoptosis-related pathways in cisplatin-treated T2 samples. Reactome diagram for 'Death receptor signaling' (A) and 'Caspase-8 activation by cleavage' (B). Differentially expressed genes between cisplatin treated control vs. T2 are presented in purple.

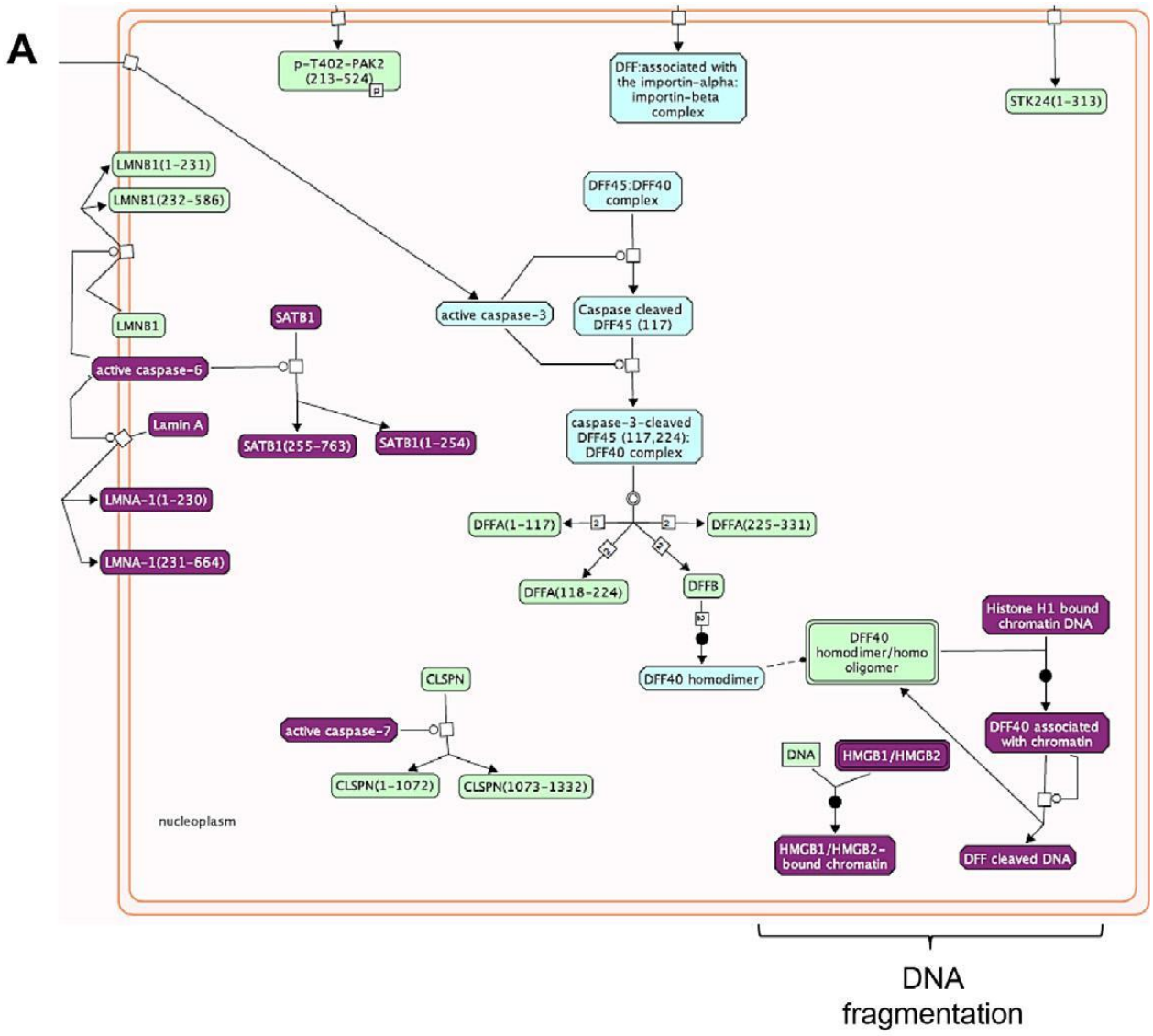
A
p-T402-PAK2 (213-524)
DFF:associated with the importin-alpha: importin-beta complex
STK24(1-313)
LMNB1(1-231)
LMNB1(232-586)
DFF45:DFF40 complex
LMNB1
SATB1
active caspase-3
Caspase cleaved DFF45 (117)
active caspase-6
Lamin A
SATB1(255-763)
SATB1(1-254)
caspase-3-cleaved DFF45 (117,224): DFF40 complex
LMNA-1(1-230)
LMNA-1(231-664)
DFFA(1-117)
DFFA(225-331)
DFFA(118-224)
DFFB
Histone H1 bound chromatin DNA
DFF40 homodimer/homo oligomer
DFF40 homodimer
CLSPN
active caspase-7
DFF40 associated with chromatin
DNA
HMGB1/HMGB2
CLSPN(1-1072)
CLSPN(1073-1332)
nucleoplasm
HMGB1/HMGB2-bound chromatin
DFF cleaved DNA
DNA fragmentation

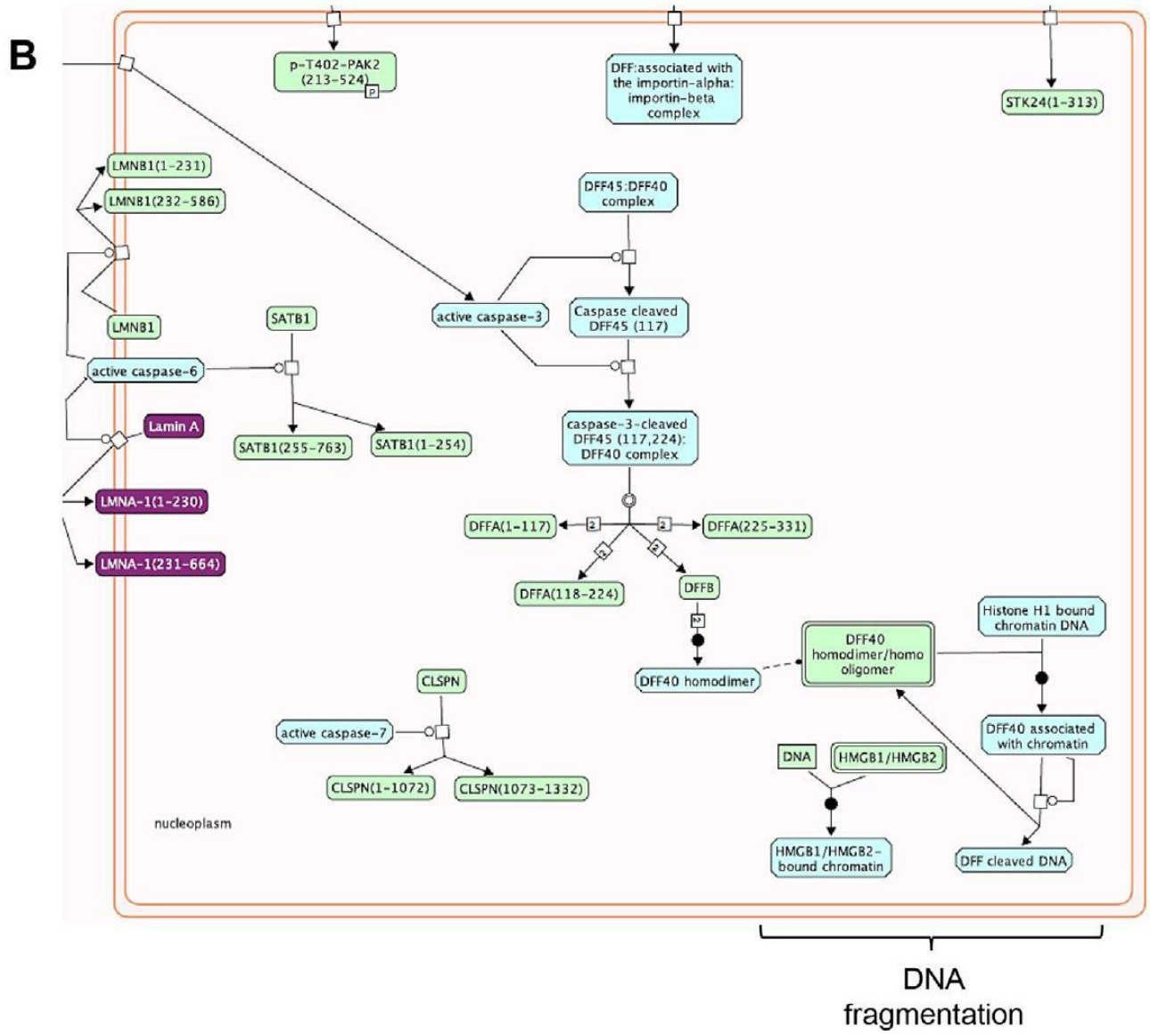

Figure 3.14 'Apoptotic execution phase' gene enrichment in cisplatin-treated samples. Differentially expressed genes between cisplatin treated control vs. T2 (A) or control vs. C4 (B) are presented in purple in a portion of the Reactome 'Apoptotic execution phase' pathway.

This in-depth pathway analysis shows that relatively low levels of *RBM5* are able to sensitize SCLC cells to cisplatin-mediated apoptosis by influencing changes in the expression of genes

involved in early apoptosis events. At relatively higher levels of RBM5 expression, this effect on cell death levels is detectable via fluorescent microscopy (Fig. 3.10C). These results suggest that the level of RBM5 expression in lung tumors could predict response to cisplatin.

Taken together, our results show that RBM5 can functionally (a) influence cell cycle progression in untreated and cisplatin-treated SCLC cells (potentially via decreased DSG2 expression), and (b) sensitize cisplatin-treated SCLC cells to cisplatin-mediated apoptosis (potentially via decreased *DSG2* and *ATP11C* expression, as well as increased *SMAD7* expression). These findings reinforce the importance of RBM5 expression to SCLC cisplatin-sensitivity and highlight the potential of RBM5 as a response marker for this chemotherapy treatment in SCLC. In fact, a recent publication suggested that *RBM5* gene therapy might be considered for NSCLC and that *RBM5* might be a predictive marker to indicate the potential success of using cisplatin on a particular lung cancer (Li et al., 2012): our results support this suggestion and extend it to SCLC.

It is important to note that *RBM5* expression was recently shown to increase autophagy levels in a NSCLC cell line (Su et al., 2016), therefore, we also examined the expression of autophagy markers *BCL2*, *NF-κB*, *LC-3*, *LAMP1* and *BECLIN1* in the RNA-Seq data from our cisplatin-treated C4 cells. Only NF-κB, however, was significantly differentially expressed compared to control; thus, autophagy does not seem to be a mechanism by which *RBM5* expression influences membrane integrity in cisplatin-treated SCLC cells.

3.4.8 In patient samples, RNA-Seq shows that RBM5 expression is reduced by 50% in tumors and that similar pathways are disrupted

To determine if the RBM5-influenced pathways that we identified in vitro were also influenced in vivo, we carried out RNA-Seq on primary tissue specimens. SCLC tumor resection is not routinely carried out in North America, but we did obtain two fresh frozen paired non-tumor and SCLC specimens. Transcriptome sequencing and analysis were performed on all four specimens.

We identified 14,346 and 14,119 genes differentially expressed between both non-tumor and tumor pairs, respectively, thus slightly more than half of the genes studied. Interestingly 12,116 (~85%) of these differentially expressed genes were common to both paired groups, suggesting that, contrary to what one might expect in a tumor, a fairly conserved mechanism is involved in the evolution of SCLC, a favorable feature for treatment development.

RBM5 expression was very similar in both non-tumor specimens, and decreased by half in the corresponding tumor specimens; from 40.43 FPKM to 18.55 FPKM in the first patient specimens, and from 39.00 FPKM to 22.30 FPKM in the second patient specimens. This significant decrease of approximately 50% suggests that loss of heterozygosity (LOH) may be the cause of decreased *RBM5* expression in SCLC. In fact, LOH of a portion of 3p21.3 close to *RBM5* has been observed in over 95% of SCLC and 70% of NSCLC (Ji et al., 2005; Kok et al., 1997; Lerman and Minna, 2000; Sutherland et al., 2010; Wei et al., 1996; Wistuba et al., 2000). It is important to note that the *RBM5* expression values in the non-tumor samples are very similar to that of T2 (58.26 FPKM), thus lending physiological relevance to our in vitro model.

Using FIDEA with the KEGG database, 34 pathways were shown to be significantly differentially regulated in both tumor specimens compared to their respective non-tumor control (Table 3.7). GSAASeqSP with MSigDB Hallmark gene set also showed that many gene sets were enriched; 18 in the first patient sample, and 26 in the second, with 15 gene sets being common between both sample pairs (Table 3.8). Differentially expressed pathways, as determined by both FIDEA and GSAASeqSP, included almost all of the RBM5-influenced pathways identified above, including many transformation-associated pathways, notably 'Pathways in cancer', 'Cell cycle', 'Small cell lung cancer', 'Axon guidance', 'p53 signaling', 'TNFα signaling via NFκB' and 'Apoptosis'. This high level of correlation between significantly differentially expressed pathways in our SCLC patient samples and the *RBM5* expressing cell lines supports, once again, our conclusion that RBM5 plays a role influencing pathways that are very important to the transformed state of SCLC cells.

Table 3.7: Significantly altered pathways between both patient SCLC tumor/non-tumor pairs as determined by FIDEA analysis with KEGG database (using the samples' RNA-Seq results). Pathways are listed based on significance of enrichment in the first patient sample.

Pathway	Non-tumor/tumor pair 1 (Benjamini value)	Non-tumor/tumor pair 2 (Benjamini value)
Pathways in cancer	1.23E-12	6.36E-14
Cell cycle	9.75E-10	1.99E-10
Regulation of actin cytoskeleton	3.03E-06	3.06E-07
Focal adhesion	3.03E-06	5.50E-08
Chronic myeloid leukemia	2.60E-05	7.09E-10
p53 signaling pathway	2.60E-05	2.23E-06
Fc gamma R-mediated phagocytosis	2.64E-05	3.95E-06
Neurotrophin signaling pathway	1.11E-04	3.68E-10
Colorectal cancer	1.64E-04	5.82E-08
Bacterial invasion of epithelial cells	1.82E-04	1.22E-06
Pancreatic cancer	1.82E-04	1.22E-06
Phosphatidylinositol signaling system	2.81E-04	4.93E-04
Prostate cancer	3.58E-04	1.58E-06
Small cell lung cancer	6.00E-04	3.74E-04
Axon guidance	1.04E-03	1.16E-06
Leukocyte transendothelial migration	1.37E-03	3.74E-04
Acute myeloid leukemia	1.73E-03	1.27E-05
Renal cell carcinoma	1.79E-03	3.74E-04
Inositol phosphate metabolism	2.29E-03	1.39E-02
Ubiquitin mediated proteolysis	4.01E-03	6.36E-04
Salmonella infection	4.20E-03	1.68E-02
Adherens junction	4.20E-03	9.09E-06
DNA replication	4.20E-03	1.39E-02
T cell receptor signaling pathway	7.53E-03	2.78E-05
mTOR signaling pathway	8.57E-03	4.60E-04
Base excision repair	1.69E-02	1.26E-02
Glioma	1.72E-02	1.31E-04
Shigellosis	1.76E-02	2.25E-05
B cell receptor signaling pathway	1.78E-02	8.53E-04
MAPK signaling pathway	1.78E-02	4.77E-02
ErbB signaling pathway	1.97E-02	1.57E-05
Endometrial cancer	2.21E-02	1.57E-05
N-Glycan biosynthesis	3.89E-02	1.23E-02
Chemokine signaling pathway	4.69E-02	1.35E-04

Table 3.8: Altered gene sets with FDRs below 1% in both patient SCLC tumor/non-tumor pairs, as determined by GSAASeqSP analysis with the MSigDB Hallmark gene set (using the samples' RNA-Seq results). Pathways are listed based on FDR in the first patient sample.

	Non-tumor/tumor pair 1		Non-tumor/tumor pair 2	
Gene set	p-value	FDR	p-value	FDR
TNFα signaling via NFκB*	0.0	0.0	0.0	0.0
IL6 JK STAT3 signaling*	0.0	0.0	0.0	0.0
G2M checkpoint	0.0	0.0	0.0	0.0
Estrogen response late*	0.0	0.0	0.0	0.0
Interferon γ response	0.0	0.0	0.0	0.0
E2F targets	0.0	0.0	0.0	0.0
EMT*	0.0	0.0	0.0	0.0
Inflammatory response*	0.0	0.0	0.0	0.0
KRAS signaling up*	0.0	0.0	0.0	0.0
Pancreas β cells*	0.0	0.0	0.0	0.0
UV response down*	0.0	0.01	0.0	0.0
Interferon α response*	0.0	0.01	0.0	0.01
IL2 STAT5 signaling*	0.0	0.01	0.0	0.0
Apoptosis*	0.0	0.01	0.0	0.0
Coagulation*	0.0	0.01	0.0	0.0

* Beside a gene set name indicates it's enrichment in untreated control vs. C4 samples, at an FDR < 10%.

3.5 Conclusion

Lung cancer is the leading cause of cancer-related deaths worldwide. The most aggressive form of lung cancer is SCLC, with a staggering 95% of diagnosed patients succumbing to the disease (Govindan et al., 2006). This high mortality rate clearly demonstrates the need for more effective screening techniques and treatment options. Our results show, for the first time, that *RBM5* expression is important to the maintenance of the non-transformed state of lung cells, and that this is accomplished via direct regulation of the cell cycle and apoptosis, and indirect regulation of overall cell death, angiogenesis, and cell adhesion. Functional studies confirmed that *RBM5* expression in SCLC (1) slowed the cell cycle, and (2) decreased membrane integrity, partially

via increased apoptosis when cells were treated with the chemotherapy agent cisplatin. Therefore, decreased *RBM5* expression, as is observed in 95% of SCLC, may be a critical step in the establishment of this disease. In a clinical setting, downregulation of *RBM5* expression could be a novel biomarker for the determination of SCLC risk. Therapeutic options involving RBM5 and/or direct targets, or pathways altered by *RBM5* expression, may also be very fruitful avenues to pursue. Furthermore, due to the significant sensitization RBM5 expression had on cisplatin-treated samples, *RBM5* expression could be a valuable predictive aid for assessing how a patient may respond to this chemotherapy. Ultimately, this work demonstrates, for the first time, the importance of RBM5 to SCLC. Our results present a stepping-off point for additional targeted functional work.

3.6 References

Abreu, A.P., Dauber, A., Macedo, D.B., Noel, S.D., Brito, V.N., Gill, J.C., Cukier, P., Thompson, I.R., Navarro, V.M., Gagliardi, P.C., et al. (2013). Central precocious puberty caused by mutations in the imprinted gene MKRN3. N Engl J Med 368, 2467-2475.

Angeloni, D. (2007). Molecular analysis of deletions in human chromosome 3p21 and the role of resident cancer genes in disease. Brief. Funct. Genomic. Proteomic.

Bechara, E.G., Sebestyen, E., Bernardis, I., Eyras, E., and Valcarcel, J. (2013). RBM5, 6, and 10 Differentially Regulate NUMB Alternative Splicing to Control Cancer Cell Proliferation. Mol Cell 52, 720-733.

Brennan, D., Hu, Y., Joubeh, S., Choi, Y.W., Whitaker-Menezes, D., O'Brien, T., Uitto, J., Rodeck, U., and Mahoney, M.G. (2007). Suprabasal Dsg2 expression in transgenic mouse skin confers a hyperproliferative and apoptosis-resistant phenotype to keratinocytes. J Cell Sci 120, 758-771.

Brennan, D., and Mahoney, M.G. (2009). Increased expression of Dsg2 in malignant skin carcinomas: A tissue-microarray based study. Cell Adh Migr 3, 148-154.

Chedotal, A., Kerjan, G., and Moreau-Fauvarque, C. (2005). The brain within the tumor: new roles for axon guidance molecules in cancers. Cell Death Differ 12, 1044-1056.

D'Andrea, D., Grassi, L., Mazzapioda, M., and Tramontano, A. (2013). FIDEA: a server for the functional interpretation of differential expression analysis. Nucleic Acids Res 41, W84-88.

Del Fabbro, C., Scalabrin, S., Morgante, M., and Giorgi, F.M. (2013). An extensive evaluation of read trimming effects on Illumina NGS data analysis. PLoS One 8, e85024.

Delfino, F.J., Stevenson, H., and Smithgall, T.E. (2006). A growth-suppressive function for the c-fes protein-tyrosine kinase in colorectal cancer. J Biol Chem 281, 8829-8835.

Forsyth, C.B., Tang, Y., Shaikh, M., Zhang, L., and Keshavarzian, A. (2010). Alcohol stimulates activation of Snail, epidermal growth factor receptor signaling, and biomarkers of epithelial-mesenchymal transition in colon and breast cancer cells. Alcohol Clin Exp Res 34, 19-31.

Funakoshi, T., Tachibana, I., Hoshida, Y., Kimura, H., Takeda, Y., Kijima, T., Nishino, K., Goto, H., Yoneda, T., Kumagai, T., et al. (2003). Expression of tetraspanins in human lung cancer cells: frequent downregulation of CD9 and its contribution to cell motility in small cell lung cancer. Oncogene 22, 674-687.

Fushimi, K., Ray, P., Kar, A., Wang, L., Sutherland, L.C., and Wu, J.Y. (2008). Up-regulation of the proapoptotic caspase 2 splicing isoform by a candidate tumor suppressor, RBM5. Proc. Natl Acad Sci U. S. A 105, 15708-15713.

Gaspar, L.E., McNamara, E.J., Gay, E.G., Putnam, J.B., Crawford, J., Herbst, R.S., and Bonner, J.A. (2012). Small-cell lung cancer: prognostic factors and changing treatment over 15 years. Clin. Lung Cancer 13, 115-122.

Govindan, R., Page, N., Morgensztern, D., Read, W., Tierney, R., Vlahiotis, A., Spitznagel, E.L., and Piccirillo, J. (2006). Changing epidemiology of small-cell lung cancer in the United States over the last 30 years: analysis of the surveillance, epidemiologic, and end results database. J Clin. Oncol 24, 4539-4544.

Guallar, D., and Wang, J. (2014). RNA-binding proteins in pluripotency, differentiation, and reprogramming. Front Biol (Beijing) 9, 389-409.

Gupta, A., Nitoiu, D., Brennan-Crispi, D., Addya, S., Riobo, N.A., Kelsell, D.P., and Mahoney, M.G. (2015). Cell cycle- and cancer-associated gene networks activated by Dsg2: evidence of cystatin A deregulation and a potential role in cell-cell adhesion. PLoS One 10, e0120091.

Hall, M.D., Telma, K.A., Chang, K.E., Lee, T.D., Madigan, J.P., Lloyd, J.R., Goldlust, I.S., Hoeschele, J.D., and Gottesman, M.M. (2014). Say no to DMSO: dimethylsulfoxide inactivates cisplatin, carboplatin, and other platinum complexes. Cancer Res 74, 3913-3922.

Harada, H., Iwatsuki, K., Ohtsuka, M., Han, G.W., and Kaneko, F. (1996). Abnormal desmoglein expression by squamous cell carcinoma cells. Acta Derm Venereol 76, 417-420.

Hegele, A., Kamburov, A., Grossmann, A., Sourlis, C., Wowro, S., Weimann, M., Will, C.L., Pena, V., Luhrmann, R., and Stelzl, U. (2012). Dynamic protein-protein interaction wiring of the human spliceosome. Mol Cell 45, 567-580.

Huan, J., Gao, Y., Xu, J., Sheng, W., Zhu, W., Zhang, S., Cao, J., Ji, J., Zhang, L., and Tian, Y. (2015). Overexpression of CD9 correlates with tumor stage and lymph node metastasis in esophageal squamous cell carcinoma. Int J Clin Exp Pathol 8, 3054-3061.

Humphries, A.D., Streimann, I.C., Stojanovski, D., Johnston, A.J., Yano, M., Hoogenraad, N.J., and Ryan, M.T. (2005). Dissection of the mitochondrial import and assembly pathway for human Tom40. J Biol Chem 280, 11535-11543.

Jackman, D.M., and Johnson, B.E. (2005). Small-cell lung cancer. Lancet 366, 1385-1396.

Jain, R., Devine, T., George, A.D., Chittur, S.V., Baroni, T.E., Penalva, L.O., and Tenenbaum, S.A. (2011). RIP-Chip Analysis: RNA-Binding Protein Immunoprecipitation-Microarray (Chip) Profiling. In RNA, H. Nielsen, ed. (Humana Press), pp. 247-263.

Jeon, W.K., Hong, H.Y., Seo, W.C., Lim, K.H., Lee, H.Y., Kim, W.J., Song, S.Y., and Kim, B.C. (2012). Smad7 sensitizes A549 lung cancer cells to cisplatin-induced apoptosis through heme oxygenase-1 inhibition. Biochem Biophys Res Commun 420, 288-292.

Ji, L., Minna, J.D., and Roth, J.A. (2005). 3p21.3 tumor suppressor cluster: prospects for translational applications. Future. Oncol 1, 79-92.

Jin, W., Niu, Z., Xu, D., and Li, X. (2012). RBM5 promotes exon 4 skipping of AID pre-mRNA by competing with the binding of U2AF65 to the polypyrimidine tract. FEBS Lett 586, 3852-3857.

Johnson, D.H., Schiller, J.H., and Bunn, P.A., Jr. (2014). Recent clinical advances in lung cancer management. J Clin. Oncol 32, 973-982.

Kanda, S., Miyata, Y., Kanetake, H., and Smithgall, T.E. (2009). Downregulation of the c-Fes protein-tyrosine kinase inhibits the proliferation of human renal carcinoma cells. Int J Oncol 34, 89-96.

Kanehisa, M., and Goto, S. (2000). KEGG: kyoto encyclopedia of genes and genomes. Nucleic Acids Res 28, 27-30.

Kanehisa, M., Goto, S., Sato, Y., Kawashima, M., Furumichi, M., and Tanabe, M. (2014). Data, information, knowledge and principle: back to metabolism in KEGG. Nucleic Acids Res 42, D199-205.

Kanehisa, M., Sato, Y., Kawashima, M., Furumichi, M., and Tanabe, M. (2016). KEGG as a reference resource for gene and protein annotation. Nucleic Acids Res 44, D457-462.

Kim, D., Pertea, G., Trapnell, C., Pimentel, H., Kelley, R., and Salzberg, S.L. (2013). TopHat2: accurate alignment of transcriptomes in the presence of insertions, deletions and gene fusions. Genome Biol 14, R36.

Kobayashi, T., Ishida, J., Musashi, M., Ota, S., Yoshida, T., Shimizu, Y., Chuma, M., Kawakami, H., Asaka, M., Tanaka, J., et al. (2011). p53 transactivation is involved in the antiproliferative activity of the putative tumor suppressor RBM5. Int J Cancer 128, 304-318.

Kok, K., Naylor, S.L., and Buys, C.H. (1997). Deletions of the short arm of chromosome 3 in solid tumors and the search for suppressor genes. Adv. Cancer Res 71, 27-92.

Kok, K., van den Berg, A., Veldhuis, P.M., van der Veen, A.Y., Franke, M., Schoenmakers, E.F., Hulsbeek, M.M., van der Hout, A.H., de Leij, L., van de Ven, W., et al. (1994). A homozygous

deletion in a small cell lung cancer cell line involving a 3p21 region with a marked instability in yeast artificial chromosomes. Cancer Res 54, 4183-4187.

Kurzen, H., Munzing, I., and Hartschuh, W. (2003). Expression of desmosomal proteins in squamous cell carcinomas of the skin. J Cutan Pathol 30, 621-630.

Lerman, M.I., and Minna, J.D. (2000). The 630-kb lung cancer homozygous deletion region on human chromosome 3p21.3: identification and evaluation of the resident candidate tumor suppressor genes. The International Lung Cancer Chromosome 3p21.3 Tumor Suppressor Gene Consortium. Cancer Res 60, 6116-6133.

Li, H., Handsaker, B., Wysoker, A., Fennell, T., Ruan, J., Homer, N., Marth, G., Abecasis, G., Durbin, R., and Genome Project Data Processing, S. (2009). The Sequence Alignment/Map format and SAMtools. Bioinformatics 25, 2078-2079.

Li, P., Wang, K., Zhang, J., Zhao, L., Liang, H., Shao, C., and Sutherland, L.C. (2012). The 3p21.3 tumor suppressor RBM5 resensitizes cisplatin-resistant human non-small cell lung cancer cells to cisplatin. Cancer Epidemiol 36, 481-489.

Liberzon, A., Birger, C., Thorvaldsdottir, H., Ghandi, M., Mesirov, J.P., and Tamayo, P. (2015). The Molecular Signatures Database (MSigDB) hallmark gene set collection. Cell Syst 1, 417-425.

Liu, Y., Zhou, J., and White, K.P. (2014). RNA-seq differential expression studies: more sequence or more replication? Bioinformatics 30, 301-304.

Loiselle, J.J., and Sutherland, L.C. (2014). Differential downregulation of Rbm5 and Rbm10 during skeletal and cardiac differentiation. In Vitro Cell Dev. Biol. Anim 50, 331-339.

Longthorne, V.L., and Williams, G.T. (1997). Caspase activity is required for commitment to Fas-mediated apoptosis. EMBO J 16, 3805-3812.

Martin, M. (2011). Cutadapt removes adapter sequences from high-throughput sequencing reads. EMBnet. journal 17, 10-12.

Mueller, C.F., Berger, A., Zimmer, S., Tiyerili, V., and Nickenig, G. (2009). The heterogenous nuclear riboprotein S1-1 regulates AT1 receptor gene expression via transcriptional and posttranscriptional mechanisms. Arch Biochem Biophys 488, 76-82.

Network, T.C.G.A.R. (2014). Comprehensive molecular profiling of lung adenocarcinoma. Nature 511, 543-550.

Niu, Z., Jin, W., Zhang, L., and Li, X. (2012). Tumor suppressor RBM5 directly interacts with the DExD/H-box protein DHX15 and stimulates its helicase activity. FEBS Lett 586, 977-983.

O'Bryan, M.K., Clark, B.J., McLaughlin, E.A., D'Sylva, R.J., O'Donnell, L., Wilce, J.A., Sutherland, J., O'Connor, A.E., Whittle, B., Goodnow, C.C., et al. (2013). RBM5 Is a Male Germ Cell Splicing Factor and Is Required for Spermatid Differentiation and Male Fertility. PLoS Genet 9, e1003628.

Oh, J.J., Boctor, B.N., Jimenez, C.A., Lopez, R., Koegel, A.K., Taschereau, E.O., Phan, D.T., Jacobsen, S.E., and Slamon, D.J. (2008). Promoter methylation study of the H37/RBM5 tumor suppressor gene from the 3p21.3 human lung cancer tumor suppressor locus. Hum. Genet 123, 55-64.

Oh, J.J., Koegel, A.K., Phan, D.T., Razfar, A., and Slamon, D.J. (2007). The two single nucleotide polymorphisms in the H37/RBM5 tumour suppressor gene at 3p21.3 correlated with different subtypes of non-small cell lung cancers. Lung Cancer 58, 7-14.

Oh, J.J., Razfar, A., Delgado, I., Reed, R.A., Malkina, A., Boctor, B., and Slamon, D.J. (2006). 3p21.3 tumor suppressor gene H37/Luca15/RBM5 inhibits growth of human lung cancer cells through cell cycle arrest and apoptosis. Cancer Res 66, 3419-3427.

Oh, J.J., West, A.R., Fishbein, M.C., and Slamon, D.J. (2002). A candidate tumor suppressor gene, H37, from the human lung cancer tumor suppressor locus 3p21.3. Cancer Res 62, 3207-3213.

Palmieri, F. (2013). The mitochondrial transporter family SLC25: identification, properties and physiopathology. Mol Aspects Med 34, 465-484.

Ramaswamy, S., Ross, K.N., Lander, E.S., and Golub, T.R. (2003). A molecular signature of metastasis in primary solid tumors. Nat. Genet 33, 49-54.

Rappa, G., Green, T.M., Karbanova, J., Corbeil, D., and Lorico, A. (2015). Tetraspanin CD9 determines invasiveness and tumorigenicity of human breast cancer cells. Oncotarget 6, 7970-7991.

Ray, D., Kazan, H., Cook, K.B., Weirauch, M.T., Najafabadi, H.S., Li, X., Gueroussov, S., Albu, M., Zheng, H., Yang, A., et al. (2013). A compendium of RNA-binding motifs for decoding gene regulation. Nature 499, 172-177.

Rintala-Maki, N.D., Abrasonis, V., Burd, M., and Sutherland, L.C. (2004). Genetic instability of RBM5/LUCA-15/H37 in MCF-7 breast carcinoma sublines may affect susceptibility to apoptosis. Cell Biochem. Funct 22, 307-313.

Rintala-Maki, N.D., and Sutherland, L.C. (2004). LUCA-15/RBM5, a putative tumour suppressor, enhances multiple receptor-initiated death signals. Apoptosis 9, 475-484.

Rintala-Maki, N.D., and Sutherland, L.C. (2009). Identification and characterisation of a novel antisense non-coding RNA from the RBM5 gene locus. Gene 445, 7-16.

Segawa, K., Kurata, S., Yanagihashi, Y., Brummelkamp, T.R., Matsuda, F., and Nagata, S. (2014). Caspase-mediated cleavage of phospholipid flippase for apoptotic phosphatidylserine exposure. Science 344, 1164-1168.

Sehgal, L., Mathur, R., Braun, F.K., Wise, J.F., Berkova, Z., Neelapu, S., Kwak, L.W., and Samaniego, F. (2014). FAS-antisense 1 lncRNA and production of soluble versus membrane Fas in B-cell lymphoma. Leukemia 28, 2376-2387.

Shamas-Din, A., Brahmbhatt, H., Leber, B., and Andrews, D.W. (2011). BH3-only proteins: Orchestrators of apoptosis. Biochim Biophys Acta 1813, 508-520.

Shao, C., Zhao, L., Wang, K., Xu, W., Zhang, J., and Yang, B. (2012). The tumor suppressor gene RBM5 inhibits lung adenocarcinoma cell growth and induces apoptosis. World J Surg Oncol 10, 160.

Smit, E.F., de Vries, E.G., Timmer-Bosscha, H., de Leij, L.F., Oosterhuis, J.W., Scheper, R.J., Weening, J.J., Postmus, P.E., and Mulder, N.H. (1992). In vitro response of human small-cell lung-cancer cell lines to chemotherapeutic drugs; no correlation with clinical data. Int. J. Cancer 51, 72-78.

Su, Z., Wang, K., Li, R., Yin, J., Hao, Y., Lv, X., Li, J., Zhao, L., Du, Y., Li, P., et al. (2016). Overexpression of RBM5 induces autophagy in human lung adenocarcinoma cells. World J Surg Oncol 14, 57.

Sutherland, L.C., Edwards, S.E., Cable, H.C., Poirier, G.G., Miller, B.A., Cooper, C.S., and Williams, G.T. (2000). LUCA-15-encoded sequence variants regulate CD95-mediated apoptosis. Oncogene 19, 3774-3781.

Sutherland, L.C., Wang, K., and Robinson, A.G. (2010). RBM5 as a putative tumor suppressor gene for lung cancer. J Thorac. Oncol 5, 294-298.

Tam, W.L., and Ng, H.H. (2014). Sox2: masterminding the root of cancer. Cancer Cell 26, 3-5.

Trapnell, C., Hendrickson, D.G., Sauvageau, M., Goff, L., Rinn, J.L., and Pachter, L. (2013). Differential analysis of gene regulation at transcript resolution with RNA-seq. Nat Biotechnol 31, 46-53.

Trapnell, C., Roberts, A., Goff, L., Pertea, G., Kim, D., Kelley, D.R., Pimentel, H., Salzberg, S.L., Rinn, J.L., and Pachter, L. (2012). Differential gene and transcript expression analysis of RNA-seq experiments with TopHat and Cufflinks. Nat Protoc 7, 562-578.

Trapnell, C., Williams, B.A., Pertea, G., Mortazavi, A., Kwan, G., van Baren, M.J., Salzberg, S.L., Wold, B.J., and Pachter, L. (2010). Transcript assembly and quantification by RNA-Seq

reveals unannotated transcripts and isoform switching during cell differentiation. Nat Biotechnol 28, 511-515.

Travis W.D., B.E., Muller-Hermelink H.K., Harris C.C. (2004). World Health Organization Classification of Tumours. Pathology and Genetics of Tumours of the Lung, Pleura, Thymus and Heart (Lyon, France: IARC Press).

Unni, A.M., Lockwood, W.W., Zejnullahu, K., Lee-Lin, S.Q., and Varmus, H. (2015). Evidence that synthetic lethality underlies the mutual exclusivity of oncogenic KRAS and EGFR mutations in lung adenocarcinoma. Elife 4, e06907.

Wei, M.H., Latif, F., Bader, S., Kashuba, V., Chen, J.Y., Duh, F.M., Sekido, Y., Lee, C.C., Geil, L., Kuzmin, I., et al. (1996). Construction of a 600-kilobase cosmid clone contig and generation of a transcriptional map surrounding the lung cancer tumor suppressor gene (TSG) locus on human chromosome 3p21.3: progress toward the isolation of a lung cancer TSG. Cancer Res 56, 1487-1492.

Wistuba, I.I., Behrens, C., Virmani, A.K., Mele, G., Milchgrub, S., Girard, L., Fondon, J.W., III, Garner, H.R., McKay, B., Latif, F., et al. (2000). High resolution chromosome 3p allelotyping of human lung cancer and preneoplastic/preinvasive bronchial epithelium reveals multiple, discontinuous sites of 3p allele loss and three regions of frequent breakpoints. Cancer Res 60, 1949-1960.

Xiong, Q., Mukherjee, S., and Furey, T.S. (2014). GSAASeqSP: a toolset for gene set association analysis of RNA-Seq data. Sci Rep 4, 6347.

Yabas, M., Jing, W., Shafik, S., Broer, S., and Enders, A. (2016). ATP11C Facilitates Phospholipid Translocation across the Plasma Membrane of All Leukocytes. PLoS One 11, e0146774.

Chapter 4

4 RBM10 promotes transformation-associated processes in small cell lung cancer and is directly regulated by RBM5

Loiselle JJ, Roy JG and Sutherland LC. (2017) *RBM10 promotes transformation-associated processes in small cell lung cancer and is directly regulated by RBM5*. **PLoS ONE**. **12**(6):e0180258.

Full text, open access document can be accessed through the journal's website:

http://journals.plos.org/plosone/article?id=10.1371/journal.pone.0180258

4.1 Abstract

Lung cancers are the leading cause of cancer-related deaths worldwide, with small cell lung cancer (SCLC) being the most aggressive type. At the time of diagnosis, SCLC has usually already metastasized, and an astonishing 95% of patients eventually succumb to the disease. This highlights the need for more effective SCLC screening and treatment options. Interestingly, the earliest and most frequent genetic alteration associated with lung cancers involves a lesion in the region to which the RNA binding protein *RBM5* maps. We have recently shown that a decrease in *RBM5* expression may be a key step in SCLC development, as RBM5 regulated many transformation-associated processes in SCLC cells. RBM5 is structurally and functionally similar to another RNA binding protein, RBM10. Both proteins have tumor-suppressor properties in a variety of cancer cell lines, and it has been suggested that RBM5 expression can influence *RBM10*. Due to their similarities, and the recent evidence that *RBM10* is mutated in up to 21% of lung cancers, we hypothesized that RBM10 would share RBM5's tumor-suppressor properties in SCLC. Using transcriptome analysis and functional assays, we show, however, that RBM10's function was significantly altered by RBM5; in the endogenously *RBM5*-null GLC20 SCLC cell line, RBM10 actually promoted cell proliferation and other transformation-associated processes. Using RNA immunoprecipitation followed by next generation sequencing (RIP-Seq) and Western blotting, we demonstrate that RBM5 post-transcriptionally regulated *RBM10* expression *via* direct interaction with specific *RBM10* splice variants. We propose a working model describing the impact of this interaction on cellular processes. Our results provide evidence that *RBM10* expression, in *RBM5*-null tumors, may contribute to tumor growth and metastasis. Measurement of both *RBM10* and *RBM5* expression in clinical samples may therefore hold prognostic and/or potentially predictive value.

4.2 Introduction

According to the World Health Organization, cancer is one of the main causes of morbidity and mortality worldwide. Lung cancers are not only one of the most diagnosed cancers, but also the main cause of these cancer-related deaths, claiming over 1.6 million lives in 2012 [1]. The most aggressive form of lung cancer is small cell lung cancer (SCLC) [2]. In 90% of SCLC cases, the disease has already metastasized when the patient is diagnosed, which limits treatment options [3]. An astonishing 95% of SCLC patients eventually succumb to the disease, highlighting the need for more effective detection and treatment options [4]. Interestingly, the earliest and most frequent genetic alteration that occurs in lung cancer involves deletion within the 3p21.3 region [5-7]. The RNA binding protein, *RBM5*, resides within this region and is significantly downregulated [8], but not deleted [6], in the majority of lung cancers. Recently, our group demonstrated that this decline in RBM5 expression may be a key step in the establishment of the transformed state of lung cells; RBM5 is responsible for slowing the cell cycle, promoting apoptosis, and downregulating transformation-associated processes such as angiogenesis in SCLC cells [9]. RBM5 may therefore be an important marker for SCLC risk, and could guide the development of more effective screening and/or treatment options.

RBM5 is structurally similar to another RNA binding protein, RBM10. *RBM10* has two main alternative splice variants termed *RBM10* variant 1 (*RBM10v1*) and *RBM10* variant 2 (*RBM10v2*) [10-12]. Each main RBM10 splice variant also codes for alternative isoforms with or without the

addition of one valine residue (Fig 4.1) [13]. Structurally, RBM10v2 has 53% identity to RBM5 [12].

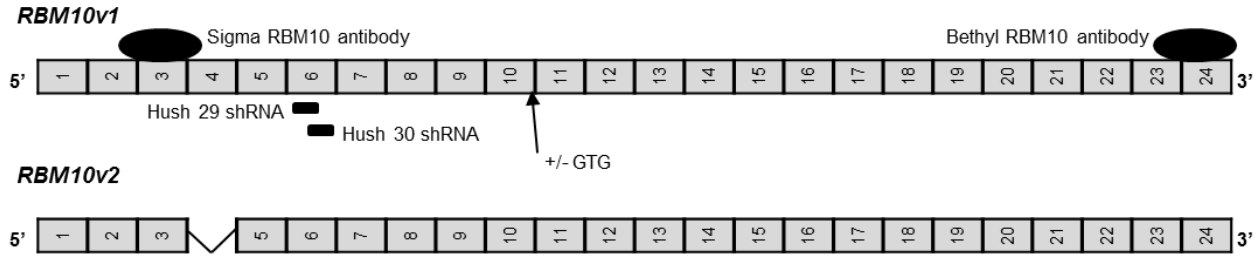

Figure 4.1 Schematic representation of RBM10v1/v2 exons. Exons are represented by grey boxes outlined in black. Box sizes are not representative of actual exon size. Black ovals represent approximate location of the epitopes recognized by the antibodies used in this study. Solid black lines represent the approximate location of shRNA RBM10 targets, which were not variant specific. Corresponding names of antibodies and shRNA are listed next to their approximate location. Arrow indicates position of the GTG codon coding for the valine residue that can be differentially spliced from RBM10 transcripts (last amino acid coded by exon 10).

RBM5 and RBM10 also share functional similarities, and both have tumor-suppressor properties in various cancer cell lines [10, 12, 14]. Functional data for RBM10 are limited, but in certain studies, RBM10 promoted apoptosis and/or decreased cell proliferation; (1) *RBM10* expression correlated with decreased cell proliferation and increased apoptosis in primary chondrocytes induced to hypertrophy [15], (2) *RBM10v1* expression in breast cancer specimens correlated with the expression of proapoptotic BAX and the tumor suppressor gene p53 [16], (3) stable *RBM10* knockdown (KD) in cervical cancer cells (HeLa) correlated with a significant increase in colony formation by clonogenic assays [17], (4) in lymphoblastic leukemia (Jurkat) and breast cancer (MCF-7) cells, transient *RBM10* overexpression correlated with increased levels of apoptosis, whereas stable RBM10KD correlated with lower TNF-α protein levels, as well as decreased TNF-α mediated apoptosis [10], and (5) in a mouse xenograft tumor model with HeLa cells, RBM10KD enhanced tumor growth [14]. In contrast, other studies suggest an anti-apoptotic function for RBM10; (1) RBM10KD in SHSY5Y human neuronal cells augmented proapoptotic

caspase activity after staurosporine exposure [18], (2) expression of both *RBM10* mRNA variants in breast cancer cells positively correlated with *VEGF* mRNA, a promoter of new blood vessel growth [16], and (3) in patients with metastatic melanoma, high *RBM10* expression correlated with increased disease aggressiveness [19]. Considered as a whole, these results suggest that the regulation of cell growth is an important aspect of RBM10 function, but that the mechanism regulating this function requires elucidation. Limited evidence suggests that this regulation depends, at least in part, on the related RNA binding protein RBM5 [20].

Considering the similarities between RBM5 and RBM10, and the recent finding that *RBM10* is mutated in up to 21% of invasive lung adenocarcinomas [21], we hypothesized that RBM10 shares RBM5's tumor-suppressor properties in SCLC. Consequently, RBM10 may also hold prognostic potential for assessing SCLC risk and provide important information regarding the development and/or progression of this particularly aggressive form of lung cancer. To this end, we set out to determine RBM10's role in SCLC, and compare it to that of RBM5.

4.3 Materials and Methods

4.3.1 Cell culture & subline establishment

SCLC GLC20 cells were gifted by the late Dr. Charles Buys from the University of Groningen (Groningen, Netherlands) and cultured as previously described [9]. Stable RBM5-expressing T2 and C4 GLC20 sublines were established as previously described [9].

SCLC GLC20 RBM10 stable KD sublines were generated from passage 7 GLC20 wild type cells. Several different dilutions of GLC20 cells were plated in 24-well flat-bottom plates (Sarstedt AG & Co., Nümbrecht, Germany) and incubated at 37°C with 5% CO2 in a humidified chamber for 24 hours. Half of the cells were transfected with a control shRNA vector "Hush 300" (TR30003, Origene Technologies, Inc, Rockville, U.S.A) and the other half with a 50:50 shRNA mix of "Hush 29" (TI308329, Origene, 5'-GCCTTCGTCGAGTTTAGTCACTTGCAGGA) and "Hush 30" (TI308330, Origene, 5'-AGTCACTTGCAGGACGCTACACGATGGAT). Hush 29 and 30 both target exon 6 of RBM10 and are not variant 1 or variant 2 specific (Fig 4.1). Cells were transfected using Lipofectamine 2000 (L2000) (Invitrogen, Life Technologies, Burlington, Canada). Transfected cells were selected using 0.1 μg/mL puromycin (Invitrogen) starting at 48 hours post-transfection. After seven days of selection, cells were treated with a Histopaque solution (Sigma-Aldrich) to separate live from dead cells. The stable negative control shRNA subline was named G300.3, and three surviving RBM10KD sublines were named G29/30.1, G29/30.3 and G29/30.4.

4.3.2 RNA sequencing and analysis

RNA samples were isolated using Tri-Reagent (BioCan Scientific, Mississauga, Canada). All sequencing was performed by the Donnelly Sequencing Centre (Toronto, Canada) on the Illumina HiSeq 2500 platform. RNA-Seq library preparation and sequencing specifications were as previously described [9]. All specimens, therefore, had (1) quality score distributions over all sequences above 37 (on a phred 33 quality scale), as determined by FastQC (Babraham Bioinformatics, http://bioinformatics.bbsrc.ac.uk/projects/fastqc/), and (2) low quality ends

trimmed during adapter trimming (quality cut-off of 26), as previously recommended [22]. Specifications for the GLC20 stable scramble control and RBM10KD (G29/30.4) were as follows; (1) RNA was not DNAse treated prior to sequencing, (2) reads were 125 bp long, and (3) both samples were multiplexed together and run in one lane. Sequencing data has been deposited to the NCBI Sequence Read Archive (SRA) database, under the submission ID SUB2649287.

Sequencing results were analyzed and pathway analysis carried out as previously described [9].

4.3.3 Western blotting

Performed as previously described [9]. Two rabbit anti-human RBM10 primary antibodies were also used: Sigma-Aldrich, HPA034972 and Bethyl Laboratories, A301-006A-1.

4.3.4 RNA immunoprecipitation followed by next generation sequencing (RIP-Seq)

The basic RIP technique was carried out as previously described [23]. RNA was sequenced by the Donnelly Sequencing Centre on the Illumina HiSeq 2500 platform. Libraries were prepared using the Illumina TruSeq Stranded Total RNA library preparation kit with Ribozero Gold depletion and random priming. Associated samples were multiplexed together for sequencing, and each run was 125 bp and pair-ended. The RBM10 antibody used for RBM10 immunoprecipitation was from Sigma-Aldrich (catalogue number: HPA034972), and the non-

specific IgG Control was from Cell Signaling (catalogue number: 2729). Sequencing data has been deposited to the NCBI Sequence Read Archive (SRA) database, under the submission ID SUB2649287.

The FPKM and log2-fold change expression values generated by Cuffdiff were used to determine protein targets. The potential target had to meet the following inclusion criteria in the RBM5 or RBM10 RIP sample, as previously described [9]: (1) an FPKM value above one, and (2) a log2-fold change above one (and necessarily positive, indicating it was more highly expressed than in the Control RIP).

4.3.5 Cell growth assay

GLC20 cells and RBM10-knockdowns were plated, as previously described [9], and monitored every day for five days by MTT assays. At the indicated time intervals, cells were treated with 10 μL of 5 mg/mL MTT (3-(4,5-dimethylthiazol-2-yl)-2,5-diphenyltetrazolium bromide) Reagent (Life Technologies) in PBS (Gibco) for 2 hours and 45 min at 37°C, as previously described [24]. Following incubation, cells were transferred to a 96-well Vee-bottom plate (Sarstedt) and subjected to centrifugation. Supernatant was discarded and the blue formazan precipitate was dissolved in DMSO (BDH Chemicals, VWR). Dissolved crystals were then transferred to a 96-well flat-bottom plate and, after a ten minute incubation, absorbances were read at 540 nm using a BioTek Synergy S4 Spectrophotometer (BioTek Instruments, Inc). Three biological replicates, using cells with different passage numbers, were performed.

Absorbances of each biological replicate were normalized to their respective day 0 absorbance value, and the averages of three or four biological replicates for each day are presented. A Two-way ANOVA statistical analysis was performed with the Bonferroni post-hoc test, comparing all growth to the pcDNA3 subline for the RBM5 sublines or G300.3 for the RBM10KD sublines, using Graphpad Prism 5 (Graphpad Software, Inc., San Diego, U.S.A).

4.4 Results

4.4.1 RBM10 RNA targets in GLC20 cells that express RBM5 cDNA

We first set out to compare RBM5 and RBM10 targets in SCLC. As RBM10 is an RNA binding protein, and was previously shown to be a part of prespliceosomal complexes A and B [25, 26], we determined that RNA Immunoprecipitation followed by next generation sequencing (RIP-Seq) was the most suitable method for identification of RBM10 targets. RIP-Seq involves antibody-driven immunoprecipitation of targeted endogenous protein without breakdown of protein-protein interactions, thus any RNA that is either directly bound to RBM10, and/or bound to RBM10 *via* another RBM10-bound protein would be captured. We anticipated that, having homology and similar functions, RBM10 targets would overlap with those of RBM5. Our group recently identified RBM5 targets using an endogenously RBM5-null SCLC cell line (4S1 Table), GLC20 [24], from which three stable sublines - an empty vector control and two RBM5 expressing (T2 and C4) – had been generated [9]. The "T2" subline was derived from a pool of transfected cells, and had *RBM5* expression levels comparable to non-tumor lung tissue, while the "C4" subline was derived from a single transfected cell, and had 6-fold higher levels of RBM5 than the T2 subline [9]. As RBM5 targets were previously identified in the C4 GLC20

subline, RBM10 RIP-Seq experiments were also performed in this subline in order to directly compare RBM5 and RBM10 targets. Specifically, RBM10 RIP-Seq was performed in biological duplicate in C4 cells using a non-specific IgG as a Control IP and an anti-RBM10 antibody for RBM10-specific IP. Following confirmation of successful IP (Fig 4.2A), the associated RNA was sequenced (4S1 Table).

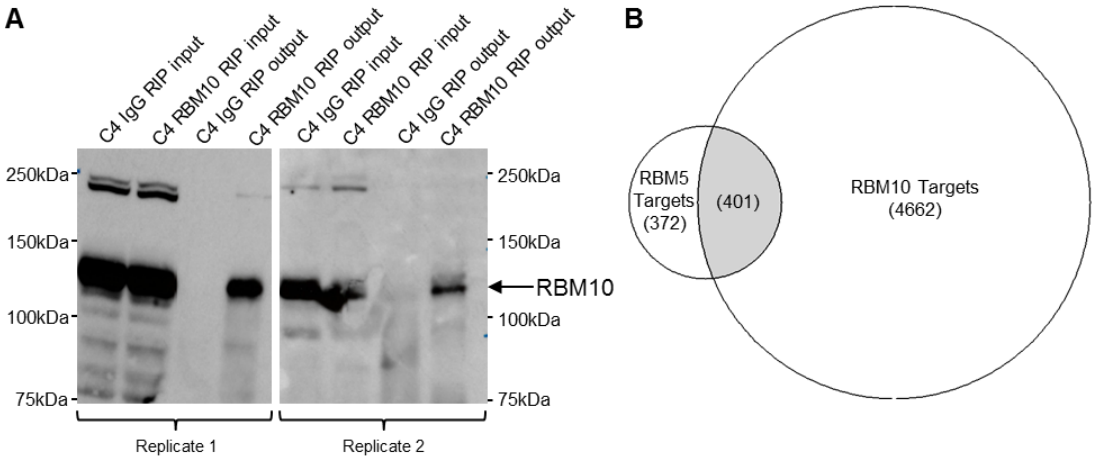

C

GO Molecular Function	Benjamini value
Protein binding	1.14E-10
RNA binding	1.14E-10
Binding	3.78E-07
Heterocyclic compound binding	8.42E-07
Organic cyclic compound binding	8.42E-07
Small molecule binding	2.86E-06
Nucleoside phosphate binding	2.18E-06
Nucleotide binding	2.18E-06
ATP binding	3.37E-04
Adenyl ribonucleotide binding	5.26E-04

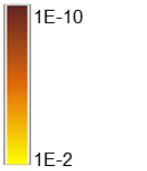

Figure 4.2 RBM10 RIP-Seq results and comparison to identified RBM5 targets. (A) Successful immunoprecipitation of RBM10 from C4 cells, demonstrated by Western Blot of input and output protein samples. Blots probed for RBM10, using the same RBM10 antibody used in the immunoprecipitation experiment (Sigma-Aldrich). Control immunoprecipitation performed, using a non-specific rabbit IgG antibody. (B) Overlap between RBM5 and RBM10 targets in C4 GLC20 subline. (C) GO Molecular Function gene sets enriched in common RBM5 and RBM10 RIP-Seq targets, as determined by FIDEA. Values indicated are Benjamini values.

Using moderate binding criteria, as previously described [9], we identified 5063 RBM10 targets. In our previous study, using the same RIP-Seq procedure and binding criteria, we had identified

773 RBM5 targets in this GLC20 subline [9]. RBM10, therefore, had many more targets than RBM5, suggesting the scope of RBM10's influence in SCLC may be greater than that of RBM5.

Interestingly, more than half of RBM5's targets were shared by RBM10 (Fig 4.2B), confirming that they do have overlapping targets. Furthermore, this suggests that RBM10 plays a key role in RBM5 regulated processes but not *vice versa*. To determine the functional relevance of these common targets, we performed pathway analyses using the Functional Interpretation of Differential Expression Analysis (FIDEA) Program, a program that can be used to analyze various types of differential expression data [27]. Two different databases were used with the FIDEA Program; (1) the Kyoto Encyclopedia of Genes and Genomes (KEGG) Database, which groups genes based on established molecular interactions [28, 29], and (2) the Gene Ontology's (GO) Molecular Function Database, which groups genes based on cellular functions [30, 31]. Using a Benjamini value cut off of 0.005, no KEGG pathways were found to be enriched, a not unexpected result since multiple targets within a single signaling pathway would not necessarily be required for an effect. Using the same Benjamini value parameter, ten GO Molecular Function gene sets were enriched (Fig 4.2C). Interestingly, all enriched gene sets involved binding, including to ATP, nucleotides, protein, RNA and small molecules. Thus RBM5 and RBM10's common targets may regulate a plethora of cellular processes, which may also explain why no individual KEGG pathways were enriched.

Since RBM10 had so many RNA targets that were not shared by RBM5 (Fig 4.2B), we went on to determine the functional importance of these RBM10-specific genes (will be referred to as RBM10-only targets). Using the FIDEA Program with the KEGG Database, we identified eight

significantly enriched pathways (Table 4.1). The most enriched pathway was ‘Metabolic pathways’, consistent with the top RBM10 targets, which are all involved in different aspects of cell metabolism: *NDUFA6* (oxidoreductase activity), *MDP1* (phosphatase activity) and *ATP6VIF* (ion transfer). We were particularly interested to see that the ‘Oxidative phosphorylation’ pathway was the second most-enriched pathway. Notably, changes in oxidative phosphorylation are not only linked to metabolism (the top enriched pathway identified), but also the three disease states enriched in RBM10-only targets: Parkinson’s [32, 33], Huntington’s [34] and Alzheimer’s [35, 36]. The fact that five of the eight enriched KEGG pathways are intimately linked to oxidative phosphorylation strongly suggests that RBM10 plays a particularly important role in this process.

Table 4.1: Pathways and gene sets enriched in RBM10-only RIP-Seq targets.

Pathways & gene sets	Benjamini value
KEGG	
Metabolic pathways	1.78E-8
Oxidative phosphorylation	9.34E-5
Base excision pair	1.56E-4
Huntington's disease	4.37E-4
Alzheimer's disease	1.77E-3
Neurotrophin signaling pathway	1.79E-3
RNA transport	1.79E-3
Parkinson's disease	2.46E-3
GO Molecular Function	
Protein binding	3.62E-34
Binding	6.15E-21
RNA binding	1.07E-13
Structural constituent of ribosome	1.63E-7
Catalytic activity	5.31E-7
Transcription cofactor activity	2.07E-7
Heterocyclic compound binding	2.07E-6
Organic cyclic compound binding	2.07E-6
Transcription factor binding transcription factor activity	4.98E-6
Transferase activity	3.29E-6
Protein binding transcription factor activity	4.34E-6
Enzyme binding	2.30E-6
Nucleic acid binding	2.30E-5
Kinase binding	2.30E-5
Transcription corepressor activity	3.61E-4
Protein kinase binding	1.19E-4
Mitogen-activated protein kinase binding	2.13E-3

Significantly enriched gene sets with Benjamini values below 0.005 are listed.

To determine if these RBM10-only targets shared similar functionality, we used the GO Molecular Function Database with the FIDEA Program. Enriched gene sets are listed in Table 4.1. Many of the enriched gene sets are still showing RBM10 targets involved in a plethora of

binding activities, but a new functional activity involving transcription regulation emerged, suggesting that RBM10 has distinct RBM5-independent functions.

Taken together our RIP-Seq results show that although RBM5 and RBM10 share many common targets, both have distinct targets, with RBM10 having over six times more than RBM5. RBM5 and RBM10 targets, themselves, bind various cellular components, suggesting that RBM5 and RBM10 work together to regulate a variety of cellular processes in SCLC. On the other hand, targets bound by RBM10, but not RBM5, regulated oxidative phosphorylation and numerous aspects of gene expression and protein activity, suggesting RBM10 has distinct mechanisms of action that could be RBM5-independent.

4.4.2 Effect of RBM10 inhibition on dehydrogenase activity in GLC20 cells

Our RIP-Seq results showed that RBM10 directly influenced metabolism, most specifically oxidative phosphorylation. Work in HeLa cells and primary chondrocytes had previously correlated RBM10 expression with decreased cell proliferation [15, 17]. Taken together, these observations suggested that *RBM10* expression would result in decreased SCLC cell proliferation and/or metabolic activity. We therefore chose to use the MTT assay to examine the functional significance of *RBM10* expression to SCLC.

As a first step, we generated stable *RBM10* knockdowns (KDs) in the parental *RBM5*-null GLC20 cells. It is important to note that this GLC20 SCLC cell line is a particularly appropriate model for aggressive SCLC, as RBM5 is downregulated in the majority of lung cancers [8]. RBM10KD was not performed in the T2 or C4 sublines since all *RBM5* expressed in these sublines results from exogenously introduced *RBM5* cDNA. These sublines, therefore, do not express any of the various *RBM5* splice variants that are present in endogenously *RBM5*-expressing systems, rendering results from RBM10KD experiments in these sublines non-physiological. As noted in Materials and Methods, GLC20 cells were subjected to transfection with two RBM10KD shRNA plasmids, together termed 29/30, that targeted an exon common to both *RBM10v1* and *RBM10v2*. Thus, knockdown of *RBM10v1* was not specifically targeted in this study, but due to the almost exclusive expression of RBM10v1 in the GLC20 cells at the protein level (Fig 4.3C), all decreases in RBM10 protein were reported as RBM10v1. Three stable sublines derived from three distinct pooled RBM10KD populations were produced, termed G29/30.1, G29/30.3 and G29/30.4, as well as one control subline, termed G300.3. Somewhat surprisingly, but in line with one of the known mechanisms of shRNA regulation [37, 38], RNA levels of *RBM10* were not diminished in any of the KDs (Fig 4.3A and B). At the protein level, although the G29/30.1 subline demonstrated great variance in protein expression, with no significant decrease in RBM10v1 expression relative to Control (99% expression, p=0.9836), both G29/30.3 and G29/30.4 had significantly lower RBM10v1 protein levels relative to G300/3, with 55% (p=0.0026) and 16% (p=0.0033) the level of Control cells, respectively (Fig 4.3C and D).

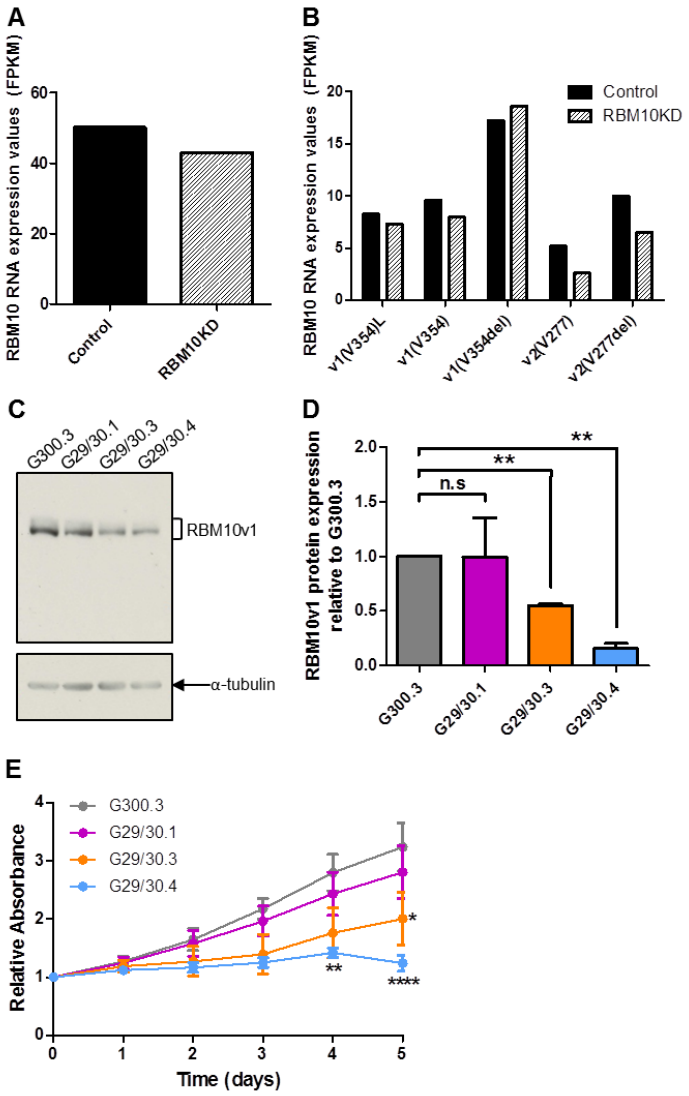

Figure 4.3 RBM10 expression and dehydrogenase activity in control and stable RBM10KD GLC20 sublines. (A & B) RBM10 mRNA levels, determined by RNA-Seq, for all RBM10 variants combined (A) or for individual splice variants (B). 'Control' represents values from parental GLC20 cells and the control G300.3 GLC20 subline. RBM10KD sample used was the G29/30.4 subline, as it showed greatest decrease in RBM10 protein expression. (C & D) RBM10v1 protein levels were monitored in the G300.3, G29/30.1, G29/30.3 and G29/30.4 sublines using the Bethyl RBM10 antibody. (C) One representative Western blot result is presented for RBM10v1 and α-tubulin (loading control). (D) Densitometric results of the average RBM10v1 protein levels from three biological replicates performed in duplicate. Analysis was performed using the AlphaEaseFC, '1D-Multi' analysis tool. Values of RBM10v1 were normalized to the α-tubulin of each biological replicate, and then made relative to the G300.3 control subline. Standard error is presented. Subline expression levels were compared using the Student's unpaired t-test, between sublines. (E) G300.3, G29/30.1, G29/30.3 and G29/30.4 were grown for five days and dehydrogenase activity was monitored daily using an MTT assay. Absorbance was plotted relative to day 0. The average of three biological replicates performed in eight technical replicates with standard error is presented. A Two-way ANOVA was performed between the G300.3 and other sublines, with Bonferroni post-hoc analysis. * $p < 0.05$, ** $p < 0.01$, and **** $p < 0.0001$.

The effect of RBM10KD on dehydrogenase activity was analyzed by MTT assay over a five day period (Fig 4.3E). The G300.3 and G29/30.1 sublines had similar dehydrogenase activity, a result that was anticipated as both sublines had nearly identical levels of RBM10v1 protein expression (Fig 4.3D). The G29/30.3 and G29/30.4 sublines, however, both displayed significantly reduced activity, relative to the G300.3 control. G29/30.4 had the greatest reduction in dehydrogenase activity, with significant differences on day four and day five ($p < 0.01$ and $p < 0.0001$, respectively), compared to G300.3.

These results indicate that the effect of RBM10 was level-dependent. More importantly, however, is the observation that inhibition of *RBM10* expression correlated with dehydrogenase activity that was decreased. Decreased activity could have resulted from either a decrease in cell number and/or a decrease in the metabolic rate of existing cells. Since this finding in an *RBM5*-null background is in contradiction to the previous work in *RBM5*-retaining HeLa cells [14, 17], our results suggest that RBM10 function can not only be altered, but actually reversed by RBM5.

4.4.3 Effect of RBM10 inhibition on signaling pathways in GLC20 cells

To gain a more comprehensive understanding of the extent of RBM10's influence in SCLC, we carried out RNA-Seq, because the MTT assay used above identifies only one functional consequence resulting from inhibition of RBM10. For these experiments, the stable RBM10KD G29/30.4 subline was used, as it had the greatest RBM10KD (referred to simply as RBM10KD in the following figures and the Discussion). As our Control, we sequenced and combined data for the stable pcDNA3 transfected GLC20 cells [9] and the stable scramble shRNA control

G300.3. Sequencing and analysis were performed as previously described [9]. Specific parameters are listed in Materials and Methods. Using the Cufflinks suite, we identified 1157 significantly differentially expressed genes, representing approximately 4.45% of the transcriptome (4S2 Table).

To determine the functional relevance of the differentially expressed genes, we performed pathway analyses. To ensure the validity of our results, as for the RIP-Seq data analyses, two different pathway analysis programs were used, each with their own database. We began with the FIDEA Program and the KEGG Database. With these tools, that group genes based on molecular interactions, we identified four enriched pathways (Fig 4.4A). The only upregulated pathway upon RBM10KD was 'Axon guidance'. Genes involved in axon guidance are deleted or the subject of promoter hypermethylation in many cancers [39]. As *RBM10* expression would correlate with decreased expression of these 'Axon guidance' factors, this may be one way by which RBM10 could promote the transformed state of lung cells. On the other hand, all three pathways that were significantly downregulated upon RBM10KD are positively linked with cancer; (1) 'Alcoholism'-related pathways have been shown to promote the transformed state, in part via increased EMT [40], (2) 'Glycolysis' is upregulated in cancers and is the main pathway for ATP production, even in the presence of oxygen [41], and (3) 'Systemic lupus erythematosus', an autoimmune disease, is linked with an increased risk of cancer, especially cancers of hematologic origin, as well as lung and hepatobiliary cancers [42, 43]. These results suggest that RBM10 could promote the transformed state in a wide variety of ways, including modulation of the immune system and various aspects of cell metabolism.

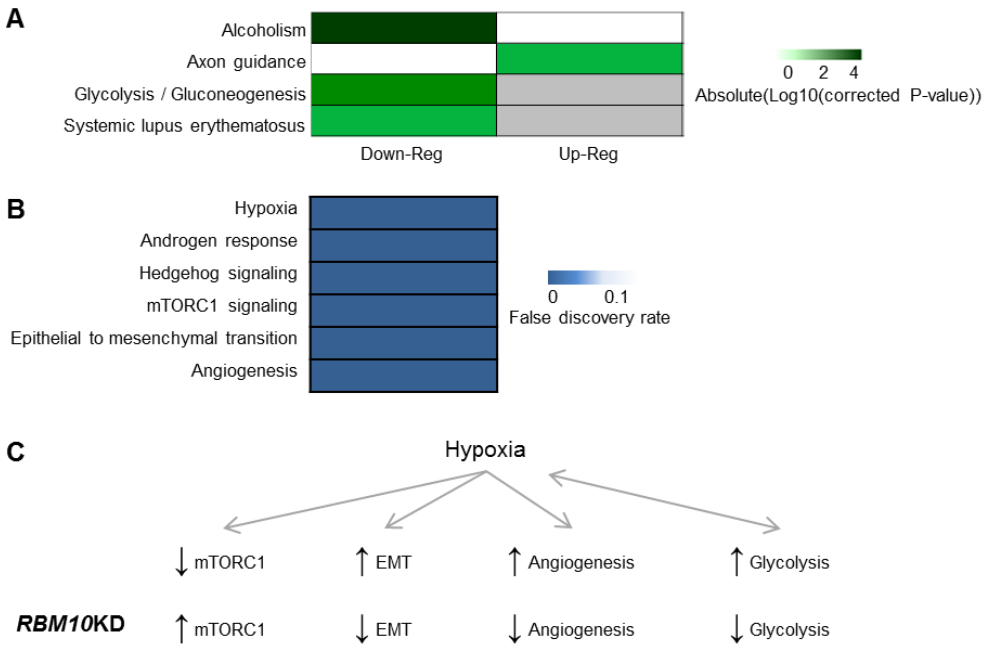

Figure 4.4 Pathway analysis of genes differentially expressed upon RBM10KD in GLC20 cells. (A) KEGG pathways significantly enriched upon RBM10KD in GLC20 cells. Analysis performed using subline RNA-Seq expression data and the FIDEA pathways analysis program. (B) MSigDB Hallmark gene sets enriched at a false discovery rate of below 5% upon RBM10KD in GLC20 cells. Analysis performed using subline RNA-Seq expression data and the GSAASeqSP pathway analysis program. (C) Relationship between select RBM10-altered pathways in GLC20 cells. Hypoxia is associated with decreased levels of mTORC1 signaling, and promotion of EMT and angiogenesis. In addition, hypoxia is associated with increased levels of glycolysis, and likewise, survival in hypoxic conditions is promoted by increased levels of glycolysis. The influence of RBM10KD on these pathways, as determined by RNA-Seq is indicated.

To complement our FIDEA and KEGG pathway analysis, we used the Gene Set Association Analysis with Sequence Permutation (GSAASeqSP) Program, which is specific for RNA-Seq data [43], with the Broad Institute's Molecular Signatures Hallmark Database (MSigDB), which groups genes based on known functions [45]. As shown in Fig 4.4B, six gene sets with false discovery rates (FDR) below 5% were enriched upon RBM10KD in GLC20 cells. The most enriched gene set was 'Hypoxia', which coordinates well with the KEGG pathway analysis results described above; hypoxic conditions increase rates of glycolysis, and likewise, increased glycolysis supports tumor growth in hypoxic conditions [46]. Interestingly, three of the other five gene sets significantly enriched upon RBM10KD are also influenced by hypoxia; 'mTORC1

signaling', 'Epithelial to Mesenchymal Transition' (EMT) and 'Angiogenesis'. Of note, the 'mTORC1 signaling' pathway, which regulates cell growth, is downregulated during hypoxia [47]. Conversely, EMT and angiogenesis can be promoted during hypoxia [48, 49] (Fig 4.4C). Although our GSAASeqSP analysis showed that these three hypoxia-related gene sets were enriched upon RBM10KD, we went on to determine if RBM10KD specifically promoted or inhibited these processes.

Firstly, in hypoxic conditions, downregulation of mTORC1 signaling is accomplished, in part, by ATM protein kinase, REDD1 and BNIP3 [47, 50, 51]. Interestingly, in our system, RBM10KD correlated with decreased levels of all three of these genes: *ATM* levels decreased from 27.98 fragments per kilobase of transcript per million mapped read (FPKM) (Control) to 20.188 FPKM (RBM10KD), *REDD1* levels decreased from 71.65 FPKM (Control) to 30.96 FPKM (RBM10KD), and *BNIP3* levels decreased from 58.02 FPKM (Control) to 19.70 FPKM (RBM10KD). These results suggest that mTORC1 signaling is promoted upon RBM10KD (Fig 4.4C).

Secondly, we examined the impact of RBM10KD on the expression of previously published EMT-associated genes [52]. Notably, all genes listed as downregulated during EMT in the referenced review were significantly upregulated upon RBM10KD in GLC20 cells, or showed no significant change in expression. The significantly upregulated genes included *CDH1*, *TJP1*, *PATJ*, *JUP* and *DSC2*. On the other hand, all genes listed as upregulated during EMT, except fibronectin, were either significantly downregulated upon RBM10KD in GLC20 cells or showed

no significant change expression. The significantly downregulated genes included *VIM*, *ID1* and *ZEB1*. Our results therefore show that RBM10KD is associated with decreased EMT (Fig 4.4C). This is in line with our KEGG pathway analysis, which showed that RBM10KD decreased the EMT-promoting 'Alcoholism' pathway.

Finally, we examined the expression of angiogenesis markers [49] in our RBM10KD samples: RBM10KD significantly decreased the expression of three by at least nine FPKM (*VEGF* from 20 to 9 FPKM; *FGF10* from 10 to 1 FPKM; *PLGF* from 75 to 33 FPKM), and increased the expression of two others, but only by 1-2 FPKM (*THBS1* from 1.75 to 3.8 FPKM; *ANGPT1* from 0.89 to 1.8 FPKM). These results show that, in general, RBM10KD correlates with decreased angiogenic marker expression (Fig 4.4C).

In summary, our GSAASeqSP pathway analysis showed that RBM10KD correlated with increased mTORC1 signaling, and decreased EMT and angiogenesis. Therefore, *RBM10* expression would be expected to downregulate mTORC1 signaling and promote EMT and angiogenesis, thereby influencing these processes in a similar way as hypoxia, and consequently promoting the transformed state. The large overlap in the results obtained using the two different pathway analysis programs (FIDEA and GSAASeqSP), each with their own database (KEGG and MSigDB), strongly supports our conclusion that RBM10 influences various hypoxia-related pathways to promote the transformed state. Together, our pathway analysis results suggest that, unlike RBM5, RBM10 promotes the transformed state. RBM10 does this specifically by (1) increasing glycolysis, (2) reducing mTORC1 signaling, which is associated with deregulated cell

growth and could contribute to the higher viable cell metabolism activity observed in *RBM10* expressing GLC20 cells by MTT (Fig 4.3E), (3) promoting EMT, thereby contributing to the establishment and progression of the transformed state, and (4) promoting angiogenesis. This wide scope of influence is supported by the large number of RBM10-only targets identified by RIP-Seq.

4.4.4 Differential gene expression in GLC20 RBM10KD cells compared to RBM5 expressing GLC20 cells

Having determined that RBM5 and RBM10 share similar targets in the C4 subline, and affect similar processes in SCLC, but with opposing functional consequences, we decided to identify and compare the genes influenced by both proteins. To this end, we examined differential gene expression following either RBM10KD or *RBM5* expression in GLC20 cells. We anticipated that many of the same genes would be influenced, but in an opposite manner, by each protein.

Comparing the RNA-Seq data from our G29/30.4 GLC20 RBM10KD subline with the RNA-Seq data from the stable RBM5-expressing GLC20 sublines T2 and C4, we determined that many of the same genes were in fact differentially expressed following either RBM10KD or RBM5 expression; of the significantly differentially expressed genes in RBM10KD, 53.8% were also significantly differentially expressed between Control and T2, and 60.7% were also differentially expressed between Control and C4 (Fig 4.5). As expected, well over half of these common differentially expressed genes (428 genes) were the same whether RBM10KD was compared to T2 or C4. Therefore, RBM5 and RBM10 do affect the expression of many of the same genes.

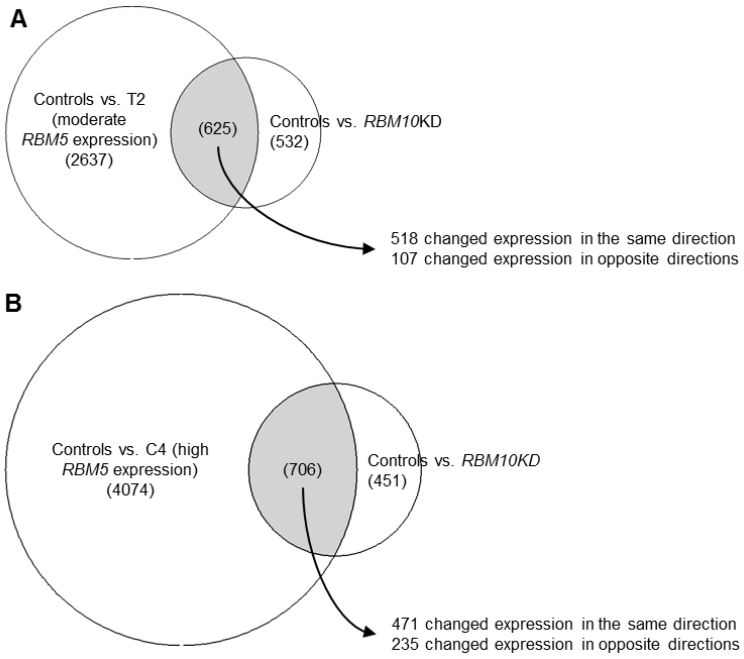

Figure 4.5 Comparison of genes differentially expressed upon RBM10KD in GLC20 cells or RBM5 expression in GLC20 sublines. Differentially expressed genes, based on RNA-Seq results, in GLC20 cells upon RBM10KD, and moderate (A) or high (B) expression levels of RBM5 expression.

We then went on to determine how RBM5 and RBM10 levels affected the expression of these commonly differentially expressed genes. Between RBM10KD and T2 *RBM5* expression, 82% of the common significantly differentially expressed genes changed expression in the same direction (Fig 4.5A). As for RBM10KD and C4 *RBM5* expression, 67% of the differentially expressed genes changed expression in the same direction (Fig 4.5B). Next, we wanted to determine if this similarity would extend to genes specifically associated with SCLC. In June 2014, the National Cancer Institute compiled a list of 'Genes of Interest in SCLC', as part of their report entitled Scientific Framework for Small Cell Lung Cancer. We recently demonstrated that *RBM5* expression in C4 significantly altered the expression of 11 of these SCLC-associated genes in a way which would suppress tumor growth [9]. Here we now show

that RBM10KD altered the expression of nine of these 11 genes in the same direction as *RBM5* expression; *BLC2*, *CCNE1*, *CREBBP*, *EPHA7*, *MED12L*, *MYCL*, *SLIT2*, *SMO* and *SOX2* (Table 4.2). This high level of similarity between the effect of *RBM5* expression and RBM10KD on gene expression, especially SCLC-associated genes, suggests opposing roles for RBM5 and RBM10 in aggressive SCLC, and supports our MTT and RNA-Seq findings.

Table 4.2: Expression of select National Cancer Institute (NCI) 'Genes of Interest in SCLC' in Control and RBM10KD samples, as determined by RNA-Seq.

Gene name	**Control**	**RBM10KD**	***p*-value**
BCL2	1.81928	1.26218	0.29525
CCNE1	18.6741	15.4965	0.2551
COBL †	0.774161	1.82919	0.00095
CREBBP ‡	5.54439	9.8752	0.0001
EPHA7	16.5578	21.467	0.09965
MED12L †	4.10916	2.75174	0.0181
MYCL	11.3944	8.92857	0.17185
RAB37	0.737284	0.803781	0.758
SLIT2 ‡	5.30312	10.1706	0.00005
SMO †	5.8898	4.02038	0.04565
SOX2 †	13.317	8.46985	0.0124

† Genes significantly downregulated upon RBM10KD ($p < 0.05$).
‡ Genes significantly upregulated upon RBM10KD ($p < 0.05$).

4.4.5 Effect of RBM5 on RBM10 expression

Previous studies have shown tumor-suppressor properties for both RBM5 and RBM10. In the results presented herein, however, using an aggressive *RBM5*-null SCLC model, we show an opposite effect for RBM10, correlating its expression with promotion of various transformation-associated processes. These results suggested to us that RBM5 may be a regulator of RBM10 function, a relationship previously supported by our work in a rat myoblast system [20]. To investigate if and how RBM5 might influence RBM10, we examined *RBM10* mRNA and protein expression in our stable *RBM5*-expressing GLC20 sublines T2 and C4.

RBM10 mRNA levels in T2 and C4 were determined from RNA-Seq data [9]. Since *RBM10* splice variants differ, in some cases, by only one amino acid, this level of resolution was required to precisely quantify the expression of each variant (Fig 4.1). Differential expression analysis of RNA-Seq results showed no significant change in *RBM10* mRNA expression levels following *RBM5* expression in GLC20 cells (Fig 4.6A). There was also no significant change in the expression of any *RBM10* splice variant when RBM5 levels were altered (Fig 4.6B). RBM5 did not, therefore, influence *RBM10* transcription or alternative splicing.

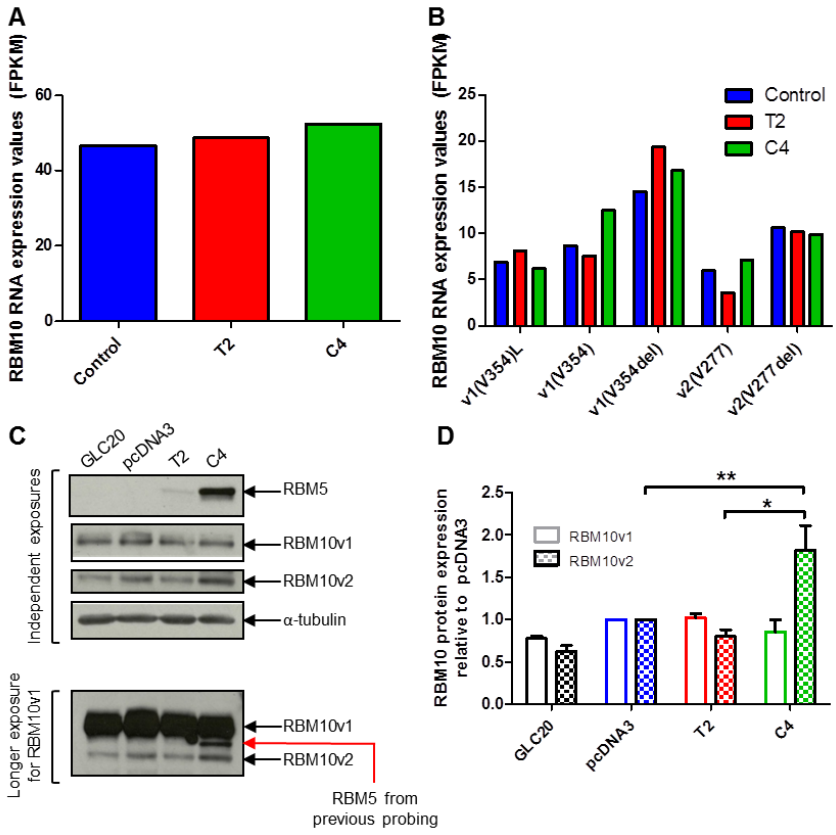

Figure 4.6 RBM10 expression in the parental GLC20 cell line and stable RBM5-expressing sublines. (A) Expression of all *RBM10* mRNA variants, as determined by RNA-Seq. (B) mRNA expression of specific RBM10 splice variants, as determined by RNA-Seq. 'Control' in A and B refers to the GLC20 parental cell line and stable pcDNA3-transfected GLC20 subline. (C) Representative Western blot for RBM5 and RBM10 (Sigma antibody) protein expression levels. Alpha-tubulin was used as loading control. (D) Densitometric results of the average RBM10v1/v2 expression of three biological replicates each performed in technical duplicate. Analysis was performed using AlphaEaseFC, '1D-Multi' analysis tool. Values of RBM10v1 and RBM10v2 were normalized to the α-tubulin of each biological technical duplicate, and then made relative to the pcDNA3 controls. Standard error is presented. One-way ANOVA was performed with Tukey post-hoc analysis, between sublines. * $p < 0.05$ and ** $p < 0.01$.

To determine if RBM5 is capable of influencing *RBM10* post-transcriptionally, RBM10 protein levels were investigated via Western blot. To note, only the two major isoforms of RBM10 (v1 and v2) are distinguishable on Western blots. Interestingly, RBM10v1 levels were not altered between sublines, whereas RBM10v2 levels were significantly increased in C4 compared to either T2 or the Control (Fig 4.6C and D). These results demonstrated that RBM5 was capable of

influencing *RBM10* expression, that this influence occurred post-transcriptionally, and that the effect was restricted to *RBM10v2*.

This increase in RBM10v2 levels could potentially have resulted from a targeted increase of *RBM10v2* translation, or from stabilization of the RBM10v2 isoform, by high levels of RBM5. Increased *RBM10v2* translation would likely involve binding of RBM5 protein to *RBM10v2* transcript, whereas stabilization of the RBM10v2 isoform by RBM5 would involve a protein/protein interaction. As a next step in our investigations, we decided to examine the ability of RBM5 protein to interact with *RBM10* transcripts. Towards this end, we re-examined our previous RBM5 RIP-Seq data (from C4 cells) [9]. As RIP-Seq provides a single nucleotide resolution of all RNA targets, we would be able to determine if RBM5 interacted with specific *RBM10* splice variants. As shown in Fig 4.7A, RBM5 bound only the one specific *RBM10* splice variant, *RBM10v2(V277del)*. RBM5 bound 186.357 FPKM of *RBM10v2(V277del)*, compared to 2.62 FPKM of IgG bound *RBM10v2(V277del)* in the Control RIP. All other RBM10 splice variants had counts of 0.1 FPKM or below, in the RBM5 RIP sample, a result clearly unrelated to variant expression levels in C4 (Fig 4.6B). This level of specificity, in regards to RBM5's binding of only one RBM10 splice variant, is likely due to structural differences between RBM10 alternative splice transcripts, which is supported by our preliminary RNA structure analysis (Fig 4.S1 – Thesis Fig 4.8) [53]. Interestingly, in an RBM5-null environment, we found that RBM10 was also capable of binding self; specifically, using our RIP-Seq data, we found that just like RBM5, RBM10 bound *RBM10v2(V277del)* mRNA. Unlike RBM5, which was only able to bind the one *RBM10v2* variant, RBM10 was able to bind not only both variants of *RBM10v2*,

at high levels (Fig 4.7B), but also *RBM10v1(V354del)*, to a lesser extent (28.1 FPKM). These results show that RBM10 protein can in fact bind *RBM10* mRNA and thus it may, like RBM5, be involved in regulating RBM10 isoform expression.

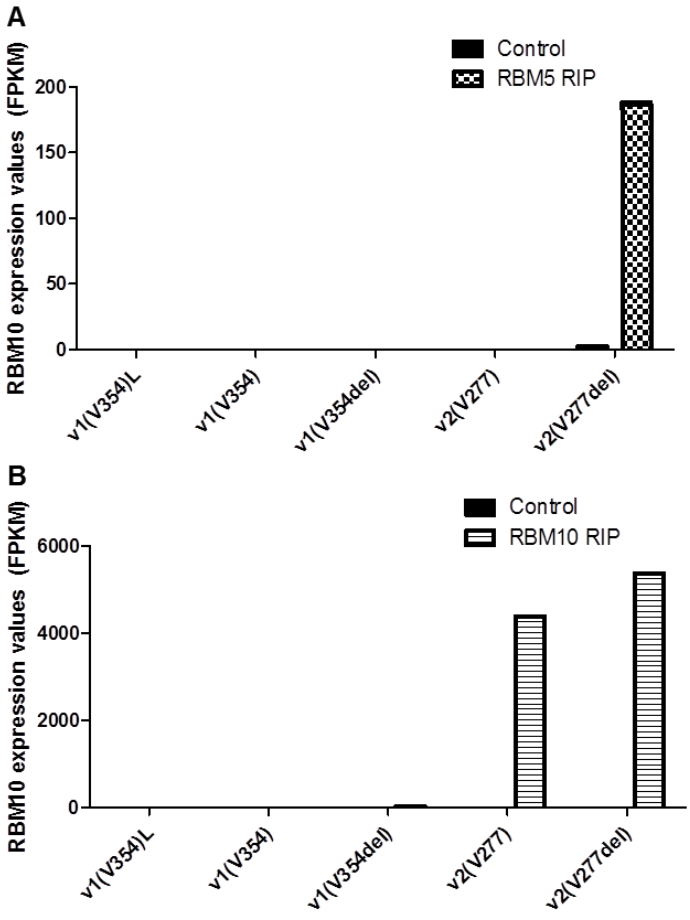

Figure 4.7 RBM5 and RBM10 RIP-Seq results for *RBM10* splice variants. Graph representing the expression of the various *RBM10* splice variants in RBM5 (A) and RBM10 (B) RIP-Seq experiments, which were carried out in C4 cells.

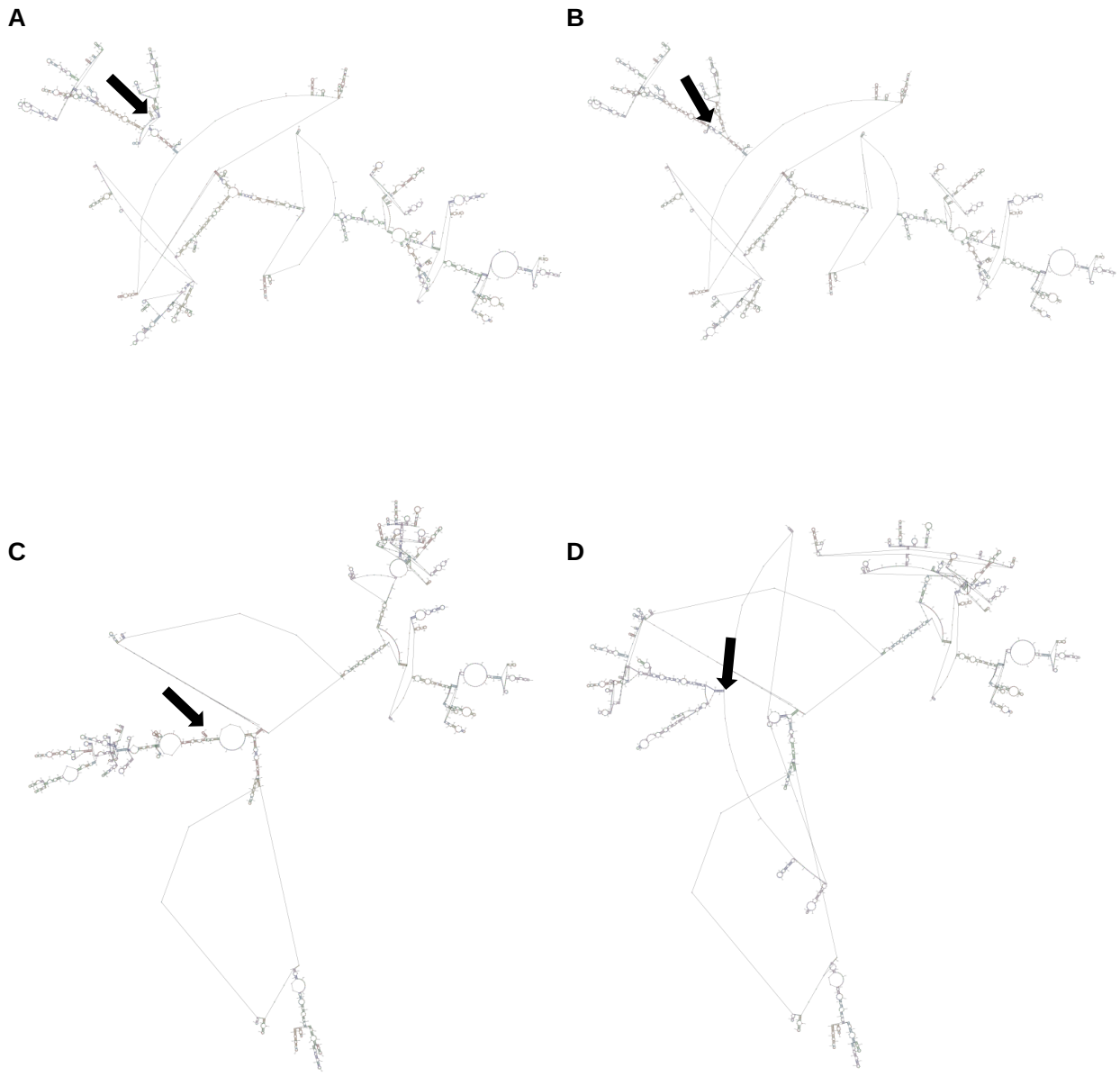

Figure 4.8 Predicted mRNA structure of *RBM10* splice variants. Most probable RNA structure for (A) RBM10v1(V354), (B) RBM10v1(V354del), (C) RBM10v2(V277) and (D) RBM10v2(V277del), as determined by RNAstructure MaxExpect with standard settings. Structure generated is composed of highly probable base pairs. Black arrow indicates position of the 'GTG' codon alternatively spliced from both RBM10v1 and RBM10v2, which results in their respective +/- valine isoforms. *This figure is part of the supplementary materials of the published manuscript (Fig S1)*

4.5 Discussion

Functional RBM10 is important for normal cellular processes. For instance, mutations in *RBM10* are the cause of TARP syndrome, which results in many developmental abnormalities and often lethality before or soon after birth [11, 54, 55]. Furthermore, *RBM10* is mutated in pancreatic intraductal papillary mucinous neoplasms [56], 7% of lung adenocarcinomas [57], and 21% of invasive lung adenocarcinomas [21]. *RBM10* has also been suggested to be important to rat myoblast differentiation [20]. Therefore, understanding the regulation of RBM10, as well as the range of its downstream effects, is of interest to various areas of cell, developmental and cancer biology.

Previous studies relating to RBM10, which have been performed in *RBM5*-expressing systems, have primarily linked *RBM10* expression with reduced cell proliferation and promotion of apoptosis [10, 14-17]. The study reported here explores, for the first time, the function of RBM10 in an RBM5-null system, and the regulation of *RBM10* by RBM5. As *RBM5* is downregulated in many cancers [8, 58-62], this work is particularly meaningful. Here we show that RBM10 actually promotes transformation-associated processes in an *RBM5*-null environment. Supporting our findings, *RBM10* has been associated with increased expression of *VEGF*, a promoter of new blood vessel growth, in breast cancer samples [16]. In addition, in patients with metastatic melanoma, high *RBM10* expression was correlated with increased disease aggression [19]. Of note, the *RBM5* promoter was identified as a "Signature of accelerated somatic evolution" in melanomas, with mutations in this region correlating with significantly lower survival rates and a higher incidence of metastasis [63]. Therefore, altered

RBM5 levels in melanoma may result in decreased translational regulation of RBM10, and thus the pro-transformation characteristics associated with RBM10 in melanomas, and here in our *RBM5*-null system. In fact, in solid tumors in general, *RBM5* is one of nine genes, within a 17 gene signature associated with metastasis, that are downregulated in various humans [64] and mice [65]. Thus, the increased metastatic characteristics of tumors with decreased RBM5 levels could in part involve decreased translational regulation of RBM10 by RBM5. This is particularly relevant as we show that RBM10 upregulates processes such as EMT and angiogenesis in an *RBM5*-null system.

The majority of functional studies relating to RBM10 have focused on its role in modulation of alternative splicing [14, 17, 66-69], likely due to the early findings that RBM10 is a core component of spliceosomal A and B complexes [25, 26, 70]. Our RNA-Seq results show, however, no significant shifts in alternative splicing upon RBM10KD in GLC20 cells (no genes had a significant increase in the expression of one alternative splice variant and a significant decrease in the expression of another) (4S2 Table), a finding we postulate may be dependent on RBM5 expression. Of note, upon RBM5 expression in GLC20 cells, using the same techniques and analysis parameters, we detected multiple alternative splicing changes. Our transcriptomic analyses, which show no effect of RBM10 downregulation on alternative splicing in GLC20 cells, are supported by (1) our RBM10-only targets (Table 4.1), which are involved in various aspects of gene expression regulation, excluding alternative splicing, (2) RBM10's mRNA stabilization effect on its only identified direct RNA target, the AT1 receptor [71], and (3) RBM10's interaction with the 2A-DUB deubiquitinase protein complex [72] and the Rac-

specific GTPase-activitating protein FilGAP [73]. These findings are not unanticipated considering RNA binding proteins are known to participate in multiple aspects of RNA metabolism, including RNA editing, polyadenylation, export, localization, translation and stability [74]. Future studies regarding RBM10 should therefore attempt to capture its influence on these other aspects of RNA biology, and not be restricted to alternative splicing. Falling to do so would result in an incomplete view of the scope of RBM10's influence on the cell.

More important than the role of RBM10 in the regulation of alternative splicing might be the role of alternative splicing of *RBM10* itself. The single valine residue that differentiates the two *RBM10v1* variants, as well as the two *RBM10v2* variants, occurs within the second RNA Recognition Motif (RRM) of RBM10. The presence or absence of this valine residue can influence the α-helical structure of this RRM domain, and could thus influence RBM10's binding targets [13, 14]. Although the functional implications of this modification have yet to be tested, the level of binding specificity exhibited by RBM5 suggests that (1) the presence or absence of this valine residue modifies RBM10's structure sufficiently for proteins (at least RBM5) to be able to distinguish between variants, and (2) RBM10 splice variants have specific, potentially opposing, roles in the cell, and thus require specific regulation.

Based on our results and those of previous RBM10-related studies, we propose a working model describing RBM5's influence on *RBM10* and yet to be confirmed functional interactions between RBM5 and RBM10 (Fig 4.S2 – Thesis Fig 4.9). This is an extension of a previous model we developed in a non-transformed rat myoblast system, which described how RBM10 might

influence RBM5 [20]. We hypothesize that RBM10's binding to *RBM10v2* mRNA results in a downregulation of RBM10v2 protein expression levels. This would explain the much lower levels of RBM10v2 protein, compared to RBM10v1, that we observed in all GLC20 sublines (Fig 4.6C), even though mRNA levels for both variants were very similar (Fig 4.6A, B). Furthermore, we suggest that RBM5's binding to *RBM10v2(V277del)* promotes this transcript's translation or prevents its degradation, resulting in the higher levels of RBM10v2 protein seen in the C4 population. The lack of significantly higher RBM10v2 protein expression in T2 (Fig 4.6C), compared to Control, is not unexpected since this subline has substantially less RBM5 expressed than C4. We postulate that RBM10v2 is an essential component, or participates in the formation, of certain RBM5 protein complexes, which would explain why (1) RBM5 would upregulate RBM10v2 protein levels, (2) such a large proportion of RBM5 targets were also shared by RBM10 in our RIP-Seq experiments, and (3) RBM10 would have so many RBM10-only targets; these targets would represent RBM10v1 targets, which would be independent from those targeted by the RBM5-RBM10v2 complex.

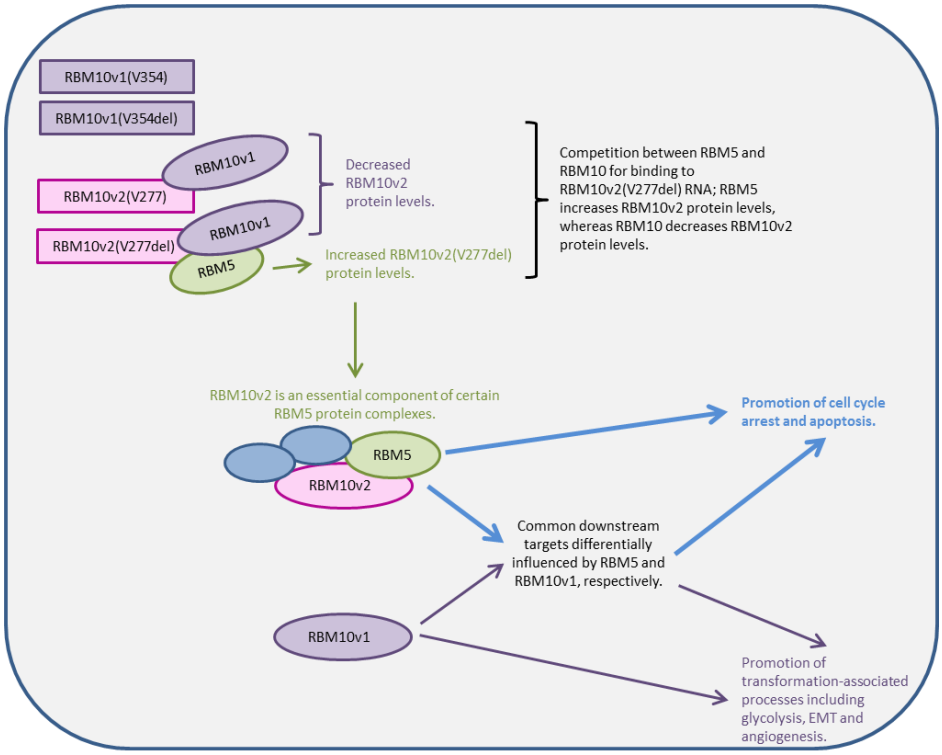

Figure 4.9 Working model representing RBM5 and RBM10 function and interactions in SCLC. Rectangles represent mRNA, whereas ovals represent protein. Blue ovals are unspecified proteins. *This figure is part of the supplementary materials of the published manuscript (Fig S2)*

We propose that the RBM5-RBM10v2 complex regulates cell cycle progression and promotes apoptosis, functions with which RBM5 has been previously associated. We suggest that most, but not all, RBM5's tumor-suppressor properties occur via this RBM5-RBM10v2 complex. The RBM5-RBM10v2 complex could also be responsible for the alternative splicing events previously associated with RBM10. This would explain why, in an *RBM5*-null system, these alternative splicing events do not appear to be influenced by RBM10 (e.g., there would be no RBM5-RBM10v2 complex). On the other hand, we suggest that RBM10v1 promotes transformation-associated processes, including glycolysis, EMT and angiogenesis. Some of the downstream RBM5-RBM10v2 and RBM10v1 targets overlap, with both complexes affecting the

expression of these genes in an opposing manner. This would explain the similarity of differentially expressed genes upon *RBM5* expression and RBM10KD in GLC20 cells, but why RBM5 and RBM10 affected the expression of these genes in contrasting ways (Fig 4.5). We also propose that the RBM5-RBM10v2 complex has a more significant influence on transformation-associated pathways than RBM10v1, explaining why cells expressing physiological levels of both RBM5 and RBM10 have regulated cell growth (as seen in the T2 subline) [9].

According to our working model, upon *RBM5* expression, an RBM5-RBM10v2 complex would be formed, resulting in higher levels of apoptosis and cell cycle arrest (Fig 4.S3A – Thesis Fig 4.10A). This is in line with what we have previously shown experimentally upon *RBM5* expression in GLC20 cells [9]. Inversely, upon RBM5KD, less RBM5-RBM10v2 complex would be formed, resulting in decreased apoptosis and deregulated cell growth, as well as less competition for RBM10v1 regarding their common targets (Fig 4.S3B – Thesis Fig 4.10B). This would all contribute to promotion of a transformation-like phenotype. Indeed, this is what we observed previously in parental GLC20 cells, compared to the *RBM5*-expressing sublines [9]. Upon RBM10KD in an *RBM5*-expressing system, we would expect almost no RBM5-RBM10v2 complex to be formed, especially as RBM10v2 levels are already so much lower than RBM10v1 in GLC20 cells (Fig 4.S3C – Thesis Fig 4.10C). This would result in a significant decrease in apoptosis, as well as reduced regulation of cell cycle progression. Although knockdown of *RBM10* would also significantly decrease RBM10v1 levels, since RBM10 would not be completely knocked out in this situation, some RBM10v1 would remain in the cell. This small amount of RBM10v1 could still promote transformation-associated processes to a certain point,

especially with much less competition from the RBM5-RBM10v2 complex. In this case, we would expect a slight increase in cell growth upon RBM10KD in *RBM5*-expressing systems. This hypothesis is in line with previous functional work performed for RBM10 in endogenously *RBM5*-expressing HeLa cells [17]. Finally, upon RBM10KD in an RBM5-null system, since there would be no influence from the RBM5-RBM10v2 complex, RBM10KD would only significantly reduce levels of RBM10v1 (Fig 4.S3D – Thesis Fig 4.10D). This would result in diminished promotion of transformation-associated processes, and thus lower levels of cell growth and/or metabolism. This proposition is in line with the MTT and RNA-Seq results presented herein regarding RBM10KD in endogenously *RBM5*-null GLC20 cells (Figs 4.3E and 4).

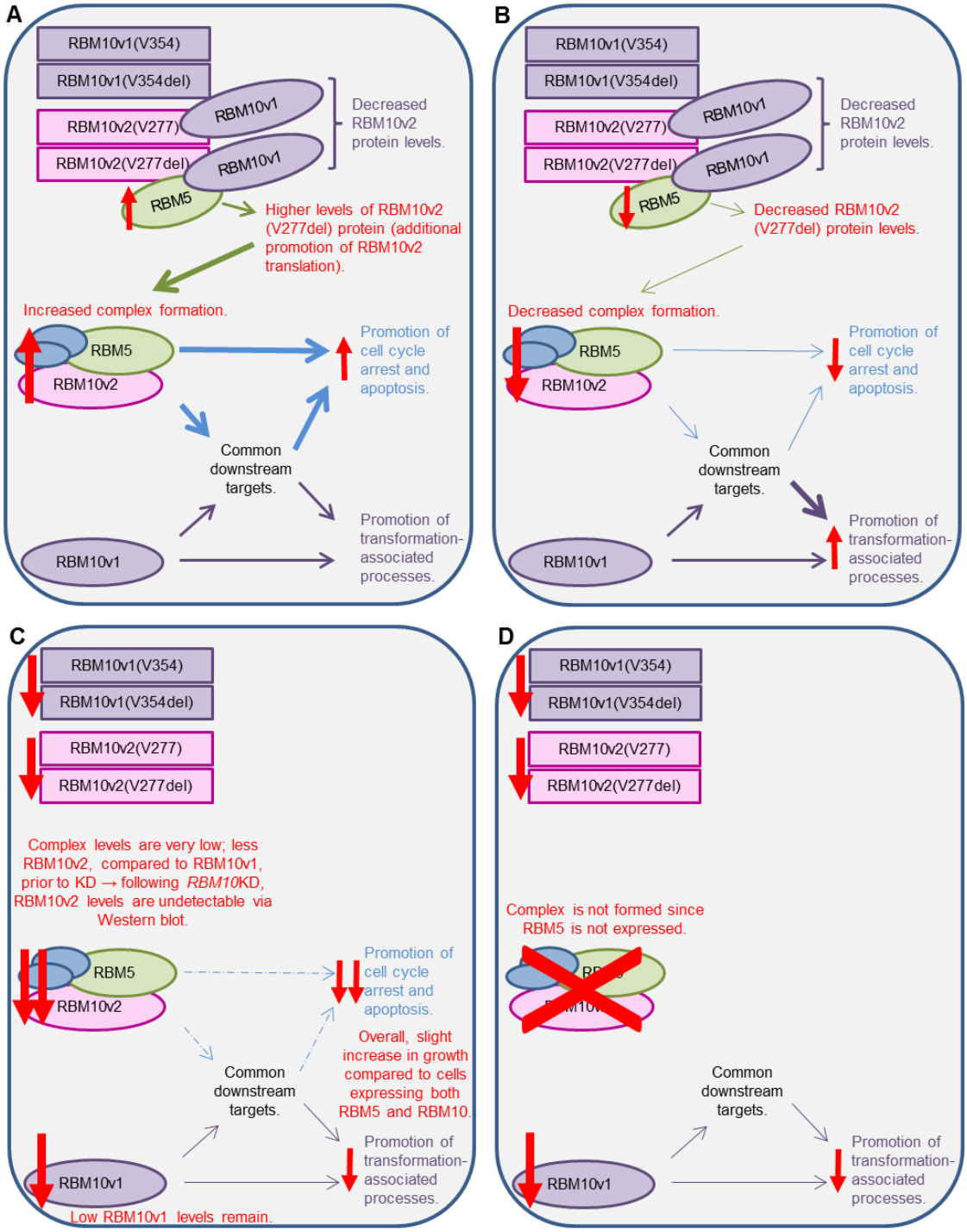

Figure 4.10 Prediction of the effects of modulating RBM5 and/or RBM10 levels. Using our working model, we predict the effects of (A) *RBM5* overexpression, (B) RBM5KD, (C) RBM10KD in an *RBM5*-expressing system, and (D) RBM10KD in an *RBM5*-null system. Open green, blue and purple arrows indicate effect, and thickness of said arrows indicates activity levels (dotted arrows indicate least activity). Closed red arrows indicate direction of expression change only. For detailed description of model, refer to text. *This figure is part of the supplementary materials of the published manuscript (Fig S3)*

Interestingly, *RBM10* mutations have recently been associated with lung adenocarcinoma pathogenesis [66]. Loss-of-function *RBM10* mutations would result in no functional RBM10 in the cell and, based on our working model, no RBM5-RBM10v2 complex. This would have two opposing consequences; (1) loss of RBM10v1 would result in reduced promotion of transformation-associated processes, and (2) loss of RBM5-RBM10v2 complex would result in reduced regulation of the cell cycle and decreased apoptosis, and thus promotion of transformation. Since, as we proposed above, the influence of RBM5-RBM10v2 is greater than RBM10v1, we would expect the overall effect of loss-of-function *RBM10* mutations to be pro-transformatory, similar to the effects of RBM5KD. This is indeed the result seen in clinical samples; loss-of-function *RBM10* mutations were associated with increased pathogenesis of lung adenocarcinomas [21]. These findings further support our working model.

A very recent study in non-transformed mouse cells not only supports our working model, but extends its relevance beyond cancer-based systems [75]. In that study, Rodor *et al.* knocked out *RBM10* in mouse cells and examined a number of processes, including cell proliferation. According to our working model, since RBM10 would be completely depleted in this scenario, RBM10v1 could no longer promote transformation-associated processes and RBM5-RBM10v2 complexes would be completely eliminated. Since RBM10 would no longer influence cellular processes, RBM5 could exercise its RBM10v2-independent tumor-suppressor properties. We would thus predict that RBM10 knockout would result in a decrease in cell proliferation. This is indeed what the authors found. Although *Rodor et al.* strongly associated RBM10 with the

regulation of alternative splicing in that study [75], as mouse cells in general express RBM5 [76], this could be an RBM5-dependent function of RBM10, as we propose above.

Considered together, our results suggest that the RBM10 reversal-of-function associated with downregulation of *RBM5* is one means by which cells transition to a cancerous state, largely through processes that involve regulation of a hypoxic state. Our results shed light on the relationship between RBM5 and RBM10, a particularly important aspect to remember when studying either of these genes individually. We not only determine, for the first time, the role of RBM10 in an *RBM5*-null system, but also propose a working model to explain how RBM10 is influenced by *RBM5* expression. We also identify all RBM10 targets and explore the extent of RBM10's influence on cellular processes. In addition, we show that RBM5 directly binds *RBM10* to regulate its expression post-transcriptionally, and that RBM5 and RBM10 share similar direct (RIP-Seq) and downstream (RNA-Seq) targets. These results lay the groundwork for additional studies to examine the role(s) of specific RBM10 isoforms, and the relationship between RBM5 and RBM10 in different systems and disease states.

4.6 References

1. Ferlay J, Soerjomataram I, Dikshit R, Eser S, Mathers C, Rebelo M, et al. Cancer incidence and mortality worldwide: sources, methods and major patterns in GLOBOCAN 2012. Int J Cancer. 2015;136(5):E359-E86. doi: 10.1002/ijc.29210 [doi].

2. Jackman DM, Johnson BE. Small-cell lung cancer. Lancet. 2005;366(9494):1385-96. doi: S0140-6736(05)67569-1 [pii];10.1016/S0140-6736(05)67569-1 [doi].

3. Johnson DH, Schiller JH, Bunn PA, Jr. Recent clinical advances in lung cancer management. J Clin Oncol. 2014;32(10):973-82. doi: JCO.2013.53.1228 [pii];10.1200/JCO.2013.53.1228 [doi].

4. Chute JP, Chen T, Feigal E, Simon R, Johnson BE. Twenty years of phase III trials for patients with extensive-stage small-cell lung cancer: perceptible progress. J Clin Oncol. 1999;17(6):1794-801.

5. Lerman MI, Minna JD. The 630-kb lung cancer homozygous deletion region on human chromosome 3p21.3: identification and evaluation of the resident candidate tumor suppressor genes. The International Lung Cancer Chromosome 3p21.3 Tumor Suppressor Gene Consortium. Cancer Res. 2000;60(21):6116-33.

6. Wistuba II, Behrens C, Virmani AK, Mele G, Milchgrub S, Girard L, et al. High resolution chromosome 3p allelotyping of human lung cancer and preneoplastic/preinvasive bronchial epithelium reveals multiple, discontinuous sites of 3p allele loss and three regions of frequent breakpoints. Cancer Res. 2000;60(7):1949-60.

7. Hung J, Kishimoto Y, Sugio K, Virmani A, McIntire DD, Minna JD, et al. Allele-specific chromosome 3p deletions occur at an early stage in the pathogenesis of lung carcinoma. JAMA. 1995;273(24):1908. PubMed PMID: 7783298.

8. Oh JJ, West AR, Fishbein MC, Slamon DJ. A candidate tumor suppressor gene, H37, from the human lung cancer tumor suppressor locus 3p21.3. Cancer Res. 2002;62(11):3207-13.

9. Loiselle JJ, Roy JG, Sutherland LC. RBM5 reduces small cell lung cancer growth, increases cisplatin sensitivity and regulates key transformation-associated pathways. Heliyon. 2016;2(11):e00204. doi: 10.1016/j.heliyon.2016.e00204. PubMed PMID: 27957556; PubMed Central PMCID: PMCPMC5133678.

10. Wang K, Bacon ML, Tessier JJ, Rintala-Maki ND, Tang V, Sutherland LC. RBM10 Modulates Apoptosis and Influences TNA-a Gene Expression. Journal of Cell Death. 2012;5:1-19.

11. Johnston JJ, Teer JK, Cherukuri PF, Hansen NF, Loftus SK, Chong K, et al. Massively parallel sequencing of exons on the X chromosome identifies RBM10 as the gene that causes a syndromic form of cleft palate. Am J Hum Genet. 2010;86(5):743-8.

12. Sutherland LC, Rintala-Maki ND, White RD, Morin CD. RNA binding motif (RBM) proteins: a novel family of apoptosis modulators? J Cell Biochem. 2005;94(1):5-24.

13. Tessier SJ, Loiselle JJ, McBain A, Pullen C, Koenderink BW, Roy JG, et al. Insight into the role of alternative splicing within the RBM10v1 exon 10 tandem donor site. BMC Res Notes. 2015;8:46. doi: 10.1186/s13104-015-0983-5 [doi];10.1186/s13104-015-0983-5 [pii].

14. Hernandez J, Bechara E, Schlesinger D, Delgado J, Serrano L, Valcarcel J. Tumor suppressor properties of the splicing regulatory factor RBM10. RNA Biol. 2016;13(4):466-72. doi: 10.1080/15476286.2016.1144004. PubMed PMID: 26853560.

15. James CG, Ulici V, Tuckermann J, Underhill TM, Beier F. Expression profiling of Dexamethasone-treated primary chondrocytes identifies targets of glucocorticoid signalling in endochondral bone development. BMC Genomics. 2007;8:205.

16. Martinez-Arribas F, Agudo D, Pollan M, Gomez-Esquer F, az-Gil G, Lucas R, et al. Positive correlation between the expression of X-chromosome RBM genes (RBMX, RBM3,

RBM10) and the proapoptotic Bax gene in human breast cancer. J Cell Biochem. 2006;97(6):1275-82.

17. Bechara EG, Sebestyen E, Bernardis I, Eyras E, Valcarcel J. RBM5, 6, and 10 Differentially Regulate NUMB Alternative Splicing to Control Cancer Cell Proliferation. Mol Cell. 2013;52(5):720-33.

18. Jackson TC, Du L, Janesko-Feldman K, Vagni VA, Dezfulian C, Poloyac SM, et al. The nuclear splicing factor RNA binding motif 5 promotes caspase activation in human neuronal cells, and increases after traumatic brain injury in mice. J Cereb Blood Flow Metab. 2015;35(4):655-66. doi: jcbfm2014242 [pii];10.1038/jcbfm.2014.242 [doi].

19. Garrisi VM, Strippoli S, De SS, Pinto R, Perrone A, Guida G, et al. Proteomic profile and in silico analysis in metastatic melanoma with and without BRAF mutation. PLoS One. 2014;9(12):e112025. doi: 10.1371/journal.pone.0112025 [doi];PONE-D-14-20054 [pii].

20. Loiselle JJ, Tessier SJ, Sutherland LC. Post-transcriptional regulation of Rbm5 expression in undifferentiated H9c2 myoblasts. In Vitro Cell Dev Biol Anim. 2015. doi: 10.1007/s11626-015-9976-x. PubMed PMID: 26659391.

21. Vinayanuwattikun C, Le Calvez-Kelm F, Abedi-Ardekani B, Zaridze D, Mukeria A, Voegele C, et al. Elucidating Genomic Characteristics of Lung Cancer Progression from In Situ to Invasive Adenocarcinoma. Sci Rep. 2016;6:31628. doi: 10.1038/srep31628. PubMed PMID: 27545006; PubMed Central PMCID: PMCPMC4992872.

22. Del Fabbro C, Scalabrin S, Morgante M, Giorgi FM. An extensive evaluation of read trimming effects on Illumina NGS data analysis. PLoS One. 2013;8(12):e85024. doi: 10.1371/journal.pone.0085024. PubMed PMID: 24376861; PubMed Central PMCID: PMCPMC3871669.

23. Jain R, Devine T, George AD, Chittur SV, Baroni TE, Penalva LO, et al. RIP-Chip Analysis: RNA-Binding Protein Immunoprecipitation-Microarray (Chip) Profiling. In: Nielsen H, editor. RNA. Methods in Molecular Biology: Humana Press; 2011. p. 247-63.

24. Smit EF, de Vries EG, Timmer-Bosscha H, de Leij LF, Oosterhuis JW, Scheper RJ, et al. In vitro response of human small-cell lung-cancer cell lines to chemotherapeutic drugs; no correlation with clinical data. Int J Cancer. 1992;51(1):72-8.

25. Behzadnia N, Golas MM, Hartmuth K, Sander B, Kastner B, Deckert J, et al. Composition and three-dimensional EM structure of double affinity-purified, human prespliceosomal A complexes. EMBO J. 2007;26(6):1737-48.

26. Deckert J, Hartmuth K, Boehringer D, Behzadnia N, Will CL, Kastner B, et al. Protein composition and electron microscopy structure of affinity-purified human spliceosomal B complexes isolated under physiological conditions. Mol Cell Biol. 2006;26(14):5528-43.

27. D'Andrea D, Grassi L, Mazzapioda M, Tramontano A. FIDEA: a server for the functional interpretation of differential expression analysis. Nucleic Acids Res. 2013;41(Web Server issue):W84-8. doi: 10.1093/nar/gkt516. PubMed PMID: 23754850; PubMed Central PMCID: PMCPMC3692084.

28. Kanehisa M, Goto S. KEGG: kyoto encyclopedia of genes and genomes. Nucleic Acids Res. 2000;28(1):27-30. PubMed PMID: 10592173; PubMed Central PMCID: PMCPMC102409.

29. Kanehisa M, Sato Y, Kawashima M, Furumichi M, Tanabe M. KEGG as a reference resource for gene and protein annotation. Nucleic Acids Res. 2016;44(D1):D457-62. doi: 10.1093/nar/gkv1070. PubMed PMID: 26476454; PubMed Central PMCID: PMCPMC4702792.

30. Ashburner M, Ball CA, Blake JA, Botstein D, Butler H, Cherry JM, et al. Gene ontology: tool for the unification of biology. The Gene Ontology Consortium. Nat Genet. 2000;25(1):25-9. doi: 10.1038/75556. PubMed PMID: 10802651; PubMed Central PMCID: PMCPMC3037419.

31. Gene Ontology C. Gene Ontology Consortium: going forward. Nucleic Acids Res. 2015;43(Database issue):D1049-56. doi: 10.1093/nar/gku1179. PubMed PMID: 25428369; PubMed Central PMCID: PMCPMC4383973.

32. Finsterer J, Jarius C, Baumgartner M. Parkinson's disease associated with impaired oxidative phosphorylation. Neuroradiology. 2001;43(11):997-1000. PubMed PMID: 11760809.

33. Shoffner JM, Watts RL, Juncos JL, Torroni A, Wallace DC. Mitochondrial oxidative phosphorylation defects in Parkinson's disease. Ann Neurol. 1991;30(3):332-9. doi: 10.1002/ana.410300304. PubMed PMID: 1952821.

34. Damiano M, Galvan L, Deglon N, Brouillet E. Mitochondria in Huntington's disease. Biochim Biophys Acta. 2010;1802(1):52-61. doi: 10.1016/j.bbadis.2009.07.012. PubMed PMID: 19682570.

35. Biffi A, Sabuncu MR, Desikan RS, Schmansky N, Salat DH, Rosand J, et al. Genetic variation of oxidative phosphorylation genes in stroke and Alzheimer's disease. Neurobiol Aging. 2014;35(8):1956 e1-8. doi: 10.1016/j.neurobiolaging.2014.01.141. PubMed PMID: 24650791; PubMed Central PMCID: PMCPMC4329419.

36. Manczak M, Park BS, Jung Y, Reddy PH. Differential expression of oxidative phosphorylation genes in patients with Alzheimer's disease: implications for early mitochondrial dysfunction and oxidative damage. Neuromolecular Med. 2004;5(2):147-62. doi: 10.1385/NMM:5:2:147. PubMed PMID: 15075441.

37. Gu S, Kay MA. How do miRNAs mediate translational repression? Silence. 2010;1(1):11. doi: 10.1186/1758-907X-1-11. PubMed PMID: 20459656; PubMed Central PMCID: PMCPMC2881910.

38. Valencia-Sanchez MA, Liu J, Hannon GJ, Parker R. Control of translation and mRNA degradation by miRNAs and siRNAs. Genes Dev. 2006;20(5):515-24. doi: 10.1101/gad.1399806. PubMed PMID: 16510870.

39. Chedotal A, Kerjan G, Moreau-Fauvarque C. The brain within the tumor: new roles for axon guidance molecules in cancers. Cell Death Differ. 2005;12(8):1044-56. doi: 10.1038/sj.cdd.4401707. PubMed PMID: 16015381.

40. Forsyth CB, Tang Y, Shaikh M, Zhang L, Keshavarzian A. Alcohol stimulates activation of Snail, epidermal growth factor receptor signaling, and biomarkers of epithelial-mesenchymal transition in colon and breast cancer cells. Alcohol Clin Exp Res. 2010;34(1):19-31. doi: 10.1111/j.1530-0277.2009.01061.x. PubMed PMID: 19860811; PubMed Central PMCID: PMCPMC3689303.

41. Warburg O. On the origin of cancer cells. Science. 1956;123(3191):309-14. PubMed PMID: 13298683.

42. Dey D, Kenu E, Isenberg DA. Cancer complicating systemic lupus erythematosus--a dichotomy emerging from a nested case-control study. Lupus. 2013;22(9):919-27. doi: 10.1177/0961203313497118. PubMed PMID: 23857987; PubMed Central PMCID: PMCPMC4107831.

43. Bernatsky S, Boivin JF, Joseph L, Rajan R, Zoma A, Manzi S, et al. An international cohort study of cancer in systemic lupus erythematosus. Arthritis Rheum. 2005;52(5):1481-90. doi: 10.1002/art.21029. PubMed PMID: 15880596.

44. Xiong Q, Mukherjee S, Furey TS. GSAASeqSP: a toolset for gene set association analysis of RNA-Seq data. Sci Rep. 2014;4:6347. doi: 10.1038/srep06347. PubMed PMID: 25213199; PubMed Central PMCID: PMCPMC4161965.

45. Liberzon A, Birger C, Thorvaldsdottir H, Ghandi M, Mesirov JP, Tamayo P. The Molecular Signatures Database (MSigDB) hallmark gene set collection. Cell Syst. 2015;1(6):417-25. doi: 10.1016/j.cels.2015.12.004. PubMed PMID: 26771021; PubMed Central PMCID: PMCPMC4707969.

46. Robin ED, Murphy BJ, Theodore J. Coordinate regulation of glycolysis by hypoxia in mammalian cells. J Cell Physiol. 1984;118(3):287-90. doi: 10.1002/jcp.1041180311. PubMed PMID: 6699103.

47. Cam H, Easton JB, High A, Houghton PJ. mTORC1 signaling under hypoxic conditions is controlled by ATM-dependent phosphorylation of HIF-1alpha. Mol Cell. 2010;40(4):509-20.

doi: 10.1016/j.molcel.2010.10.030. PubMed PMID: 21095582; PubMed Central PMCID: PMCPMC3004768.

48. Yang MH, Wu MZ, Chiou SH, Chen PM, Chang SY, Liu CJ, et al. Direct regulation of TWIST by HIF-1alpha promotes metastasis. Nat Cell Biol. 2008;10(3):295-305. doi: 10.1038/ncb1691. PubMed PMID: 18297062.

49. Krock BL, Skuli N, Simon MC. Hypoxia-induced angiogenesis: good and evil. Genes Cancer. 2011;2(12):1117-33. doi: 10.1177/1947601911423654. PubMed PMID: 22866203; PubMed Central PMCID: PMCPMC3411127.

50. Li Y, Wang Y, Kim E, Beemiller P, Wang CY, Swanson J, et al. Bnip3 mediates the hypoxia-induced inhibition on mammalian target of rapamycin by interacting with Rheb. J Biol Chem. 2007;282(49):35803-13. doi: 10.1074/jbc.M705231200. PubMed PMID: 17928295.

51. Brugarolas J, Lei K, Hurley RL, Manning BD, Reiling JH, Hafen E, et al. Regulation of mTOR function in response to hypoxia by REDD1 and the TSC1/TSC2 tumor suppressor complex. Genes Dev. 2004;18(23):2893-904. doi: 10.1101/gad.1256804. PubMed PMID: 15545625; PubMed Central PMCID: PMCPMC534650.

52. Lamouille S, Xu J, Derynck R. Molecular mechanisms of epithelial-mesenchymal transition. Nat Rev Mol Cell Biol. 2014;15(3):178-96. doi: 10.1038/nrm3758. PubMed PMID: 24556840; PubMed Central PMCID: PMCPMC4240281.

53. Reuter JS, Mathews DH. RNAstructure: software for RNA secondary structure prediction and analysis. BMC Bioinformatics. 2010;11:129. doi: 10.1186/1471-2105-11-129. PubMed PMID: 20230624; PubMed Central PMCID: PMCPMC2984261.

54. Gorlin RJ, Cervenka J, Anderson RC, Sauk JJ, Bevis WD. Robin's syndrome. A probably X-linked recessive subvariety exhibiting persistence of left superior vena cava and atrial septal defect. Am J Dis Child. 1970;119(2):176-8. PubMed PMID: 5410571.

55. Kurpinski KT, Magyari PA, Gorlin RJ, Ng D, Biesecker LG. Designation of the TARP syndrome and linkage to Xp11.23-q13.3 without samples from affected patients. Am J Med Genet A. 2003;120A(1):1-4. doi: 10.1002/ajmg.a.10201. PubMed PMID: 12794682.

56. Furukawa T, Kuboki Y, Tanji E, Yoshida S, Hatori T, Yamamoto M, et al. Whole-exome sequencing uncovers frequent GNAS mutations in intraductal papillary mucinous neoplasms of the pancreas. Sci Rep. 2011;1:161.

57. Imielinski M, Berger AH, Hammerman PS, Hernandez B, Pugh TJ, Hodis E, et al. Mapping the hallmarks of lung adenocarcinoma with massively parallel sequencing. Cell. 2012;150(6):1107-20.

58. Welling DB, Lasak JM, Akhmametyeva E, Ghaheri B, Chang LS. cDNA microarray analysis of vestibular schwannomas. Otol Neurotol. 2002;23(5):736-48.

59. Zhao L, Li R, Shao C, Li P, Liu J, Wang K. 3p21.3 tumor suppressor gene RBM5 inhibits growth of human prostate cancer PC-3 cells through apoptosis. World J Surg Oncol. 2012;10:247.

60. Miller G, Socci ND, Dhall D, D'Angelica M, DeMatteo RP, Allen PJ, et al. Genome wide analysis and clinical correlation of chromosomal and transcriptional mutations in cancers of the biliary tract. J Exp Clin Cancer Res. 2009;28:62.

61. Peng J, Valeshabad AK, Li Q, Wang Y. Differential expression of RBM5 and KRAS in pancreatic ductal adenocarcinoma and their association with clinicopathological features. Oncol Lett. 2013;5(3):1000-4.

62. Kim YS, Hwan JD, Bae S, Bae DH, Shick WA. Identification of differentially expressed genes using an annealing control primer system in stage III serous ovarian carcinoma. BMC Cancer. 2010;10:576.

63. Smith KS, Yadav VK, Pedersen BS, Shaknovich R, Geraci MW, Pollard KS, et al. Signatures of accelerated somatic evolution in gene promoters in multiple cancer types. Nucleic Acids Res. 2015;43(11):5307-17. doi: gkv419 [pii];10.1093/nar/gkv419 [doi].

64. Ramaswamy S, Ross KN, Lander ES, Golub TR. A molecular signature of metastasis in primary solid tumors. Nat Genet. 2003;33(1):49-54.

65. Qiu TH, Chandramouli GV, Hunter KW, Alkharouf NW, Green JE, Liu ET. Global expression profiling identifies signatures of tumor virulence in MMTV-PyMT-transgenic mice: correlation to human disease. Cancer Res. 2004;64(17):5973-81.

66. Zhao J, Sun Y, Huang Y, Song F, Huang Z, Bao Y, et al. Functional analysis reveals that RBM10 mutations contribute to lung adenocarcinoma pathogenesis by deregulating splicing. Sci Rep. 2017;7:40488. doi: 10.1038/srep40488. PubMed PMID: 28091594; PubMed Central PMCID: PMCPMC5238425.

67. Wang Y, Gogol-Doring A, Hu H, Frohler S, Ma Y, Jens M, et al. Integrative analysis revealed the molecular mechanism underlying RBM10-mediated splicing regulation. EMBO Mol Med. 2013;5(9):1431-42.

68. Zheng S, Damoiseaux R, Chen L, Black DL. A broadly applicable high-throughput screening strategy identifies new regulators of Dlg4 (Psd-95) alternative splicing. Genome Res. 2013;23(6):998-1007.

69. Inoue A, Yamamoto N, Kimura M, Nishio K, Yamane H, Nakajima K. RBM10 regulates alternative splicing. FEBS Lett. 2014;588(6):942-7. doi: S0014-5793(14)00094-5 [pii];10.1016/j.febslet.2014.01.052 [doi].

70. Rappsilber J, Ryder U, Lamond AI, Mann M. Large-scale proteomic analysis of the human spliceosome. Genome Res. 2002;12(8):1231-45.

71. Mueller CF, Berger A, Zimmer S, Tiyerili V, Nickenig G. The heterogenous nuclear riboprotein S1-1 regulates AT1 receptor gene expression via transcriptional and posttranscriptional mechanisms. Arch Biochem Biophys. 2009;488(1):76-82.

72. Zhu P, Zhou W, Wang J, Puc J, Ohgi KA, Erdjument-Bromage H, et al. A histone H2A deubiquitinase complex coordinating histone acetylation and H1 dissociation in transcriptional regulation. Mol Cell. 2007;27(4):609-21.

73. Yamada H, Tsutsumi K, Nakazawa Y, Shibagaki Y, Hattori S, Ohta Y. Src Family Tyrosine Kinase Signaling Regulates FilGAP through Association with RBM10. PLoS One. 2016;11(1):e0146593. doi: 10.1371/journal.pone.0146593. PubMed PMID: 26751795; PubMed Central PMCID: PMCPMC4709192.

74. Glisovic T, Bachorik JL, Yong J, Dreyfuss G. RNA-binding proteins and post-transcriptional gene regulation. FEBS Lett. 2008;582(14):1977-86. doi: S0014-5793(08)00207-X [pii];10.1016/j.febslet.2008.03.004 [doi].

75. Rodor J, FitzPatrick DR, Eyras E, Caceres JF. The RNA-binding landscape of RBM10 and its role in alternative splicing regulation in models of mouse early development. RNA Biol. 2017;14(1):45-57. doi: 10.1080/15476286.2016.1247148. PubMed PMID: 27763814; PubMed Central PMCID: PMCPMC5270529.

76. Ozuemba B, Masilamani TJ, Loiselle JJ, Koenderink B, Vanderbeck KA, Knee J, et al. Co- and post-transcriptional regulation of Rbm5 and Rbm10 in mouse cells as evidenced by tissue-specific, developmental and disease-associated variation of splice variant and protein expression levels. Gene. 2016;580(1):26-36. doi: 10.1016/j.gene.2015.12.070. PubMed PMID: 26784654

4.7 Supporting information

4S1 Table. RBM5 and RBM10 RIP-Seq results. RNA expression levels of all genes examined in RBM5 and RBM10 RIP-Seq experiments. Gene expression quantification was performed using Cuffdiff v2.2.1; however, targets were identified using the inclusion criteria elaborated in the Materials and Methods section. Genes listed based on log2(fold-change) in expression, and then their value in the experimental RIP sample.

S1_Table.xlsx

4S2 Table. RNA-Seq gene expression data for Control and RBM10KD GLC20 cells. RNA expression levels for all genes examined, as well as their specific splice variants. Genes listed based on their q-value, and log2(fold-change) in expression. Ctrl refers to combined gene expression values for parental GLC20 cells and the stable pcDNA3 transfected GLC20 subline. Differential expression testing was performed using Cuffdiff v2.2.1. The third sheet contains the information required to identify a particular gene's alternative splice variant(s) (based on their TCONS assigned number from Cufflinks).

S2_Table.xlsx

Chapter 5

5 Post-transcriptional regulation of Rbm5 expression in undifferentiated H9c2 myoblasts

Loiselle JJ, Tessier SJ and Sutherland LC. (2016) *Post-transcriptional regulation of Rbm5 expression in undifferentiated H9c2 myoblasts*. **In Vitro Cellular & Developmental Biology - Animal. 52**(3):327-336.

Full text, open access document can be accessed through the journal's website:
https://link.springer.com/article/10.1007%2Fs11626-015-9976-x

In Vitro Cell.Dev.Biol.—Animal (2016) 52:327–336
DOI 10.1007/s11626-015-9976-x

Post-transcriptional regulation of Rbm5 expression in undifferentiated H9c2 myoblasts

Julie J. Loiselle[1,2] & Sarah J. Tessier[3] & Leslie C. Sutherland[1,2,4,5,6]

Received: 17 July 2015 / Accepted: 4 November 2015 / Published online: 10 December 2015 / Editor: T. Okamato

* Julie J. Loiselle
jloiselle@amric.ca

1 Biomolecular Sciences Program, Laurentian University, 935 Ramsey Lake Road, Sudbury, ON P3E 2C6, Canada

2 AMRIC, Health Sciences North, 41 Ramsey Lake Road, Sudbury, ON P3E 5J1, Canada

3 Department of Biology, Laurentian University, 935 Ramsey Lake Road, Sudbury, ON P3E 2C6, Canada

4 Department of Chemistry and Biochemistry, Laurentian University, 935 Ramsey Lake Road, Sudbury, ON P3E 2C6, Canada

5 Division of Medical Sciences, Northern Ontario School of Medicine, Laurentian University, 935 Ramsey Lake Road, Sudbury, ON P3E 2C6, Canada

6 Department of Medicine, Division of Medical Oncology, University of Ottawa, Ottawa, ON, Canada

5.1 Abstract

We previously examined the expression of Rbm5 during myoblast differentiation and found significantly more protein in the early stages of skeletal myoblast differentiation than during the later stages. We decided to determine if this elevated level was necessary for differentiation. Our hypothesis was that if high levels of Rbm5 protein expression were necessary for the initiation of skeletal myoblast differentiation, then inhibition of expression would prevent differentiation. Our long-term objective is to inhibit Rbm5 expression and examine the effect on H9c2

differentiation. Towards this end, stable knockdown clones and transient knockdown populations were generated. Expression analyses in H9c2 myoblasts demonstrated significant Rbm5 messenger RNA (mRNA) inhibition but, surprisingly, no effect on RBM5 protein levels. Expression of the Rbm5 paralogue Rbm10 was examined in order to (a) ensure no off-target knockdown effect, and (b) investigate any possible compensatory effects. RBM10 protein levels were found to be elevated, in both the clonal and transiently transfected populations. These results suggest that myoblast RBM5 expression is regulated by a process that includes RNA sequestration and/or controlled translation, and that (a) RBM5 function is compensated for by RBM10, and/or (b) RBM5 regulates RBM10 expression. We have developed a model to describe our findings, and suggest further experiments for testing its validity. Since up-regulation of Rbm10 might compensate for downregulated Rbm5, and consequently might mask any potential knock-down effect, it could lead to incorrect conclusions regarding the importance of Rbm5 for differentiation. It is therefore imperative to determine how both RBM5 and RBM10 protein expression is regulated.

5.2 Introduction

In general, the expression of RNA-binding motif domain protein 5 (RBM5) is highest in cells that have reduced proliferation such as aging cells (Geigl et al. 2004), dormant seeds (Sugliani et al. 2010), and in adult thymus compared to fetal liver (Drabkin et al. 1999), and lowest in highly proliferating cells, e.g., most cancers such as non-small cell lung cancers (Oh et al. 2002), vestibular schwannomas (Welling et al. 2002), prostate cancers (Zhao et al. 2012), stage III serious ovarian carcinomas (Kim et al. 2010), pancreatic cancers (Peng et al. 2013), and biliary tract cancers (Miller et al. 2009). In fact, RBM5 was shown to be one of nine genes down

regulated in metastasis as part of the 17-gene signature associated with metastasis in various solid tumor types (Ramaswamy et al. 2003; Qiu et al. 2004). The triggers for these expression fluctuations are unknown; however, using cancer cell lines, some of the mechanisms by which RBM5 expression can be regulated have been identified. For instance, RBM5 can be downregulated at the transcriptional level by a process that involves the read-through of polymerase from the upstream RBM6 gene and the consequent generation of transcription-induced chimeras (Wang et al. 2007). Changes in RBM5 expression also occur via the regulation of alternative splicing, a role played by human epidermal growth factor receptor 2 (Rintala-Maki et al. 2007) and potentially, the antisense non-coding RBM5-related factor, LUST (Rintala-Maki and Sutherland 2009). Post-transcriptionally, RBM5 can be differentially phosphorylated (Shu et al. 2007).

Changes in RBM5 expression levels are associated with changes in both the expression level and the alternative splicing of downstream transcripts. For example, overexpression of RBM5 in the human leukemic cell line CEM-C7 was associated with altered expression of 35 genes, including cyclin-dependent kinase 2 (CDK2) and signal transducer and activator of transcription 5B (Stat5b), which are involved in processes such as G1/S transition and apoptosis, respectively (Mourtada-Maarabouni et al. 2006). Knockdown of RBM5 was associated with altered expression of many genes in a number of different cell lines (a normal lung epithelial cell line (BEAS-2B), a normal breast epithelial cell line (MCF-10A) and three different lung cancer cell lines with varying RBM5 expression levels (A549, Calu-6 and NCI-H1299), notably increasing the expression of genes involved in cell adhesion, migration, and motility, all processes important to metastasis (Oh et al. 2010). In addition, in the MCF-7 breast adenocarcinoma cell

line, RBM5 and tumor necrosis factor alpha (TNF-α) expression were shown to be positively correlated, TNF-α being an important apoptosis regulatory factor (Wang et al. 2012). RBM5 also regulates alternative splicing of pre-messenger RNAs (mRNAs) involved in apoptosis (exclusion of caspase-2 exon 9 (Fushimi et al. 2008) and FAS receptor exon 6 (Bonnal et al. 2008)), seed maturation (the inclusion of an ABIα/β exon (Sugliani et al. 2010), muscular dystrophy (exclusion of dystrophin exons 40 and 72 (O'Leary et al. 2009) and immunoglobulin diversification (exclusion of activation-induced cytidine deaminase exon 4 (Jin et al. 2012).

Is it important to note that RBM5 shares highest homology with another RBM protein, RNA-binding motif domain protein 10 (RBM10) (Sutherland et al. 2005). In fact, RBM5 and RBM10 are approximately 50% homologous at the transcript level in both human and rat. Also, endogenous RBM5 and RBM10v1 protein expression levels have been shown to be significantly positively correlated in primary breast cancer samples (Rintala-Maki et al. 2007).

Similar to RBM5, RBM10 has been shown to influence the alternative splicing of many genes (Behzadnia et al. 2007; Bechara et al. 2013; Wang et al. 2013; Zheng et al. 2013; Inoue et al. 2014). RBM10 is also important for the regulation of apoptosis and proliferation (James et al. 2007; Wang et al. 2012). Very little is known in regards to the importance of RBM5 and RBM10 in muscle differentiation; however, (a) both Rbm5 and Rbm10 are downregulated in H9c2 skeletal muscle differentiation (Loiselle and Sutherland 2014) and highly expressed in skeletal and cardiac muscle (Drabkin et al. 1999; Johnston et al. 2010), (b) RBM5 influences the alternative splicing of dystrophin, an important muscle protein (O'Leary et al. 2009), and (c) RBM10 is important to spermatid differentiation (O'Bryan et al. 2013).

In our previous study, we identified the rat H9c2 myoblast differentiation model as a suitable function-based muscle model in which to study Rbm5 and Rbm10 (Loiselle and Sutherland 2014). Our long-term objective is to determine the importance of Rbm5 to myoblast differentiation. In the study described herein, we manipulated Rbm5 expression levels in undifferentiated myoblasts, in order to characterize expression prior to differentiation. The effects of knockdown and overexpression of Rbm5 on Rbm10 mRNA and protein expression levels were also examined, to rule out off-target knockdown effects and to determine if changes in Rbm5 ex-pression effected the expression of Rbm10, prior to differentiation. The interesting observations that were made have been incorporated into a model that will be tested in future experiments.

5.3 Materials and Methods

5.3.1 Cell culture

Cells were grown as previously described (Loiselle and Sutherland 2014).

5.3.2 Stable knockdown

At 24 h prior to transfection, cells were passed in 100-mm plates (Sarstedt, Montreal, Canada) and as such that they would be approximately 35% confluent at the time of transfection. Twenty-four hours following appropriate plating, 12 µl of Lipofectamine 2000 transfection re-agent (Life Technologies, Burlington, Canada) was mixed with 1.5 ml of Opti-MEM reduced serum media (Life Technologies) with GlutaMAX (Life Technologies), and incubated at room temperature for

5 min. The appropriate small hairpin RNA (shRNA) construct (12 μg) was also mixed with 1.5 ml of Opti-MEM reduced serum media with GlutaMAX, and incubated at room temperature for five minutes. Control samples were transfected with CSHCTR001-nU6 shRNA scrambled control (GeneCopoeia, Rockville, MD). Rbm5 knockdown samples were transfected with both MSH039757-1 and MSH039757-6 Rbm5-specific shRNAs (6 μg of each) (GeneCopoeia) (Table 5.1). The Rbm5-specific shRNAs were 100% homologous to both rat and mouse Rbm5 sequence. Following, the Lipofectamine 2000 + Opti-MEM and shRNA + Opti-MEM solutions were mixed together and incubated at room temperature for 35 min. The transfection solution was then added to the normal, serum-containing media on the cells. Selection began 24 h post-transfection by treating cells with 1 μg/ml of puromycin. Cells were then cultured in antibiotic-containing media to select for successful transfectants for at least 28 days following transfection and until they filled a 100-mm plate (Sarstedt).

5.3.3 Transient knockdown

Twenty-four hours prior to transfection, cells were passed to 6-well plates (Sarstedt) so as to be 40% confluent at the time of transfection. Twenty-four hours after appropriately plating cells, 5 μl of Lipofectamine 2000 transfection reagent (Life Technologies) was added to 245 μl of Opti-MEM reduced serum media (Life Technologies) with GlutaMAX (Life Technologies), and incubated at room temperature for 5 min. The appropriate small interfering RNA (siRNA) or shRNA was also added to 245 μl of Opti-MEM reduced serum media with GlutaMAX, and incubated at room temperature for 5 min. The first transient knockdown experiment was performed with siRNA. The siRNA used for the control sample was Trilencer-27mer universal scrambled negative control siRNA duplex (OriGene, Rockville, MD). For Rbm5 knockdown

samples, custom on-target RBM5 duplex siRNA (Dharmacon, Thermo Fisher Scientific, Ottawa, Canada) was used (Table 5.1). The second and third transient knockdown experiments were performed with shRNAs (same constructs used for stable knockdown experiments). Thus, control samples were transfected with the scramble control CSHCTR001-nU6, and Rbm5 transient knockdown experiments two and three were transfected with MSH039757-1 and MSH039757-6 Rbm5-specific shRNAs, respectively (GeneCopoeia) (Table 5.1). siRNAs and shRNAs had a final concentration of 10 nM when administered to cells. Following a 5-min incubation, the Lipofectamine 2000 + Opti-MEM and siRNA + Opti-MEM solutions were mixed together and incubated at room temperature for 20 min. Next, the transfection solution was added to the normal, serum-containing media on the cells. Medium was not changed after addition of transfection solution, and cell pellets were collected at 72 h post-transfection.

Table 5.1: Small interfering RNA Rbm5 knockdown oligonucleotides.

Type	Name	Sequence	Location	Homology to Rbm10
shRNA	CSHCTR001-nU6		Scrambled	
	MSH039757-1	5′ GTAGTGGAAGATATGGTTC 3′	Exon 3	(12/19) 63%
	MSH039757-6	5′ GAGCGATATTCGAGAAATG 3′	Exon 4/5	(12/19) 63%
siRNA	Trilencer-27mer universal scrambled negative control		Scrambled	
	ON-TARGET RBM5 duplex siRNA	5′ GAGCGATATTCGAGAAATG 3′	Exon 4/5	(12/19) 63%

5.3.4 Transient overexpression

The plasmid used for the transient overexpression of RBM5 was pcDNA3.RBM5 (Rintala- Maki and Sutherland 2004), with pcDNA3 empty vector as the negative control. Note that RBM5 sequence in the vector was human, which has approximately 80% homology with rat. Cells were passaged such that a confluency of 35% would be obtained on the day of the experiment. At that point, 12 μg of the respective pcDNA3 plasmid and 18 μl of Lipofectamine 2000 transfection reagent (Life Technologies) were each mixed separately with 1.5 ml of Opti-MEM reduced serum medium (Life Technologies) with GlutaMAX (Life Technologies). After a 5-min incubation at room temperature, the DNA + Opti-MEM and Lipofectamine 2000 + Opti-MEM mixtures were mixed together, and incubated at room temperature for 20 min. Following this, the transfection mixture was added to the cells. The medium was not changed after addition of the transfection mixture, and cell pellets were collected at 72 h post-transfection.

5.3.5 RNA expression analysis

RNA extraction, reverse transcription, and end-point semi-quantitative PCR were performed as previously described (Loiselle and Sutherland 2014), except in this case, 24 amplification cycles

were used for glyceraldehyde 3-phosphate dehydrogenase (Gapdh), and 38 cycles for Rbm5 and Rbm10 (Table 5.2).

Table 5.2: Primers for end-point PCR.

Gene name	Accession no.	Primer sequence (5′ to 3′)	Amplicon length (bp)	Annealing temp. (°C)
Actb	NM_031144	F: TGAGCGCAAGTACTCTGTGTGGAT	129	62
		R: TAGAAGCATTTGCGGTGCACGATG		
Gapdh	BC059110	F: ACCACAGTCCATGCCATCAC	452	58
		R: TCCACCACCCTGTTGCTGTA		
Rbm5	BC166477	F: ATGGGTTCAGACAAAAGAG	520	55
		R: GCATTGCAATGTGCTTTCCTTGA		
Rbm10	F1LWMO	F: ATTGGCTCCCGTCGAACTAACAGT	916 (10v1)	63
		R: ACTTCTCTCGGCGCTTGAAGTTCT	682 (10v2)	

F forward primer (5′ primer), R reverse primer (3′ primer)

Densitometric analysis was performed using AlphaEase FC software (Alpha Innotec, Kasendorf, Germany). Rbm5 and Rbm10 mRNA expression values were first normalized to the 300-bp ladder band to account for gel exposure differences between replicates, then to Gapdh, the reference gene used. Next, the average of the normalized expression value obtained for all technical replicates of a biological replicate was determined. This average normalized expression value was then expressed as a fold-change from the control sample of that biological replicate, and averaged for the various biological replicates. This gave the final expression value that was graphed.

5.3.6 Protein expression analysis

Protein samples were prepared as previously described (Sutherland et al. 2000). Primary antibodies used were mouse anti-α-tubulin (1:10,000, sc-8035, Santa Cruz Biotechnologies Inc., Santa Cruz, CA); rabbit anti-RBM10 (1:1000, A301-006A, Bethyl Laboratories Inc/ Cedarlane,

Burlington, Canada); rabbit anti-RBM5 (1:2500, ab85504, Abcam, Toronto, Canada); rabbit anti-RBM5 LUCA-15UK (1:2000, non-commercially available (Sutherland et al. 2000)); and rabbit anti-RBM5 SP1 and SP2 (1:1000, non-commercially available (Bonnal et al. 2008)). A goat anti-mouse horseradish peroxidase (HRP)-conjugated secondary antibody (1:20,000, sc-2005, Santa Cruz Biotechnologies Inc.) and a goat anti-rabbit HRP-conjugated secondary antibody (1:10,000, sc-2004, Santa Cruz Biotechnologies Inc.) were employed. The presence of anti-bodies on the membrane was detected using Amersham ECL Western Blotting Detection Reagents (GE Healthcare, Mississauga, Canada) and Amersham Hyperfilm ECL (GE Healthcare).

The membranes were stripped between probing with different primary antibodies using the following mild stripping procedure: two 10-min washes in mild stripping buffer (1.5% glycine, 0.1% SDS, 0.1% Tween 20, pH 2.2); two 10-min washes in phosphate-buffered saline (1× PBS, pH 7.4, Life Technologies); and finally, two 5-min washes with Tris-buffered saline with Tween 20 (TBS-T). Densitometric analysis was performed on the resulting blots using AlphaEase FC software. The resulting RBM5 and RBM10 expression values were first normalized to α-tubulin, the reference gene used. Normalized expression values were then expressed as fold-change from the control sample for that biological replicate (control sample present on each gel), and the average of the technical replicates for each biological replicate determined. Following, the average across biological replicates was determined and graphed.

5.4 Results and Discussion

5.4.1 Rbm5 mRNA knockdown has no effect on Rbm5 protein levels.

One hundred seventeen Rbm5 shRNA transfected H9c2 clones were obtained following 28 or 29 days of selection in puromycin. All 117 clones were screened for Rbm5 mRNA expression. Three clones (clones 87, 9, and 100) with significant inhibition of Rbm5 mRNA expression (>80%),compared to the scrambled control, were chosen for further analysis, along with two clones (clones 12 and 104) with no visible knockdown (Fig. 5.1A). Surprisingly, Rbm5 protein levels were not significantly inhibited in any of the Rbm5 knockdown clones (Fig. 5.1B, C). To rule out any possible clonal effect that could account for abnormal regulation of protein expression, three transient transfections were performed. The first transient transfection used siRNA-specific to Rbm5 sequence (but different from one of the shRNA sequences used) (KD1). The second and third transient transfections used the shRNA from the stable knock-down experiments, MSH039757-1 and MSH039757-6, respectively. mRNA knockdowns ranged between 55% and 70% (Fig. 5.2A), but, once again, there was no decrease in Rbm5 protein expression levels (Fig. 5.2B, C). To ensure that antibody affinity was not an issue, three different anti-RBM5 antibodies were used in the stable knockdown analysis, and two in the transient knock-down work (Figs. 5.1B and 5.2B).

A (i)

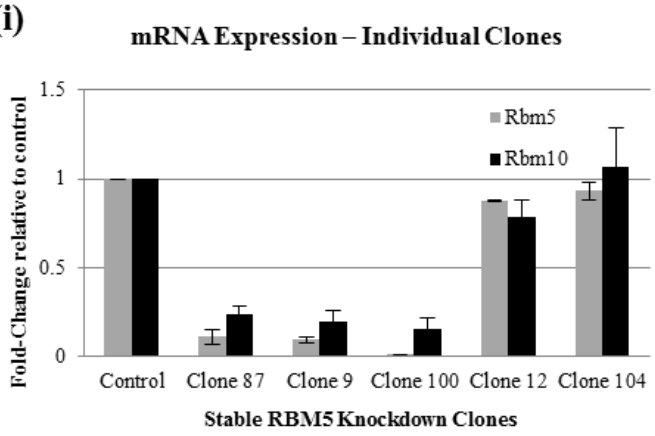
mRNA Expression – Individual Clones
Fold-Change relative to control
1.5
1
0.5
0
Rbm5
Rbm10
Control
Clone 87
Clone 9
Clone 100
Clone 12
Clone 104
Stable RBM5 Knockdown Clones

(ii)

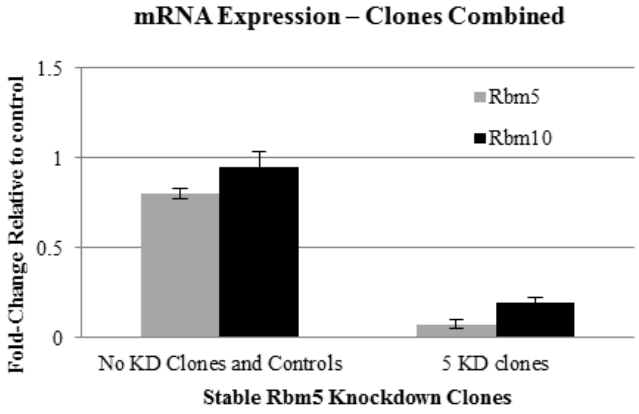
mRNA Expression – Clones Combined
Fold-Change Relative to control
1.5
1
0.5
0
Rbm5
Rbm10
No KD Clones and Controls
5 KD clones
Stable Rbm5 Knockdown Clones

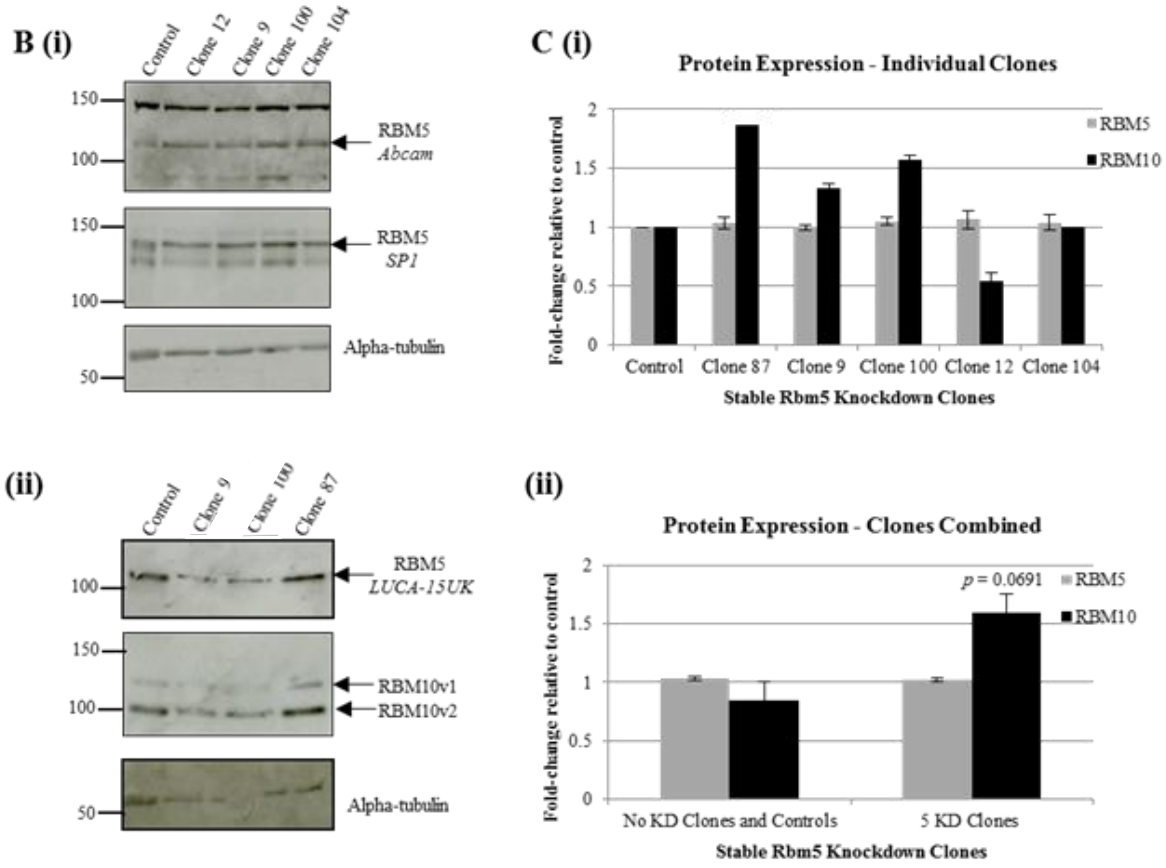

Figure 5.1 Rbm5 and Rbm10 expression in Rbm5 shRNA stably transfected H9c2 clones. (A) RT-PCR results for Rbm5 and Rbm10 expression in the various RBM5 knockdown (KD) clones, individually from technical duplicates (i) and pooled (ii). Gapdh was used as reference gene. (B) Representative raw Western blot protein expression data for RBM5 and RBM10 using one anti-RBM10 antibody and various anti-RBM5 antibodies (antibody name or manufacturer indicated on the right of the blots). Precision Plus ladder (BioRad) was used, and ladder values refer to weight in kilodalton (kDa). (C) Densitometric analysis of protein expression in the various clones, individually (from technical duplicates for each clone except clone 87 and 104 in regards to RBM10 expression) (i) and pooled (ii). Results were normalized to alpha-tubulin. In the pooled figures (Aii, Cii), BNo KD Clones and Controls^ represents results from the scrambled control as well as clones which did not show at least 70% knockdown of Rbm5 at the RNA level (clones 12 and 104), whereas B5 KD Clones^ represent results from those clones that did show mRNA knockdown of Rbm5 (clones 87, 9, and 100). Values represent mean±standard error (SE). Asterisk placed directly above a bar indicates value is statistically different from control as determined by unpaired t test (**indicates $p<0.01$).

5.4.2 Rbm5 knockdown correlates with increased Rbm10 protein levels.

Since rat Rbm10 has 57% homology with rat Rbm5, to ensure no off-target effect of the theoretically Rbm5-specific sh/siRNAs on Rbm10 expression, Rbm10 expression was also examined in the knockdowns. Both shRNA and siRNA sequences were chosen to limit the potential for off-target effects on Rbm10: Rbm5 shRNA and siRNA sequences were 19-mers with seven mismatches to rat Rbm10, meaning they had 63% homology. In the clones, at the RNA level (Fig. 5.1A), Rbm10 expression significantly decreased in of all the clones with the most significant Rbm5 RNA knockdown (clones 87, 9, and 100). At the protein level (Fig. 5.1C), Rbm10 expression was surprisingly increased, but only in the Rbm5 clones with the most significant Rbm5 RNA knockdown. Additionally, Rbm10 protein expression was unexpectedly decreased in clone 12, which had shown no change in Rbm5 mRNA expression levels as a result of knockdown. In the transient Rbm5 knockdown, RBM10 mRNA and protein expression were increased almost two-fold, compared to the scrambled control (Fig. 5.2A, C).

A (i)

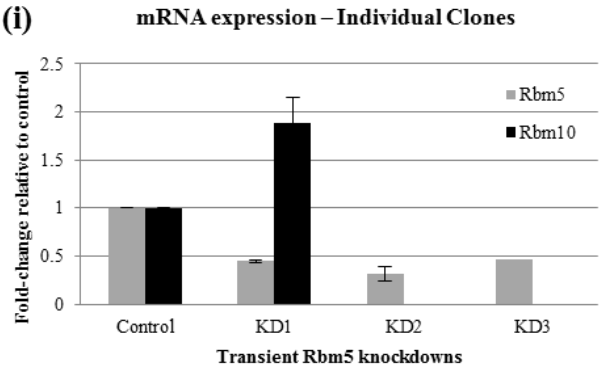
mRNA expression – Individual Clones
Fold-change relative to control
2.5
2
1.5
1
0.5
0
Rbm5
Rbm10
Control
KD1
KD2
KD3
Transient Rbm5 knockdowns

(ii)

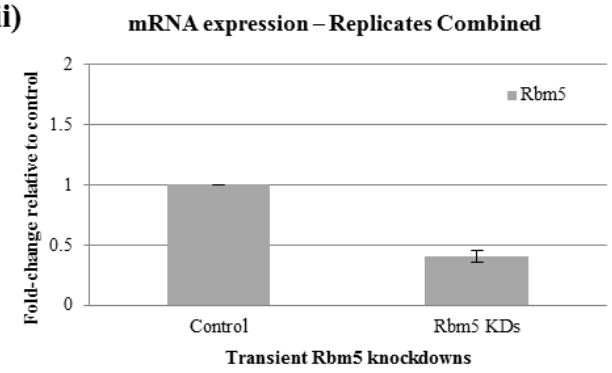
mRNA expression – Replicates Combined
Fold-change relative to control
2
1.5
1
0.5
0
Rbm5
Control
Rbm5 KDs
Transient Rbm5 knockdowns

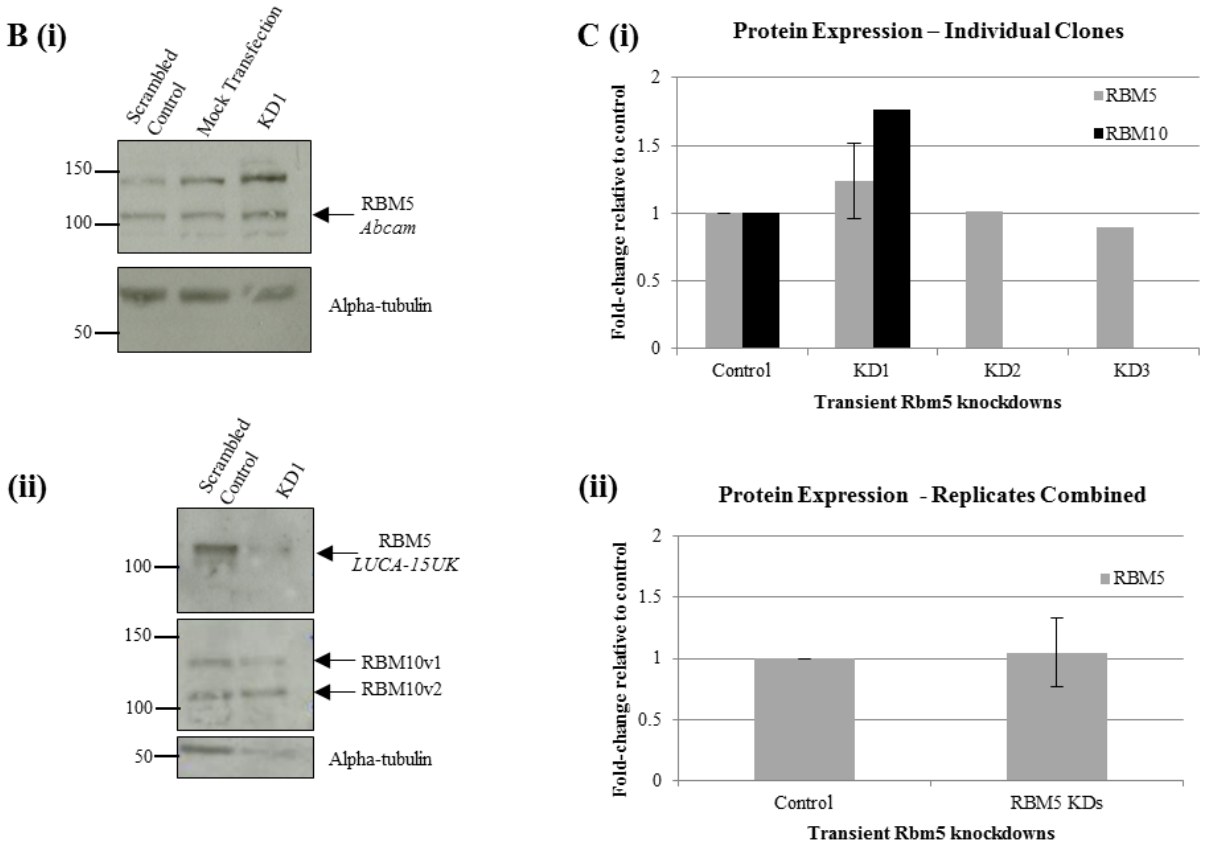

Figure 5.2 Rbm5 and Rbm10 expression in Rbm5 shRNA/siRNA transiently transfected H9c2 cells. (A) RT-PCR results for Rbm5 and Rbm10 expression in the various transient RBM5 knockdown (KD) experiments, individually (from technical duplicates, except KD3 (one technical replicate)) (i) and pooled (ii). Gapdh was used as reference gene. (B) Representative raw Western Blot protein expression data for RBM5 and RBM10 using one anti-RBM10 antibody and various anti-RBM5 antibodies (antibody name or manufacturer indicated on the right of the blots). Precision Plus ladder (BioRad) was used, and ladder values refer to weight in kDa. (C) Densitometric analysis of protein expression in the various KD experiments, individually from one technical replicate (two for KD1 expression of RBM5) (i) and pooled (ii). Results were normalized to alpha-tubulin. Values represent mean±SE. Asterisk placed directly above a bar indicates value is statistically different from control as determined by unpaired t test (** indicates $p<0.01$).

5.4.3 Rbm5 overexpression does not correlate with decreased Rbm10 protein levels.

Since inhibition of Rbm5 correlated with increased expression of RBM10 in both the stable and transient knockdowns, we sought to determine if the reverse were true, and overexpression of Rbm5 correlated with decreased Rbm10 expression. Transient overexpression of RBM5 protein from the human complementary DNA (cDNA) sequence (which has approximately 80% homology with rat) was confirmed with three different anti-RBM5 anti-bodies (Fig. 5.3B), but Rbm10 protein expression levels remained unchanged, compared to the scrambled control transfectants (Fig. 5.3B,C).

A (i)

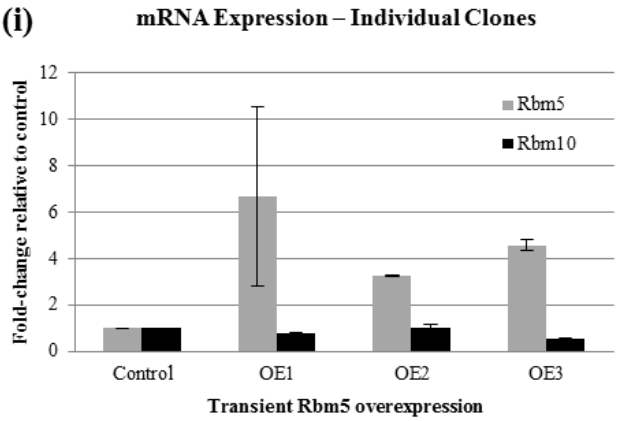
mRNA Expression – Individual Clones
Fold-change relative to control
12
10
8
6
4
2
0
Rbm5
Rbm10
Control
OE1
OE2
OE3
Transient Rbm5 overexpression

(ii)

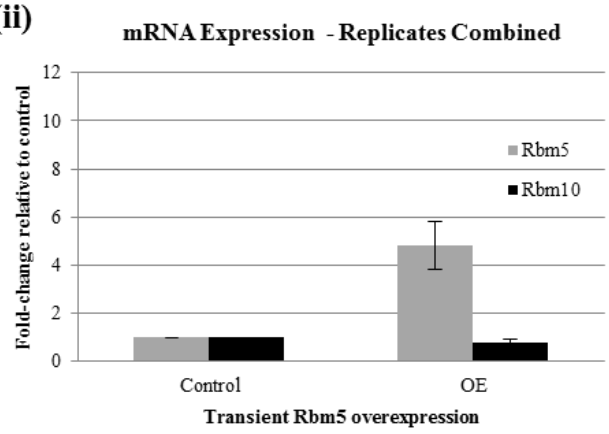
mRNA Expression - Replicates Combined
Fold-change relative to control
12
10
8
6
4
2
0
Rbm5
Rbm10
Control
OE
Transient Rbm5 overexpression

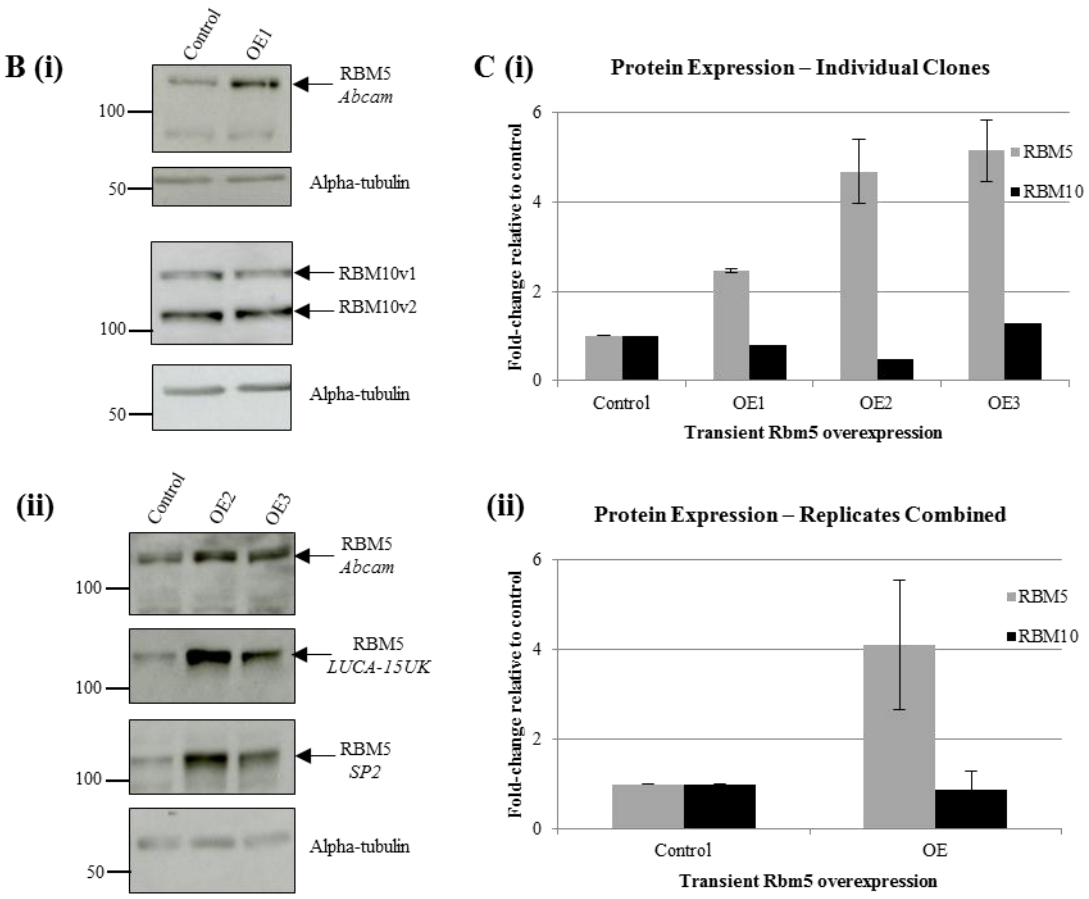

Figure 5.3 Rbm5 and Rbm10 expression in Rbm5 transiently overexpressed H9c2 cells. (A) RT-PCR results for Rbm5 and Rbm10 expression in the various transient RBM5 overexpression (OE) experiments, individually from technical duplicates (i) and pooled (ii). Gapdh was used as reference gene. (B) Representative raw Western Blot protein expression data for RBM5 and RBM10 using one anti-RBM10 antibody and various anti-RBM5 antibodies (antibody name or manufacturer indicated on the right of the blots). Precision Plus ladder (BioRad) was used, and ladder values refer to weight in kDa. (C) Densitometric analysis of protein expression in the various OE experiments, individually from technical duplicates for RBM5 expression and one technical replicate for RBM10 expression (i) and pooled (ii). Results were normalized to alpha-tubulin. Values represent mean±SE. Statistical significance was evaluated using an unpaired t test for each sample compared to their respective control.

Based on our findings, a number of conclusions can be drawn. Firstly, only a small quantity of Rbm5 mRNA is translated. Secondly, regulation of Rbm5 protein expression in H9c2 myoblasts has unique characteristics. Thirdly, decreased Rbm5 mRNA levels regulate Rbm10 protein expression. In the following sections, we discuss each of these conclusions, and present a model that depicts them.

5.4.4 Only a small quantity of Rbm5 mRNA is translated.

Knockdown of Rbm5 mRNA in either stable or transient transfections is not reflected at the protein level. Lack of a positive correlation between Rbm5 mRNA and protein expression in the transient transfections could possibly relate to the fact that (a) Rbm5 protein is very stable or (b) the mRNA was not inhibited sufficiently to have an effect. When these transient data are combined with the lack of correlation between Rbm5 mRNA and protein expression in the stable clones, the data suggest that unchanged Rbm5 protein expression levels was not due to (a) any possible clonal effect in the stable clones or (b) Rbm5 protein stability. A precedented explanation for the lack of correlation between Rbm5 mRNA and protein expression levels in the knockdown experiments is that only a fraction of endogenous Rbm5 mRNA is actually translated into protein. The shRNA was able to degrade up to 90% of the Rbm5 mRNA in the stable clones, but the ~10% that was left might be all that is normally translated in the wild-type myoblasts.

One possible reason to account for the fact that only a small portion of Rbm5 mRNA may be translated is that messenger ribonucleoproteins (mRNPs) may be involved in sequestering the majority of Rbm5 mRNA in H9c2 cells. Precedent for this occurs in Xenopus oogenesis, where 80% of maternal mRNAs are sequestered in mRNP storage particles, and translation is inhibited until specific time-points during early embryogenesis when the mRNAs are recruited to ribosomes and finally translated (Spirin 1966; Tafuri and Wolffe 1993). A second precedent occurs in P19 murine embryonic carcinoma cell differentiation, where the composition of mRNP-sequestered mRNAs changes following exposure to differentiation-inducing stimuli (Tenenbaum et al. 2000). Furthermore, in satellite cells, transcripts of Myf5, an important regulator of myogenesis, have been shown to be sequestered in mRNP granules. Upon activation

of the satellite cell, these granules dissociate, leading to liberation of myogenic factor 5(Myf5) transcripts and consequently higher levels of Myf5 (Crist et al. 2012). This regulatory mechanism thus allows quiescent satellite cells to transcribe Myf5 without activating differentiation. A similar mechanism could be occurring in the H9c2 cells, which would explain not only why a 90% knockdown of Rbm5 mRNA is not reflected at the protein level, and why the changes in Rbm5 protein levels during cardiac differentiation were not positively correlated with changes in Rbm5 mRNA levels (i.e., during differentiation, it is not the total amount of Rbm5 mRNA in the cell that is important but the amount that is not sequestered, and thus available for translation) (Loiselle and Sutherland 2014).

In the overexpression experiments, exogenous Rbm5 mRNA was translated. If our sequestering hypothesis is correct, this result suggests that either (a) the cell could distinguish between exogenously and endogenously transcribed Rbm5 transcript, or (b) there was a finite quantity of Rbm5 message that could be sequestered, a quantity that might be regulated by levels of endogenous Rbm5 protein or Rbm10 mRNA/protein levels.

5.4.5 Regulation of Rbm5 protein expression in H9c2/myoblasts has unique characteristics.

Correlations between RBM5 expression at both the mRNA and protein levels have been examined in breast (Oh et al. 2002; Rintala-Maki et al. 2007), lung (Liang et al. 2012), and pancreatic (Peng et al. 2013) non-tumor and tumor tissue, and various cell lines including A549 (lung adenocarcinoma) (Oh et al. 2010; Li et al. 2012), Calu-6 (possibly lung carcinoma) (Oh et al. 2010), NCI-H1299 (non-small cell lung carcinoma) (Oh et al. 2010), U2OS (osteosarcoma)

(Kobayashi et al. 2011), PC-3 (prostate adenocarcinoma) (Zhao et al. 2012), BEAS-2B (immortalized human bronchial epithelial cells) (Oh et al. 2010), HEK293 (human embryonic kidney cells) (Fushimi et al. 2008), MCF-10A (immortalized epithelial cells derived from human fibrocystic mammary tissue) (Oh et al. 2010), and those of various mantle cell and follicular lymphomas (Weinkauf et al. 2007): a positive correlation between mRNA and protein expression levels was consistently observed. Only in non-tumor breast tissue was a positive correlation between RBM5 mRNA and protein expression not observed (Rintala-Maki et al. 2007). Therefore, the mechanism suggested earlier in which only a percentage of Rbm5 mRNA is translated, and the rest is sequestered (perhaps in mRNPs) may be a restricted phenomenon that occurs in, for example, particular cell types or in cells with certain growth characteristics, including rat myoblasts.

5.4.6 Decreased Rbm5 mRNA levels regulate Rbm10 protein expression.

It was interesting to note that, despite unchanged levels of Rbm5 protein, Rbm10 protein levels went up. This observation was particularly interesting in view of the fact that Rbm10 mRNA levels significantly decreased in the stable knockdowns. Any potential off-target effect of Rbm5 shRNA on Rbm10 was considered highly unlikely once the elevated levels of Rbm10 protein were observed. The results suggest a complex regulatory mechanism linking degradation of Rbm5 mRNA with Rbm10 protein expression. It is important to note that another group has also recently reported that decreased expression of Rbm5 correlated with increased levels of Rbm10. Their study was performed in injured mouse brain homogenates (Jackson et al. 2015).

5.4.7 Model

Based on the results of the Rbm5 knockdown and overexpression experiments, we hypothesize that the majority of Rbm5 transcripts are sequestered, possibly in mRNPs, and unavailable for translation. Release of sequestered Rbm5 transcripts would occur at certain points during differentiation, as required. Therefore, this could be the post-transcriptional mechanism regulating Rbm5 expression throughout H9c2 skeletal and cardiac differentiation suggested by our group previously (Loiselle and Sutherland 2014).

We postulate that two things are occurring in H9c2 cells regarding RBM10. Firstly, that RBM10 is a component of the mRNP complexes sequestering Rbm5 mRNA in H9c2 cells (Fig. 5.4A), as RBM proteins have been shown to play important roles in these structures, as previously reviewed (Hieronymus and Silver 2004). Secondly, that RBM10 can bind the 3′ UTR of its own mRNA transcript and thereby increase its own stability. The rat homologue of RBM10, S1-1, has already been shown to bind the 3′ UTR of angiotensin II receptor type 1 (AT1), stabilizing the message, and ultimately decreasing transcription (Mueller et al . 2009). Furthermore, previously identified RBM10 binding sequences are located within the Rbm10 3′ UTR (Fig. 5.5) (Bechara et al. 2013). It is important to note that Bechara et al. demonstrated that even 2/7 mismatches from the top selected motifs still enabled good RBM10 binding.

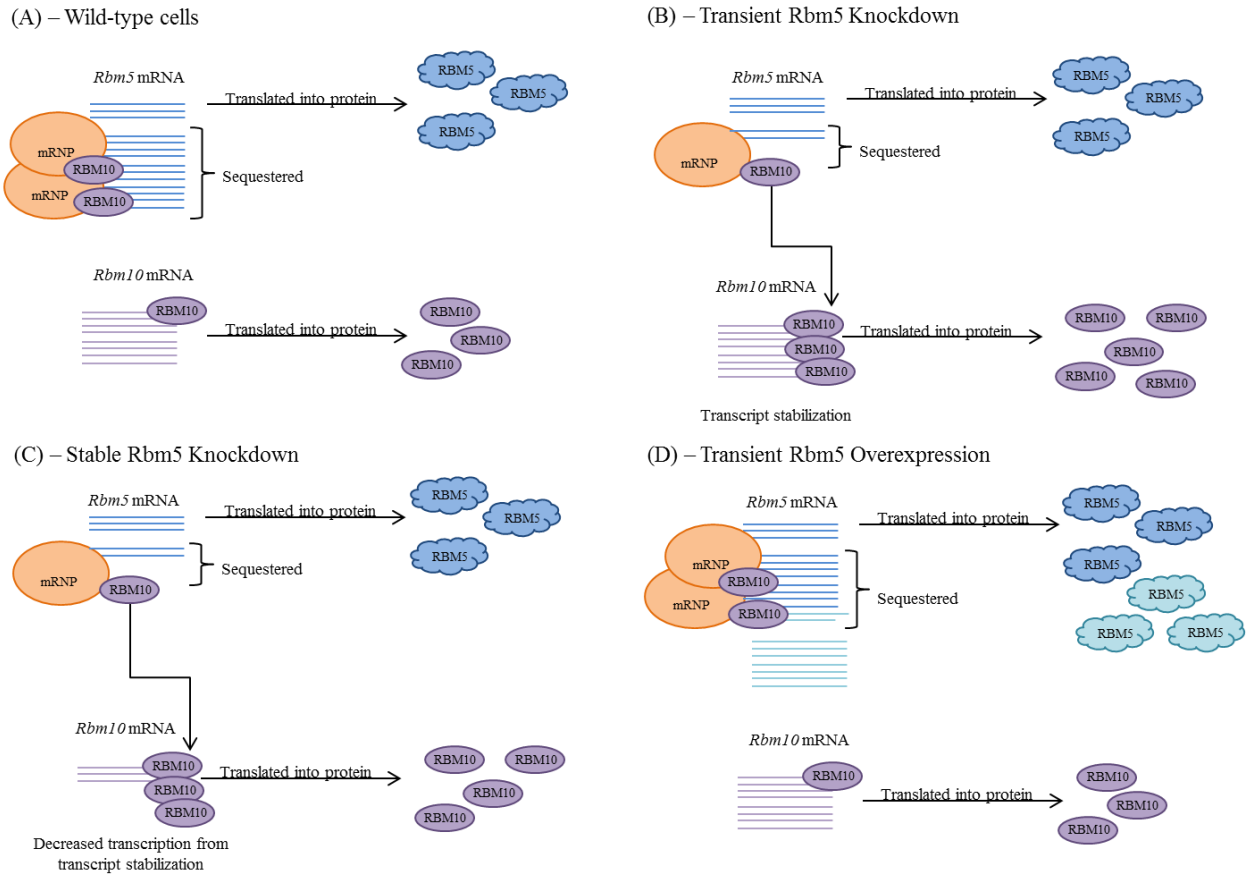

Figure 5.4 Model representing the effects of varying levels of Rbm5 mRNA on the expression of RBM5 and RBM10. Rbm5 and Rbm10 expression in H9c2 wild-type cells (A), upon transient Rbm5 knockdown (B), upon stable Rbm5 knockdown (C), and upon transient Rbm5 overexpression (D). RBM5 protein is represented by blue clouds, with lighter blue representing overexpressed protein, and RBM10 protein is represented by purple ovals. Orange mRNP ovals represent complex mRNP particles with various components. For in-depth model description, refer to text.

Rbm10 3’ UTR sequence:

GCAGCTTCAAGAGCAACTTCTCCACATGTTGGGTGTCCATCCTGGGGCAGGGAAGGACAGAGTGTTGGA

TGGCTGGGACGGGGCCTTGCTCTTGTCGGCCAGCCCACTCCCCAGCCAGAGAGGGCTTGACCAAATCAA

ATTGAGGTGGTGACTTTTGTTGGAAAATTGGGCTGGGATCACGTCCTGTTTTGTAATAAAAGCTGAAAAG

TCTG

Figure 5.5 RBM10 binding sites in the Rbm10 3'UTR. Segments of the top consensus motifs for RBM10 binding sites, as determined by Bechara et al. (2013), underlined at their respective locations in the Rbm10 3′ UTR. Double underlined sequences are part of the motifs on each side. All sequences have two mismatches compared to the top previously identified motif, except the most 3′- motif which is a complete match.

In our model, when Rbm5 mRNA is decreased and its associated mRNP complexes disassembled, RBM10protein would be released into the cell. This RBM10 would be free to bind the 3′ UTR of Rbm10 mRNA, stabilizing the transcript (Fig. 5.4B). Initially, this may lead to increased levels of Rbm10 mRNA and protein, which is what we observed in our transient Rbm5 knockdown experiments (Fig. 5.2). Ultimately, however, this stabilization may lead to decreased transcription of Rbm10, as has been shown upon rat RBM10 stabilization of AT-1 transcript (Mueller et al. 2009) (Fig. 5.4C). As a result, lower levels of Rbm10 mRNA would be expected. This is, in fact what we observed in our Rbm5 stable knockdown clones (Fig. 5.1).

On the other hand, upon overexpression of Rbm5, we would expect these non-physiological levels to be too high to all be sequestered in mRNP complexes, resulting in their transcription, translation, and, as a result, higher levels RBM5 (Fig. 5.4D). Furthermore, since the mRNP complexes sequestering Rbm5 would not be disrupted by this overexpression, we would expect Rbm10 mRNA and protein levels to remain constant. As shown in Fig. 5.3, this is what we

observed experimentally; higher levels of RBM5 upon Rbm5 overexpression, but no change in Rbm10 mRNA or protein levels.

To test the validity of this model, immunoprecipitation of Rck/p54 (p-body protein and mRNP complex component) could be performed, followed by next generation sequencing of its associated RNA (RIP-Seq). This would determine if Rbm5 is among the mRNP-sequestered transcripts in H9c2 myoblasts. Furthermore, RNA-binding protein purification and identification (RaPID) could be used to determine if Rbm10 is a component of the mRNP/Rbm5 mRNA complexes. This would involve tagging Rbm5 mRNA, transfecting it into H9c2 cells, purifying the tagged transcripts, then detecting associated proteins via mass-spectrometry (Slobodin and Gerst 2010). Direct binding of Rbm10 to its own transcript could be analyzed *via* electromobility shift assays (EMSAs), using tagged Rbm10 3′ UTR probes. Knockdown and overexpression of Rbm10 would not be useful to test this model since it would involve directly manipulating levels of Rbm10, which may mask any effect that protein levels have on transcript expression.

5.4.8 Conclusion

The results from this work suggest that Rbm5 is post-transcriptionally regulated in rat myoblasts. More specifically, our results suggest that only a small portion of Rbm5 mRNA may be translated in myoblasts, while the rest is sequestered in the cell. Results from Rbm10 mRNA and protein expression in Rbm5 knockdown and overexpression samples also suggest that Rbm10 expression is influenced by Rbm5 and by its own protein levels. This co-regulation has already

been shown in neuronal cells (Jackson et al. 2015), and suggests that, as in transformed cells (Sutherland et al. 2000; Bonnal et al. 2008; Fushimi et al. 2008; Wang et al. 2012; Inoue et al. 2014), Rbm5 and Rbm10 may influence similar cellular processes in myoblasts. Finally, the intricate regulation of Rbm5 protein levels in H9c2 cells suggest a function of the utmost importance to myoblast differentiation, and perhaps, muscle development in general.

5.5 References

Bechara EG, Sebestyen E, Bernardis I, Eyras E, Valcarcel J (2013) RBM5, 6, and 10 differentially regulate NUMB alternative splicing to control cancer cell proliferation. Mol Cell 52:720–733

Behzadnia N, Golas MM, Hartmuth K, Sander B, Kastner B, Deckert J, Dube P, Will CL, Urlaub H, Stark H, Luhrmann R (2007) Composition and three-dimensional EM structure of double affini-ty-purified, human prespliceosomal A complexes. EMBO J 26: 1737–1748

Bonnal S, Martinez C, Forch P, Bachi A, Wilm M, Valcarcel J (2008) RBM5/Luca-15/H37 regulates Fas alternative splice site pairing af-ter exon definition. Mol Cell 32:81–95

Crist CG, Montarras D, Buckingham M (2012) Muscle satellite cells are primed for myogenesis but maintain quiescence with sequestration of Myf5 mRNA targeted by microRNA-31 in mRNP granules. Cell Stem Cell 11:118–126

Drabkin HA, West JD, Hotfilder M, Heng YM, Erickson P, Calvo R, Dalmau J, Gemmill RM, Sablitzky F (1999) DEF-3(g16/NY-LU-12), an RNA binding protein from the 3p21.3 homozygous deletion region in SCLC. Oncogene 18:2589–2597

Fushimi K, Ray P, Kar A, Wang L, Sutherland LC, Wu JY (2008) Up-regulation of the proapoptotic caspase 2 splicing isoform by a can-didate tumor suppressor, RBM5. Proc Natl Acad Sci U S A 105: 15708–15713

Geigl JB, Langer S, Barwisch S, Pfleghaar K, Lederer G, Speicher MR (2004) Analysis of gene expression patterns and chromosomal changes associated with aging. Cancer Res 64:8550–8557

Hieronymus H, Silver PA (2004) A systems view of mRNP biology. Genes Dev 18:2845–2860

Inoue A, Yamamoto N, Kimura M, Nishio K, Yamane H, Nakajima K (2014) RBM10 regulates alternative splicing. FEBS Lett 588: 942–947

Jackson TC, Du L, Janesko-Feldman K, Vagni VA, Dezfulian C, Poloyac SM, Jackson EK, Clark RS, Kochanek PM (2015) The nuclear splicing factor RNA binding motif 5 promotes caspase activation in human neuronal cells, and increases after traumatic brain injury in mice. J Cereb Blood Flow Metab 35:655–666

James CG, Ulici V, Tuckermann J, Underhill TM, Beier F (2007) Expression profiling of dexamethasone-treated primary chondrocytes identifies targets of glucocorticoid signalling in endo-chondral bone development. BMC Genomics 8:205

Jin W, Niu Z, Xu D, Li X (2012) RBM5 promotes exon 4 skipping of AID pre-mRNA by competing with the binding of U2AF65 to the polypyrimidine tract. FEBS Lett 586: 3852–3857

Johnston JJ, Teer JK, Cherukuri PF, Hansen NF, Loftus SK, Chong K, Mullikin JC, Biesecker LG (2010) Massively parallel sequencing of exons on the X chromosome identifies RBM10 as the gene that causes a syndromic form of cleft palate. Am J Hum Genet 86: 743–748

Kim YS, Hwan JD, Bae S, Bae DH, Shick WA (2010) Identification of differentially expressed genes using an annealing control primer system in stage III serous ovarian carcinoma. BMC Cancer 10:576

Kobayashi T, Ishida J, Musashi M, Ota S, Yoshida T, Shimizu Y, Chuma M, Kawakami H, Asaka M, Tanaka J, Imamura M, Kobayashi M, Itoh H, Edamatsu H, Sutherland LC, Brachmann RK (2011) p53 transactivation is involved in the antiproliferative activity of the putative tumor suppressor RBM5. Int J Cancer 128:304–318

Li P, Wang K, Zhang J, Zhao L, Liang H, Shao C, Sutherland LC (2012) The 3p21.3 tumor suppressor RBM5 resensitizes cisplatin-resistant human non-small cell lung cancer cells to cisplatin. Cancer Epidemiol 36:481–489

Liang H, Zhang J, Shao C, Zhao L, Xu W, Sutherland LC, Wang K (2012) Differential expression of RBM5, EGFR and KRAS mRNA and protein in non-small cell lung cancer tissues. J Exp Clin Cancer Res 31:36

Loiselle JJ, Sutherland LC (2014) Differential downregulation of Rbm5 and Rbm10 during skeletal and cardiac differentiation. In Vitro Cell Dev Biol Anim 50:331–339

Miller G, Socci ND, Dhall D, D'Angelica M, DeMatteo RP, Allen PJ, Singh B, Fong Y, Blumgart LH, Klimstra DS, Jarnagin WR (2009) Genome wide analysis and clinical correlation of chromosomal and transcriptional mutations in cancers of the biliary tract. J Exp Clin Cancer Res 28:62

Mourtada-Maarabouni M, Keen J, Clark J, Cooper CS, Williams GT (2006) Candidate tumor suppressor LUCA-15/RBM5/H37 modu-lates expression of apoptosis and cell cycle genes. Exp Cell Res 312: 1745–1752

Mueller CF, Berger A, Zimmer S, Tiyerili V, Nickenig G (2009) The heterogenous nuclear riboprotein S1-1 regulates AT1 receptor gene expression via transcriptional and posttranscriptional mechanisms. Arch Biochem Biophys 488:76–82

O'Bryan MK, Clark BJ, McLaughlin EA, D'Sylva RJ, O'Donnell L, Wilce JA, Sutherland J, O'Connor AE, Whittle B, Goodnow CC, Ormandy CJ, Jamsai D (2013) RBM5 is a male germ

cell splicing factor and is required for spermatid differentiation and male fertility. PLoS Genet 9:e1003628

O'Leary DA, Sharif O, Anderson P, Tu B, Welch G, Zhou Y, Caldwell JS, Engels IH, Brinker A (2009) Identification of small molecule and genetic modulators of AON-induced dystrophin exon skipping by high-throughput screening. PLoS One 4:e8348

Oh JJ, Taschereau EO, Koegel AK, Ginther CL, Rotow JK, Isfahani KZ, Slamon DJ (2010) RBM5/H37 tumor suppressor, located at the lung cancer hot spot 3p21.3, alters expression of genes involved in me-tastasis. Lung Cancer 70:253–262

Oh JJ, West AR, Fishbein MC, Slamon DJ (2002) A candidate tumor suppressor gene, H37, from the human lung cancer tumor suppres-sor locus 3p21.3. Cancer Res 62:3207–3213

Peng J, Valeshabad AK, Li Q, Wang Y (2013) Differential expression of RBM5 and KRAS in pancreatic ductal adenocarcinoma and their association with clinicopathological features. Oncol Lett 5: 1000–1004

Qiu TH, Chandramouli GV, Hunter KW, Alkharouf NW, Green JE, Liu ET (2004) Global expression profiling identifies signatures of tumor virulence in MMTV-PyMT-transgenic mice: correlation to human disease. Cancer Res 64:5973–5981

Ramaswamy S, Ross KN, Lander ES, Golub TR (2003) A molecular signature of metastasis in primary solid tumors. Nat Genet 33:49–54

Rintala-Maki ND, Goard CA, Langdon CE, Wall VE, Traulsen KE, Morin CD, Bonin M, Sutherland LC (2007) Expression of RBM5 related factors in primary breast tissue. J Cell Biochem 100: 1440–1458

Rintala-Maki ND, Sutherland LC (2009) Identification and characterisa-tion of a novel antisense non-coding RNA from the RBM5 gene locus. Gene 445:7–16

Shu Y, Rintala-Maki ND, Wall VE, Wang K, Goard CA, Langdon CE, Sutherland LC (2007) The apoptosis modulator and tumour suppressor protein RBM5 is a phosphoprotein. Cell Biochem Funct 25:643–653

Slobodin B, Gerst JE (2010) A novel mRNA affinity purification tech-nique for the identification of interacting proteins and transcripts in ribonucleoprotein complexes. RNA 16:2277–2290

Spirin AS (1966) BMasked^ forms of messenger RNA in early embryo-genesis and in other differentiating systems. In: Moscona AA, Monroy A (eds) Current topics in developmental biology. Elsevier, New York, pp 1–38

Sugliani M, Brambilla V, Clerkx EJ, Koornneef M, Soppe WJ (2010) The conserved splicing factor SUA controls alternative splicing of the developmental regulator ABI3 in Arabidopsis. Plant Cell 22: 1936–1946

Sutherland LC, Edwards SE, Cable HC, Poirier GG, Miller BA, Cooper CS, Williams GT (2000) LUCA-15-encoded sequence variants reg-ulate CD95-mediated apoptosis. Oncogene 19:3774–3781

Sutherland LC, Rintala-Maki ND, White RD, Morin CD (2005) RNA binding motif (RBM) proteins: a novel family of apoptosis modula-tors? J Cell Biochem 94:5–24

Tafuri SR, Wolffe AP (1993) Selective recruitment of masked maternal mRNA from messenger ribonucleoprotein particles containing FRGY2 (mRNP4). J Biol Chem 268:24255–24261

Tenenbaum SA, Carson CC, Lager PJ, Keene JD (2000) Identifying mRNA subsets in messenger ribonucleoprotein complexes by using cDNA arrays. Proc Natl Acad Sci U S A 97:14085–14090

Wang K, Bacon ML, Tessier JJ, Rintala-Maki ND, Tang V, Sutherland LC (2012) RBM10 modulates apoptosis and influences TNA-α gene expression. J Cell Death 5:1–19

Wang K, Ubriaco G, Sutherland LC (2007) RBM6-RBM5 transcription-induced chimeras are differentially expressed in tumours. BMC Genomics 8:348

Wang Y, Gogol-Doring A, Hu H, Frohler S, Ma Y, Jens M, Maaskola J, Murakawa Y, Quedenau C, Landthaler M, Kalscheuer V, Wieczorek D, Wang Y, Hu Y, Chen W (2013) Integrative analysis revealed the molecular mechanism underlying RBM10-mediated splicing regu-lation. EMBO Mol Med 5:1431–1442

Weinkauf M, Christopeit M, Hiddemann W, Dreyling M (2007) Proteome- and microarray-based expression analysis of lymphoma cell lines identifies a p53-centered cluster of differentially expressed proteins in mantle cell and follicular lymphoma. Electrophoresis 28: 4416–4426

Welling DB, Lasak JM, Akhmametyeva E, Ghaheri B, Chang LS (2002) cDNA microarray analysis of vestibular schwannomas. Otol Neurotol 23:736–748

Zhao L, Li R, Shao C, Li P, Liu J, Wang K (2012) 3p21.3 tumor suppressor gene RBM5 inhibits growth of human prostate cancer PC-3 cells through apoptosis. World J Surg Oncol 10:247

Zheng S, Damoiseaux R, Chen L, Black DL (2013) A broadly applicable high-throughput screening strategy identifies new regulators of Dlg4 (Psd-95) alternative splicing. Genome Res 23:998–1007

Chapter 6

6 Discussion

The **objectives** of this study were **(1)** identify all cellular processes and events enriched by changes in RBM5 and/or RBM10 expression in a particular cultured cell line, and **(2)** to determine the extent of functional overlap for RBM5 and RBM10 in these cells. Entering into this study, I **hypothesized** that processes influenced by changes in RBM5 and RBM10 expression are not limited to apoptosis and cell cycle regulation. I also **hypothesized** that RBM5 and RBM10 influence many events in addition to differentiation. Finally, based on their structural similarities, I **hypothesized** some overlap in functional roles for RBM5 and RBM10.

My results suggest that RBM5 and RBM10 influence many events, in addition to differentiation. RBM5-altered events typically involved apoptosis and cell cycle regulation, whereas RBM10-altered events involved additional processes. These results suggest that even though RBM5 and RBM10's consensus functional motifs are very homologous, the sequence variations between RBM5 and RBM10 do have functional implications. Furthermore, I demonstrated that while both proteins have overlapping roles, sharing similar targets and influencing similar processes and events, the functional implications of their expression were quite different. In fact, the putative tumor suppressor RBM10, in an *RBM5*-null environment, actually promoted transformation associated processes. This suggests that *RBM5* expression levels can significantly alter the function of RBM10. The complex relationship demonstrated in this body of work between RBM5 and RBM10, in both transformed and non-transformed cells, also underscores the importance of their regulated expression.

Since the beginning of this project, many studies, in addition to those presented herein, have continued to confirm RBM5's tumor suppressive properties. There has been an overall growing interest in regards to RBM10 – a greater than 50% increase in RBM10-related Pubmed-indexed publications (i.e. 27 manuscripts) since the beginning of this study. These studies, together with my doctoral research work, have provided a much more comprehensive understanding of the roles of, and relationship between, these two RBPs. Specific aspects of RBM5's and RBM10's functions that are now much better understood, compared to the beginning of this study, will be briefly discussed to truly highlight the range of processes altered by these proteins, and the impact and novelty of the findings presented in this thesis.

6.1. RBM5 and RBM10 are not only modulators of alternative splicing

Prior to the beginning of this study, mechanistic information regarding RBM5 had been solely focused on its role as a modulator of alternative splicing. As for RBM10, although a role in alternative splicing had been suggested, no mechanism of action had been demonstrated. Since then, a number of studies have confirmed RBM5's role as a modulator of alternative splicing (Sebestyen et al., 2016; Zhang et al., 2014). Of note, RNA splicing by RBM5 was shown to be dependent on its OCRE and RRM domains (Mourao et al., 2016; Zhang et al., 2014). A role for RBM10 in the modulation of alternative splicing was also established by many groups (Hernandez et al., 2016; Inoue et al., 2014; Rodor et al., 2017; Wang et al., 2013; Zhao et al., 2017; Zheng et al., 2013). In addition, some studies have identified RNA consensus binding

sequences for RBM5 and RBM10 (Bechara et al., 2013; Maaskola and Rajewsky, 2014; Ray et al., 2013; Rodor et al., 2017; Wang et al., 2013). The similarity between the identified sequences between studies, however, is quite low. This may be due to the difference in techniques used in each study, or could indicate that secondary RNA structure is important to consider when predicting RBM5 and RBM10 targets, rather than simply a short consensus binding sequence in the target RNA.

The target identification and gene expression data presented herein support a role for RBM5 in the modulation of alternative splicing. We suggest, however, that RBM10's ability to influence alternative splicing is largely dependent on *RBM5* expression since (a) RBM10 knockdown in an *RBM5*-null system resulted in no significant changes in alternative splicing, and (b) no RBM10 mRNA targets are involved in any aspect of alternative splicing. In addition, we determined that, mechanistically, RBM5 and RBM10 are much more than modulators of apoptosis, and influence RNA metabolism in various ways. In fact, although RBM5 influenced the expression of thousands of genes, only 47 genes underwent significant changes in alternative splicing upon modulating *RBM5* expression levels. The fact that only 47 of thousands of differentially expressed genes experienced alternative splicing suggests that RBM5 influences not only alternative splicing but other aspects of RNA metabolism. This is in line with a recent study showing that RBM5 knockdown in HeLa cells altered only 30 alternative splicing events (Bechara et al., 2013). Alternate methods of regulation of gene expression by RBM5 and RBM10 suggested by our results include nonsense-mediated decay (NMD), transcriptional and post-translational control (elaborated in Chapters 3 and 4). Actually, we showed that RBM5 directly interacted with *RBM10v2(V277del)* and influenced its expression post-transcriptionally.

Furthermore, we demonstrated that RBM10 interacted with both *RBM10v2(V277)* and *RBM10v2(V277del),* and suggested that this interaction ultimately influenced RBM10v2 protein expression levels. Supporting our suggestion that these RBPs function in ways other than modulating alternative splicing are the reports that; (a) RBM10 interacted with the FilGAP protein independently of RNA to control FilGAP localization and function (Yamada et al., 2016), (b) RBM10's rat homologue, S1-1, bound mRNA's 3-UTR and influenced transcript stability (Inoue et al., 1996), (c) RBM10 interacted with 2A-DUB deubiquitinase protein complex, which influences histone modifications and thus gene transcription (Zhu et al., 2007), (d) RBM5 co-localized with p53 and caspase 3 in the cytoplasm upon spinal cord injury in rat, and correlated with increased levels of apoptosis (Zhang et al., 2015), (e) RBM5 was associated with decreased phosphorylation of β-catenin and GSK-3B (Hao et al., 2015), and (f) in mouse spermatid differentiation, RBM5 had putative protein partners involved in various aspects of RNA metabolism (O'Bryan et al., 2013). In all, our work suggests that RBM5 and RBM10 have multiple functions, independent of their role in alternative splicing. Future studies involving RBM5 and/or RBM10 should, therefore, recognize the limitations of alternative splicing focused assays.

6.2. RBM5 regulates many cellular events, in addition to differentiation

RBM5 is an established tumor suppressor gene and its inhibition of cell division (Jiang et al., 2017; Lv et al., 2016; Zhang et al., 2014) and promotion of apoptosis (Bechara et al., 2013; Jiang et al., 2017; Lv et al., 2016; Zhang et al., 2015; Zhang et al., 2014) have been recently confirmed

in a number of cell lines. In addition, RBM5's regulation of differentiation, an event involving control of both the cell cycle and apoptosis, has been further explored (Di Cecilia et al., 2016; Loiselle and Sutherland, 2014).

The work presented herein supports a role for RBM5 in the control of the cell cycle and apoptosis, as well as differentiation. RBM5's importance to development is particularly highlighted by our identification and description of its complex post-transcriptional regulation in H9c2 myoblasts (Chapter 5). Our data also suggests that RBM5 expression influences two transformation-associated events: angiogenesis and EMT. In fact, *RBM5* expression correlated with downregulation of angiogenesis and EMT markers; two events which, like differentiation, involve cell cycle control and apoptosis. Supporting our suggestion that RBM5 influences angiogenesis is the correlation previously established between *RBM5* overexpression and lower levels of epidermal growth factor receptor (EGFR), an angiogenesis promoter (Ellis, 2004), in an *in vitro* model and a xenograft mouse model (Su et al., 2014). Supporting our suggestion that RBM5 influences EMT is RBM5's association with inhibition of cell migration and invasion (Jiang et al., 2017; Lv et al., 2016), and inhibition of the Wnt/β-catenin pathway (positive regulator of EMT) (Hao et al., 2015; Lamouille et al., 2014). Importantly, the Wnt/β-catenin signaling is also critical to development and is associated with a number of diseases (MacDonald et al., 2009; Morin, 1999), suggesting a link between RBM5's regulation of both EMT and development. In sum, RBM5 likely influences many cellular events, and may prevent many facets of the transformed state.

6.3. Decreased *RBM5* expression may be a key step in SCLC development

The earliest and most frequent genetic alteration observed in lung cancer occurs at a chromosomal location very close to *RBM5*, within region 3p21.3 (Hung et al., 1995; Lerman and Minna, 2000; Wei et al., 1996; Wistuba et al., 2000). In addition, *RBM5* was found to be downregulated in 70-95% of lung cancers (Travis W.D., 2004). Our findings provide insight into the impact of *RBM5* downregulation to SCLC development and progression: (a) modification of only *RBM5* expression levels influenced many SCLC transformation-associated processes and events, and (b) RBM5 regulated the expression of many SCLC-associated genes. Of note, SCLC occurs almost exclusively in tobacco smokers (Toyooka et al., 2003), which has in turn been associated with decreased *RBM5* expression in two different *in vitro* systems (Hao et al., 2015; Lv et al., 2016). Taken together, these findings suggest that downregulation of *RBM5*, by smoke exposure, is important to SCLC risk. Furthermore, RBM5 is required for aryl hydrocarbon receptor (AHR) expression and consequent CYP1A1 induction in mouse Hepa-1 cells (Solaimani et al., 2013). The role of CYP1A1 is two-pronged; it can detoxify environmental toxins, but also bioactivate procarcinogens (Stejskalova and Pavek, 2011). Such procarcinogens include polycyclic aromatic hydrocarbons (PAH), which are found in cigarette smoke. Therefore, as CYP1A1 can have beneficial, as well as cancer-promoting functions, its strict regulation of function is extremely necessary (Androutsopoulos et al., 2009). Taken together, these results not only support our suggestion that *RBM5* downregulation is an early and important step in SCLC development and progression, but suggest a mechanism by which this may occur.

6.4. RBM10 influences many processes and events, ultimately promoting transformation in a number of ways

RBM10's role as a promoter of apoptosis (Inoue et al 2014) and inhibitor of proliferation (Zhao et al 2017, Hernandez et al 2016) have, like RBM5, been recently confirmed in a number of studies. My results, however, extend the influence of RBM10 past cell cycle arrest and apoptosis, and suggest its ability to alter many transformation- and hypoxia-associated processes and events. Unexpectedly, in an *RBM5*-null environment, RBM10 may influence these processes and events in a way that would promote transformation. Specifically, knockdown of *RBM10* expression induced changes in gene expression predicted to reduce glycolysis, EMT, angiogenesis, and inhibition of mTORC1 pathways – potentially by direct regulation of cell metabolism, particularly oxidative phosphorylation.

Interestingly, RBM10 has been previously shown to influence the expression of genes associated with various neurodegenerative disorders (Bechara et al., 2013). As elaborated in Chapter 4, such diseases usually involve impairments in oxidative phosphorylation and, therefore, these findings support a potential role for RBM10 in the regulation of oxidative phosphorylation. In addition, RBM10's association with FilGAP, a regulator of cell spreading (Yamada et al., 2016), supports a role for RBM10 in the regulation of EMT. Finally, RBM10's potential role in the promotion of angiogenesis is supported by its phosphorylation by c-SRC, and consequent involvement in the PDGF signaling pathway (Amanchy et al., 2008), which controls motility, and angiogenesis (Heldin et al., 1998; Sato et al., 1993). Our comprehensive study suggests

compelling links between these disparate findings regarding RBM10, and suggests processes by which RBM10 may influence these transformation-associated events.

In fact, this overall pro-transformatory role for RBM10 has been previously demonstrated in embryonic stem cells and mouse mandibular cells, where knockdown of RBM10 was associated with decreased cell growth (Rodor et al., 2017). Furthermore, RBM10 knockdown in neuronal cells increased caspase activation induced by staurosporine, an apoptosis inducer (Jackson et al., 2015). Despite one brief recognition of a functional RBM10 dichotomy (Rodor et al., 2017), no previous study had ever investigated it. Chapter 4 directly tackled the opposing functional findings regarding RBM10, even proposing a working model which described the regulatory measures that determine the functional outcome of *RBM10* expression, whether tumor suppressive or transformation-promoting.

6.5. RBM10's pro-transformatory role may be RBM5-dependent

One important factor we identified that influenced RBM10 expression and function was RBM5. In fact, my work suggests that the pro-transformatory characteristics of RBM10 are largely regulated by RBM5, with RBM10 exercising this ability in *RBM5*-deficient systems. The working model presented in Chapter 4, which describes this association, is very comprehensive, and takes into account even the most recent published findings regarding RBM10 (the Chapter 4 manuscript is very recent – currently under review).

Three recent gene expression studies involving various tumors types provide *in vivo* evidence supporting our suggestion that RBM10 promotes transformation in systems where *RBM5* is downregulated. Firstly, gene expression analysis of Cancer Genome Atlas (TCGA) samples from various tumor types showed that *RBM10* was significantly upregulated in many cancer types, while *RBM5* expression was significantly downregulated (Sebestyen et al., 2016). Secondly, RBM10 mutations in pancreactic ductal cancer correlated with better 5-year survival probability (Witkiewicz et al., 2015) and *RBM5* mRNA and protein expression was significantly reduced in pancreatic cancers (Peng et al., 2013). Thirdly, *RBM10* expression correlated with increased disease aggressiveness in metastatic melanomas (Garrisi et al., 2014) and RBM5's promoter region was found to be significantly mutated in metastatic melanomas (Smith et al., 2015), meaning that *RBM5* expression is likely compromised in this type of cancer. Taken together, these studies suggest, like our *in vitro* work, that *RBM10* expression promotes transformation in *RBM5*-reduced environments. We have, therefore, begun to elucidate how *RBM10* expression and function are regulated, a better understanding of which is key to predicting the functional consequences of its expression.

6.6. A relationship between RBM5 and RBM10 is present in many systems

The body of work presented herein demonstrates an association between RBM5 and RBM10 in human SCLC and rat myoblast cell lines. Additional studies have also shown a relationship between RBM5 and RBM10: (1) in SHSY5Y human neuronal cells, RBM10 knockdown correlated with increased levels of *RBM5* (Jackson et al., 2015), and (2) in HEK293 cells,

RBM10 overexpression correlated with increased *RBM5* exon 6 exclusion, whereas RBM10 knockdown correlated with a slight decrease in *RBM5* exon 6 exclusion (Wang et al., 2013). It is, therefore, evident that a relationship exists between RBM5 and RBM10 in many systems, highlighting their potential fundamental importance to the cell. The nature of this relationship between RBM5 and RBM10 has begun to be elucidated; however, many more studies are required to completely understand this association, and its consistencies/differences between cell types.

6.7. Significance and conclusions

This body of work represents the first comprehensive analysis of the many potential roles of RBM5 and RBM10 in cells. We determined that RBM5 and RBM10 influenced a number of cellular events, and that although they had significantly overlapping targets and altered processes/events, the functional consequences of their expression were antagonistic. Furthermore, we took preliminary steps in evaluating the impact of *RBM5* downregulation and RBM10 mutation to SCLC development, progression and treatment. Frighteningly, 70% of patients already have extensive stage SCLC at the time of diagnosis, characterized by the presence of at least one distant metastasis (Lekic et al., 2012; Micke et al., 2002). Due to the late stage diagnosis, treatment options are usually limited, and the 5-year survival rate has not improved over the past two decades, remaining at a dismal 2% (Gaspar et al., 2012; Lekic et al., 2012; Micke et al., 2002). The development of novel treatment options, with better success rates, is thus of utmost importance. Our work suggests that restoring RBM5 expression levels, or processes and events regulated by RBM5, may significantly slow SCLC progression.

Furthermore, downregulation of RBM10 or RBM10-associated processes and events in RBM5-null SCLC tumors may also be a fruitful avenue to pursue in terms of new SCLC therapeutic options.

The alarming SCLC survival statistics make it evident that earlier detection of SCLC could also significantly improve outcomes. Since, at the molecular level, the earliest and most frequent genetic alteration observed in lung cancer is very close to *RBM5*, within region 3p21.3, RBM5 may not only hold therapeutic value, but also predictive value for SCLC risk (Hung et al., 1995; Lerman and Minna, 2000; Wei et al., 1996; Wistuba et al., 2000). Such predictive tests could include evaluating RBM5 expression levels of lung tissues of at-risk patients (*e.g.* smokers). Furthermore, screening for RBM10 mutations in lung cancers with RBM5-downregulation may provide important insight as to the metastatic potential of the tumor, and thus suggest a more intensive treatment plan for the patient. Taken together, the work presented herein is an important step towards better understanding SCLC at a molecular level, and thus presents an important base for future screening and therapeutic options.

An important part of this study is the demonstration and description of a complex relationship between RBM5 and RBM10, in both transformed and non-transformed cells. This work thus greatly expands the knowledge of RBM5 and RBM10 function and regulation, which is particularly important to better understand and treat disease states, such as TARP, in which one or both of these RBPs are altered. This work also increases the general knowledge regarding the functioning of, and relationship between, similar RBPs. As RBPs control all aspects of RNA metabolism, and their aberrant expression and/or function can have devastating consequences,

strengthening the basic understanding of how this class of proteins work is important to all aspects of biology, including molecular, cellular, and developmental.

6.8. Future directions

Our study takes important preliminary steps towards understanding the roles of RBM5 and RBM10 in the cell, and the complex relationship between these two RBPs. More studies, however, are required to fully understand the nature of this relationship, how their interactions are regulated, and how these may vary between cell types and disease states. Given the significant functional consequences of altered *RBM5* or *RBM10* expression, as elaborated in the Introduction, future work in this area could have important clinical relevance.

In addition, our work particularly highlights how very similar alternative splice variants, differing in fact by only one triplet, can differentially interact with proteins, and may have varying downstream functions. Future studies should, therefore, consider the *RBM10* splice variant expression profile in the cell types used prior to undertaking functional assays related to RBM10. Furthermore, it's essential to specify which particular variants are being overexpressed or knocked down, and which are able to be detected by each experimental assay. This aspect of variant identification is often completely overlooked in RBM10-related studies. Future studies examining how each RBM10 isoform functions would also be an extremely important avenue. Particularly since we propose that different isoforms have opposing functions, the ratio of the various RBM10 isoforms, along with *RBM5* expression levels, in a patient could be of predictive significance for cancer incidence and/or progression.

In all, our results really highlight the complexity of RBP function, and how an RBP's interaction with specific proteins, or even RNA molecules, can influence the downstream effects of the RBP's expression. Future work should, therefore, not only focus on determining RBPs function, but also consider the regulatory mechanisms which may be modulating their function under specific circumstances. These types of studies would help to give a more rounded picture of RBPs, and a much better understanding of the many ways by which RNA function and metabolism are regulated.

References

Abdelmohsen, K., Kim, M.M., Srikantan, S., Mercken, E.M., Brennan, S.E., Wilson, G.M., Cabo, R., and Gorospe, M. (2010). miR-519 suppresses tumor growth by reducing HuR levels. Cell Cycle *9*, 1354-1359.

Aigner, A., Juhl, H., Malerczyk, C., Tkybusch, A., Benz, C.C., and Czubayko, F. (2001). Expression of a truncated 100 kDa HER2 splice variant acts as an endogenous inhibitor of tumour cell proliferation. Oncogene *20*, 2101-2111.

Allain, F.H., Bouvet, P., Dieckmann, T., and Feigon, J. (2000). Molecular basis of sequence-specific recognition of pre-ribosomal RNA by nucleolin. EMBO J *19*, 6870-6881.

Amanchy, R., Zhong, J., Molina, H., Chaerkady, R., Iwahori, A., Kalume, D.E., Gronborg, M., Joore, J., Cope, L., and Pandey, A. (2008). Identification of c-Src tyrosine kinase substrates using mass spectrometry and peptide microarrays. J Proteome. Res *7*, 3900-3910.

Andres, V., and Walsh, K. (1996). Myogenin expression, cell cycle withdrawal, and phenotypic differentiation are temporally separable events that precede cell fusion upon myogenesis. J Cell Biol *132*, 657-666.

Androutsopoulos, V.P., Tsatsakis, A.M., and Spandidos, D.A. (2009). Cytochrome P450 CYP1A1: wider roles in cancer progression and prevention. BMC Cancer *9*, 187.

Aravind, L., and Koonin, E.V. (1999). G-patch: a new conserved domain in eukaryotic RNA-processing proteins and type D retroviral polyproteins. Trends Biochem. Sci *24*, 342-344.

Auweter, S.D., Oberstrass, F.C., and Allain, F.H. (2006). Sequence-specific binding of single-stranded RNA: is there a code for recognition? Nucleic Acids Res *34*, 4943-4959.

Babic, I., Jakymiw, A., and Fujita, D.J. (2004). The RNA binding protein Sam68 is acetylated in tumor cell lines, and its acetylation correlates with enhanced RNA binding activity. Oncogene *23*, 3781-3789.

Bandziulis, R.J., Swanson, M.S., and Dreyfuss, G. (1989). RNA-binding proteins as developmental regulators. Genes Dev *3*, 431-437.

Banerjee, D., McDaniel, P.M., and Rymond, B.C. (2015). Limited portability of G-patch domains in regulators of the Prp43 RNA helicase required for pre-mRNA splicing and ribosomal RNA maturation in Saccharomyces cerevisiae. Genetics *200*, 135-147.

Bayer, T.S., Booth, L.N., Knudsen, S.M., and Ellington, A.D. (2005). Arginine-rich motifs present multiple interfaces for specific binding by RNA. RNA *11*, 1848-1857.

Bechara, E.G., Sebestyen, E., Bernardis, I., Eyras, E., and Valcarcel, J. (2013). RBM5, 6, and 10 Differentially Regulate NUMB Alternative Splicing to Control Cancer Cell Proliferation. Mol Cell *52*, 720-733.

Behzadnia, N., Golas, M.M., Hartmuth, K., Sander, B., Kastner, B., Deckert, J., Dube, P., Will, C.L., Urlaub, H., Stark, H., *et al.* (2007). Composition and three-dimensional EM structure of double affinity-purified, human prespliceosomal A complexes. EMBO J *26*, 1737-1748.

Blackwell, E., and Ceman, S. (2012). Arginine methylation of RNA-binding proteins regulates cell function and differentiation. Mol Reprod Dev *79*, 163-175.

Bonnal, S., Martinez, C., Forch, P., Bachi, A., Wilm, M., and Valcarcel, J. (2008). RBM5/Luca-15/H37 regulates Fas alternative splice site pairing after exon definition. Mol Cell *32*, 81-95.

Brayer, K.J., Kulshreshtha, S., and Segal, D.J. (2008). The protein-binding potential of C2H2 zinc finger domains. Cell Biochem Biophys *51*, 9-19.

Buratti, E., and Baralle, F.E. (2011). TDP-43: new aspects of autoregulation mechanisms in RNA binding proteins and their connection with human disease. FEBS J *278*, 3530-3538.

Callebaut, I., and Mornon, J.P. (2005). OCRE: a novel domain made of imperfect, aromatic-rich octamer repeats. Bioinformatics *21*, 699-702.

Castello, A., Fischer, B., Frese, C.K., Horos, R., Alleaume, A.M., Foehr, S., Curk, T., Krijgsveld, J., and Hentze, M.W. (2016). Comprehensive Identification of RNA-Binding Domains in Human Cells. Mol Cell *63*, 696-710.

Castello, A., Fischer, B., Hentze, M.W., and Preiss, T. (2013). RNA-binding proteins in Mendelian disease. Trends Genet *29*, 318-327.

Castello, A., Hentze, M.W., and Preiss, T. (2015). Metabolic Enzymes Enjoying New Partnerships as RNA-Binding Proteins. Trends Endocrinol Metab *26*, 746-757.

Chang, D.W., Xing, Z., Pan, Y., Algeciras-Schimnich, A., Barnhart, B.C., Yaish-Ohad, S., Peter, M.E., and Yang, X. (2002). c-FLIP(L) is a dual function regulator for caspase-8 activation and CD95-mediated apoptosis. EMBO J *21*, 3704-3714.

Chen, T., and Richard, S. (1998). Structure-function analysis of Qk1: a lethal point mutation in mouse quaking prevents homodimerization. Mol Cell Biol *18*, 4863-4871.

Coleman, M.P., Ambrose, H.J., Carrel, L., Nemeth, A.H., Willard, H.F., and Davies, K.E. (1996). A novel gene, DXS8237E, lies within 20 kb upstream of UBE1 in Xp11.23 and has a different X inactivation status. Genomics *31*, 135-138.

Crawford, D.C., Acuna, J.M., and Sherman, S.L. (2001). FMR1 and the fragile X syndrome: human genome epidemiology review. Genet Med *3*, 359-371.

Crawford, T.O., and Pardo, C.A. (1996). The neurobiology of childhood spinal muscular atrophy. Neurobiol Dis *3*, 97-110.

Damianov, A., and Black, D.L. (2010). Autoregulation of Fox protein expression to produce dominant negative splicing factors. RNA *16*, 405-416.

de Hoog, C.L., Foster, L.J., and Mann, M. (2004). RNA and RNA binding proteins participate in early stages of cell spreading through spreading initiation centers. Cell *117*, 649-662.

Deckert, J., Hartmuth, K., Boehringer, D., Behzadnia, N., Will, C.L., Kastner, B., Stark, H., Urlaub, H., and Luhrmann, R. (2006). Protein composition and electron microscopy structure of affinity-purified human spliceosomal B complexes isolated under physiological conditions. Mol Cell Biol *26*, 5528-5543.

Di Cecilia, S., Zhang, F., Sancho, A., Li, S., Aguilo, F., Sun, Y., Rengasamy, M., Zhang, W., Del Vecchio, L., Salvatore, F., *et al.* (2016). RBM5-AS1 Is Critical for Self-Renewal of Colon Cancer Stem-like Cells. Cancer Res *76*, 5615-5627.

Dutertre, M., and Vagner, S. (2016). DNA-Damage Response RNA-Binding Proteins (DDRBPs): Perspectives from a New Class of Proteins and Their RNA Targets. J Mol Biol.

Edamatsu, H., Kaziro, Y., and Itoh, H. (2000). LUCA15, a putative tumour suppressor gene encoding an RNA-binding nuclear protein, is down-regulated in ras-transformed Rat-1 cells. Genes Cells *5*, 849-858.

Ellis, L.M. (2004). Epidermal growth factor receptor in tumor angiogenesis. Hematol Oncol Clin North Am *18*, 1007-1021, viii.

Ferre, F., Colantoni, A., and Helmer-Citterich, M. (2016). Revealing protein-lncRNA interaction. Brief Bioinform *17*, 106-116.

Franco, D.L., Mainez, J., Vega, S., Sancho, P., Murillo, M.M., de Frutos, C.A., Del Castillo, G., Lopez-Blau, C., Fabregat, I., and Nieto, M.A. (2010). Snail1 suppresses TGF-beta-induced apoptosis and is sufficient to trigger EMT in hepatocytes. J Cell Sci *123*, 3467-3477.

Furukawa, T., Kuboki, Y., Tanji, E., Yoshida, S., Hatori, T., Yamamoto, M., Shibata, N., Shimizu, K., Kamatani, N., and Shiratori, K. (2011). Whole-exome sequencing uncovers frequent GNAS mutations in intraductal papillary mucinous neoplasms of the pancreas. Sci Rep *1*, 161.

Fushimi, K., Ray, P., Kar, A., Wang, L., Sutherland, L.C., and Wu, J.Y. (2008). Up-regulation of the proapoptotic caspase 2 splicing isoform by a candidate tumor suppressor, RBM5. Proc. Natl Acad Sci U. S. A *105*, 15708-15713.

Garber, K.B., Visootsak, J., and Warren, S.T. (2008). Fragile X syndrome. Eur J Hum Genet *16*, 666-672.

Garrisi, V.M., Strippoli, S., De, S.S., Pinto, R., Perrone, A., Guida, G., Azzariti, A., Guida, M., and Stefania, T. (2014). Proteomic profile and in silico analysis in metastatic melanoma with and without BRAF mutation. PLoS One *9*, e112025.

Gaspar, L.E., McNamara, E.J., Gay, E.G., Putnam, J.B., Crawford, J., Herbst, R.S., and Bonner, J.A. (2012). Small-cell lung cancer: prognostic factors and changing treatment over 15 years. Clin. Lung Cancer *13*, 115-122.

Glisovic, T., Bachorik, J.L., Yong, J., and Dreyfuss, G. (2008). RNA-binding proteins and post-transcriptional gene regulation. FEBS Lett *582*, 1977-1986.

Gorlin, R.J., Cervenka, J., Anderson, R.C., Sauk, J.J., and Bevis, W.D. (1970). Robin's syndrome. A probably X-linked recessive subvariety exhibiting persistence of left superior vena cava and atrial septal defect. Am J Dis Child *119*, 176-178.

Gripp, K.W., Hopkins, E., Johnston, J.J., Krause, C., Dobyns, W.B., and Biesecker, L.G. (2011). Long-term survival in TARP syndrome and confirmation of RBM10 as the disease-causing gene. Am J Med Genet A *155A*, 2516-2520.

Han, L.Y., Cai, C.Z., Lo, S.L., Chung, M.C., and Chen, Y.Z. (2004). Prediction of RNA-binding proteins from primary sequence by a support vector machine approach. RNA *10*, 355-368.

Hao, Y.Q., Su, Z.Z., Lv, X.J., Li, P., Gao, P., Wang, C., Bai, Y., and Zhang, J. (2015). RNA-binding motif protein 5 negatively regulates the activity of Wnt/beta-catenin signaling in cigarette smoke-induced alveolar epithelial injury. Oncol Rep *33*, 2438-2444.

Hartmuth, K., Urlaub, H., Vornlocher, H.P., Will, C.L., Gentzel, M., Wilm, M., and Luhrmann, R. (2002). Protein composition of human prespliceosomes isolated by a tobramycin affinity-selection method. Proc Natl Acad Sci U S A *99*, 16719-16724.

Heldin, C.H., Ostman, A., and Ronnstrand, L. (1998). Signal transduction via platelet-derived growth factor receptors. Biochim Biophys Acta *1378*, F79-113.

Hernandez, J., Bechara, E., Schlesinger, D., Delgado, J., Serrano, L., and Valcarcel, J. (2016). Tumor suppressor properties of the splicing regulatory factor RBM10. RNA Biol *13*, 466-472.

Hoffman, D.W., Query, C.C., Golden, B.L., White, S.W., and Keene, J.D. (1991). RNA-binding domain of the A protein component of the U1 small nuclear ribonucleoprotein analyzed by NMR spectroscopy is structurally similar to ribosomal proteins. Proc. Natl Acad. Sci. U. S. A *88*, 2495-2499.

Hung, J., Kishimoto, Y., Sugio, K., Virmani, A., McIntire, D.D., Minna, J.D., and Gazdar, A.F. (1995). Allele-specific chromosome 3p deletions occur at an early stage in the pathogenesis of lung carcinoma. JAMA *273*, 1908.

Imielinski, M., Berger, A.H., Hammerman, P.S., Hernandez, B., Pugh, T.J., Hodis, E., Cho, J., Suh, J., Capelletti, M., Sivachenko, A., *et al.* (2012). Mapping the hallmarks of lung adenocarcinoma with massively parallel sequencing. Cell *150*, 1107-1120.

Inoue, A., Takahashi, K.P., Kimura, M., Watanabe, T., and Morisawa, S. (1996). Molecular cloning of a RNA binding protein, S1-1. Nucleic Acids Res *24*, 2990-2997.

Inoue, A., Tsugawa, K., Tokunaga, K., Takahashi, K.P., Uni, S., Kimura, M., Nishio, K., Yamamoto, N., Honda, K.I., Watanabe, T., *et al.* (2008). S1-1 nuclear domains: characterization and dynamics as a function of transcriptional activity. Biol Cell *100*, 523-35.

Inoue, A., Yamamoto, N., Kimura, M., Nishio, K., Yamane, H., and Nakajima, K. (2014). RBM10 regulates alternative splicing. FEBS Lett *588*, 942-947.

Jackson, T.C., Du, L., Janesko-Feldman, K., Vagni, V.A., Dezfulian, C., Poloyac, S.M., Jackson, E.K., Clark, R.S., and Kochanek, P.M. (2015). The nuclear splicing factor RNA binding motif 5 promotes caspase activation in human neuronal cells, and increases after traumatic brain injury in mice. J Cereb. Blood Flow Metab *35*, 655-666.

James, C.G., Ulici, V., Tuckermann, J., Underhill, T.M., and Beier, F. (2007). Expression profiling of Dexamethasone-treated primary chondrocytes identifies targets of glucocorticoid signalling in endochondral bone development. BMC Genomics *8*, 205.

Jiang, Y., Sheng, H., Meng, L., Yue, H., Li, B., Zhang, A., Dong, Y., and Liu, Y. (2017). RBM5 inhibits tumorigenesis of gliomas through inhibition of Wnt/beta-catenin signaling and induction of apoptosis. World J Surg Oncol *15*, 9.

Jin, W., Niu, Z., Xu, D., and Li, X. (2012). RBM5 promotes exon 4 skipping of AID pre-mRNA by competing with the binding of U2AF65 to the polypyrimidine tract. FEBS Lett *586*, 3852-3857.

Johnston, J.J., Teer, J.K., Cherukuri, P.F., Hansen, N.F., Loftus, S.K., Chong, K., Mullikin, J.C., and Biesecker, L.G. (2010). Massively parallel sequencing of exons on the X chromosome identifies RBM10 as the gene that causes a syndromic form of cleft palate. Am J Hum. Genet *86*, 743-748.

Justice, M.J., and Bode, V.C. (1988). Three ENU-induced alleles of the murine quaking locus are recessive embryonic lethal mutations. Genet Res *51*, 95-102.

Kan, Z., Jaiswal, B.S., Stinson, J., Janakiraman, V., Bhatt, D., Stern, H.M., Yue, P., Haverty, P.M., Bourgon, R., Zheng, J., *et al.* (2010). Diverse somatic mutation patterns and pathway alterations in human cancers. Nature *466*, 869-873.

Kelemen, O., Convertini, P., Zhang, Z., Wen, Y., Shen, M., Falaleeva, M., and Stamm, S. (2013). Function of alternative splicing. Gene *514*, 1-30.

Khosravi-Far, R., and Der, C.J. (1994). The Ras signal transduction pathway. Cancer Metastasis Rev *13*, 67-89.

Kim, Y.S., Hwan, J.D., Bae, S., Bae, D.H., and Shick, W.A. (2010). Identification of differentially expressed genes using an annealing control primer system in stage III serous ovarian carcinoma. BMC Cancer *10*, 576.

Kobayashi, T., Ishida, J., Musashi, M., Ota, S., Yoshida, T., Shimizu, Y., Chuma, M., Kawakami, H., Asaka, M., Tanaka, J., *et al.* (2011). p53 transactivation is involved in the antiproliferative activity of the putative tumor suppressor RBM5. Int J Cancer *128*, 304-318.

Lamouille, S., Xu, J., and Derynck, R. (2014). Molecular mechanisms of epithelial-mesenchymal transition. Nat Rev Mol Cell Biol *15*, 178-196.

Lee, C.B., Morris, D.E., Fried, D.B., and Socinski, M.A. (2006). Current and evolving treatment options for limited stage small cell lung cancer. Curr Opin Oncol *18*, 162-172.

Lekic, M., Kovac, V., Triller, N., Knez, L., Sadikov, A., and Cufer, T. (2012). Outcome of small cell lung cancer (SCLC) patients with brain metastases in a routine clinical setting. Radiol Oncol *46*, 54-59.

Lerman, M.I., and Minna, J.D. (2000). The 630-kb lung cancer homozygous deletion region on human chromosome 3p21.3: identification and evaluation of the resident candidate tumor

suppressor genes. The International Lung Cancer Chromosome 3p21.3 Tumor Suppressor Gene Consortium. Cancer Res *60*, 6116-6133.

Li, H., and Bingham, P.M. (1991). Arginine/serine-rich domains of the su(wa) and tra RNA processing regulators target proteins to a subnuclear compartment implicated in splicing. Cell *67*, 335-342.

Li, X., Kazan, H., Lipshitz, H.D., and Morris, Q.D. (2014). Finding the target sites of RNA-binding proteins. Wiley Interdiscip Rev RNA *5*, 111-130.

Liang, H., Zhang, J., Shao, C., Zhao, L., Xu, W., Sutherland, L.C., and Wang, K. (2012). Differential expression of RBM5, EGFR and KRAS mRNA and protein in non-small cell lung cancer tissues. J Exp Clin Cancer Res *31*, 36.

Loiselle, J.J., and Sutherland, L.C. (2014). Differential downregulation of Rbm5 and Rbm10 during skeletal and cardiac differentiation. In Vitro Cell Dev. Biol. Anim *50*, 331-339.

Loughlin, F.E., Mansfield, R.E., Vaz, P.M., McGrath, A.P., Setiyaputra, S., Gamsjaeger, R., Chen, E.S., Morris, B.J., Guss, J.M., and Mackay, J.P. (2009). The zinc fingers of the SR-like protein ZRANB2 are single-stranded RNA-binding domains that recognize 5' splice site-like sequences. Proc Natl Acad Sci U. S. A *106*, 5581-5586.

Lukong, K.E., Chang, K.W., Khandjian, E.W., and Richard, S. (2008). RNA-binding proteins in human genetic disease. Trends Genet *24*, 416-425.

Lunde, B.M., Moore, C., and Varani, G. (2007). RNA-binding proteins: modular design for efficient function. Nat Rev Mol. Cell Biol *8*, 479-490.

Lv, X.J., Du, Y.W., Hao, Y.Q., Su, Z.Z., Zhang, L., Zhao, L.J., and Zhang, J. (2016). RNA-binding motif protein 5 inhibits the proliferation of cigarette smoke-transformed BEAS-2B cells through cell cycle arrest and apoptosis. Oncol Rep *35*, 2315-2327.

Maaskola, J., and Rajewsky, N. (2014). Binding site discovery from nucleic acid sequences by discriminative learning of hidden Markov models. Nucleic Acids Res *42*, 12995-13011.

MacDonald, B.T., Tamai, K., and He, X. (2009). Wnt/beta-catenin signaling: components, mechanisms, and diseases. Dev Cell *17*, 9-26.

Maquat, L.E., and Carmichael, G.G. (2001). Quality control of mRNA function. Cell *104*, 173-176.

Maris, C., Dominguez, C., and Allain, F.H. (2005). The RNA recognition motif, a plastic RNA-binding platform to regulate post-transcriptional gene expression. FEBS J *272*, 2118-2131.

Martinez-Arribas, F., Agudo, D., Pollan, M., Gomez-Esquer, F., az-Gil, G., Lucas, R., and Schneider, J. (2006). Positive correlation between the expression of X-chromosome RBM genes (RBMX, RBM3, RBM10) and the proapoptotic Bax gene in human breast cancer. J Cell Biochem *97*, 1275-1282.

Masilamani, T.J., Rintala-Maki, N.D., Wang, K., and Sutherland, L.C. (2012). Downregulating activated epidermal growth factor receptor has no effect on RBM5 expression. Chin Med J (Engl) *125*, 2378-2381.

Matter, N., Herrlich, P., and Konig, H. (2002). Signal-dependent regulation of splicing via phosphorylation of Sam68. Nature *420*, 691-695.

Micke, P., Faldum, A., Metz, T., Beeh, K.M., Bittinger, F., Hengstler, J.G., and Buhl, R. (2002). Staging small cell lung cancer: Veterans Administration Lung Study Group versus International Association for the Study of Lung Cancer--what limits limited disease? Lung Cancer *37*, 271-276.

Miller, G., Socci, N.D., Dhall, D., D'Angelica, M., DeMatteo, R.P., Allen, P.J., Singh, B., Fong, Y., Blumgart, L.H., Klimstra, D.S., *et al.* (2009). Genome wide analysis and clinical correlation of chromosomal and transcriptional mutations in cancers of the biliary tract. J Exp Clin Cancer Res *28*, 62.

Morin, P.J. (1999). beta-catenin signaling and cancer. Bioessays *21*, 1021-1030.

Mourao, A., Bonnal, S., Soni, K., Warner, L., Bordonne, R., Valcarcel, J., and Sattler, M. (2016). Structural basis for the recognition of spliceosomal SmN/B/B' proteins by the RBM5 OCRE domain in splicing regulation. Elife *5*.

Mourtada-Maarabouni, M., Keen, J., Clark, J., Cooper, C.S., and Williams, G.T. (2006). Candidate tumor suppressor LUCA-15/RBM5/H37 modulates expression of apoptosis and cell cycle genes. Exp. Cell Res *312*, 1745-1752.

Mourtada-Maarabouni, M., Sutherland, L.C., Meredith, J.M., and Williams, G.T. (2003). Simultaneous acceleration of the cell cycle and suppression of apoptosis by splice variant delta-6 of the candidate tumour suppressor LUCA-15/RBM5. Genes Cells *8*, 109-119.

Mueller, C.F., Berger, A., Zimmer, S., Tiyerili, V., and Nickenig, G. (2009). The heterogenous nuclear riboprotein S1-1 regulates AT1 receptor gene expression via transcriptional and posttranscriptional mechanisms. Arch Biochem Biophys *488*, 76-82.

Nagai, K., Oubridge, C., Jessen, T.H., Li, J., and Evans, P.R. (1990). Crystal structure of the RNA-binding domain of the U1 small nuclear ribonucleoprotein A. Nature *348*, 515-520.

Nagase, T., Seki, N., Tanaka, A., Ishikawa, K., and Nomura, N. (1995). Prediction of the coding sequences of unidentified human genes. IV. The coding sequences of 40 new genes (KIAA0121-

KIAA0160) deduced by analysis of cDNA clones from human cell line KG-1. DNA Res *2*, 167-210.

Nakahata, S., and Kawamoto, S. (2005). Tissue-dependent isoforms of mammalian Fox-1 homologs are associated with tissue-specific splicing activities. Nucleic Acids Res *33*, 2078-2089.

Network, T.C.G.A.R. (2014). Comprehensive molecular profiling of lung adenocarcinoma. Nature *511*, 543-550.

Nguyen, C.D., Mansfield, R.E., Leung, W., Vaz, P.M., Loughlin, F.E., Grant, R.P., and Mackay, J.P. (2011). Characterization of a family of RanBP2-type zinc fingers that can recognize single-stranded RNA. J Mol Biol *407*, 273-283.

Niu, Z., Jin, W., Zhang, L., and Li, X. (2012). Tumor suppressor RBM5 directly interacts with the DExD/H-box protein DHX15 and stimulates its helicase activity. FEBS Lett *586*, 977-983.

O'Bryan, M.K., Clark, B.J., McLaughlin, E.A., D'Sylva, R.J., O'Donnell, L., Wilce, J.A., Sutherland, J., O'Connor, A.E., Whittle, B., Goodnow, C.C., *et al.* (2013). RBM5 Is a Male Germ Cell Splicing Factor and Is Required for Spermatid Differentiation and Male Fertility. PLoS Genet *9*, e1003628.

O'Connor, C.M., and Adams, J.U. (2010). Proteins Are Responsible for a Diverse Range of Structural and Catalytic Functions in Cells. In Essentials of Cell Biology (Cambridge, MA: NPG Education).

O'Leary, D.A., Sharif, O., Anderson, P., Tu, B., Welch, G., Zhou, Y., Caldwell, J.S., Engels, I.H., and Brinker, A. (2009). Identification of small molecule and genetic modulators of AON-induced dystrophin exon skipping by high-throughput screening. PLoS One *4*, e8348.

Oh, J.J., Boctor, B.N., Jimenez, C.A., Lopez, R., Koegel, A.K., Taschereau, E.O., Phan, D.T., Jacobsen, S.E., and Slamon, D.J. (2008). Promoter methylation study of the H37/RBM5 tumor suppressor gene from the 3p21.3 human lung cancer tumor suppressor locus. Hum. Genet *123*, 55-64.

Oh, J.J., Razfar, A., Delgado, I., Reed, R.A., Malkina, A., Boctor, B., and Slamon, D.J. (2006). 3p21.3 tumor suppressor gene H37/Luca15/RBM5 inhibits growth of human lung cancer cells through cell cycle arrest and apoptosis. Cancer Res *66*, 3419-3427.

Oh, J.J., West, A.R., Fishbein, M.C., and Slamon, D.J. (2002). A candidate tumor suppressor gene, H37, from the human lung cancer tumor suppressor locus 3p21.3. Cancer Res *62*, 3207-3213.

Oubridge, C., Ito, N., Evans, P.R., Teo, C.H., and Nagai, K. (1994). Crystal structure at 1.92 A resolution of the RNA-binding domain of the U1A spliceosomal protein complexed with an RNA hairpin. Nature *372*, 432-438.

Pan, Q., Shai, O., Lee, L.J., Frey, B.J., and Blencowe, B.J. (2008). Deep surveying of alternative splicing complexity in the human transcriptome by high-throughput sequencing. Nat Genet *40*, 1413-1415.

Panda, A.C., Abdelmohsen, K., Yoon, J.H., Martindale, J.L., Yang, X., Curtis, J., Mercken, E.M., Chenette, D.M., Zhang, Y., Schneider, R.J., *et al.* (2014). RNA-binding protein AUF1 promotes myogenesis by regulating MEF2C expression levels. Mol Cell Biol *34*, 3106-3119.

Paronetto, M.P., Cappellari, M., Busa, R., Pedrotti, S., Vitali, R., Comstock, C., Hyslop, T., Knudsen, K.E., and Sette, C. (2010). Alternative splicing of the cyclin D1 proto-oncogene is regulated by the RNA-binding protein Sam68. Cancer Res *70*, 229-239.

Peng, J., Valeshabad, A.K., Li, Q., and Wang, Y. (2013). Differential expression of RBM5 and KRAS in pancreatic ductal adenocarcinoma and their association with clinicopathological features. Oncol Lett *5*, 1000-1004.

Pont, A.R., Sadri, N., Hsiao, S.J., Smith, S., and Schneider, R.J. (2012). mRNA decay factor AUF1 maintains normal aging, telomere maintenance, and suppression of senescence by activation of telomerase transcription. Mol Cell *47*, 5-15.

Popovitchenko, T., Thompson, K., Viljetic, B., Jiao, X., Kontonyiannis, D.L., Kiledjian, M., Hart, R.P., and Rasin, M.R. (2016). The RNA binding protein HuR determines the differential translation of autism-associated FoxP subfamily members in the developing neocortex. Sci Rep *6*, 28998.

Price, S.R., Evans, P.R., and Nagai, K. (1998). Crystal structure of the spliceosomal U2B"-U2A' protein complex bound to a fragment of U2 small nuclear RNA. Nature *394*, 645-650.

Pullmann, R., Jr., Kim, H.H., Abdelmohsen, K., Lal, A., Martindale, J.L., Yang, X., and Gorospe, M. (2007). Analysis of turnover and translation regulatory RNA-binding protein expression through binding to cognate mRNAs. Mol Cell Biol *27*, 6265-6278.

Qiu, T.H., Chandramouli, G.V., Hunter, K.W., Alkharouf, N.W., Green, J.E., and Liu, E.T. (2004). Global expression profiling identifies signatures of tumor virulence in MMTV-PyMT-transgenic mice: correlation to human disease. Cancer Res *64*, 5973-5981.

Rajan, P., Gaughan, L., Dalgliesh, C., El-Sherif, A., Robson, C.N., Leung, H.Y., and Elliott, D.J. (2008). Regulation of gene expression by the RNA-binding protein Sam68 in cancer. Biochem Soc Trans *36*, 505-507.

Ramaswamy, S., Ross, K.N., Lander, E.S., and Golub, T.R. (2003). A molecular signature of metastasis in primary solid tumors. Nat. Genet *33*, 49-54.

Rappsilber, J., Ryder, U., Lamond, A.I., and Mann, M. (2002). Large-scale proteomic analysis of the human spliceosome. Genome Res *12*, 1231-1245.

Ray, D., Kazan, H., Cook, K.B., Weirauch, M.T., Najafabadi, H.S., Li, X., Gueroussov, S., Albu, M., Zheng, H., Yang, A., *et al.* (2013). A compendium of RNA-binding motifs for decoding gene regulation. Nature *499*, 172-177.

Revil, T., Gaffney, D., Dias, C., Majewski, J., and Jerome-Majewska, L.A. (2010). Alternative splicing is frequent during early embryonic development in mouse. BMC Genomics *11*, 399.

Rintala-Maki, N.D., Goard, C.A., Langdon, C.E., Wall, V.E., Traulsen, K.E., Morin, C.D., Bonin, M., and Sutherland, L.C. (2007). Expression of RBM5-related factors in primary breast tissue. J Cell Biochem *100*, 1440-1458.

Rintala-Maki, N.D., and Sutherland, L.C. (2004). LUCA-15/RBM5, a putative tumour suppressor, enhances multiple receptor-initiated death signals. Apoptosis *9*, 475-484.

Rintala-Maki, N.D., and Sutherland, L.C. (2009). Identification and characterisation of a novel antisense non-coding RNA from the RBM5 gene locus. Gene *445*, 7-16.

Rodor, J., FitzPatrick, D.R., Eyras, E., and Caceres, J.F. (2017). The RNA-binding landscape of RBM10 and its role in alternative splicing regulation in models of mouse early development. RNA Biol *14*, 45-57.

Sandri, M., and Carraro, U. (1999). Apoptosis of skeletal muscles during development and disease. Int. J. Biochem. Cell Biol *31*, 1373-1390.

Sato, N., Beitz, J.G., Kato, J., Yamamoto, M., Clark, J.W., Calabresi, P., Raymond, A., and Frackelton, A.R., Jr. (1993). Platelet-derived growth factor indirectly stimulates angiogenesis in vitro. Am J Pathol *142*, 1119-1130.

Savagner, P. (2010). The epithelial-mesenchymal transition (EMT) phenomenon. Ann Oncol *21 Suppl 7*, vii89-92.

Sebestyen, E., Singh, B., Minana, B., Pages, A., Mateo, F., Pujana, M.A., Valcarcel, J., and Eyras, E. (2016). Large-scale analysis of genome and transcriptome alterations in multiple tumors unveils novel cancer-relevant splicing networks. Genome Res *26*, 732-744.

Sehgal, L., Mathur, R., Braun, F.K., Wise, J.F., Berkova, Z., Neelapu, S., Kwak, L.W., and Samaniego, F. (2014). FAS-antisense 1 lncRNA and production of soluble versus membrane Fas in B-cell lymphoma. Leukemia *28*, 2376-2387.

Sela-Brown, A., Silver, J., Brewer, G., and Naveh-Many, T. (2000). Identification of AUF1 as a parathyroid hormone mRNA 3'-untranslated region-binding protein that determines parathyroid hormone mRNA stability. J Biol Chem *275*, 7424-7429.

Shao, C., Zhao, L., Wang, K., Xu, W., Zhang, J., and Yang, B. (2012). The tumor suppressor gene RBM5 inhibits lung adenocarcinoma cell growth and induces apoptosis. World J Surg Oncol *10*, 160.

Shedlovsky, A., King, T.R., and Dove, W.F. (1988). Saturation germ line mutagenesis of the murine t region including a lethal allele at the quaking locus. Proc Natl Acad Sci U S A *85*, 180-184.

Shu, Y., Rintala-Maki, N.D., Wall, V.E., Wang, K., Goard, C.A., Langdon, C.E., and Sutherland, L.C. (2007). The apoptosis modulator and tumour suppressor protein RBM5 is a phosphoprotein. Cell Biochem Funct *25*, 643-653.

Smit, E.F., de Vries, E.G., Timmer-Bosscha, H., de Leij, L.F., Oosterhuis, J.W., Scheper, R.J., Weening, J.J., Postmus, P.E., and Mulder, N.H. (1992). In vitro response of human small-cell lung-cancer cell lines to chemotherapeutic drugs; no correlation with clinical data. Int. J. Cancer *51*, 72-78.

Smith, K.S., Yadav, V.K., Pedersen, B.S., Shaknovich, R., Geraci, M.W., Pollard, K.S., and De, S. (2015). Signatures of accelerated somatic evolution in gene promoters in multiple cancer types. Nucleic Acids Res *43*, 5307-5317.

Solaimani, P., Damoiseaux, R., and Hankinson, O. (2013). Genome-wide RNAi high-throughput screen identifies proteins necessary for the AHR-dependent induction of CYP1A1 by 2,3,7,8-tetrachlorodibenzo-p-dioxin. Toxicol. Sci *136*, 107-119.

Song, Z., Wu, P., Ji, P., Zhang, J., Gong, Q., Wu, J., and Shi, Y. (2012). Solution structure of the second RRM domain of RBM5 and its unusual binding characters for different RNA targets. Biochemistry *51*, 6667-6678.

Srikantan, S., and Gorospe, M. (2012). HuR function in disease. Front Biosci (Landmark Ed) *17*, 189-205.

Stejskalova, L., and Pavek, P. (2011). The function of cytochrome P450 1A1 enzyme (CYP1A1) and aryl hydrocarbon receptor (AhR) in the placenta. Curr Pharm Biotechnol *12*, 715-730.

Su, Z., Yin, J., Zhao, L., Li, R., Liang, H., Zhang, J., and Wang, K. (2014). Lentiviral vector-mediated RBM5 overexpression downregulates EGFR expression in human non-small cell lung cancer cells. World J Surg. Oncol *12*, 367.

Sutherland, L.C., Edwards, S.E., Cable, H.C., Poirier, G.G., Miller, B.A., Cooper, C.S., and Williams, G.T. (2000). LUCA-15-encoded sequence variants regulate CD95-mediated apoptosis. Oncogene *19*, 3774-3781.

Sutherland, L.C., Rintala-Maki, N.D., White, R.D., and Morin, C.D. (2005). RNA binding motif (RBM) proteins: a novel family of apoptosis modulators? J. Cell Biochem *94*, 5-24.

Thapar, R. (2015). Structural basis for regulation of RNA-binding proteins by phosphorylation. ACS Chem Biol *10*, 652-666.

Thiselton, D.L., McDowall, J., Brandau, O., Ramser, J., d'Esposito, F., Bhattacharya, S.S., Ross, M.T., Hardcastle, A.J., and Meindl, A. (2002). An integrated, functionally annotated gene map of the DXS8026-ELK1 interval on human Xp11.3-Xp11.23: potential hotspot for neurogenetic disorders. Genomics *79*, 560-572.

Timmer, T., Terpstra, P., van den Berg, A., Veldhuis, P.M., Ter Elst, A., van der Veen, A.Y., Kok, K., Naylor, S.L., and Buys, C.H. (1999a). An evolutionary rearrangement of the Xp11.3-11.23 region in 3p21.3, a region frequently deleted in a variety of cancers. Genomics *60*, 238-240.

Timmer, T., Terpstra, P., van den Berg, A., Veldhuis, P.M., Ter Elst, A., Voutsinas, G., Hulsbeek, M.M., Draaijers, T.G., Looman, M.W., Kok, K., *et al.* (1999b). A comparison of

genomic structures and expression patterns of two closely related flanking genes in a critical lung cancer region at 3p21.3. Eur. J. Hum. Genet *7*, 478-486.

Toyooka, S., Tsuda, T., and Gazdar, A.F. (2003). The TP53 gene, tobacco exposure, and lung cancer. Hum Mutat *21*, 229-239.

Travis W.D., B.E., Muller-Hermelink H.K., Harris C.C. (2004). World Health Organization Classification of Tumours. Pathology and Genetics of Tumours of the Lung, Pleura, Thymus and Heart (Lyon, France: IARC Press).

Valdes, F., Alvarez, A.M., Locascio, A., Vega, S., Herrera, B., Fernandez, M., Benito, M., Nieto, M.A., and Fabregat, I. (2002). The epithelial mesenchymal transition confers resistance to the apoptotic effects of transforming growth factor Beta in fetal rat hepatocytes. Mol Cancer Res *1*, 68-78.

Venter, J.C., Adams, M.D., Myers, E.W., Li, P.W., Mural, R.J., Sutton, G.G., Smith, H.O., Yandell, M., Evans, C.A., Holt, R.A., *et al.* (2001). The sequence of the human genome. Science *291*, 1304-1351.

Walsh, K., and Perlman, H. (1997). Cell cycle exit upon myogenic differentiation. Curr Opin Genet Dev *7*, 597-602.

Wang, J., and Walsh, K. (1996). Resistance to apoptosis conferred by Cdk inhibitors during myocyte differentiation. Science *273,* 359-361.

Wang, K., Bacon, M.L., Tessier, J.J., Rintala-Maki, N.D., Tang, V., and Sutherland, L.C. (2012). RBM10 Modulates Apoptosis and Influences TNA-a Gene Expression. Journal of Cell Death *5*, 1-19.

Wang, Y., Gogol-Doring, A., Hu, H., Frohler, S., Ma, Y., Jens, M., Maaskola, J., Murakawa, Y., Quedenau, C., Landthaler, M., *et al.* (2013). Integrative analysis revealed the molecular mechanism underlying RBM10-mediated splicing regulation. EMBO Mol Med *5*, 1431-1442.

Wei, M.H., Latif, F., Bader, S., Kashuba, V., Chen, J.Y., Duh, F.M., Sekido, Y., Lee, C.C., Geil, L., Kuzmin, I., *et al.* (1996). Construction of a 600-kilobase cosmid clone contig and generation of a transcriptional map surrounding the lung cancer tumor suppressor gene (TSG) locus on human chromosome 3p21.3: progress toward the isolation of a lung cancer TSG. Cancer Res *56*, 1487-1492.

Welling, D.B., Lasak, J.M., Akhmametyeva, E., Ghaheri, B., and Chang, L.S. (2002). cDNA microarray analysis of vestibular schwannomas. Otol. Neurotol *23*, 736-748.

Williams, P.A., Krug, M.S., McMillan, E.A., Peake, J.D., Davis, T.L., Cocklin, S., and Strochlic, T.I. (2016). Phosphorylation of the RNA-binding protein Dazl by MAPKAP kinase 2 regulates spermatogenesis. Mol Biol Cell *27*, 2341-2350.

Wistuba, I.I., Behrens, C., Virmani, A.K., Mele, G., Milchgrub, S., Girard, L., Fondon, J.W., III, Garner, H.R., McKay, B., Latif, F., *et al.* (2000). High resolution chromosome 3p allelotyping of human lung cancer and preneoplastic/preinvasive bronchial epithelium reveals multiple, discontinuous sites of 3p allele loss and three regions of frequent breakpoints. Cancer Res *60*, 1949-1960.

Witkiewicz, A.K., McMillan, E.A., Balaji, U., Baek, G., Lin, W.C., Mansour, J., Mollaee, M., Wagner, K.U., Koduru, P., Yopp, A., *et al.* (2015). Whole-exome sequencing of pancreatic cancer defines genetic diversity and therapeutic targets. Nat Commun *6*, 6744.

Wurth, L. (2012). Versatility of RNA-Binding Proteins in Cancer. Comp Funct Genomics *2012*, 178525.

Xiao, S.J., Wang, L.Y., Kimura, M., Kojima, H., Kunimoto, H., Nishiumi, F., Yamamoto, N., Nishio, K., Fujimoto, S., Kato, T., *et al.* (2013). S1-1/RBM10: multiplicity and cooperativity of nuclear localisation domains. Biol Cell *105*, 162-174.

Yahi, H., Philipot, O., Guasconi, V., Fritsch, L., and Ait-Si-Ali, S. (2006). Chromatin modification and muscle differentiation. Expert Opin Ther Targets *10*, 923-934.

Yamada, H., Tsutsumi, K., Nakazawa, Y., Shibagaki, Y., Hattori, S., and Ohta, Y. (2016). Src Family Tyrosine Kinase Signaling Regulates FilGAP through Association with RBM10. PLoS One *11*, e0146593.

Yi, J., Chang, N., Liu, X., Guo, G., Xue, L., Tong, T., Gorospe, M., and Wang, W. (2010). Reduced nuclear export of HuR mRNA by HuR is linked to the loss of HuR in replicative senescence. Nucleic Acids Res *38*, 1547-1558.

Zhang, J., Cui, Z., Feng, G., Bao, G., Xu, G., Sun, Y., Wang, L., Chen, J., Jin, H., Liu, J., *et al.* (2015). RBM5 and p53 expression after rat spinal cord injury: implications for neuronal apoptosis. Int J Biochem Cell Biol *60*, 43-52.

Zhang, L., Zhang, Q., Yang, Y., and Wu, C. (2014). The RNA recognition motif domains of RBM5 are required for RNA binding and cancer cell proliferation inhibition. Biochem Biophys. Res. Commun *444*, 445-450.

Zhao, J., Sun, Y., Huang, Y., Song, F., Huang, Z., Bao, Y., Zuo, J., Saffen, D., Shao, Z., Liu, W., *et al.* (2017). Functional analysis reveals that RBM10 mutations contribute to lung adenocarcinoma pathogenesis by deregulating splicing. Sci Rep *7*, 40488.

Zhao, L., Li, R., Shao, C., Li, P., Liu, J., and Wang, K. (2012). 3p21.3 tumor suppressor gene RBM5 inhibits growth of human prostate cancer PC-3 cells through apoptosis. World J Surg Oncol *10*, 247.

Zheng, S., Damoiseaux, R., Chen, L., and Black, D.L. (2013). A broadly applicable high-throughput screening strategy identifies new regulators of Dlg4 (Psd-95) alternative splicing. Genome Res *23*, 998-1007.

Zhu, P., Zhou, W., Wang, J., Puc, J., Ohgi, K.A., Erdjument-Bromage, H., Tempst, P., Glass, C.K., and Rosenfeld, M.G. (2007). A histone H2A deubiquitinase complex coordinating histone acetylation and H1 dissociation in transcriptional regulation. Mol Cell *27*, 609-621.